

**PRECISION QCD STUDY FOR
SPIN-2 PRODUCTION
AT THE LARGE HADRON COLLIDER**

By
GOUTAM DAS
(PHYS05201304001)

*Saha Institute of Nuclear Physics
Kolkata, India*

*A thesis submitted to the
Board of Studies in Physical Sciences
In partial fulfillment of requirements
For the Degree of*

DOCTOR OF PHILOSOPHY
of
HOMI BHABHA NATIONAL INSTITUTE



June, 2017

Homi Bhabha National Institute

Recommendations of the Viva Voce Committee

As members of the Viva Voce Committee, we certify that we have read the dissertation prepared by Goutam Das entitled "**Precision QCD Study for Spin-2 Production at the Large Hadron Collider**" and recommend that it may be accepted as fulfilling the thesis requirement for the award of Degree of Doctor of Philosophy.

Chairman - Partha Sarathi Mitra	<u>Partha Sarathi Mitra</u>	Date: 15. 6. 17
Guide/Convener - Prakash Mathews	<u>Prakash Mathews</u>	Date: 15/6/17
Co-guide(if any) - NA		Date:
Examiner - Sreerup Raychaudhuri	<u>Sreerup Raychaudhuri</u>	Date: 15-06-2017
Member 1 - Asit Kumar De	<u>Asit Kumar De</u>	Date: 15/6/2017
Member 2 - Munshi Golam Mustafa	<u>Munshi Golam Mustafa</u>	Date: 15/6/2017
Member 3 - Palash Baran Pal	<u>Palash Baran Pal</u>	Date: 15/6/2017

Final approval and acceptance of this thesis is contingent upon the candidate's submission of the final copies of the thesis to HBNI.

I hereby certify that I have read this thesis prepared under my direction and recommend that it may be accepted as fulfilling the thesis requirement.

Date: 15/6/17
Place: KOLKATA

Prakash Mathews
Guide
(P. MATHEW'S)

STATEMENT BY AUTHOR

This dissertation has been submitted in partial fulfillment of requirements for an advanced degree at Homi Bhabha National Institute (HBNI) and is deposited in the Library to be made available to borrowers under rules of the HBNI.

Brief quotations from this dissertation are allowable without special permission, provided that accurate acknowledgement of source is made. Requests for permission for extended quotation from or reproduction of this manuscript in whole or in part may be granted by the Competent Authority of HBNI when in his or her judgement the proposed use of the material is in the interests of scholarship. In all other instances, however, permission must be obtained from the author.

Goutam Das

DECLARATION

I, hereby declare that the investigation presented in the thesis has been carried out by me. The work is original and has not been submitted earlier as a whole or in part for a degree/diploma at this or any other Institution/University.

Goutam Das

LIST OF PUBLICATIONS ARISING FROM THE THESIS

1. *RS resonance in di-final state production at the LHC to NLO+PS accuracy.*

G. Das, P. Mathews, V. Ravindran, S. Seth, **JHEP 1410 (2014) 188** [arXiv:1408.3970]

2. *Neutral Triple Vector Boson Production in Randall-Sundrum Model at the LHC.*

G. Das, P. Mathews, **Phys.Rev. D92 (2015) 9, 094034** [arXiv: 1507.08857]

3. *Two-loop QCD Correction to Massive Spin-2 Resonance $\rightarrow q \bar{q} g$.*

T. Ahmed, **G. Das**, P. Mathews, N. Rana, V. Ravindran, **EPJC (2016) 76: 667**
[arXiv: 1608.05906]

Goutam Das

To My Family and Friends . . .

ACKNOWLEDGEMENTS

First and foremost I would like to express my deepest gratitude to my advisor Prof. Prakash Mathews. His constant motivation, enthusiasm and supervision helped me to complete my journey in Ph.D. and writing this thesis. Working with him has been a very rewarding and joyful experience on a professional and personal level that I will always be grateful for.

I will be always grateful to Prof. V. Ravindran for sharing his knowledge with me and for bearing all my stupid questions. I have enjoyed discussing and learned a lot from you during all these years. I am thankful to you for accepting me as a post-doc. I hope to learn a lot from you in future.

My special thanks to Prof. Fabio Maltoni who gave me the opportunity to work as a Marie Curie fellow. I have learned a lot from you as well as I enjoyed a lot for my stay at Louvain.

The members of my doctoral committee, Prof. Asit De, Prof. Munshi Golam Mustafa and Prof. Palash Baran pal, have generously given their time and expertise to better my work. I thank them for their contribution and their good-natured support. I am thankful to all the members of the Theory and APC divisions for all the support in these long five years. Thanks to Richard and Sangita for all the help related to the clusters.

I am thankful to all my teachers starting from my school age who developed me to be what I am now, particularly I would like to mention my mom, Dipankar sir (my father-in-law), Debananda sir, Haraprasad sir, Bimal sir, Barui sir, Prof. Debabrata Das, Prof. Indrajit Mitra, Prof. Abhijit Bhattacharya, Prof. Anirban Kundu and Prof. Anindya Dutta.

I have enjoyed working with Hua-Sheng Shao, Valentin Hirschi, Celine De-Grande, Taushif Ahmed, Narayan Rana, M. C. Kumar and Satyajit Seth. I am thankful to Manoj Kumar Mandal, David Lopez-Val, Georgious Krintiras, Paolo Torrielli, Marco

Zaro, Olivier Mattelaer for all the moral and academical supports.

My life is incomplete without my friends. I have spent a fun and cheerful time with Prasanta, Apurba, Gourab, Abhijit, Sourav, Mithun, Santanu, Ashis, Rajendra, Abdul, Arka, Debaleen, Sabyasachi, Arijit, Sourav(pong). I will surely miss all of you guys and miss all the food adventures! I am also fortunate to have company of Dipankar (Giri), Dipsikha, Puja, Debasish (vai), Nabarun, Indrani, Dipenda, Gupida, Bishwapratim (Goddi), Wasiur, Indrajit (Laltu) and Saswata. I am thankful to all of you for spending a cheerful time all these years in Kolkata.

I am thankful to Kuntal, Chiranjib and Aritra for spending so much fun time at SINP, discussing a lot of issues! I have been fortunate to have seniors like Aminulda, Dipankarda, Pritibhajan da, Chandrachur da, Amit da, Kamakshya da from whom I have learned a lot. I would like to thank all my colleagues of the Theory division and APC division who have always maintained a charming and enthusiastic work environment, thanks to Augniva, Avik (Boro), Avik (Choto), Chitradekha, Kumar, Mugdha, Naosad, Rohit, Sukannya, Udit, Anshu, Biswajit, Madhurima, Rome, Roopam, Sajad, Susnatadi and Suvankar.

I am thankful to my family- mom, dad, dida, my brothers Buddhadeb and Tathagata, my elder brother Siddhartha and sister-in-law Sanchita for bearing with me all these years, for believing in me. I have no words to acknowledge you mom and dad, the sacrifices that you have made and the dreams that you had to let go, just to give me a shot at achieving mine.

Lastly, I am thankful to my friend, my life-partner, my wife Monalisa. Thanks for accepting me as what I am!! Thanks for tolerating me, keeping patience with me all these years. Thanks for having been my roots during these five years.

Goutam Das

CONTENTS

Synopsis	iv
List of Figures	xiii
List of Tables	xvii
1 Introduction to the Standard Model	1
1.1 A brief history towards the Standard Model	1
1.2 Standard Model in a nutshell	4
1.3 Standard Model as a gauge theory	5
1.3.1 Spontaneous Symmetry Breaking	8
1.3.2 Goldstone theorem: Spontaneous breaking of continuous symmetry	9
1.3.3 Brout-Englert-Higgs mechanism	11
1.3.4 Electroweak unification	12
1.4 Experimental tests on the Standard Model	18
2 Basics of QCD	21
2.1 Introduction	21
2.2 QCD as non-abelian gauge theory	22
2.3 The quark-parton model	24
2.4 Introduction to Color	26
2.4.1 Color Algebra	27
2.5 Running of Coupling	30
2.6 QCD Lagrangian	33
2.7 Structure of NLO calculation	35
2.7.1 Dimensional Regularization	36
2.7.2 Renormalization	37
2.8 Parton Shower	45
2.8.1 Sudakov Form Factor	48

2.9	Matching Parton Shower with Fixed Order	49
2.10	Conclusion	51
3	Gravity Beyond the Standard Model	53
3.1	Introduction	53
3.2	Spin-2 in BSM physics	54
3.3	Extra Dimensions	57
3.3.1	Kaluza-Klein Reduction	60
3.3.2	ADD model	61
3.3.3	RS model	64
3.4	Conclusion	68
4	Triple Neutral gauge bosons production in RS model	71
4.1	Introduction	71
4.2	Merging Matrix Element with Parton Shower	73
4.2.1	CKKW	74
4.2.2	MLM	75
4.2.3	Shower- k_T	76
4.3	Triple Neutral Gauge boson production in RS	77
4.4	Numerical Result	79
4.4.1	$\gamma\gamma\gamma$	82
4.4.2	$\gamma\gamma Z$	84
4.4.3	γZZ	86
4.4.4	ZZZ	87
4.4.5	Event Estimation at the LHC	88
4.5	Conclusions	88
5	Di-final production at NLO+PS accuracy in RS model	91
5.1	Introduction	91
5.2	NLO with PS : MC@NLO	92
5.3	Di-final State Production in RS Model	95
5.4	Numerical Results	99
5.4.1	$\ell^+\ell^-$	103
5.4.2	$\gamma\gamma$	106
5.4.3	ZZ	107
5.4.4	W^+W^-	110
5.5	Search sensitivity at LHC-14	112
5.6	Conclusions	113
6	Two-Loop QCD correction to massive Graviton $\rightarrow q\bar{q}g$	115
6.1	Introduction	115
6.2	Method of Diagram Reduction	119
6.2.1	Reduction to Master Integrals	119
6.3	Spin-2 in association with a jet	125
6.3.1	Effective Action	126

6.3.2	Notations	127
6.3.3	Ultraviolet Renormalization	128
6.3.4	Infrared Factorization	130
6.4	Calculation of Amplitudes	132
6.4.1	Generation of Feynman Diagrams and Simplification	132
6.4.2	Reduction of Tensor Integrals	133
6.4.3	Master Integrals	135
6.5	Results	136
6.6	Conclusion	141
7	Conclusion	143
A		147
A.1	Color algebra	147
A.2	Dirac Algebra in D-dimension	149
A.3	QCD Feynman rules	151
A.3.1	Propagators	151
A.3.2	Vertices	152
B		153
B.1	Feynman rules for SM-graviton interactions	153
C		155
C.1	Harmonic polylogarithms	155
C.2	Two-loop coefficients	158
Bibliography		199

SYNOPSIS

This is an exciting era of particle physics, the most powerful accelerators ever built are now exploring physics at scales and distances never probed before. The theory which describes the physics of elementary particles, known as the Standard Model (SM) has been very successful so far. Over the last few years the predictions of the SM have been well tested in different experiments. The last and the most wanted missing piece of the SM, the Higgs boson, has been discovered at the Large Hadron Collider (LHC) recently in early 2012. With the advancement of the detector technology, it has been possible to study the predictions of the SM to a very high degree of precision at the hadron colliders like Tevatron and LHC. To match the precision of the experimental data, very precise and accurate predictions are needed from theoretical side. Precise predictions for the SM processes are important as the quantum corrections are often very large. In spite of its tremendous success, SM is not complete on many accounts. There are hints from theoretical questions, such as the hierarchy problem as well as experimental observations, such as the neutrino mass, existence of dark matter etc., to expect new physics beyond the SM (BSM). SM successfully describes three forces *viz.* the strong force, the weak force and the electromagnetic force through the gauge group $SU(3)_c \otimes SU(2)_L \otimes U(1)_Y$. $SU(3)_c$ describes the color group of Quantum Chromo Dynamics (QCD) where the interactions of strongly interacting particles (quarks and gluons) are described.

$SU(2)_L \otimes U(1)_Y$ gauge group describes the electro-weak sector of the SM. After the electro-weak symmetry breaking through the Brout-Englert-Higgs mechanism this gives three massive gauge bosons of weak interaction and one massless gauge boson- the photon of electromagnetic interaction. Gravity on the other hand is excluded from the SM. The main reason behind this, is the large scale hierarchy between the gravity scale or Planck scale and the electro-weak scale, commonly known as the hierarchy problem. Many solutions have been proposed over the past few decades to address this issue. Extra-dimensional models which predict the existence of a spin-2 graviton could be an interesting solution which can be tested at the LHC energies.

LHC collides protons with protons at high centre-of-mass energies and luminosities and can scan a large energy range, hence it is an ideal discovery machine. The observables like cross-section, distributions etc., suffer from large QCD radiative corrections. These QCD corrections are needed to take into account for precise prediction of any result. Precise measurements are needed not only to test the SM more accurately, to probe its gauge structure but also any deviation from the SM prediction can lead to potential BSM signature. In addition, they are essential to reduce the theoretical uncertainties arising from the missing higher order quantum corrections through the renormalisation and factorisation scales. This necessitates the calculation of observables to a very high degree of accuracy in the SM and the BSM physics. SM and the BSM scenarios are mostly based on the perturbation theory where the scattering amplitudes are expanded to an infinite series in powers of coupling constant. Since QCD strong coupling constant dominates over the weak and electromagnetic couplings, it has the most pronounced effect at hadron colliders like the LHC. Therefore the perturbative amplitudes are expanded in terms of strong coupling constant to an infinite series. The first term of this series is known as the leading order (LO), next one is the next-to-leading order (NLO) and so on. The LO approximation fails to make accurate predictions of observables at the hadron colliders, whereas a tiny deviation from the SM result could lead to the signature of new

physics. Therefore NLO, NNLO or in some cases even N^3LO corrections are needed to have precise description of observables.

The main theme of this thesis is to explore theoretical and phenomenological aspects of spin-2 particle at the LHC. In particular, the focus is kept on the extra dimensional theories that can incorporate gravity with the SM. Analyses are performed at LO, NLO and NNLO level, employing simulations and computational tools to directly link theories with experimental data.

To address the hierarchy problem Randall and Sundrum proposed a model named as RS model based on the warped 5-dimensional space-time. Only gravity is allowed to explore the full space-time, whereas SM fields are confined to the usual 4-dimensional 3-brane. The effect of gravity on the 3-brane is realized through a tower of Kaluza-Klein (KK) excitations. Due to the exponential warping, the Planck scale could be of the order of the electroweak scale thus solving the hierarchy problem. These KK states couple universally to the SM fields. Their signature could be observed in di-final scattering amplitudes *viz.*, di-photon ($\gamma\gamma$), di-lepton ($\ell^+\ell^-$), di-electro-weak gauge bosons (ZZ, W^+W^-), di-jet etc., as well as in triple neutral gauge bosons productions $\gamma\gamma\gamma, \gamma\gamma Z, \gamma ZZ$ and ZZZ , through the virtual KK graviton exchange. The LO predictions for cross-section or distributions are not adequate to make precise prediction. Therefore NLO corrections have to be considered for these processes. While NLO accuracy is good enough to predict the cross-section to a good accuracy, some kinematical distributions are not well described by the fixed order NLO computation. This happens due to extra QCD radiations from initial or final legs of the scattering amplitudes. Particularly the soft region of some kinematical variables suffers from such extra QCD radiation and gives unreliable distributions which can not be compared to the experimental outputs. For example, the total transverse momenta (P_T) of the di-photon pair in case of di-photon production at fixed order NLO computation diverges in the soft region. These effects of extra soft radiations can be included at the NLO level using a Parton Shower (PS) monte carlo algorithm.

Combining NLO along with PS would make the final state more realistic to be compared with experimental situation. This thesis includes all the important color-neutral di-final state productions $\gamma\gamma$, $\ell^+\ell^-$, ZZ and W^+W^- in the RS model at NLO+PS accuracy. NLO results are matched to the HERWIG PS at the MC@NLO formalism. For the first time the MC@NLO formalism have been used for these processes in the RS model. Different kinematical distributions have been presented along with flexible kinematical cuts. Based on the $\gamma\gamma$ and $\ell^+\ell^-$ channels a search sensitivity is presented for the search of RS KK states at the LHC. All the codes are automatized and are publicly available at the website <http://amcatnlo.cern.ch> to be used in the analysis at the LHC. These codes are flexible enough to be used for any centre-of-mass energy or any cuts which would be useful in the upcoming LHC runs.

This thesis also includes the study of triple neutral gauge boson production processes within the RS model. Triple neutral gauge bosons final states are also phenomenologically important, as they could effectively participate in interesting new physics searches at the TeV scale. In the SM, the triple gauge boson processes serve as potential backgrounds to a number of new physics signals coming from different BSM scenarios. For example, the SM $\gamma\gamma\gamma$ process is a background to single photon production, together with one techni-pion in technicolor model, whereas $\gamma\gamma Z$ process in the SM is a background to the signal with di-photon plus missing energy in gauge-mediated supersymmetric theories. Moreover the tri-gauge final state provides the measurement of quartic gauge couplings, which can be used to test not only the electroweak sector of the SM but also to probe any new physics beyond the SM. In this thesis the neutral triple gauge bosons productions are considered at the LO level merged to one extra jet. In LHC, additional jets are often produced from initial state radiation and can alter the LO predictions for relevant observables. Generally these additional jets are simulated using PS monte carlo. But these QCD radiations in the PS programs are generated in the soft and collinear approximation based on Sudakov form factors. The widely separated and hard emissions are not well-described in the PS

approach, whereas the fixed order tree level amplitudes can provide reliable predictions in the hard region, but it fails in the collinear and soft limits. Therefore it is also essential to take into account the tree level amplitude containing additional jets. Both descriptions have to be combined in an appropriate matching method by avoiding double counting or gaps between samples with different multiplicity. The fixed order merging approach gives a better description of the region of hard and well separated jet, whereas the parton shower takes care of the infrared region correctly. These merged-matched events provide a realistic framework to be compared to the experimental outcomes. This thesis contains the production of neutral triple electroweak gauge bosons in warped extra dimension model at the LHC, *i.e.*, $PP \rightarrow V_1 V_2 V_3 X$, where $V_i = \gamma, Z$ and X denotes some hadronic final states. The study of these processes in the RS scenario bears much importance, as their contributions in searching new physics using the triple gauge boson productions are undeniable, particularly in distinguishing physics arising from the potential BSM candidates like supersymmetry or technicolor. Event samples for $PP \rightarrow V_1 V_2 V_3$ and $PP \rightarrow V_1 V_2 V_3 + j$ have been merged for better prediction of the distributions. Any final state Z bosons are decayed leptonically. It is observed that the addition of the extra jet gives harder distributions compared to the un-merged sample. To make theoretical prediction closer to the experimental situation, the merged events have been matched to PYTHIA6 parton shower. All these computations have been carried out in the MADGRAPH5_AMC@NLO framework which provides a nice interface to merge event samples of different jet-multiplicity and to link to parton shower programs for proper matching. Numerical results of some selective differential distributions for a set of kinematical variables have been presented for the merged samples. Using the $\gamma\gamma\gamma$ channel an estimate of signal over background events has been provided for 100 fb^{-1} luminosity at the LHC.

The processes with missing energy associated with a SM particle can also give significant information about new physics. Particularly, the jet+missing energy is one important process studied at the LHC to look for BSM signature like dark matter in simplified

models. A massive spin-2 particle which goes undetected could be an important dark matter candidate. The NLO correction for this process in large extra dimension model is known to have large QCD corrections, it could be as large as 50% and suffers from large scale uncertainties. Therefore a full NNLO correction is important for such process to have accurate prediction of cross-section and distributions and also to have the scale uncertainties under control. Although the gluon-gluon (gg) initiated sub-process is the dominant contribution at the LHC, as the perturbative order increases, the other sub-processes like the quark-anti-quark ($q\bar{q}$) and the quark(anti-quark)-gluon ($q(\bar{q})g$) begin to contribute significantly. In fact, for full NNLO correction to spin-2+jet, one needs to have the virtual contributions from all the sub-processes, the real-virtual piece and the pure real corrections. This thesis includes the two-loop virtual QCD correction to the process massive spin-2 $\rightarrow q + \bar{q} + g$. After appropriate analytical continuation of the kinematical variables to the respective regions, the result can be used for other scattering sub-processes *viz.* $q + \bar{q} \rightarrow G + g$ and $q(\bar{q}) + g \rightarrow G + q(\bar{q})$, where G denotes the spin-2 field. Feynman diagrammatic approach has been employed to achieve the goal. As expected, the computation becomes very tedious not only due to the presence of a large number of Feynman diagrams but also due to the involvement of a spin-2 tensorial coupling. In-house codes and state-of-the-art techniques, in particular, Integration-by-parts and Lorentz-invariance identities, are employed extensively to execute the computation successfully. The Lorentz, Dirac and color algebra are performed in a systematic way. The bare matrix elements contain ultraviolet (UV) as well as infrared (IR) divergences. The strong coupling constant renormalization is sufficient to make it UV finite. No extra UV renormalization is required for the spin-2 coupling as a consequence of the conserved SM energy-momentum tensor through which it couples universally to the SM fields. The UV finite matrix elements exhibit poles of infrared origin in dimensional regularization. The resulting infrared pole structure ensures the universal factorization property of QCD amplitudes even in the presence of spin-2 field. This serves a crucial check on the correct-

ness of the computation. The result presented here is an important piece, which can be used for full NNLO calculation of real graviton production associated with a jet.

LIST OF FIGURES

1.1	The full particle content of the Standard Model [1].	5
1.2	Spontaneous symmetry breaking.	9
2.1	Running of strong coupling [2].	32
4.1	Typical SM Feynman diagrams for neutral tri-boson production.	77
4.2	Typical RS contribution for neutral tri-boson production. The double-line represents RS graviton. For diagrams with one extra jet one can attach a gluon to any of the initial or internal lines.	78
4.3	Invariant masses of $\gamma\gamma\gamma$ (left) and of two hardest photons (right) for $\gamma\gamma\gamma$ production.	81
4.4	Transverse momentum distributions of hardest photon γ_1 (left) and next hard photon γ_2 (right) for $\gamma\gamma\gamma$ production.	83

4.5	Rapidity distributions of hardest photon (left) and hardest pair (right) for $\gamma\gamma\gamma$ production.	83
4.6	Invariant mass distributions of $\gamma\gamma\mu^+\mu^-$ (left) and $\gamma\gamma$ (right) for $\gamma\gamma Z$ production.	84
4.7	Transverse momentum distributions of hardest photon γ_1 (left) and second hard photon γ_1 (right) for $\gamma\gamma Z$ production.	85
4.8	Invariant mass distributions of $\gamma e^+e^-\mu^+\mu^-$ (left) and $e^+e^-\mu^+\mu^-$ (right) for γZZ production.	86
4.9	Invariant mass distributions of $e^+e^-\mu^+\mu^-\mu^+\mu^-$ (left) and hardest two lepton pairs (right) for ZZZ production.	87
5.1	Born contribution for colorless di-final production through RS graviton. The long-dash line represents the di-final states <i>viz.</i> $\gamma\gamma$, $\ell^+\ell^-$, ZZ and W^+W^-	95
5.2	Virtual corrections for colorless di-final production through RS graviton. The last diagram involves ghost loop (dotted line) appearing due to the use of Feynman Gauge.	95
5.3	Real corrections ($q\bar{q}$ initiated) for colorless difinal production through RS graviton.	96
5.4	Real corrections (qg initiated) for colorless difinal production through RS graviton.	96
5.5	Real corrections (gg initiated) for colorless difinal production through RS graviton.	97

5.6 Transverse momentum distribution of RS contribution, shown in log-log scale at fixed order NLO and NLO+PS for the Drell-Yan (left) and di-photon (right) production processes.	100
5.7 Transverse momentum distribution of RS contribution, shown in log-log scale at fixed order NLO and NLO+PS for the ZZ (left) and W^+W^- (right) production processes.	102
5.8 Invariant mass distribution of the di-lepton pair in Drell-Yan process for RS and SM.	104
5.9 Transverse momentum (left) and rapidity (right) distribution of the di-lepton pair in both RS and SM.	104
5.10 Transverse momentum (left) and rapidity (right) distribution of the positron for the Drell-Yan production process in SM and RS.	105
5.11 Transverse momentum (left) and rapidity (right) distribution of the electron for the Drell-Yan production process in SM and RS.	106
5.12 Invariant mass distribution of the di-photon pair (left) in RS and SM. The right panel shows the separation between two hardest photons in the rapidity-azimuthal angle plane.	107
5.13 Di-photon transverse momentum (left) and rapidity (right) distribution in RS and SM.	108
5.14 Transverse momentum (left) and rapidity (right) distribution of the hardest photon in di-photon production process in RS and SM.	108
5.15 Four-lepton invariant mass ($M^{e^+e^-\mu^+\mu^-}$) distribution for RS and SM coming from the decay products of ZZ process.	109

5.16 Transverse momentum (left) and rapidity (right) distribution of the e^+e^- pair coming from the decay products of ZZ process in RS and SM.	109
5.17 Transverse momentum (left) and rapidity (right) distribution of the $\mu^+\mu^-$ pair coming from ZZ decay for RS and SM.	110
5.18 Invariant mass (left) distribution of the decay products of W^\pm and the total missing E_T distribution (right) in SM and RS.	111
5.19 Transverse momentum distribution of e^+ (left) and μ^- (right) coming from W^\pm decay in RS and SM.	111
6.1 The different components of NNLO calculation (graviton+jet). VV is the double virtual piece which contains two-loop diagrams. RV is the one loop diagrams with one extra radiation. RR is the pure double radiation diagram.	118
6.2 Two-loop massive Sunrise diagram.	121
6.3 Planar and non-planar topologies for the master integrals.	136
B.1 Feynman rules for graviton interaction with scalar, vector and fermions. .	154

LIST OF TABLES

2.1	Masses and electric charges (in the unit of $+e$) of quarks [2]. Top quark mass is given as the pole mass.	26
5.1	Bounds on M_1 for various \bar{c}_0 values at the 14 TeV LHC with integrated luminosity of 50 fb^{-1} at 3-sigma and 5-sigma signal significance, coming from Drell-Yan process.	112
5.2	Bounds on M_1 for various \bar{c}_0 values at the 14 TeV LHC with integrated luminosity of 50 fb^{-1} at 3-sigma and 5-sigma signal significance, coming from di-photon production process.	113

1

INTRODUCTION TO THE STANDARD MODEL

1.1 A brief history towards the Standard Model

We are living in an interesting era of particle physics. We have the largest collider- the Large Hadron Collider running perfectly. It has already given interesting results in it's first phase of run (Run-I). Recently it is running with higher energy (13 TeV) and luminosity with the hope to explore the properties of the elementary particles in more detail and to shed some light into new physics. The theory of elementary particles is described by the Standard Model (SM). The development of the SM started with the advancement of theoretical ideas and experimental verification around 1960s.

Prior to accelerators, Rutherford had shown that atoms have relatively tiny but massive nuclei. By the mid 1930s, protons, neutrons and electrons provided the building blocks of all matter, the understanding of the fundamental structure of matter seemed almost complete. But some questions remained unanswered, like what holds protons together to form a nucleus; or, what causes radioactive decays to produce alpha, beta, gamma rays etc. To study the nucleus and the interactions of neutrons and protons, we needed

accelerators that can make scattering experiments at high energies as well as we needed a well-defined mathematically formulated theory. Around 1960s, accelerator experiments had revealed that the world of particles is very rich, many more particle types similar to protons and neutrons (called baryons) and a whole new family of particles (called mesons) were discovered. Physicists realized that their previous understanding, where all matter is composed of the fundamental protons, neutrons, and electrons, was insufficient to explain the myriad of new particles being discovered. Thus theoretical ideas were developed and experimental findings backed those ideas and played important role to construct and test the theory of elementary particles which is now known as the SM.

In 1948 Feynman [3,4], Schwinger [5,6], Tati and Tomonaga [7,8] created the covariant theory of Quantum Electrodynamics (QED) which describes the interactions of photons with fermions. In subsequent few years, several important theoretical ideas were developed. For example, the Ward identity [9] in QED, the invention of renormalization group by Stukelberg, Gell-Mann *etc. all* [10, 11] in 1953, non-abelian gauge theory by Yang and Mills [12] in 1954, to name a few. In 1957, Salam [13], Lee, Yang [14], Landau [15] proposed the two-component theory of neutrinos *i.e.* neutrinos are either left-handed or right-handed. This was crucial to measure the structure of weak-current. At the same time, experiments showed some interesting results. Parity violation in weak decays was observed [16] by Wu in 1957 motivated by theoretical review [17] by Lee and Yang. Reines and Cowan confirmed [18] the detection of anti-electron neutrino ($\bar{\nu}_e$) in 1959 and so on.

The interplay between theory and experiments continued. In fact around 1960s there was a revolution in the field of particle physics. Feynman, Gell-Mann [19], Marshak and Sudarshan [20] and Sakurai [21] proposed the universal $V-A$ type interaction for the weak force. Gell-Mann [22] and Zweig [23,24] put forth the idea of quarks to explain the newly discovered mesons and baryons from the accelerator experiments. They proposed three quarks *viz. up, down and strange* with spin $1/2$ and electric charges $2/3, -1/3, -1/3$

respectively. At the same year, Glashow and Bjorken [25] proposed a partner for strange quark and named as *charm* quark which was discovered later. In 1961, Goldstone predicted [26] the massless Goldstone bosons if Lagrangian is spontaneously broken. Later in 1964, Higgs [27], Englert and Brout [28], Guralnik, Hagen and Kibble [29] proposed an example of field theory with spontaneous symmetry breaking but no massless Goldstone bosons, rather the degrees of freedom is used to generate masses for vector bosons, which is now known as the *Brout-Englert-Higgs* mechanism. In 1965 Greenberg [30], Han and Nambu [31] introduced the idea of Color charge for the strong interaction. Along the road, Weinberg [32] and Salam [33] proposed in 1967, a theory to unify electromagnetism and weak interaction. The unified theory is known as the electro-weak theory which proposes two charged W^\pm bosons which explains the beta decay along with the existence of one new neutral Z boson.

The linear accelerator of electrons at Stanford took the first clean look inside the atomic nucleus in 1968 and discovered that what we know as protons and neutrons are actually made of *quarks*. This was the first evidence of the quarks as proposed by Gell-Mann and Zweig. Later in 1969 Feynman and Bjorken analyzed the data from SLAC and proposed the Parton model [34–36] to describe the structure of proton although they did not use the name ‘quark’ for the constituents of the proton. They calculated that roughly half of the proton momenta is carried by quark type partons whereas other half is carried by gluons- carrier of the strong force. A quantum theory for the strong interaction is formulated with quarks and gluons similar to the QED. Quarks and gluons are colored charged and thus it is named as *Quantum Chromo Dynamics* (QCD). In 1973 Politzer [37], Gross and Wilczek [38] proved the asymptotic freedom of strong interaction. The electro-weak interactions along with the inclusion of strong force now form the theory which is known as the SM.

Although the theoretical set up for the SM was almost complete by the year 1974,

still the predictions of the SM were yet to confirm. In 1974 a new particle J/ψ was discovered [39, 40] which is a bound state of charm-anti-charm quarks confirming the existence of the charm quark. In 1977 a new quark was discovered through the discovery of a new meson Υ (a bound state of $b\bar{b}$) in Fermilab, which is called *bottom* quark. Since quarks come in pairs, this demands the existence of a sixth quark- the *top* quark. In 1983, the weak bosons *i.e.* W^\pm and Z are discovered in UA1 [41, 42] and UA2 [43, 44] experiments. They predicted the W^\pm mass, $M_W = 81 \pm 5 \text{ GeV}$ which is in good agreement with the SM prediction. In 1995 CDF [45] and D \emptyset [46] experiments found the top quark. Finally the last missing piece of the SM, the Higgs boson has been discovered at the LHC by ATLAS [47] and CMS [48] collaborations in 2012.

1.2 Standard Model in a nutshell

The SM contains 12 elementary fermions which are broken into three classes formed out of quarks and leptons. There are six quarks, oddly named up, down, charm, strange, top and bottom. Out of the leptons, the most familiar is the electron. There are two other charged leptons, called *muon* and *tau*. There are also some electrically neutral leptons called *neutrinos*. Neutrinos originate in nuclear reactions through the weak decays. They rarely interact with matter due to their weak interactions. For each of the 12 regular particles, there are another 12 anti-particles, there are anti-neutrinos, anti-muons, anti-up quarks, and anti-electrons etc. In addition to the particle content, the SM also includes three forces that govern the behavior of matter. These forces are electromagnetism, the strong force and the weak forces. These forces are governed through the exchange particles: photons, gluons, Z bosons, and W^\pm bosons. Gravity is currently not included in the standard model and it will be the subject of discussion in this thesis.

The SM also contains another important particle- the higgs boson, which is the only

scalar particle present in the SM. Higgs Boson is responsible for giving mass to all the SM particles.

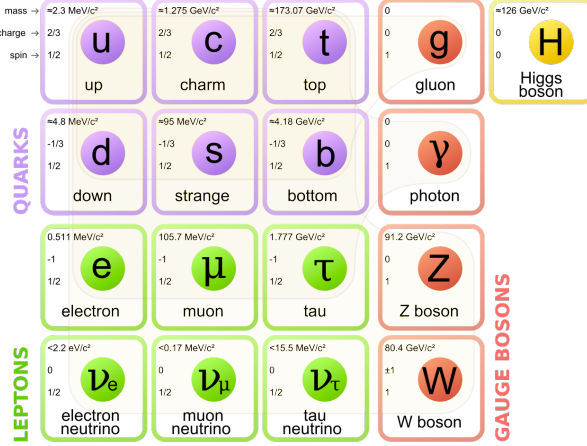


Figure 1.1: The full particle content of the Standard Model [1].

1.3 Standard Model as a gauge theory

Gauge symmetry plays an important role in constructing the Lagrangian for the fundamental forces. The basic idea of gauge symmetry is that if we start with a quantum field theory of a free matter field and promote a global symmetry to a local one, then we automatically get interaction between the matter fields with spin-1 bosons. For example, let us consider the Lagrangian for a massive free fermion,

$$\mathcal{L}_{free} = \bar{\psi}(i\cancel{\partial} - m)\psi \quad (1.1)$$

Now this Lagrangian is invariant under a global phase transformation *i.e.* $U(1)$ symmetry.

$$\psi \rightarrow \psi' = \exp(i\alpha)\psi. \quad (1.2)$$

Let us impose a stronger requirement *i.e.* if we consider a phase transformation which depends on the local space-time,

$$\psi \rightarrow \psi' = \exp(i\alpha(x))\psi \quad (1.3)$$

then the Lagrangian 1.1 is no longer invariant. However the gauge invariance can be restored if we make the following replacement

$$\partial_\mu \rightarrow D_\mu = \partial_\mu + ieA_\mu \quad (1.4)$$

The physical properties must not depend on the phases of the fields. Thus the effect of the local phase change in ψ is compensated by the introduction of a gauge field A_μ . As a result the free Lagrangian now becomes,

$$\begin{aligned} \mathcal{L} &= \bar{\psi}(iD^\dagger - m)\psi \\ &= \bar{\psi}(i\cancel{\partial} - m)\psi - e\bar{\psi}\mathcal{A}(x)\psi \end{aligned} \quad (1.5)$$

Under the gauge transformation, the field A_μ transforms as

$$A'_\mu(x) = A_\mu(x) - \frac{1}{e}\partial_\mu\alpha(x) \quad (1.6)$$

The field strength of the gauge field A_μ is given by

$$F_{\mu\nu} = \partial_\mu A_\nu - \partial_\nu A_\mu \quad (1.7)$$

D_μ in Eq. 1.4 is called the covariant derivative which transforms as

$$D_\mu\psi \rightarrow \exp(i\alpha(x))D_\mu\psi \quad (1.8)$$

This local phase transformation is an example of the Abelian gauge theory. With the inclusion of the kinetic term of the gauge field, the Lagrangian represents QED and is given by

$$\mathcal{L}_{QED} = -\frac{1}{4}F_{\mu\nu}F^{\mu\nu} + \bar{\psi}(i\cancel{D} - m)\psi - e\bar{\psi}\cancel{A}\psi \quad (1.9)$$

The last term in the Lagrangian comes due to the demand of gauge invariance of the theory which describes the interaction of the gauge field with the fermions.

This idea has been generalized to non-abelian cases in order to describe the Weak and Strong forces which corresponds to the $SU(2)_L$ and $SU(3)_c$ gauge groups respectively. We see that to enforce the invariance of the Lagrangian under a local gauge transformation, it is necessary to introduce vector fields. In case of $SU(2)_L$ we will need three such gauge bosons which are actually two W^\pm bosons and one Z boson, whereas in case of $SU(3)_c$ there are eight such colored gluons. The electromagnetic and the weak forces in the SM, are unified through $SU(2)_L \otimes U(1)_Y$ gauge theory. The fermions which are represented as four-component Dirac fields (ψ), can be split, in the chiral representation, into two separate pieces for the left-handed and right-handed fermions:

$$\psi_L = \frac{1 - \gamma_5}{2}\psi, \quad \psi_R = \frac{1 + \gamma_5}{2}\psi \quad (1.10)$$

The left handed charged fermion together with left-handed neutrino form a doublet under the $SU(2)_L$. Similarly, left handed up-type quark and left-handed down-type quark form a quark doublet under the $SU(2)_L$. However, the right-handed fermions (or quarks) transform as singlets under the same gauge group.

1.3.1 Spontaneous Symmetry Breaking

In physics, symmetries play important roles; studying the symmetries of the system (Lagrangian), a lot of information can be obtained. Noether provided an important theorem [49] to particle physics by studying the symmetries and conserved quantities. According to the Noether's theorem, if there is symmetry in a Lagrangian then there must be some conserved quantities. For example, space translation symmetry gives conservation of energy, rotational symmetry gives conservation of angular momentum etc. Actually, Noether's theorem is a consequence of the invariance of both the Lagrangian and the vacuum of the theory. However there could be cases where the Lagrangian is invariant under a symmetry but the vacuum is not. In such a case the symmetry is broken. Let us consider the Lagrangian for a real scalar field,

$$\mathcal{L}_\phi = \frac{1}{2}(\partial_\mu\phi)(\partial^\mu\phi) - \frac{1}{2}\mu^2\phi^2 - \frac{1}{4}\lambda\phi^4 \quad (1.11)$$

with $\lambda > 0$ to guarantee that the Hamiltonian is bounded. This Lagrangian is invariant under the transformation $\phi \rightarrow -\phi$ which is a discrete \mathbb{Z}_2 symmetry to the Lagrangian.

Now if $\mu^2 > 0$, then the vacuum expectation value (VEV) $\langle\phi\rangle_0 = 0$, and thus the vacuum is also invariant under the symmetry. However, if $\mu^2 < 0$, then the vacuum is no longer invariant under the symmetry. In fact the VEV is found to be

$$\langle\phi\rangle_0 = \pm\sqrt{\frac{-\mu^2}{\lambda}} = \pm v \quad (1.12)$$

Clearly the vacuum is degenerate (see Fig. 1.3.1). But once the choice is made for the vacuum, the symmetry is then told to be *spontaneously broken* since the Lagrangian is invariant but the vacuum is not. We can redefine the field to have the vacuum at the

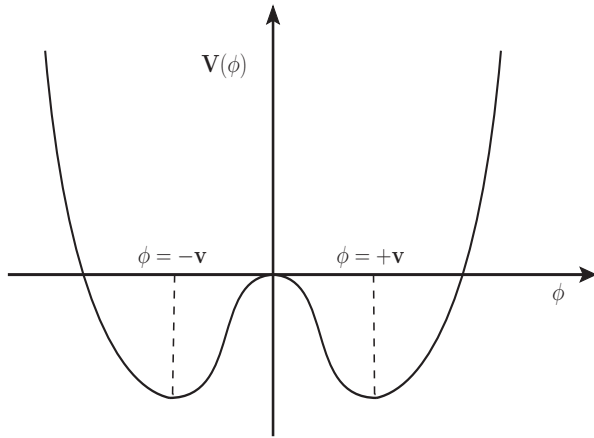


Figure 1.2: Spontaneous symmetry breaking.

origin,

$$h = \phi - v \quad (1.13)$$

for which the VEV $\langle h \rangle = 0$. Therefore the Lagrangian after the spontaneous symmetry breaking (SSB) becomes

$$\mathcal{L} = \frac{1}{2} \partial_\mu h \partial^\mu h - \frac{1}{2} m_h^2 h^2 - \lambda v h^3 - \frac{1}{4} \lambda h^4 + \frac{1}{4} \lambda v^4 \quad (1.14)$$

where $m_h = \sqrt{-2\mu^2}$ is the mass for the scalar field (h). This Lagrangian now loses the original \mathbb{Z}_2 symmetry due to the cubic term in h . Note that the last term has less importance which is a constant contribution to the potential and we always measure energy difference.

1.3.2 Goldstone theorem: Spontaneous breaking of continuous symmetry

Goldstone explained [26] that if the Lagrangian has a continuous symmetry which is spontaneously broken, then there will be massless scalars known as Goldstone bosons.

The number of such Goldstone bosons is equal to the number of broken generators of the symmetry group. Let us now consider a complex scalar doublet Φ given by,

$$\Phi = \frac{1}{\sqrt{2}} \begin{pmatrix} \phi_1 + i \phi_2 \\ \phi_0 + i \phi_3 \end{pmatrix} \quad (1.15)$$

and the scalar potential $V(\Phi)$ is given by,

$$V(\Phi) = \mu^2 \Phi^\dagger \Phi + \lambda (\Phi^\dagger \Phi)^2 \quad (1.16)$$

The Lagrangian thus has a continuous rotational symmetry corresponding to $O(4)$ which has six generators. For the SSB, let us choose the VEV at $\langle \phi_0 \rangle$. So we choose,

$$\langle \phi_0 \rangle = v \quad \text{and} \quad \langle \phi_i \rangle = 0 \quad \text{for } i = 1, 2, 3 \quad (1.17)$$

As before we will redefine the field ϕ_0 to have the vacuum at 0. Thus

$$\phi_0 = h + v \quad (1.18)$$

The potential can be written as

$$V(h, \phi_i) = \frac{1}{2} \mu^2 \left((h + v)^2 + \sum_{i=1}^3 \phi_i^2 \right) + \frac{1}{4} \lambda \left((h + v)^2 + \sum_{i=1}^3 \phi_i^2 \right)^2 \quad (1.19)$$

It is easy to check from Eq. 1.19 that only h field gets mass whereas the other three fields ϕ_i , $i = 1, 2, 3$ are still massless after SSB. These are the Goldstone bosons. After SSB the Lagrangian still has an $O(3)$ symmetry with 3 generators.

1.3.3 Brout-Englert-Higgs mechanism

In gauge theories, the mass of the gauge boson does not come naturally. The explicit introduction of the mass term for the gauge bosons will break the gauge symmetry. However the mass term for the gauge bosons can be generated through SSB by introducing a scalar doublet in a gauge invariant way. Let us consider a real scalar doublet given by,

$$\phi = \begin{pmatrix} \phi^1 \\ \phi^2 \end{pmatrix} \quad (1.20)$$

The kinetic part of the scalar and the gauge field (abelian) is

$$\begin{aligned} \mathcal{L}_{\phi-A} &= (D_\mu \phi)^\dagger (D^\mu \phi) - \frac{1}{4} F_{\mu\nu} F^{\mu\nu} \\ &= [(\partial_\mu - igA_\mu)\phi_1(\partial^\mu + igA^\mu)\phi_1] + [(\partial_\mu - igA_\mu)\phi_2(\partial^\mu + igA^\mu)\phi_2] - \frac{1}{4} F_{\mu\nu} F^{\mu\nu} \end{aligned} \quad (1.21)$$

For SSB we choose $\phi_2 = h + v$. The Lagrangian after SSB thus written as,

$$\mathcal{L}_{\phi-A} = (D_\mu h)^\dagger (D^\mu h) + (D_\mu \phi_1)^\dagger (D^\mu \phi_1) + 2g^2 v^2 A_\mu A^\mu h^2 + g^2 v^2 A_\mu A^\mu - \frac{1}{4} F_{\mu\nu} F^{\mu\nu} \quad (1.22)$$

Note that the gauge field (A_μ) acquires mass term $g^2 v^2 A_\mu A^\mu$ even though the gauge symmetry is unbroken. However there is one ambiguity, the number of degrees of freedom before SSB was four, two corresponding to the massless gauge field and two from the two real scalars. However after SSB, there is one extra degrees of freedom, three from the massive gauge field and two from the real scalars. This can be avoided by choosing a particular gauge. We can rewrite the fields ϕ_1 and ϕ_2 as

$$\phi^+ = \frac{1}{\sqrt{2}}(\phi_1 + i\phi_2) \quad \text{and} \quad \phi^- = \frac{1}{\sqrt{2}}(\phi_1 - i\phi_2) \quad (1.23)$$

When gauge transformation is applied, these fields transform as,

$$\phi^+(x) \rightarrow \exp(i\alpha(x))\phi^+(x) \quad \text{and} \quad \phi^-(x) \rightarrow \exp(-i\alpha(x))\phi^-(x) \quad (1.24)$$

The vacuum-shifted configuration can be written as

$$\phi^+ = \frac{1}{\sqrt{2}}(h + v + i\phi_2) \equiv \frac{1}{\sqrt{2}}(h + v)\exp(i\phi_2/v), \quad (1.25)$$

keeping terms linear in fields. Note that we have the freedom to choose the gauge transformation $\alpha(x)$. Therefore we could choose it such a way that it exactly cancels with the exponential part. Thus we choose,

$$\alpha(x) = -\frac{\phi_2(x)}{v} \quad (1.26)$$

Thus after the gauge transformation there is no ϕ_2 field in the potential and we can remove this degree of freedom. Thus we can say that the gauge boson acquires mass by *eating* the Goldstone boson. This is known as the Brout-Englert-Higgs mechanism ¹.

1.3.4 Electroweak unification

The SM unifies the weak and the electromagnetic forces through the $SU(2)_L \otimes U(1)_Y$ theory, which was first realized by Sheldon Glashow. Later Salam and Weinberg formulated the theory in great detail. Electromagnetic interaction is governed by the exchange of photons. The theory is described by the quantum field theory known as the Quantum Electrodynamics (QED) which is a $U(1)$ gauge theory. It has been successful to describe the Lamb shift in hydrogen, anomalous magnetic moment of electron etc. On the other side the weak force is the theory of $SU(2)$, involves point-like Fermi interaction. It suffers

¹Anderson, Englert and Brout, and Guralnik, Hagen, and Kibble came to the same idea as P. Higgs did at the same time. However in the Higgs's paper, he had predicted (in a single line) that a massive scalar could exist.

from the problem of renormalization. The weak current is charge-changing and identified as the $V - A$ form (vector-axial vector). In early 50's many have attempted to unify the QED with weak-interaction. In 1961 it was Glashow who realized that the weak interaction and QED can be described through the $SU(2)_L \otimes U(1)_Y$ theory with the introduction of heavy bosons.

The weak interaction belongs to the $SU(2)$ gauge group which has three generators corresponding to three gauge bosons. The weak bosons are massive. To generate the masses for these three weak gauge bosons we must choose a complex scalar doublet which gives rise to three Goldstone bosons, to be *eaten up* by the three weak gauge bosons. The weak isospin (T_3) quantum number can be used to label $SU(2)$. Different experiments suggests that weak interaction violates parity, also neutrinos are completely left-handed. These suggested that left handed fermions (ψ_L) are doublet under $SU(2)$ *i.e.* they live in fundamental representation. However the right-handed fermions (ψ_R) are singlet under the $SU(2)$. The gauge group is thus labeled as $SU(2)_L$.

The $U(1)$ in the unbroken theory is not the electromagnetism we know, because the $U(1)$ generator must commute with all the generators of $SU(2)$ which leads to the fact that all component of $SU(2)$ doublet must have same charge under $U(1)$. However we know that this is not true. Thus this $U(1)$ is not electromagnetism. However after the spontaneous symmetry breaking, we need one unbroken sub-group $U(1)_{em}$ to keep the electric charge conserved. Thus

$$SU(2)_L \otimes U(1)_Y \rightarrow U(1)_{em} . \quad (1.27)$$

For the unbroken $U(1)$ however one can choose $2(Q - T_3)$ as the charge since this is same for each component of the $SU(2)$ doublet. Thus the $U(1)$ hypercharge (Y) is defined

through,

$$Q = T_3 + \frac{Y}{2} . \quad (1.28)$$

The unbroken $U(1)$ group is labeled as $U(1)_Y$.

In 1967 Weinberg and Salam have shown that it is possible to incorporate the Brout-Englert-Higgs mechanism to give the masses for the W^\pm and Z bosons. The electro-weak symmetry is broken by the Brout-Englert-Higgs mechanism and thus producing one massless photon, one neutral Z boson and two massive charged W^\pm bosons. However we have to use a complex higgs doublet as given in Eq. 1.15.

The Lagrangian for the $SU(2)_L \otimes U(1)_Y$ is given as

$$\mathcal{L}_{EW} = \bar{L} \not{D} L + \bar{e}_R \not{D}' e_R - \frac{1}{4} W^{\mu\nu i} W_{\mu\nu}^i - \frac{1}{4} B^{\mu\nu} B_{\mu\nu} . \quad (1.29)$$

Here L represents an isospin doublet for the left-handed neutrino and electron. e_R is the right handed electron. g and g' are the couplings in $SU(2)_L$ and $U(1)_Y$ theories respectively. $W_{\mu\nu}, B_{\mu\nu}$ are the corresponding field strength tensors, given by,

$$\begin{aligned} W_{\mu\nu}^i &= \partial_\mu W_\nu^i - \partial_\nu W_\mu^i - g\epsilon_{ijk}W_\mu^j W_\nu^k, \\ B_{\mu\nu} &= \partial_\mu B_\nu - \partial_\nu B_\mu . \end{aligned} \quad (1.30)$$

To maintain the gauge invariance under $SU(2)_L \otimes U(1)_Y$, the covariant derivative is given by

$$D_\mu = \partial_\mu + ig\frac{\tau^i}{2}W_\mu^i + i\frac{g'}{2}YB_\mu \quad (1.31)$$

where τ^i are the Pauli matrices corresponding to the $SU(2)_L$ generators given by,

$$\tau^1 = \begin{pmatrix} 0 & 1 \\ 1 & 0 \end{pmatrix}, \quad \tau^2 = \begin{pmatrix} 0 & -i \\ i & 0 \end{pmatrix}, \quad \tau^3 = \begin{pmatrix} 1 & 0 \\ 0 & -1 \end{pmatrix}.$$

The right handed electron being singlet under the $SU(2)_L$ transforms only under the $U(1)_Y$ group. The covariant derivative is thus given as,

$$D'_\mu = \partial_\mu + i \frac{g'}{2} Y B_\mu . \quad (1.32)$$

Note that $SU(2)_L$ introduces three massless gauge fields W^i , $i = 1, 2, 3$ and $U(1)_Y$ introduces one massless gauge field B_μ .

For the SSB, the Higgs doublet can be parametrized as

$$\Phi = \begin{pmatrix} i\omega^+ \\ (v + h - iz^0)/\sqrt{2} \end{pmatrix}$$

where ω^\pm, z^0 are the Goldstone bosons. These Goldstone bosons will give mass to the W^\pm, Z bosons after the SSB. The scalar Lagrangian can now be written as

$$\mathcal{L} = \left| \left(\partial_\mu + ig \frac{\tau^i}{2} W_\mu^i + i \frac{g'}{2} Y B_\mu \right) \begin{pmatrix} 0 \\ \frac{(v+h)}{\sqrt{2}} \end{pmatrix} \right|^2 - \mu^2 \frac{(v+h)^2}{2} - \lambda \frac{(v+h)^4}{4} \quad (1.33)$$

The two W -bosons (W_μ^\pm) are defined through the linear combination of two fields W^1 and W^2 ,

$$W_\mu^\pm = \frac{1}{\sqrt{2}} (W_\mu^1 \pm W_\mu^2) . \quad (1.34)$$

The mass term of W -bosons found from the 1.33 is given by

$$M_{W^\pm}^2 W_\mu^+ W_\mu^- = \frac{g^2 v^2}{4} W_\mu^+ W_\mu^- \quad (1.35)$$

The remaining two fields W_μ^3 and B_μ can be rotated to get right orthogonal combinations

which actually give the Z -boson and a photon A ,

$$\begin{pmatrix} A_\mu \\ Z_\mu \end{pmatrix} = \begin{pmatrix} \cos \theta_W & \sin \theta_W \\ -\sin \theta_W & \cos \theta_W \end{pmatrix} \begin{pmatrix} B_\mu \\ W_\mu^3 \end{pmatrix} \quad (1.36)$$

where θ_W is the Weinberg angle,

$$\sin \theta_W = \frac{g'}{\sqrt{g^2 + g'^2}} \quad \text{and} \quad \cos \theta_W = \frac{g}{\sqrt{g^2 + g'^2}} . \quad (1.37)$$

Photon still remains massless whereas the mass term of the Z boson as found from Eq. 1.33 using Eq. 1.36 is given by

$$\frac{1}{2} M_Z^2 Z_\mu Z^\mu = \frac{g^2 v^2}{8 \cos^2 \theta_W} Z_\mu Z^\mu . \quad (1.38)$$

Note that the usual electric charge of QED can be found in terms of the gauge couplings as,

$$e = \frac{gg'}{\sqrt{g^2 + g'^2}} . \quad (1.39)$$

The masses of the W^\pm and Z bosons are given by

$$M_{W^\pm} = \frac{g v}{2} \quad \text{and} \quad M_Z = \frac{g v}{2 \cos \theta_W} . \quad (1.40)$$

The coupling constant associated with the $SU(2)_L$ group *i.e.* g can be related to the Fermi constant (G_F) at the low energy limit as,

$$\frac{g}{2\sqrt{2}} = \left(\frac{M_W^2 G_F}{\sqrt{2}} \right)^{1/2} . \quad (1.41)$$

Thus the vacuum expectation value is found to be

$$v = \left(\sqrt{2} G_F \right)^{-1/2} \approx 246 \text{ GeV} \quad (1.42)$$

The value of $\sin^2\theta_W$ as measured in experiment is ~ 0.22 . Thus the SM prediction for the mass of the W^\pm bosons and Z boson are 80.38 GeV and 91.18 GeV respectively. Another important quantity derived is the ρ -parameter defined by

$$\rho = \frac{M_W^2}{\cos^2\theta_W M_Z^2}, \quad (1.43)$$

which actually represents the ratio of the strength of the neutral current and charged current. In SM the value of ρ parameter is 1 at the tree level. The ρ -parameter provides a good test for the SM particularly the isospin structure of the SM.

The masses for the fermions can be generated using the Higgs doublet. The explicit introduction of a fermion mass like $(m_\psi \bar{\psi}\psi)$ violets the $SU(2)_L$ gauge symmetry. However the fermion mass can be introduced into the SM after electroweak symmetry breaking (EWSB) through the Yukawa interaction of Higgs field with the fermions,

$$\mathcal{L}_{yukawa} = -\lambda_e \bar{L}\Phi e_R - \lambda_d \bar{Q}_L\Phi d_R - \lambda_u \bar{Q}_L \tilde{\Phi} u_R + h.c. \quad (1.44)$$

Here λ_f with $f = e, u, d$ are the Yukawa couplings. Q_L is the left-handed iso-spin doublet containing the left-handed up-type and down-type quarks, u_R and d_R are the right-handed up-type and down-type quarks respectively. $\tilde{\Phi}$ is given by,

$$\tilde{\Phi} = i\tau^2 \Phi^*. \quad (1.45)$$

After the SSB, neutrinos remain massless whereas other fermions acquire mass given by,

$$M_f = \frac{y_f v}{\sqrt{2}}. \quad (1.46)$$

The mass of the Higgs boson can also be found from Eq. 1.33 and is given by,

$$M_h = \sqrt{2\lambda}v . \quad (1.47)$$

1.4 Experimental tests on the Standard Model

SM is the most extensively tested theory in physics. Colliders are the best tools for discovering fundamental particles and measuring their properties as predicted by the SM. Colliders like SLC, LEP, PEP-II, KEKB etc. collided e^+e^- at different energies. Some other kind of collider uses only hadrons as colliding particles like Tevatron ($p\bar{p}$) or LHC (pp). On the other hand collider like HERA collided e^- with proton (p) mainly to study deep inelastic scattering. e^+e^- colliders are best used for detailed study due to the clean signature whereas hadron colliders are well-suited for discovery as they can scan over a broad energy range.

The predictions of the SM are verified in these experiments at a very high accuracy. Anomalous magnetic moment of electron ($g - 2$) has been measured to a great precision and it agrees very well with the SM. The electro-weak $V-A$ theory is verified with the discovery of W^\pm [41, 43] and Z bosons [42, 44] in UA1, UA2 experiments. The masses of these bosons are found to be in agreement with the SM. Three generations of matter are found as SM predicts. The properties of the strong force are also precisely measured. Observance of 3-jet events in e^+e^- collision in PETRA collider confirms the existence of gluons [50–53]. The LEP collaborations also used four-jet events to verify the QCD predictions for the three-gluon coupling, a crucial consequence of the non-Abelian nature of QCD which we will discuss in the next chapter.

All the predictions of the SM were verified by 1995 with the discovery of the top quark

by CDF and D \emptyset at Fermilab. The last missing piece was the Higgs boson. The Higgs mass can not be found from the SM since the quartic coupling λ is an unknown parameter. However if we assume the SM to be valid at energy scales all the way up to the Planck scale, then the Higgs mass should lie between 115 and 180 GeV. Finally in 2012, the Higgs boson was found with mass 125.7 ± 0.3 GeV by the ATLAS [47] and CMS [48] collaborations at the LHC. With the discovery of the Higgs boson, all the predictions of the SM are experimentally verified. However SM is not a complete theory of nature as it lacks to explain many observations which are currently beyond the scope of SM and requires new physics beyond the SM.

2

BASICS OF QCD

2.1 Introduction

After the discovery of proton in 1919 by E. Rutherford, it was felt that there should be something stronger force than the electromagnetic force present to bind the positively charged protons together. This binding force must be of short range so that it can confine protons and neutrons within the distance of nuclear size at the same time it should be strong enough to overcome the Coulomb repulsion of positively charged protons. In fact the force through which the protons are bound together inside the nucleus is one of the fundamental forces in the nature and is known as the *strong force*. The theory which describes the strong interaction is known as the quantum chromodynamics (QCD), which is an $SU(3)$ Yang-Mills gauge theory of colored quarks. Similar to the electromagnetic and weak theory, QCD is governed by the exchange of spin-1 vector boson, known as gluons. The dynamics among quarks and gluons leads to the theory of QCD.

Each quark comes in one of three color quantum numbers: red (r), green (g) or blue (b) whereas the anti-quarks are anti-colored ($\bar{r}, \bar{g}, \bar{b}$). In QCD color plays the role of charge and gluons are also colored which is in contrary to the QED. However all the physical states appear as *color-singlet* *i.e.* they are invariant under the rotation in color space.

Different quarks or anti-quarks with different color quantum number pair up to form colorless hadrons. The non-observance of colored object is an important property of QCD and is known as the *color confinement*.

The vacuum of QCD consists of infinite numbers of $q\bar{q}$ pairs as well as virtual gluon pairs as a result of gluon self couplings. Gluons however give negative contribution to the beta function of QCD. This negative contribution dominates over the positive contribution coming from quarks, resulting a negative beta function in case of QCD. The result is that the effective strong coupling becomes small at short distances or at high energies. This property is known as the *asymptotic freedom*. This enables us to use perturbation theory for the strong force at high energies. Contrary to the W^\pm and Z bosons, gluons are massless which is compatible to the experiments.

2.2 QCD as non-abelian gauge theory

The generalization of local gauge transformation to non-abelian groups $SU(N)$ leads to the theory of strong interaction. Let us consider the free Lagrangian for n-plet Dirac field (Ψ) as

$$\mathcal{L}_\Psi = \bar{\Psi}(i\not{\partial} - m_\Psi)\Psi \quad (2.1)$$

where Ψ transforms in the fundamental representation of $SU(N)$,

$$\psi(x) \rightarrow \psi'(x) = U(x)\psi(x) \quad . \quad (2.2)$$

Here $U(x)$ is $n \times n$ unitary matrix dependent on space-time. They are hermitian and traceless since U is special unitary *i.e.*

$$U^\dagger U = 1, \quad \det(U) = 1 \quad . \quad (2.3)$$

Note that as long as U is space-time independent the theory is still gauge invariant, however once it depends on the local space-time the gauge invariance is lost.

To retain the gauge invariance we need to introduce extra gauge fields as we did in the local $U(1)$ case. However unlike the $U(1)$ case where only one gauge field was needed, here we need $N^2 - 1$ gauge fields (A_μ^a) since this is the number of independent parameters in case of $SU(N)$ group. The local gauge transformation thus can be written in the following form,

$$U(x) = \exp(-ig\alpha^a(x)T^a) \approx 1 - ig\alpha^a(x)T^a \in SU(N), \quad (2.4)$$

where T^a , $a = 1, \dots, N^2 - 1$ are the generators of the $SU(N)$ in the fundamental representation.

QCD belongs to non-abelian $SU(3)_c$ gauge, where the subscript c denotes the color quantum number associated to the $SU(3)$ charge. The covariant derivative takes the form

$$D_\mu = \partial_\mu - igT^a A_\mu^a. \quad (2.5)$$

Under the gauge transformation, the fermion fields transform in the fundamental representation of $SU(3)$ as,

$$\psi'_i = \psi_i - ig\alpha^a(x)T_{ij}^a\psi_j. \quad (2.6)$$

The gauge fields (A_μ^a) transform in the adjoint representation as

$$A'_\mu{}^a = A_\mu^a - ig\alpha^b(x)\left[T^{b,(adj)}\right]^{ac}A_\mu^c, \quad (2.7)$$

where $\left[T^{b,(adj)}\right]^{ac} \equiv if^{abc}$ is the generator in the adjoint representation. Here f^{abc} is the anti-symmetric tensor. In case of QCD there are 8 such gauge fields which are actually gluon fields. The field strength of the gluon field is not gauge invariant on its own in

contrast to the QED. The field strength $F_{\mu\nu}^a$ is given by,

$$F_{\mu\nu}^a = \partial_\mu A_\nu^a - \partial_\nu A_\mu^a + g f^{abc} A_\mu^b A_\nu^c \quad (2.8)$$

Note that the last term in the above equation gives the self-interactions among the gluons fields which is absent in abelian gauge theories.

2.3 The quark-parton model

In 1950s-60s experiments revealed a jungle of new hadrons produced through the strong interaction for which a theory was still lacking. Gell-Mann [22] and Zweig [23, 24] independently came forward with a bold idea in 1964. They proposed that the observed mesons and hadrons are bound states of some hypothetical fundamental particles. Gell-Mann named them as quarks. The quark picture is a nice mathematical scheme to classify the hadronic world. At that time three quarks were proposed to describe the observed hadrons. For example, a proton is a bound state of two u-quarks and one d-quark whereas neutron is a bound state of two d-quark and one u-quark. In 1972 Gell-Mann and Fritzsch [54] interpreted that the dynamics of the quarks follow the color gauge group. The interaction of the quarks is described by an octet of massless color gauge bosons, which are called gluons. The resulting gauge theory is similar to the QED, however unlike QED here the gluons interact among themselves. The self interaction among gluons leads to the reduction of the coupling constant with higher energy, *i.e.* the theory is asymptotically free, as discovered in 1972 by 't Hooft (unpublished) and in 1973 by Gross and Wilczek [38] and by David Politzer [37].

By the mid-1970s, almost 10 years after quarks were first proposed, evidence for quark has showed up, that quarks do exist but are locked within the individual hadrons in such

a way that they can never escape as single entities. It is also observed that the quarks can indeed have fractional charges of $+2/3e$ or $-1/3e$ and thus confirmed one of the more surprising predictions of the quark model. Gell-Mann and Zweig required only three quarks to build the particles known in 1964. These quarks are the ones known as up (u), down (d), and strange (s). Later experiments have revealed a number of heavy hadrons which show that there are more than three quarks. In fact, the $SU(3)$ symmetry is part of a larger mathematical symmetry that incorporates quarks of several flavors. There are quarks known as charm (c), bottom (or beauty, b), and top (or truth, t) which were discovered subsequently. Quarks can also change from one flavor to another only by way of the weak force, which is responsible for the decay of these particles.

In 1969 Bjorken predicted that scattering of high-energy electrons on the proton is independent of Q^2 . This phenomenon is called scale invariance (Bjorken scaling) [36]. The experiments at SLAC studied the scattering of high-energy electrons on the proton and found similar behavior. This implied that the proton is built up of point-like constituents. In 1969 R. Feynman proposed the *parton model* to explain the deep-inelastic scattering experiments from SLAC [55, 56]. The idea was similar, that the nucleons are made up of point-like constituents known to be partons which behave as free particles at the high energy. Parton model provides a very simple framework for calculating the e - P scattering cross section in terms of the subprocess cross section involving partons and their probability of finding inside a proton. Bjorken scaling is, however, not exact. In fact, by explicit calculation in various perturbation theories (Adler and Tung 1969 [57, 58], Jackiw and Preparata 1969 [59]) it was found that Bjorken limit and Bjorken scaling can not hold exactly in any realistic interacting quantum field theory; scaling-breaking terms appear invariably order-by-order in perturbative calculations. A mild violation of scaling would be possible in a special class of theories that are asymptotically free, characterized by effective couplings that approach zero as the renormalization scale increases indefinitely.

The experimental discovery of such approximate scaling behavior of the DIS structure functions set off an urgent search in the theoretical physics community for quantum field theories that are asymptotically free which essentially gives birth to QCD. This picture was very successful in describing a large set of data. Later partons are identified with quarks and gluons.

The different quark flavors organize themselves into families under the weak interactions. Up and down form the first family (or generation), charm and strange the second, and top and bottom the third. These three families are basically repetitions of the same pattern *i.e.* same quantum numbers. For example, the electric charges of the up, charm and top quarks are all $2/3$ of that of the proton, and the charges of the down, strange, and bottom are all $-1/3$. They are distinguished by their masses and associated flavor quantum numbers. Quark masses are free parameters in QCD and depend on momentum scale and renormalization scheme. In the $\overline{\text{MS}}$ scheme they are given by,

Quark type	Electric charge	Mass
u	$+2/3$	$\overline{m}_u(2 \text{ GeV}) = 2.2_{-0.4}^{+0.6} \text{ MeV}$
d	$-1/3$	$\overline{m}_d(2 \text{ GeV}) = 4.7_{-0.4}^{+0.5} \text{ MeV}$
s	$-1/3$	$\overline{m}_s(2 \text{ GeV}) = 96_{-4}^{+8} \text{ MeV}$
c	$+2/3$	$\overline{m}_c(\overline{m}_c) = 1.27_{-0.03}^{+0.03} \text{ GeV}$
b	$-1/3$	$\overline{m}_b(\overline{m}_b) = 4.18_{-0.03}^{+0.04} \text{ GeV}$
t	$+2/3$	$m_t = 174.2_{-1.4}^{+1.4} \text{ GeV}$

Table 2.1: Masses and electric charges (in the unit of $+e$) of quarks [2]. Top quark mass is given as the pole mass.

2.4 Introduction to Color

Quark model appeared to be very useful to describe the observed hadrons but it suffered from Fermi-Dirac statistics of the quarks. Contradiction arises with the discovery of Δ^{++}

baryon in 1957. The flavor and spin content of Δ^{++} is given as

$$|\Delta^{++}\rangle = |u_{\uparrow}u_{\uparrow}u_{\uparrow}\rangle \quad (2.9)$$

which appears to be a highly symmetric state whereas Δ^{++} baryon being a fermion should have an anti-symmetric wave function. This puzzle has been addressed in 1965 through the introduction of a new quantum number called *color*. In 1965 O. Greenberg introduced [30] the notion of the color charge as a way out to describe how quarks could coexist inside a hadron without violating the Pauli's exclusion principle. This new quantum number is associated with the group $SU(3)$. Through the introduction of color quantum number, the Δ^{++} baryon can now be written as anti-symmetric wave function by arranging the quarks anti-symmetrically in the color quantum numbers.

$$|\Delta^{++}\rangle = \epsilon^{ijk} |u_{i\uparrow}u_{j\uparrow}u_{k\uparrow}\rangle \quad . \quad (2.10)$$

2.4.1 Color Algebra

Color is associated to the generator (T_{ij}^a) of the $SU(3)_c$ gauge group. T_{ij}^a s are proportional to the Gell-Mann matrices of $SU(3)_c$. The proportional constant is taken to be $1/2$, *i.e.*

$$T_{ij}^a = \frac{1}{2} \lambda_{ij}^a \quad . \quad (2.11)$$

The Gell-Mann matrices (λ_{ij}^a) are given as

$$\lambda^1 = \begin{pmatrix} 0 & 1 & 0 \\ 1 & 0 & 0 \\ 0 & 0 & 0 \end{pmatrix}, \quad \lambda^2 = \begin{pmatrix} 0 & -i & 0 \\ i & 0 & 0 \\ 0 & 0 & 0 \end{pmatrix}, \quad \lambda^3 = \begin{pmatrix} 1 & 0 & 0 \\ 0 & -1 & 0 \\ 0 & 0 & 0 \end{pmatrix}, \quad \lambda^4 = \begin{pmatrix} 0 & 0 & 1 \\ 0 & 0 & 0 \\ 1 & 0 & 0 \end{pmatrix},$$

$$\lambda^5 = \begin{pmatrix} 0 & 0 & -i \\ 0 & 0 & 0 \\ i & 0 & 0 \end{pmatrix}, \quad \lambda^6 = \begin{pmatrix} 0 & 0 & 0 \\ 0 & 0 & 1 \\ 0 & 1 & 0 \end{pmatrix}, \quad \lambda^7 = \begin{pmatrix} 0 & 0 & 0 \\ 0 & 0 & -i \\ 0 & i & 0 \end{pmatrix}, \quad \lambda^8 = \frac{1}{\sqrt{3}} \begin{pmatrix} 1 & 0 & 0 \\ 0 & 1 & 0 \\ 0 & 0 & -2 \end{pmatrix}. \quad (2.12)$$

The generators follow the Lie algebra,

$$[T^a, T^b] = i f^{abc} T^c . \quad (2.13)$$

The structure constants f^{abc} are the adjoint representation of the $SU(3)$ group. They follow the Jacobi identity,

$$f^{abd} f^{cde} + f^{bcd} f^{ade} + f^{cad} f^{bde} = 0 . \quad (2.14)$$

The generators T_{ij}^a are traceless Hermitian matrices *i.e.*

$$\text{Tr}(T^a) = 0, \quad (T^a)^\dagger = T^a . \quad (2.15)$$

The generators (T_{ij}^a) and the anti-symmetric tensors (f^{abc}) follow some algebra, which are needed for calculation of Feynman amplitudes and are listed in the Appendix A.1. The two Casimir in QCD are given by,

$$C_A = N = 3 \quad \text{and} \quad C_F = \frac{N^2 - 1}{2N} = \frac{4}{3} \quad (2.16)$$

It can be very easy to prove that to C_A, C_F are indeed Casimir of $SU(3)_c$ corresponding to the adjoint and fundamental representations respectively (see Appendix A.1).

Color charge however is not directly observed in nature, all the hadrons appear as color neutral entity. This is an important property of QCD known as *color confinement*. Color confinement is a peculiar property of QCD. Its a phenomenon which predicts that

quarks and gluons can not be isolated and thus can not be directly observed as a singular particle. Although there is no mathematical proof of color confinement so far, the naive idea is rather very simple. When a quark-anti-quark pair separates from each other, the gluon field forms a narrow tube of color field between them. Since gluons also carry color charges, the strong force between the quark pair acts constantly, regardless of their distance. Which means the pair can not be separated. However if the external energy is very large, then this procedure becomes less favorable and new quark-anti-quark pairs appear from the vacuum which essentially lead to hadronisation forming new mesons or baryons. The mesons are bound state of quark-anti-quark pair and baryons are bound state of three valence quarks. The Belle and BES III experiments confirmed the existence of tetra-quark bound state which is formed out of four valence quarks. Very recently in 2016, the LHCb experiment of CERN has also confirmed the existence of new tetra-quark bound state [60, 61]. LHCb has also reported the existence of penta quark [62] formed out of five valence quarks. With upcoming runs at the LHC with higher statistics it will be possible to understand the color structure of QCD in great detail.

Direct observation of colored state is not possible by means of color confinement. However evidence can be found from indirect measurements. Particularly, through measuring cross-section for e^+e^- collision producing hadrons in the final state and looking at some kinematical region. For this purpose the following ratio is defined,

$$R_{e^+e^-} = \frac{\sigma(e^+e^- \rightarrow \text{hadrons})}{\sigma(e^+e^- \rightarrow \mu^+\mu^-)} . \quad (2.17)$$

At energies below the Z -peak, the cross-section is dominated by γ^* exchange, so that the ratio $R_{e^+e^-}$ is given by the sum of electric charge squared of the quarks. Therefore,

$$R_{e^+e^-} = N_C \sum_{f=1}^{N_f} Q_f^2 . \quad (2.18)$$

For $N_f = 5$, the value of $R_{e^+e^-} = 11/3$ which agrees very well with the experimental measurements.

2.5 Running of Coupling

Like QED vacuum consists of e^+e^- pairs, the QCD vacuum also consists of infinite virtual $q\bar{q}$ pairs which lead to positive contribution in the beta-function. But unlike the QED, QCD has self-couplings among the gluons, thus the vacuum is also filled with virtual gluon pairs. It turns out that the effective charge thus becomes larger with larger distance, which leads to the negative contribution to the beta function. This phenomena is known as the *anti-screening* effect. As a result of this, the QCD beta function becomes negative and the effective strong coupling becomes small in short distances. The strong coupling (α_s) thus depends on the energy scale. The running of α_s is governed by the beta function,

$$Q^2 \frac{\partial \alpha_s}{\partial Q^2} = \frac{\partial \alpha_s}{\partial \ln Q^2} = \beta(\alpha_s) \quad (2.19)$$

where the beta function is defined as,

$$\begin{aligned} \beta(\alpha_s) &= -\alpha_s^2(b_0 + b_1\alpha_s + b_2\alpha_s^2 + \dots) \\ &= -\alpha_s \sum_{n=0}^{\infty} \beta_n \left(\frac{\alpha_s}{4\pi} \right)^{n+1} \end{aligned} \quad (2.20)$$

where b_0 is the 1-loop coefficient, b_1 is the 2-loop coefficient and so on. These coefficients are calculated upto five loops [63]. b_i 's are given by

$$\begin{aligned} b_0 &= \frac{11C_A - 4T_R n_f}{12\pi} \\ b_1 &= \frac{17C_A^2 - 10T_R C_A n_f - 6T_R C_F n_f}{24\pi^2} . \end{aligned} \quad (2.21)$$

Each term in the expressions for b_0, b_1 etc. can be traced back to the Feynman diagrams. For example, the first term in b_0 corresponds to a gluon loop whereas the second term belongs to a quark loop. Similarly, the first term in b_1 comes from a double gluon loop, whereas the second and the third terms are from mixed gluon-quark loop. It is to be noted that the higher b_i coefficients are renormalization scheme dependent. Solving Eq. 2.19, we can get the expression for strong coupling at one loop as

$$\alpha_s(Q^2) = \frac{\alpha_s(\mu_0^2)}{1 + \beta_0 \alpha_s(\mu_0^2) \ln\left(\frac{Q^2}{\mu_0^2}\right)} + \mathcal{O}(\alpha_s) \quad (2.22)$$

For $Q^2 \gg \mu_0^2$ the strong coupling $\alpha_s \ll 1$, which enables us to use perturbation theory in terms of expansion of the small parameter α_s . However, perturbation theory fails at some lower scale roughly of the order of hadron masses. This reference scale is known as Λ_{QCD} which is roughly 200 MeV. In the figure 2.5 we show the summary of measurements of the strong coupling at various energy scales, which is in agreement with the theoretical prediction for the running of α_s .

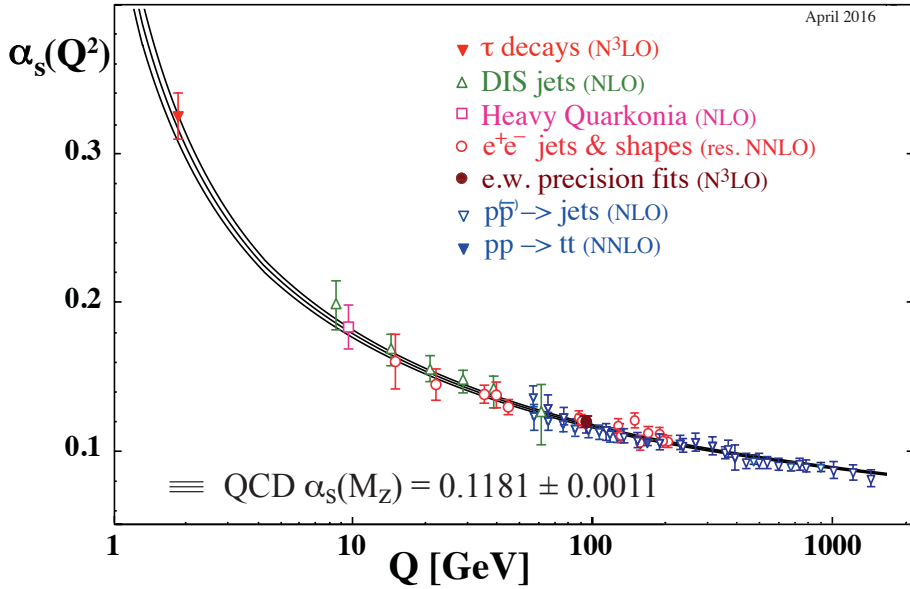


Figure 2.1: Running of strong coupling [2].

Apart from the quark masses, strong coupling is the only free parameter in QCD as well as a fundamental parameter to the SM. This coupling constant is not a constant but it varies with the energy scale for the process involved. The interesting property of the strong coupling is that its strength decreases with energy. This leads to the distinguished phenomena in QCD known as the *asymptotic freedom*. When the quarks are close together, they don't feel each other presence, as if they are free particle. But when they try to move away, they feel the force strongly. The reason behind this is that, the gluons are themselves colored charged. Therefore QCD vacuum also consists of gluon pairs in addition to the quark-anti-quark pairs. Since in case of QCD, the anti-screening effect from gluons wins over the screening effect of the quark-anti-quark pairs, at higher energies, the effective charge becomes weaken. In fact asymptotic freedom is a property of any non-abelian gauge theory. The discovery of asymptotic freedom led to Nobel prize

to Gross, Wilczek and Politzer in 2004.

2.6 QCD Lagrangian

QCD is based on the $SU(3)$ gauge group. It has 8 generators corresponding to 8 different gluons. The gauge invariant QCD Lagrangian is given by

$$\mathcal{L}_{QCD} = \bar{\psi}_q^i \left(i\gamma^\mu (D_\mu)_{ij} - m_q \delta_{ij} \right) \psi_q^j - \frac{1}{4} F_{\mu\nu}^a F^{a\mu\nu} \quad (2.23)$$

where

$$(D_\mu)_{ij} = \delta_{ij} \partial_\mu - ig_s T_{ij}^a A_\mu^a \quad (2.24)$$

is the covariant derivative, ψ_q^i is the quark field with mass m_q and color index i . g_s is the strong coupling constant which is related to α_s by

$$\alpha_s = \frac{g_s^2}{4\pi} . \quad (2.25)$$

A_μ^a is the gluon field with color index a in adjoint representation. $F_{\mu\nu}^a$ is the strength tensor for the gluon field which is given by,

$$F_{\mu\nu}^a = \partial_\mu A_\nu^a - \partial_\nu A_\mu^a + g_s f^{abc} A_\mu^b A_\nu^c \quad (2.26)$$

Note that the last term in the above equation gives the self coupling of gluons which is the reason the theory is non-abelian in nature and differs from QED. The Feynman rules for QCD as extracted from the Lagrangian (Eq. 2.23) is given in Appendix A.3. The Lagrangian 2.23 is invariant under local gauge transformation.

The quantization of QCD gives the quarks and gluon fields, at the same time the

gluon fields A_μ^a contain too many degrees of freedom, some of them are nonphysical, which creates problem in quantising the theory. This invites the introduction of the gauge-fixing (GF) term in the Lagrangian. Several choices are possible although the final result must not depend on the choices. Particularly a clever choice of the gauge fixing term can reduce the complexity of the loop calculation in QCD. We will consider covariant gauge throughout. For this, the effect of the unphysical degrees of freedom are compensated by the auxiliary complex scalar fields with Fermi statics, known as the Fadeev-Popov ghosts.

The choice of GF term is provided by the following

$$\mathcal{L}_{GF} = -\frac{1}{2\xi}(\partial^\mu A_\mu^a)^2 \quad (2.27)$$

where ξ is the gauge parameter. Now with the introduction of the GF term, the Lagrangian must be supported by the ghost term \mathcal{L}_{ghost} given by.

$$\mathcal{L}_{ghost} = -\partial_\mu \bar{\omega}^a (D^\mu \omega^a) \quad (2.28)$$

where ω^a is the ghost field. With the introduction of the GF term the gluon propagator now takes the form as

$$\Delta_{gluon}^{ab} = \delta^{ab} \frac{i}{p^2} \left[-g_{\mu\nu} + (1 - \xi) \frac{p_\mu p_\nu}{p^2} \right] \quad (2.29)$$

$\xi = 1, 0, \infty$ correspond to the Feynman, Landau and Unitary gauge respectively. Throughout this thesis we will use the Feynman gauge for the multiloop calculations. For perturbative calculations of QCD, the total Lagrangian is thus

$$\mathcal{L}_{total} = \mathcal{L}_{QCD} + \mathcal{L}_{GF} + \mathcal{L}_{ghost} \quad (2.30)$$

The second term in \mathcal{L}_{QCD} represents the mass term for the quark fields. This however does not mean that isolated quarks can exist in nature, be accelerated, and have their masses measured by their inertia with respect to acceleration. In fact since quarks are not free (which is a result of color confinement), we do not know exactly what are their masses. Note that quark masses appear in the Lagrangian as $-m_q \bar{\psi}_q \psi_q$ which is not the same as the mass appearing as pole in the quark propagator. Since quark mass appears in the Lagrangian rather directly, it undergoes radiative corrections and it runs *i.e.* it depends on the scale at which it is measured. Usually $\overline{\text{MS}}$ renormalization scheme is used to define the quark masses (see Table 2.3).

2.7 Structure of NLO calculation

With the currently available techniques, it is not possible to compute cross-sections exactly. A powerful technique is to use the perturbative methods. Within the perturbation theory, an observable can be computed as a series expansion in the coupling constant, in the case of QCD, in terms of the strong coupling constant g_s . The first term of this series is known as the leading-order (LO) term, next one is next-to-leading-order (NLO) and so on. Note that the asymptotic property of the QCD is the reason for the weakness of strong coupling g_s at higher energies so that we can use the perturbative technique. In order to fully exploit the quality of the LHC measurements and to discriminate between different new physics models and theoretical calculations we must include quantum corrections at least to NLO. The complexity of traditional NLO approaches grows very fast with the number of scattering particles, and the abundant production of multi-particle final states at the LHC poses new challenges.

The scattering cross-section at the hadron collider for the production of a final state

X is given by,

$$d\sigma(pp \rightarrow X) = \sum_{ij} \int dx_1 dx_2 f_i^{(p)}(x_1, \mu_F) f_j^{(p)}(x_2, \mu_F) d\hat{\sigma}_{ij \rightarrow X}(x_1, x_2, Q^2, \mu_F) \quad (2.31)$$

where ij are the initial state partons. $f_i^{(p)}(x_1, \mu_F) f_j^{(p)}(x_2, \mu_F)$ are the parton distribution functions (PDF), x_1, x_2 are the momentum fraction carried by partons, μ_F is the factorization scale which is introduced to separate collinear singularities appearing in the initial legs. Thus any collinear singularities from the initial state are factored out from the hard cross-section and absorbed in the bare PDFs. The evolution of PDFs can be calculated perturbatively from DGLAP equations 2.60. Here $d\hat{\sigma}_{ij \rightarrow X}(x_1, x_2, Q^2, \mu_F)$ is the hard scattering cross-section for the process $ij \rightarrow X$ at the scale Q^2 . $d\hat{\sigma}_{ij \rightarrow X}(x_1, x_2, Q^2, \mu_F)$ can be calculated perturbatively as,

$$\begin{aligned} d\hat{\sigma}_{ij \rightarrow X}(Q^2, \mu_F) &= \alpha_s^k(\mu_F) \sum_{n=0}^{\infty} d\hat{\sigma}_{ij}^{(n)}(Q^2, \mu_F, \mu_R) \alpha_s^n(\mu_R) \\ &= d\hat{\sigma}_{ij}^{LO} + d\hat{\sigma}_{ij}^{NLO} + \dots \end{aligned} \quad (2.32)$$

The $n = 0$ term in Eq. 2.32 is the LO term ($d\hat{\sigma}_{ij}^{LO}$), $n = 1$ is the NLO ($d\hat{\sigma}_{ij}^{NLO}$) and so on. Here $\alpha_s^k(\mu_F)$ in front of the sum at the right hand side denotes any α_s dependence in the process at the LO itself. Note that at each order of the α_s , both the hard cross-section and the PDFs have a residual factorization scale (μ_F) dependence. The hard cross-section also suffers from the UV divergences at higher orders which can be renormalized at the cost of dependence on a renormalization scale μ_R .

2.7.1 Dimensional Regularization

Dimensional regularization (DR) is one of the popular as well as powerful method for regularizing the multiloop Feynman diagrams. DR is easy to implement and it preserves

Poincare invariance as well as the gauge invariance which is important in proving the renormalizability of the theory. The main idea in DR is to shift the theory to a higher space-time dimension D . Therefore all the calculations, for example, Lorentz contraction, Dirac algebra etc. are performed in the D -dimension. The divergences present in the calculation then appear as poles when we get back to the physical 4-dimension.

The idea was implemented by 't Hooft and Veltman in 1972 to regularize the UV divergences. The poles are manifested in terms of powers of ϵ when the result is expanded in terms of $D - 4 \equiv -2\epsilon$. An important feature of the DR is that it regulates the infrared singularities as well. Note that the UV divergences occur when the loop momenta $k \rightarrow \infty$, thus in general the UV behavior becomes better if $\epsilon > 0$, whereas the IR behavior becomes better if one chooses $\epsilon < 0$. In practice however both the choices can not be applied at the same time. What is done is that, first the IR divergences are regulated in some other way for example considering a small mass of the all massless particles. Next assuming $\epsilon > 0$ one obtains a well defined UV convergent result. Next the auxiliary IR regulator is removed and the IR poles appear as powers of $1/\epsilon$.

2.7.2 Renormalization

QCD is a renormalizable theory meaning all the divergences coming from the loop corrections of Green's functions constructed from the fundamental fields of the Lagrangian can be rendered finite through the redefinition of the fields and parameters appearing in the Lagrangian. The bare quantities (fields, couplings, masses) lead to the divergent Green's

functions. Thus the renormalized quantities are defined as

$$\begin{aligned}\hat{\psi} &= Z_2^{1/2} \psi, & \hat{m} &= Z_m m, \\ \hat{A}_\mu^a &= Z_3^{1/2} A_\mu^a, & \hat{g}_s &= Z_g^{1/2} g_s, \\ \hat{\omega}^a &= \tilde{Z}_3^{1/2} \omega^a, & \hat{\xi} &= Z_3^{1/2} \xi\end{aligned}\tag{2.33}$$

Here the quantities at the left hand side of these equations *i.e.* $\hat{\psi}, \hat{A}_\mu^a, \hat{\xi}, \hat{\omega}^a, \hat{m}, \hat{g}_s$, are the bare quantities appearing in the QCD Lagrangian, whereas the renormalized quantities are $\psi, A_\mu^a, \xi, \omega^a, m, g_s$ appearing on the right hand side of the equations. Z_2, Z_3 and \tilde{Z}_3 are the quark, gluon and ghost field renormalization constants respectively. Z_m and Z_g are called the mass renormalization and coupling constant renormalization constant respectively. Note that the original Lagrangian can be written in terms of renormalized quantities plus counter-term Lagrangian which contains the renormalized fields, masses, coupling constant as well as the renormalization constants, *i.e.*

$$\mathcal{L}(\hat{\psi}, \hat{A}_\mu^a, \hat{\xi}, \hat{\omega}^a, \hat{m}, \hat{g}_s) = \mathcal{L}_R(\psi, A_\mu^a, \xi, \omega^a, m, g_s) + \mathcal{L}_c(\psi, A_\mu^a, \xi, \omega^a, m, g_s, Z_2, Z_3, \tilde{Z}_3, Z_m, Z_g)\tag{2.34}$$

It is obvious that through the redefinition of the fields, masses and coupling constants, the renormalization constants Z_i 's become infinite.

In general an overall UV divergence of a l -loop amplitude is a l -degree polynomial in ϵ^{-1} , and can be written as,

$$\frac{C_l}{\epsilon^l} + \frac{C_{l-1}}{\epsilon^{l-1}} + \cdots + \frac{C_1}{\epsilon} + C_0\tag{2.35}$$

where C_i 's are some constants. Now to cancel such divergences we need a l -loop order

counter-term which has similar form,

$$\delta_Z^l \approx \frac{C_l}{\epsilon^l} + \frac{C_{l-1}}{\epsilon^{l-1}} + \cdots + \frac{C_1}{\epsilon} + C'_0 \quad (2.36)$$

Note that, in the counter term, the coefficients C_i 's are completely determined by the UV divergence of the l -loop diagram except for the finite term C'_0 . In fact the value of the finite term follows from the renormalization scheme chosen. We will work in the $\overline{\text{MS}}$ scheme where the constant $(-\gamma_E + \log(4\pi))$ accompanied with $1/\epsilon$ pole is removed by the definition,

$$\frac{1}{\bar{\epsilon}} \equiv \frac{1}{\epsilon} - \gamma_E + \log(4\pi) \quad (2.37)$$

The differential cross-section at the NLO level is given by,

$$d\hat{\sigma}^{NLO} = \left[B(\Phi_B) + \alpha_s V(\Phi_B) \right] d\Phi_B + \alpha_s R(\Phi_{B+1}) d\Phi_{B+1} \quad (2.38)$$

where $B(\Phi_B)$ is the tree-level or the Born contribution, $V(\Phi_B)$ is the order α_s one-loop virtual correction, both of these contribution have phase-space integration ($d\Phi_B$) same as the tree-level. The last term $R(\Phi_{B+1})$ is the order α_s real emission with one extra phase-space integration due to extra emission.

The virtual and the real contributions both separately contain singularities of infrared nature, only their sum is finite and free from any divergences which is possible due to the Kinoshita-Lee-Nauenberg (KLN) theorem [64, 65]. In practice one needs a regularization scheme like infrared cut-off or dimensional regularization to explicitly express the singularities. Usually the cancellation of these infrared singularities is dealt with a subtraction method, in which a counter term is introduced which has similar infrared structure as the real emission. Therefore including the subtraction term, the differential cross-section is

written as,

$$\begin{aligned} d\hat{\sigma}^{NLO} = & \left[B(\Phi_B) + \alpha_s V(\Phi_B) + \alpha_s \int S(\Phi_1) d\Phi_1 \right] d\Phi_B \\ & + \left[\alpha_s R(\Phi_{B+1}) - \alpha_s S(\Phi_1) \right] d\Phi_{B+1} \end{aligned} \quad (2.39)$$

The universality of soft and the collinear divergences enables us to write this subtraction term as follows,

$$S(\Phi_1) = B(\Phi_B) \otimes \mathcal{U} \quad (2.40)$$

where \mathcal{U} is universal in nature and analytically known in DR. The real emission terms can be written as the singular $R(\Phi_1)^s$ and the non-singular $R(\Phi_1)^{ns}$ terms as,

$$R(\Phi_1) = R^s(\Phi_1) + R^{ns}(\Phi_1) \quad (2.41)$$

Therefore the differential NLO cross-section can be written as,

$$\begin{aligned} d\hat{\sigma}^{NLO} = & \left[B(\Phi_B) + \alpha_s V(\Phi_B) + \alpha_s \int S(\Phi_1) d\Phi_1 \right] d\Phi_B \\ & + \left[\alpha_s R^s(\Phi_{B+1}) - \alpha_s S(\Phi_1) \right] d\Phi_{B+1} + \alpha_s R^{ns}(\Phi_1) d\Phi_{B+1} \end{aligned} \quad (2.42)$$

With the introduction of proper subtraction terms, it is now possible to calculate each term in the square brackets at the right hand side of Eq. 2.42 numerically.

Virtual calculation

The difficulties in the virtual loop calculation comes due to the tensorial integrand appearing in the Feynman integrals. There are several methods to perform these Feynman integrals for example Passarino-Veltmann reduction, OPP reduction etc. Most of these methods rely on the reduction of these tensorial integrals into scalar integrals which are rather easier to compute. Different methods are available based on reduction at the integral level for example Passarino-Veltman reduction (PV) [66], or reduction at the

integrand level for example OPP reduction (OPP) [67, 68].

At one-loop, the structure of the tensorial integral has a general structure in d -dimensions,

$$I_n^{\mu_1 \dots \mu_r} = \int \frac{d^d l}{(2\pi)^d} \frac{l^{\mu_1} \dots l^{\mu_r}}{((l - q_1)^2 + i\varepsilon) \dots ((l - q_n)^2 + i\varepsilon)} \quad (2.43)$$

where $q_1 = p_1$, $q_2 = p_1 + p_2, \dots$, $q_n = p_1 + p_2 + \dots + p_n$. r is the rank of the tensor integrals which has n propagators.

To evaluate the tensor integral, first one has to expand the integral in a basis of external momenta. For $r > 2$ one has to also consider the metric tensor $g_{\mu\nu}$ in the basis. Next thing is to contract the expansion with each basis vectors. After this there will be scalar products which are then converted in terms of the propagators. Finally the set of equations expressed in terms of the expansion coefficients are found in terms of the lower rank tensor integrals. The tensor integrals coefficients are proportional to inverse powers of the Gram determinant ($\det(p_i \cdot p_j)$), where p_i, p_j are independent external momenta. All loop integrals can be reduced to basic “scalar” integrals A_0, B_0, C_0, D_0 which don’t have any Lorentz index on the numerator. The basic integral with the help of which PV integrals can be computed is of the form,

$$I_d^{(n)} = \int d^d q \frac{1}{(q^2 - m^2 + i\epsilon)^n} \quad (2.44)$$

which is converging provided $m^2 > 0$ and $d < 2n$. In fact the integral of this type has the solution of the following form,

$$I_d^{(n)} = i(-1)^n \pi^{d/2} \frac{\Gamma(n - d/2)}{\Gamma(n)} (m^2 - i\epsilon)^{d/2-n} \quad (2.45)$$

However PV reduction can be problematic while considering high rank tensor integrals with more external particles, as Gram determinant might vanish and leads to numerical

instability. This can be avoided for example by eliminating such integrals at the amplitude level or by putting numerical cuts etc. Another numerically well-fitted procedure is to adopt the OPP reduction at the integrand level [67, 68]. The method is based on idea of expressing the integrand of the one-loop amplitude in terms of the propagators that depends on the integration momentum.

Real Correction

The IR singularities from the real emission can be extracted from different methods. For example, phase space slicing method, subtraction method etc. These two methods can be best described using a toy example in one dimension. Let us consider the sum of the real and virtual pieces as

$$\sigma = \int_0^1 \frac{dx}{x^{1+\epsilon}} F(x) + \frac{F(0)}{\epsilon} \quad (2.46)$$

Note that the virtual piece has pole structure of $1/\epsilon$ kind, we expect similar pole structure from the real part after the phase space integration. Now in phase space slicing method, the phase space is sliced into two parts: one is singularity free region and other is problematic singular region. This separation is done by introducing a scale δ . Thus $0 < x < \delta$ is the divergent region, with δ small. As long as δ is very small, we assume that $F(x) \approx F(0)$. Therefore the cross-section can be approximated as,

$$\sigma = \int_{\delta}^1 \frac{dx}{x^{1+\epsilon}} F(x) + \int_0^{\delta} \frac{dx}{x^{1+\epsilon}} F(0) + \frac{F(0)}{\epsilon} \quad (2.47)$$

The first term is safe from divergences and thus the limit $\epsilon \rightarrow 0$ can be taken. Performing the integration, it can be very easily seen that the poles are canceled and the result is given as,

$$\sigma = \int_{\delta}^1 \frac{dx}{x^1} F(x) + F(0) \ln(\delta) + \mathcal{O}(\delta) \quad (2.48)$$

Note that in the phase space slicing method, there is residual dependency on the scale δ chosen to slice the phase space. In the practical method however, the real phase space is decomposed into soft and hard regions. The hard region is further decomposed into hard collinear and hard non-collinear region. Correspondingly two scales δ_s, δ_c are introduced which define the boundary of these regions.

In the subtraction method, however, no such scale is chosen to slice the phase space, instead a counter-term is added and subtracted to the virtual and to the real pieces respectively. This subtraction term must have the same pole structure as the virtual (or real). With the example of our toy model, let us choose a subtraction term $F(0)/x^{1+\epsilon}$. Therefore the cross-section can be written as,

$$\sigma = \int_0^1 \frac{dx}{x^{1+\epsilon}} [F(x) - F(0)] + \int_0^1 \frac{dx}{x^{1+\epsilon}} F(0) + \frac{F(0)}{\epsilon} \quad (2.49)$$

Since the divergent term is added and subtracted to the virtual and real terms respectively, therefore the divergences in those terms separately cancel and the cross-section finally takes the form (taking the limit $\epsilon \rightarrow 0$),

$$\sigma = \int_0^1 \frac{dx}{x^1} [F(x) - F(0)] \quad (2.50)$$

Note that unlike the phase space slicing method there is no residual δ scale dependence in the subtraction method. This makes it perfect for the implementation in monte carlo programs. Next we will discuss on the FKS subtraction scheme which is being used in the subsequent chapters.

FKS subtraction

The central idea behind the FKS subtraction [69, 70] formalism is that in the integration of the real emission matrix elements, one effectively defines partonic processes with at most one soft and one collinear singularities. As a result the subtraction structure becomes much simpler than that of the original matrix elements. The real contribution to the cross-section at NLO level can be written as the product of the matrix element squared for the real emission and the phase space for the emission,

$$d\sigma_R = |M^{(n+1)}|^2 d\Phi_{B+1} \quad (2.51)$$

One introduces a set of positive definite terms, called S-functions S_{ij} to partition the phase space such that

$$\sum_{\{ij\}} S_{ij} = 1 \quad (2.52)$$

For a given pair (ij) all the S-functions vanish in the soft and the collinear limit except for the cases where $k_i \rightarrow 0$ and $k_i \parallel k_j$. Thus the real emission term in FKS formalism can be written as,

$$d\sigma_R = \sum_{ij} S_{ij} |M^{(n+1)}|^2 d\Phi_{B+1} \quad (2.53)$$

Note that the sum in the above equation gives finite contribution in all over the phase space except the cases where $i \rightarrow 0$ or i, j become collinear. These singularities are subtracted through the following substitution,

$$S_{ij} |M^{(n+1)}|^2 d\Phi_{B+1} \rightarrow \left(\frac{1}{E_i} \right)_+ \left(\frac{1}{1 - \cos \theta_{ij}} \right)_+ \left(E_i (1 - \cos \theta_{ij}) |M^{(n+1)}|^2 \right) d\Phi_{B+1} \quad (2.54)$$

The two plus prescriptions in Eq. 2.54 is that of constructing the linear combination,

$$|M^{(n+1)}|^2 - |M^{(n+1)}|^2 \Big|_{E_i \rightarrow 0} - |M^{(n+1)}|^2 \Big|_{\theta_{ij} \rightarrow 0} + |M^{(n+1)}|^2 \Big|_{(E_i, \theta_{ij}) \rightarrow (0,0)} \quad (2.55)$$

The second, third and the last terms are respectively the soft, collinear and soft-collinear terms respectively. Each term in the sum in Eq. 2.53 must have well-defined soft, collinear, and soft-collinear limits, for each such individual term a linear combination identical to that of Eq. 2.55 can be defined, which is finite locally in the phase space. Eq. 2.54 defines the subtraction scheme in FKS formalism.

2.8 Parton Shower

While a fixed order result is essential to describe the rate precisely, in practice the distributions are not correctly described for jet exclusive observable. While the infrared divergences are canceled in a fixed order calculation, it leaves behind large logarithms due to which some observables for example P_T of lepton-pair in Drell-Yan production are not correctly described in the infrared region. The parton shower (PS) approximation takes care of these enhanced contributions from large logarithms in the soft and collinear region. In the collinear limit, the $n + 1$ body cross-section factorizes in terms of n body cross-section and a universal splitting kernel.

$$d\hat{\sigma}_{n+1}(\Phi_{n+1}) = d\hat{\sigma}_n(\Phi_n)P(\Phi_1)d\Phi_1 \quad (2.56)$$

The 1-particle phase-space can be parametrized in terms of hardness q of emitted parton, fraction of longitudinal momentum z of the emitter and the azimuthal angle ϕ of splitting.

$$P(\Phi_1)d\Phi_1 \approx \frac{\alpha_s(q)}{2\pi} \frac{dq^2}{q^2} P(z, \phi) dz \frac{d\phi}{2\pi} \quad (2.57)$$

where, $P(z, \phi)$'s when averaged over the azimuthal angle gives the universal splitting functions $P(z)$. Note that the variable q^2 , also known as the *virtuality* serves as the evolution variable of the PS. There are many other choices for the evolution variable, like

the opening angle θ or p_T of the daughter particle, all are equivalent *i.e.*

$$\frac{dq^2}{q^2} \equiv \frac{dp_T^2}{p_T^2} \equiv \frac{d\theta^2}{\theta^2} \quad (2.58)$$

Different PS generator chooses different evolution variables. For example in Pythia-6 it is virtuality q^2 , in Pythia-8 and in Pythia-6.4 it is p_T , whereas in Herwig the evolution variable is θ . The splitting $i \rightarrow j + k$ can not take place unless the partons are off-shell. The dominant contribution comes from the configuration where all the partons are strongly ordered in virtuality *i.e.* the partons nearest to the hard subprocess are farthest from its mass-shell and virtuality decreases as the parton shower evolves down to the hadronization scale Q_0^2 which is roughly of the order of 1 GeV.

In the collinear limit, the scattering amplitude can be factorized. Using this property, it is possible to derive the DGLAP equations which determines the behavior of the PDFs in the collinear limit with the changing factorization scales,

$$\mu_F^2 \frac{df_a(x, \mu_F^2)}{d\mu_F^2} = \sum_{b \in \{q, g\}} \int_x^1 \frac{dz}{z} \frac{\alpha_2}{2\pi} \hat{P}_{ba}(z) f_b(x/z, \mu_F^2) \quad (2.59)$$

Here $\hat{P}_{ba}(z)$ describes the splitting of parton a into b . They are known as the regularized Alterelli-Parisi splitting functions and are given by,

$$\begin{aligned} \hat{P}_{qq}(z) &= C_F \left[\frac{1+z^2}{(1-z)_+} + \frac{3}{2} \delta(1-z) \right] + \mathcal{O}(\alpha_s) \\ \hat{P}_{gq}(z) &= C_F \left[\frac{1+(1-z)^2}{z} \right] + \mathcal{O}(\alpha_s) \\ \hat{P}_{qg}(z) &= T_R \left[z^2 + (1-z)^2 \right] + \mathcal{O}(\alpha_s) \\ \hat{P}_{gg}(z) &= 2C_A \left[\frac{z}{(1-z)_+} + \frac{1-z}{z} + z(1-z) \right] + \delta(1-z) \left(\frac{11}{6}C_A - \frac{2}{3}n_f T_R \right) + \mathcal{O}(\alpha_s) \end{aligned} \quad (2.60)$$

The Alterelli-Parisi splitting functions are known to NNLO [71–74]. In addition to the

collinear branching, the soft emissions also give logarithmic enhancement. Note that the soft gluon emission gives a color factor times a universal spin-independent factor (\mathcal{F}_{soft}) at the amplitude level,

$$\mathcal{F}_{soft} = \frac{p \cdot \epsilon}{p \cdot q} \quad (2.61)$$

where a soft gluon with momenta q_μ and polarization ϵ_μ is emitted from a parton of momenta p_μ . It is worth noting that there is however no soft enhancement from the internal lines, since the associated denominator factor does not diverge at the soft limit. Therefore soft emission happens only from the external partons and thus at the level of cross-section the soft-enhancement is given by,

$$d\hat{\sigma}_{n+1} = d\hat{\sigma}_n \frac{\alpha_s}{2\pi} \frac{d\omega}{\omega} \frac{d\Omega}{2\pi} \sum_{\{i,j\}} C_{ij} W_{ij} \quad (2.62)$$

Here ω is the energy of the emitted gluon in the solid angle Ω . C_{ij} is the color factor. Note that this is summed over since enhancement at the amplitude level implies cross-section is summed over all pairs of external lines $\{i,j\}$. W_{ij} in the above equation is known as the radiation function, and for massless partons it is given by,

$$W_{ij} = \frac{1 - \cos \theta_{ij}}{(1 - \cos \theta_{iq})(1 - \cos \theta_{jq})} \quad (2.63)$$

Soft emission in any gauge theory is always angular ordered [75]. This can be seen by rewriting the Eq. 2.63 in the following form,

$$W_{ij} = W_{ij}^i + W_{ij}^j \quad (2.64)$$

where

$$\begin{aligned} W_{ij}^i &\equiv \frac{1}{2(1 - \cos \theta_{iq})} \left[1 + \frac{\cos \theta_{iq} - \cos \theta_{ij}}{\cos \theta_{jq}} \right] \\ W_{ij}^j &\equiv \frac{1}{2(1 - \cos \theta_{jq})} \left[1 + \frac{\cos \theta_{jq} - \cos \theta_{ij}}{\cos \theta_{iq}} \right] \end{aligned} \quad (2.65)$$

Now writing the angular integration as $d\Omega = d\cos \theta_{iq} d\phi_{iq}$ and performing integration over W_{ij}^i , it can be shown that

$$\begin{aligned} \int_0^{2\pi} \frac{d\phi_{iq}}{2\pi} W_{ij}^i &= \frac{1}{1 - \cos \theta_{iq}} && \text{when } \theta_{iq} < \theta_{ij} \\ &= 0 && \text{otherwise} \end{aligned} \quad (2.66)$$

Thus the contribution of W_{ij}^i is confined into a cone centered on the direction of i , extending to the direction to j . Similar happens when same calculation is performed on W_{ij}^j . In fact the property of angular order is common to all gauge theory. In QED it is known as the Chudakov effect, which suppresses the soft radiation from the e^+e^- pair. If a soft photon is emitted from either of the e^+ or e^- at an angle $\theta_\gamma > \theta_{e^+e^-}$, then this radiation is heavily suppressed as the photon at this large angle can not resolve e^+ and e^- separately.

2.8.1 Sudakov Form Factor

While the collinear contributions are taken into account through the Eq. 2.56, the unsolvable and virtual contributions are also considered through the Sudakov form factor (SFF). SFF gives the probability of a non-splitting between the evolution from q_1^2 to q_2^2 and is given by,

$$\Delta_i(q_1^2, q_2^2) = \exp \left(- \int_{q_2^2}^{q_1^2} \frac{dq^2}{q^2} \frac{\alpha_s(q)}{2\pi} \int_{Q_0^2/q^2}^{1-Q_0^2/q^2} dz \int_0^{2\pi} \frac{d\phi}{2\pi} P_{ji}(z, \phi) \right) \quad (2.67)$$

Parton shower develops from off-shell quarks or gluons from initial as well as final legs of the scattering amplitudes. For a final state shower *i.e.* parton shower starts from the colored final leg and with high energy and a large time-like virtuality scale Q^2 set by the hard subprocess. The parton thus continues to lose energy and ends up

with virtually below Q_0^2 where the parton shower stops and hadronization starts. For initial state parton shower, the parton coming from each of hadrons starts at a high energy but low virtuality. In contrast to final-state showers, initial-state ones are space-like. Partons are then evolved to a higher space-like virtuality by emitting partons and losing energy. The showering of these partons terminates when they collide to initiate the hard subprocess, which sets the scale that limits the endpoint virtualities of the showers. However this procedure is highly inefficient as at the end of the shower the partons have to have a precise values for momenta to set the hard scale. In practice, what is done is known as the backward evolution. What is done is that, longitudinal momentum fractions x_1 and x_2 of the incoming partons of the hard subprocess are chosen using the parton distribution functions at the high hard-subprocess scale, subjected to the kinematic constraint that $x_1 x_2 S = s$ where S and s are the collider and subprocess centre-of-mass energies-squared respectively. The incoming partons are then evolved backwards, gaining energy in each emission. However the no emission probability is no longer given by the Sudakov, rather it is reweighted through the PDF,

$$\Delta'_i(q_1^2, q_2^2) = \frac{f_i(x, q_2^2)}{f_i(x, q_1^2)} \Delta_i(q_1^2, q_2^2) . \quad (2.68)$$

2.9 Matching Parton Shower with Fixed Order

Parton shower only populates the infrared region of the phase space. However we need to describe hard cross-section with more hard jets as well, thereby achieving higher accuracy in the perturbation theory. These two procedure are complimentary to each other and to have a complete description of the cross-section and the distributions at higher accuracy we need to incorporate these two approaches in a systematic way. However care should be taken particularly in the infrared region of the phase space as both matrix element as well

as parton shower can contribute thus leading to double counting or in some cases gaps in those region. The naive way of approaching is to cut the phase space in such a way that the infrared region is populated only by parton shower whereas the hard region is taken care of by the matrix element radiation. This obviously calls for a merging scale by which the phase space region is separated. Thus the problem is that the cross-section now depends on an unphysical scale. However a proper choice of this scale could reduce the dependency of cross-section on this scale. Another useful approaches like MC@NLO, POWHEG etc. are implemented in case of matching parton shower with NLO matrix elements. In case of MC@NLO method, the subtraction term is chosen cleverly to match with the singular term in the real emission and universal parton shower splitting kernel. We will discuss more about it in Chapter 5. In the POWHEG, one starts with NLO weighted Born cross-section *i.e.* hardest emission is performed first with full NLO accuracy. The PS is used next for the subsequent emissions. The differential cross-section in this approach is given by,

$$d\sigma^{POWHEG} = d\Phi_B \bar{B}(\Phi_B) \left[\bar{\Delta}(Q^2, Q_0^2) + \int d\Phi_1 \bar{\Delta}(Q^2, q^2) \frac{R^s(\Phi_1)}{B(\Phi_B)} \right] \quad (2.69)$$

Note that the Sudakov is redefined here as,

$$\bar{\Delta}(Q^2, q^2) = \exp \left[- \int d\Phi_1 \alpha_s \frac{R^s(\Phi_1)}{B(\Phi_B)} \theta(Q^2 - q^2) \right] \quad (2.70)$$

Note that the cross-section 2.70 matches with NLO cross-section in the hard region. Moreover the infrared region also has the NLO accuracy. A fixed order and parton shower description both have advantages and disadvantages in different phase space region. For an optimal description of observables and distributions however both have to be taken into account. The matched and merged results can be directly compared to the experimental data.

2.10 Conclusion

The SM successfully describes the physics of elementary particles. However as we know SM is not complete description of the nature. It can not explain many theoretical dilemma like the hierarchy problem, strong CP problem etc. as well as experimental observations like the existence of neutrino mass, dark matter etc. One main shortcoming of the SM is that it does not include gravity. The obvious reason behind this is that gravity is very weak compared to the other three forces. However we will see in the next chapter, gravity can be incorporated in the SM to address different issues beyond the SM and more importantly the signature of these models might be observed at the LHC energies.

GRAVITY BEYOND THE STANDARD MODEL

3.1 Introduction

The Standard Model is only a “*low-energy*” effective theory, which means that it is valid only up to a certain scale (roughly $\mathcal{O}(TeV)$) and may have to be modified at TeV energies. While strong, weak and electromagnetic forces are described satisfactorily within the SM, gravity still remains unexplained in a QFT framework. Various scenarios have been discussed how to modify the SM in order to extend its validity to the Planck scale, where gravity cannot be neglected anymore.

For a long time the impact of gravity was ignored as it is the most weakly interacting force. The interaction of gravity with the SM is Planck mass suppressed. Therefore it’s effect on the SM is so small that it can be practically ignored in collider experiments and the effects of quantum gravity are only expected to non-negligible near the Planck scale. Moreover there is no consistent quantum field theoretic description for gravity till now. Any theory involving gravity suffers from a basic problem, that the theory is non-renormalizable which is due the fact that gravity coupling is not dimensionless.

Therefore when calculating higher loops with graviton one generally encounters UV divergences which can not be renormalized through redefining fundamental parameters of the theory. This also restricts the incorporation of gravity within the SM. Therefore the current understanding of gravity is based on Einstein's general theory of relativity, which is formulated within the framework of classical physics.

3.2 Spin-2 in BSM physics

Although a consistent quantum field theory for gravity is still lacking, one can build an effective field theory with gravity and comparatively low energy phenomena can be studied. The motivation is to investigate the impact of gravity on the quantum phenomena on a first approximation, relying on semi-classical theory for gravity. The action describing gravity is given by the Einstein-Hilbert action [76],

$$S_{GRAVITY} = \frac{1}{16\pi G_N} \int d^4x \sqrt{-g} [R] \quad (3.1)$$

where G_N is the universal Newton's constant, R is the Ricci scalar found from contracting Ricci tensor $R_{\mu\nu}$ with metric tensor $g^{\mu\nu}$ i.e. $R = g^{\mu\nu}R_{\mu\nu}$ and $g = \det(g_{\mu\nu})$. Ricci tensor $R_{\mu\nu}$ is given in terms of connection as,

$$R_{\mu\nu} = \partial_\nu \Gamma_{\mu\rho}^\rho - \partial_\rho \Gamma_{\mu\nu}^\rho + \Gamma_{\mu\rho}^\sigma \Gamma_{\nu\sigma}^\rho - \Gamma_{\mu\nu}^\sigma \Gamma_{\rho\sigma}^\rho \quad (3.2)$$

where the connections are defined as,

$$\Gamma_{\mu\nu}^\rho = \frac{g^{\rho\sigma}}{2} (\partial_\mu g_{\nu\sigma} + \partial_\nu g_{\mu\sigma} - \partial_\sigma g_{\mu\nu}) \quad (3.3)$$

To get the equation of motion one needs to vary the action 3.1. This leads to the Einstein's field equations given by [77, 78],

$$R^{\mu\nu} - \frac{1}{2}g^{\mu\nu}R = -8\pi G_NT^{\mu\nu} = -\frac{\kappa^2}{2}T^{\mu\nu} \quad (3.4)$$

where we have used the definition $\kappa^2 = 16\pi G_N$ and $T^{\mu\nu}$ is the stress-energy tensor of matter fields. In the semi-classical approximation, gravitational field is considered as a classical background field which satisfy the field equations of General Relativity while other fields are quantized. By varying the metric field $g_{\mu\nu}$ in weak field approximation one can obtain the action (or Lagrangian) for the gravity field ($G_{\mu\nu}$). Metric is varied as below:

$$g_{\mu\nu} = \eta_{\mu\nu} + \kappa G_{\mu\nu} \quad (3.5)$$

Correspondingly,

$$g^{\mu\nu} = \eta^{\mu\nu} - \kappa G^{\mu\nu} + \kappa^2 G_\rho^\mu G^{\rho\nu} + \dots \quad (3.6)$$

The action takes the form,

$$S_{GRAVITY} = \int d^4x \sqrt{-g} [\mathcal{L}^0 + \mathcal{L}^1 + \mathcal{L}^2 + \dots] \quad (3.7)$$

where,

$$\begin{aligned} \mathcal{L}^0 &= \frac{1}{\kappa^2}R \\ \mathcal{L}^1 &= \frac{1}{\kappa} \left(\frac{\eta^{\mu\nu}}{2}R - R^{\mu\nu} \right) G_{\mu\nu} \\ \mathcal{L}^2 &= \frac{1}{2}\partial_\rho G_{\mu\nu}\partial^\rho G^{\mu\nu} - \frac{1}{2}\partial_\rho G\partial^\rho G + \partial_\mu G\partial_\nu G^{\mu\nu} - \partial_\rho G_{\mu\sigma}\partial^\sigma G^{\mu\rho} \\ &\quad + R \left(\frac{1}{4}G^2 - \frac{1}{2}G_{\mu\nu}G^{\mu\nu} \right) + R^{\mu\nu} \left(\frac{1}{2}G_\mu^\sigma G_{\nu\sigma} - GG_{\mu\nu} \right) \end{aligned} \quad (3.8)$$

Note that the indices are raised or lowered using flat metric $\eta_{\mu\nu}$ and therefore Ricci scalar in this case is $R = \eta^{\mu\nu}R_{\mu\nu}$. By considering the variation of the action 3.7 we get the

interaction between the linearised Gravity and the SM fields in weak field approximation,

$$S_{int} = -\frac{\kappa}{2} \int d^4x G_{\mu\nu} T^{\mu\nu} \quad (3.9)$$

The stress-energy tensor of the SM ($T^{\mu\nu}$) is given by,

$$T^{\mu\nu}(\phi, \psi, A_\mu) = \left(\eta^{\mu\nu} \mathcal{L}_{SM}(\phi, \psi, A_\mu) + 2 \frac{\delta \mathcal{L}_{SM}(\phi, \psi, A_\mu)}{\delta g_{\mu\nu}} \right) \Big|_{g_{\mu\nu}=\eta_{\mu\nu}} \quad (3.10)$$

The actions for the SM for scalar (ϕ), fermion (ψ) and gauge fields (A_μ) is given as follows,

$$\begin{aligned} S_\phi &= \int d^4x \sqrt{-g} \left[\frac{1}{2} \partial_\mu \phi \partial^\mu \phi - \frac{m_\phi^2}{2} \phi^2 \right] \\ S_\psi &= \int d^4x \sqrt{-g} \left[\bar{\psi} \not{D} \psi - m_\psi \bar{\psi} \psi \right] \\ S_{A_\mu} &= \int d^4x \sqrt{-g} \left[-\frac{1}{4} F_{\mu\nu} F^{\mu\nu} \right] \end{aligned} \quad (3.11)$$

Corresponding Stress-energy tensors are given by

$$\begin{aligned} T_{\mu\nu}^\phi &= -\frac{\eta_{\mu\nu}}{2} (\partial_\rho \phi \partial^\rho \phi - m_\phi^2 \phi^2) + \partial_\mu \phi \partial_\nu \phi \\ T_{\mu\nu}^\psi &= -\eta_{\mu\nu} (\bar{\psi} \not{D} \psi - m_\psi \bar{\psi} \psi) + \frac{i}{4} [\bar{\psi} \gamma_\mu (\partial_\nu - ig_s T^a A_\nu^a) \psi - \bar{\psi} (\partial_\nu + ig_s T^a A_\nu^a) \gamma_\mu \psi + (\mu \leftrightarrow \nu)] \\ T_{\mu\nu}^{A_\mu} &= \frac{\eta_{\mu\nu}}{4} F_{\rho\sigma} F^{\rho\sigma} - F_\mu^\sigma F_{\nu\sigma} \end{aligned} \quad (3.12)$$

Using the expressions for the stress-energy tensor Eq. 3.12 in the interaction action Eq. 3.9 we can get all the Feynman rules needed to describe Gravity-SM interaction. These Feynman rules are listed in Appendix B.

3.3 Extra Dimensions

From the early Twentieth century, there has been a growing interest in unifying Einstein gravity with the other forces. The first attempt [79] was made by T. Kaluza in 1921. While trying to study Einstein's gravity in 5-dimensional space-time, he discovers that it is possible to unify gravity with electromagnetism with the incorporation of extra spacial dimensions. A few years later in 1926 O. Klein realized [80] the same and predicted that there could be extra dimension which are small and compact. But their theories were not explored for a long time since gravity interacts very weakly with SM whose signature is negligible. Later in the 80s with the advancement of superstring theories, where multiple extra dimensions are essential, the idea of Kaluza-Klein again revived.

The central idea of Kaluza-Klein theory is to consider 5-dimensional graviton field G_{MN} , where $M, N \in \{0, 1, 2, 3, 4\}$. The 5-D metric could be a flat metric like $g_{MN} = \text{diag}(1, -1, -1, -1, \pm 1)$. Here ± 1 corresponds to the time-like (space-like) extra dimension. For a time-like extra dimension *i.e.* where extra dimension has signature +1, tachyon particle with negative mass will appear which violates the causality. Therefore it is always good to choose a spacial extra dimension to have the interactions with the SM particle as well. The 5-dimensional manifold is factorizable,

$$\mathcal{M}^{(5)} \equiv \mathcal{M}^{(4)} \otimes \mathcal{M}^{(1)} \quad (3.13)$$

where $\mathcal{M}^{(4)}$ is the usual Minkowski space-time and $\mathcal{M}^{(1)}$ is the one-dimensional Euclidean manifold. The background metric can be decomposed in the following form

$$g_{MN} = \begin{pmatrix} (g_{\mu\nu} - \kappa^2 \phi^2 A_\mu A_\nu) & -\kappa \phi^2 A_\mu \\ -\kappa \phi^2 A_\nu & \phi^2 \end{pmatrix}$$

Here μ, ν represent the usual $1 + 3$ dimensional Minkowski space-time whereas $M, N \in$

$\{0, 1, 2, 3, 4\}$. In fact the $g_{\mu\nu}$, A_μ and ϕ naively look as metric, vector and scalar fields in 4-dimensions. The 5-D Christoffels are given by

$$\Gamma_{MN}^P = \frac{g^{PQ}}{2}(\partial_M g_{QN} + \partial_N g_{QM} - \partial_Q g_{MN}) \quad (3.14)$$

Here M, N, P, Q run over $0, 1, 2, 3, 4$. Correspondingly the Ricci tensor and Ricci scalar are given as

$$\begin{aligned} R_{MN} &= \partial_N \Gamma_{MP}^P - \partial_P \Gamma_{MN}^P + \Gamma_{MP}^Q \Gamma_{NQ}^P - \Gamma_{MN}^Q \Gamma_{PQ}^P \\ R_5 &= g^{MN} R_{MN} \end{aligned} \quad (3.15)$$

The 5-dimensional Einstein action is then

$$S = \frac{1}{16\pi G} \int R_5 \sqrt{-g} d^4x dy \quad (3.16)$$

Varying the action we can get the Einstein's equation in 5-dimensions as

$$\begin{aligned} \delta S &= 0 \\ R_{MN} - \frac{g_{MN}}{2} R_5 &= 0 \end{aligned} \quad (3.17)$$

If we identify $\kappa^2 = 16\pi G_N$ where $G_N = G / \int dy$, then substitution of the metric 3.3 in Eq. 3.16 leads to the action

$$S = \int d^4x \sqrt{-g} \phi \left(\frac{R}{16\pi G_N} - \frac{\phi^2 F_{\mu\nu} F^{\mu\nu}}{4} - \frac{2\partial_\mu \phi \partial^\mu \phi}{3\kappa^2 \phi^2} \right) \quad (3.18)$$

By varying action 3.18, one gets the field equations in terms of 4D quantities as:

$$\begin{aligned} G_{\mu\nu} &= R_{\mu\nu} - \frac{g_{\mu\nu}}{2}R \\ &= -\frac{\kappa^2\phi^2}{2}T_{\mu\nu}^A + \frac{1}{\phi}(\nabla_\mu(\partial_\nu\phi) - g_{\mu\nu}\square\phi) \\ \nabla^\mu F_{\mu\nu} &= 3\frac{\partial^\mu\phi}{\phi}F_{\mu\nu} \\ \square\phi &= \frac{\kappa^2\phi^3}{4}F_{\mu\nu}F^{\mu\nu} \end{aligned} \quad (3.19)$$

where $T_{\mu\nu}^A$ is given in Eq. 3.12. Thus Eqs. 3.19 imply that the 4D EM radiation can arise from a 5D geometry. In fact in Kaluza-Klein's original idea ϕ is taken to be constant (particularly $\phi = 1$). Then the fields equations Eq. 3.19 are exactly reduced to the Einstein and Maxwell equations:

$$\begin{aligned} G_{\mu\nu} &= -8\pi G_N T_{\mu\nu}^A \\ \nabla^\mu F_{\mu\nu} &= 0 \end{aligned} \quad (3.20)$$

In KK theory, it is considered that our universe is a four-dimensional subspace of $M^{(5)}$ where all derivatives with respect to the fifth coordinate vanish. This is known as the *Cylinder condition*. The scalar field ϕ is called the *dilaton* field and the vector field A_μ as the KK gauge field. In the original Kaluza-Klein idea, it was found that the $g^{\mu\nu}$ and A_μ fields satisfy the Einstein's field equation Eq. 3.4 and Maxwell's equations respectively.

Klein's idea was based on extra dimensions which are compactified, meaning that the extra dimension has a finite boundary unlike the usual Euclidean x - y - z co-ordinates which are infinitely extended. Therefore the extra-dimension is postulated to be compactified on a small circle with a periodicity

$$y \rightarrow y + 2\pi R \quad (3.21)$$

where R is the size of the extra-dimension. The topology of the space-time is given by

$$M^{(5)} = \mathcal{M}^{(4)} \otimes \mathcal{S}^{(1)} \quad (3.22)$$

where $\mathcal{M}^{(4)}$ is the usual Minkowski space-time and $\mathcal{S}^{(1)}$ is the topology of a circle. Due to the periodicity of the fifth dimension, all the fields can be Fourier expanded as,

$$\begin{aligned} \phi(x^\mu, y) &= \sum_{n=-\infty}^{\infty} \phi^{(n)}(x^\mu) \exp\left(\frac{iny}{R}\right) \\ A_\rho(x^\mu, y) &= \sum_{n=-\infty}^{\infty} A_\rho^{(n)}(x^\mu) \exp\left(\frac{iny}{R}\right) \\ G_{\rho\sigma}(x^\mu, y) &= \sum_{n=-\infty}^{\infty} G_{\rho\sigma}^{(n)}(x^\mu) \exp\left(\frac{iny}{R}\right) \end{aligned} \quad (3.23)$$

3.3.1 Kaluza-Klein Reduction

Periodicity in the extra dimension implies that the 5-dimensional fields can be Fourier expanded. The equations of motion for the Fourier modes are wave equations:

$$\begin{aligned} \partial_M \partial^M \phi &= 0 \\ \implies \sum_{n=-\infty}^{\infty} \left(\partial_\mu \partial^\mu - \frac{n^2}{R^2} \right) \phi^{(n)}(x^\mu) \exp\left(\frac{iny}{R}\right) &= 0 \\ \implies \partial_\mu \partial^\mu \phi^{(n)}(x^\mu) - \frac{n^2}{R^2} \phi^{(n)}(x^\mu) &= 0 \end{aligned} \quad (3.24)$$

Eq. 3.24 indicates an infinite number of Klein-Gordon equations for massive 4D scalar fields. This implies that each Fourier mode $\phi^{(n)}$ is a scalar particle in 4-dimension with mass given by

$$m_n^2 = \frac{n^2}{R^2} \quad (3.25)$$

The zero mode here is massless which is generally identified with the 4D field. The massive states are called Kaluza-Klein states which originates from the extra dimensions.

3.3.2 ADD model

Arkani-Hamed, Dimopoulos and Dvali revived the idea of Kaluza-Klein and proposed [81–83] a way to lower the scale of gravity to TeV scale. The main idea was to consider extra spatial dimensions which are compactified and the Planck scale is not the fundamental scale. The idea is backed from the fact that gravity has not been probed at small distances less than a centimeter. Therefore they postulated that gravity behaves quite differently in small range than the usual. Motivated by the string theory, the number of such extra dimensions can be more than one. According to ADD model, the space-time is $4 + \delta$ dimensional and only gravity can probe the full $d = 4 + \delta$ dimensional bulk, whereas the SM is contained within 4-dimensional brane. These δ extra dimensions are compactified on a torus with radius R and volume $V_\delta = (2\pi R)^\delta$. The fundamental gravity scale can be related to the 4-dimensional Planck scale simply through Gauss's law, according to which the gravitational potential at a distance $r \ll R$ is given by

$$V(r)_{r \ll R} \sim \frac{m_1 m_2}{M_F^{\delta+2}} \frac{1}{r^{\delta+1}} \quad (3.26)$$

where m_1, m_2 are two test masses placed at a distance r . Similarly the expression for potential at a distance larger than the extra dimension is given by

$$V(r)_{r > R} \sim \frac{m_1 m_2}{M_F^{\delta+2}} \frac{1}{R^\delta r} \quad (3.27)$$

which can be equated to our usual Newtonian gravity

$$V(r)_{r \gg R}^N \sim \frac{m_1 m_2}{M_{Pl}^2} \frac{1}{r}. \quad (3.28)$$

Equating Eq. 3.27 with Eq. 3.28, we find the relation between the 4-dimensional Planck scale and fundamental gravity scale as

$$M_{Pl}^2 = C_\delta M_F^{\delta+2} R^\delta, \quad (3.29)$$

where $C_\delta = 2/(4\pi)^{\frac{\delta}{2}} \Gamma(\frac{\delta}{2})$. The fundamental scale for gravity thus can be of the order of the electro-weak scale through the large volume of the extra dimension. One extra dimension *i.e.* $\delta = 1$ is excluded as this leads to $R \sim 10^{11}$ m *i.e.* roughly the astrophysical distances, and the non-observance of any deviations from Newtonian gravity at this distances basically rules out $\delta = 1$ scenario. For $\delta = 2$, $R \sim 1$ mm which is within the experimental limit, for δ even higher the radius of extra dimension becomes even smaller. The coupling strength of graviton to the SM fields are very small and thus apparently can not be relevant for the collider search. However the number of such massive states are very large. In fact there are $(ER)^\delta$ number of massive KK states which are kinematically accessible in a collider of centre of mass energy E . Therefore the sum over the contribution from each KK state removes the Planck scale suppression in a process and replaces it by powers of the fundamental scale M_F ($\mathcal{O}(TeV)$). The signature of these massive KK states at the collider can be observed in two ways. One through the signature of missing energy where the KK modes escapes the detection. Other is through the virtual KK mode exchange by which any deviations in some observable from the SM may lead to the ADD signature. The density of the KK states increases rapidly with the numbers of extra dimensions and the KK mass distribution is shifted to higher values. This is not reflected in the missing energy distribution: although the heavier KK gravitons are more likely to carry larger energy, they are also more likely to be produced at threshold due to

the rapidly decreasing parton distribution functions. These two effects compensate each other, leaving nearly identical missing energy distributions.

Searches for direct KK graviton production through the first kind of processes have been performed in LEP-II as well as at the LHC [84, 85]. LEP-II has put bound [86, 87] on the fundamental scales up to 1.45 TeV for two extra compactified dimensions and 0.6 TeV for six extra dimensions using the characteristic final states of missing energy plus a single photon or Z boson. The second kind of collider signature is through the virtual KK exchange in $2 \rightarrow 2$ scattering processes which lead to deviation of cross sections and asymmetries from the SM processes.

The Lagrangian for the ADD case is given by

$$\mathcal{L} = -\frac{\kappa}{2} \sum_{(\bar{n})} T^{\mu\nu} h_{\mu\nu}^{(\bar{n})}(x) \quad (3.30)$$

Here $h_{\mu\nu}^{(\bar{n})}(x)$ denotes the KK states which contains one spin-2 state, $(n - 1)$ spin-1 states, and $n(n - 1)/2$ spin-0 states with mass given by,

$$m_{\bar{n}}^2 = \frac{(2\pi n)^2}{R^2} \quad (3.31)$$

The sum of the KK modes is given by

$$\begin{aligned} \kappa^2 \mathcal{D}(s) &= \kappa^2 \sum_{(\bar{n})} \frac{1}{s - m_{\bar{n}}^2 + i\epsilon} \\ &= \frac{8\pi}{M_F^4} \left(\frac{\sqrt{s}}{M_F} \right)^{(\delta-2)} \left[\pi + 2iI \left(\frac{\Lambda}{\sqrt{s}} \right) \right] \end{aligned} \quad (3.32)$$

where s is the partonic centre of mass energy, Λ is the UV cut off of the KK modes which

is roughly taken of the order of M_F . The integral $I\left(\frac{\Lambda}{\sqrt{s}}\right)$ is given in [88] as,

$$\begin{aligned} I\left(\frac{\Lambda}{\sqrt{s}}\right) &= - \sum_{n=1}^{(\delta-2)/2} \frac{1}{2n} \left(\frac{\Lambda}{\sqrt{s}}\right)^{2n} - \frac{1}{2} \log\left(\frac{\Lambda^2}{s} - 1\right) && \text{for } \delta = \text{even} \\ &= - \sum_{n=1}^{(\delta-1)/2} \frac{1}{(2n-1)} \left(\frac{\Lambda}{\sqrt{s}}\right)^{(2n-1)} + \frac{1}{2} \log\left(\frac{\Lambda + \sqrt{s}}{\Lambda - \sqrt{s}}\right) && \text{for } \delta = \text{odd} \end{aligned} \quad (3.33)$$

To order κ^2 , the ADD action allows scattering processes involving SM fields and virtual gravitons in the intermediate state or real gravitons in the final state. In the context of collider phenomenology, this gives rise to a very rich and interesting signals that can be seen at the present LHC. The virtual exchange of the gravitons can lead to deviations from the SM predictions whereas the real emission of the gravitons can lead to the missing energy signals. Since the size of the extra dimension is large in ADD case, the mass splitting among the KK modes *i.e.* $2\pi/R$ is small, as a result of which one can approximate the summation of the KK modes as integral in continuum limit, with the density of the KK modes is given by,

$$\rho(m_{\bar{n}}) = \frac{R^\delta m_{\bar{n}}^{(\delta-2)}}{(4\pi)^{\frac{\delta}{2}} \Gamma(\frac{\delta}{2})} \quad (3.34)$$

The inclusive cross-section for the real graviton production at the colliders is then given by the convolution with this state density function and is given by,

$$d\sigma = \int dm_{\bar{n}}^2 d\sigma_{m_{\bar{n}}} \quad (3.35)$$

where $d\sigma_{m_{\bar{n}}}$ is the differential cross-section for producing single KK mode of mass $m_{\bar{n}}$.

3.3.3 RS model

The fundamental idea for RS model is to consider a 5-dimensional geometry which can describe the physical world through a warping in the 5 dimensional metric. The metric

thus must follow the Poincare invariance *i.e.* it must have 4-dimensional symmetry under boost, translation and rotation. This leads to the following ansatz for the metric,

$$ds^2 = e^{-2\sigma(\phi)} \eta_{\mu\nu} dx^\mu dx^\nu - r_c^2 d\phi^2 , \quad (3.36)$$

where $e^{-2\sigma(\phi)}$ is known as the warped factor and $\eta_{\mu\nu}$ represents the flat Minkowski metric. ϕ denotes the fifth dimension ($0 \leq \phi \leq \pi$) which is compactified on a S^1/\mathbb{Z}_2 orbifold with a radius r_c and κ is related to the curvature of the AdS_5 space-time. Two 3-branes with opposite tensions are situated on two fixed points ($\phi = 0, \pi$) of the extra dimension. The brane at $\phi = 0$ is called the *Planck brane* and the other one at $\phi = \pi$ is known as the *TeV brane*. Solving the 5-dimensional Einstein's equation 3.17 for the metric 3.36, we can get the form for the warped factor. In the RS model, the non-factorizable geometry is governed by the following 5-dimensional warped metric [89],

$$ds^2 = e^{-2\kappa r_c |\phi|} \eta_{\mu\nu} dx^\mu dx^\nu - r_c^2 d\phi^2 , \quad (3.37)$$

The RS action is taken as

$$S^{RS} = \int d^4x dy \sqrt{-g} M_F^3 R_5 \quad (3.38)$$

The 4-dimensional Planck scale M_{Pl} is related to the fundamental gravity scale M_F through the warp factor. With this exponential warping it is now possible to bring down the hierarchy,

$$M_{Pl}^2 = \frac{M_F^2}{\kappa} (1 - e^{-2\pi\kappa r_c}) \quad (3.39)$$

In the RS scenario, all SM fields are considered to be confined on the TeV brane, whereas the gravity can propagate in the full $4 + 1$ dimensions. The interaction among the SM fields with the massive KK excitations ($h_{\mu\nu}^{(n)}$) of the graviton [88, 90] is determined

by the following Lagrangian,

$$\mathcal{L}_{\mathcal{RS}} = -\frac{1}{\overline{M}_{Pl}} T^{\mu\nu}(x) h_{\mu\nu}^{(0)}(x) - \frac{\bar{c}_0}{m_0} T^{\mu\nu}(x) \sum_{n=1}^{\infty} h_{\mu\nu}^{(n)}(x) , \quad (3.40)$$

where $\bar{c}_0 = \frac{\kappa}{\overline{M}_{Pl}}$, $m_0 = \kappa e^{-\kappa r_c \pi}$, $T^{\mu\nu}$ is the energy-momentum tensor for the SM particles and \overline{M}_{Pl} is the reduced Planck scale which is related to the Planck mass (M_{Pl}) through $\overline{M}_{Pl} = M_{Pl}/\sqrt{8\pi}$. Note that, the couplings of the zeroth KK mode to the SM fields are \overline{M}_{Pl} suppressed and hence this term can be practically neglected. However, the contribution from the higher modes with the coupling \bar{c}_0/m_0 can be of the order of few TeV for a choice of $\kappa r_c \sim \mathcal{O}(10)$ [91, 92] and they can produce significant observable effects. The masses of the KK mode excitations are given by

$$M_n = x_n \kappa e^{-\pi \kappa r_c}, \quad (3.41)$$

where x_n s are the zeros of the Bessel function $J_1(x)$.

The effective graviton propagator after summing over all the massive KK modes except the zeroth one takes the following form [93, 94],

$$\begin{aligned} D_{eff}(s_{ij}) &= \sum_{n=1}^{\infty} \frac{1}{s_{ij} - M_n^2 + i\Gamma_n M_n} \\ &= \frac{1}{m_0^2} \sum_{n=1}^{\infty} \frac{(x^2 - x_n^2) - ix_n \frac{\Gamma_n}{m_0}}{(x^2 - x_n^2)^2 + x_n^2 \left(\frac{\Gamma_n}{m_0}\right)^2} , \end{aligned} \quad (3.42)$$

where $s_{ij} = (p_i + p_j)^2$, $x = \sqrt{s_{ij}}/m_0$ and Γ_n denotes the width of the resonance with mass M_n . Note that unlike the ADD case here individual KK mode can give rise to massive resonance. The total decay width of the graviton can be calculated with the KK states decaying to the SM particles [88, 95] in the following way,

$$\Gamma_n = m_0 \bar{c}_0^2 x_n^3 \Delta_n , \quad (3.43)$$

where Δ_n is given by,

$$\Delta_n = \Delta_n^{\gamma\gamma} + \Delta_n^{ZZ} + \Delta_n^{WW} + \Delta_n^{HH} + \sum_{\nu} \Delta_n^{\nu\nu} + \sum_l \Delta_n^{ll} + \Delta_n^{gg} + \sum_q \Delta_n^{qq} \quad . \quad (3.44)$$

Here each Δ_n^{aa} corresponds to the coefficient coming from the decay width calculation of the process $h^{(n)} \rightarrow aa$. Unlike the large extra dimension model, the individual resonances of the graviton are well-separated in the RS model and they can be probed in invariant mass distribution. All the relevant decay widths can be found in [88], nevertheless below we present them,

$$\begin{aligned} \Delta_n^{\gamma\gamma} &= \frac{\kappa^2 M_n^3}{160\pi} \\ \Delta_n^{ZZ} &= \frac{\kappa^2 M_n^3}{160\pi} \left(1 - \frac{4M_Z^2}{M_n^2}\right)^{1/2} \left(\frac{13}{12} + \frac{14}{39} \frac{M_Z^2}{M_n^2} + \frac{4}{13} \frac{M_Z^4}{M_n^4}\right) \\ \Delta_n^{W^+W^-} &= \frac{\kappa^2 M_n^3}{80\pi} \left(1 - \frac{4M_{W^\pm}^2}{M_n^2}\right)^{1/2} \left(\frac{13}{12} + \frac{14}{39} \frac{M_{W^\pm}^2}{M_n^2} + \frac{4}{13} \frac{M_{W^\pm}^4}{M_n^4}\right) \\ \Delta_n^{HH} &= \frac{\kappa^2 M_n^3}{960\pi} \left(1 - \frac{4M_H^2}{M_n^2}\right)^{5/2} \\ \Delta_n^{\nu\nu} &= \frac{\kappa^2 M_n^3}{360\pi} \\ \Delta_n^{\ell^+\ell^-} &= \frac{\kappa^2 M_n^3}{360\pi} \left(1 - \frac{4M_{\ell^\pm}^2}{M_n^2}\right)^{3/2} \left(1 + \frac{8M_{\ell^\pm}^2}{3M_n^2}\right) \\ \Delta_n^{gg} &= \frac{\kappa^2 M_n^3}{20\pi} \\ \Delta_n^{q\bar{q}} &= \frac{3\kappa^2 M_n^3}{360\pi} \left(1 - \frac{4M_q^2}{M_n^2}\right)^{3/2} \left(1 + \frac{8M_q^2}{3M_n^2}\right) \end{aligned} \quad (3.45)$$

In RS scenario, the principal collider signature is the direct resonant production of the spin-2 states in the graviton KK tower. The two parameters in RS case are chosen as

$$\begin{aligned} \bar{c}_0 &= \frac{\kappa}{\bar{M}_{Pl}} \\ m_0 &= \kappa e^{-\pi\kappa r_c} \end{aligned} \quad (3.46)$$

m_0 has the dimension of mass and sets the scale for the masses of the KK excitations whereas c_0 is an effective coupling. Searches for the first graviton KK resonance in Drell-Yan and di-jet data from Run I at the Tevatron restrict (34) the parameter space of this model.

Since κ is related to the curvature of the fifth dimension, we need to restrict it to small enough values to avoid effects of strong curvature. On the other hand κ should not be too small compared to M_P , as that would reintroduce a hierarchy. This suggest to restrict the value of \bar{c}_0 within $[0.01, 0.1]$. Although there are motivations from string theory to the theoretical bounds of \bar{c}_0 . The curvature is assumed to be less than the Planck scale *i.e.* $\kappa < \bar{M}_{Pl} \Rightarrow \bar{c}_0 < 1$. Now the tension on D3 brane from the argument of string theory is given by,

$$T_{string}^{(D3)} = \frac{M_{string}^4}{(2\pi)^3 g_{string}} \quad (3.47)$$

where g_{string} is the string coupling constant ~ 1 . M_{string} is the string scale $\sim g_{YM} \bar{M}_{Pl}$, where g_{YM} is the 4D Yang-Mills gauge coupling constant ~ 0.7 . The tension on the 3-brane from RS scenario is found to be

$$T_{RS}^{(D3)} = 24\kappa^2 \bar{M}_{Pl}^2 \quad (3.48)$$

Equating Eq. 3.47 with Eq. 3.48 gives the lower bound on \bar{c}_0 to be ~ 0.01 . Although the electro-weak precision data from LEP sets the lower bound for \bar{c}_0 to be ~ 0.03 .

3.4 Conclusion

Discovering extra dimensions could give us clues about the mysterious workings of gravity and also show the path to unify the forces. The ADD and the RS models provide simple frameworks through which gravity can be incorporated at the first order approximation

within the SM. Clearly the rates and distributions of scattering amplitudes will deviate from the SM one in the presence of such extra dimensions. LHC with its high energy run provides a great opportunity to test these models and existence of such extra dimensions. QCD corrections to the scattering amplitudes are also important to these models as often the correction is large. In the next two chapters we will consider how RS signature can be found at the hadron colliders like the LHC. In chapter-4 we will use the technique ME+PS for triple neutral gauge boson production, in chapter-5 we will use the MC@NLO formalism to consider the NLO+PS production for di-final states.

4

TRIPLE NEUTRAL GAUGE BOSONS PRODUCTION IN RS MODEL

4.1 Introduction

LHC is now running at its phase-II with higher energies and luminosity. Precision measurement of the properties of the newly discovered Higgs boson is a priority and will be matched with precise higher order theoretical predictions to look for any deviations from the SM. Now that the Higgs boson is discovered it is important to look at the massive vector boson scattering (VBS) cross section which is uniterised by the Higgs boson. The VBS gets contribution from the non-abelian couplings of the electro-weak gauge boson sector (a) triple gauge boson coupling (TGC), (b) quartic gauge boson coupling (QGC) and in addition, Higgs coupling to the massive gauge boson. The TGC will contribute to the di-boson final state and Run-I has already placed comparable limits to the anomalous couplings as the LEP experiments. The QGC coupling leads to tri-gauge boson final states, though the full process would involve the TGC, fermion mediated processes and also Higgs mediated processes. The QGC has been reported for the first time by ATLAS collaboration using the VBS process, yielding a final state with two same sign W boson in association with two jets [96] in a purely electro-weak process and also measured the $W\gamma\gamma$

production cross section [97] which is now accessible with the 8 TeV LHC data set. The CMS collaboration has also measured the QGC in the $WW\gamma$ and $WZ\gamma$ final states [98]. So far the observations are consistent with SM predictions and as the sensitivity of these measurements improves, the TGC and QGC that lead to tri-boson final states can not only test the electro-weak sector of the SM but also probe new physics. In this chapter we look at some of the tri-boson production processes merged to 1-jet in the warped extra dimension model.

In the model proposed by Randall and Sundrum (RS) [99], the non-factorizable geometry of the space-time with the inclusion of a single warped extra spatial dimension, proposes a solution to the hierarchy problem. The SM fields are confined to a 3-brane, whereas the gravity which propagates the full 5-dimensional space-time, manifests as massive Kaluza-Klein (KK) modes in 4-dimensional space-time. RS model phenomenology of the virtual graviton exchange have extensively been studied for gauge boson pair production processes *viz.*, $\gamma\gamma$ [94], ZZ [100], W^+W^- [101] and also for DY production [102] at the next-to-leading order (NLO) accuracy, because of their rich sensitivity to the model parameters. This in turn helps to reduce the theoretical uncertainties whereby constraining the RS model parameters. Recently the parton shower effect has been considered for those processes in [103]. Nevertheless, the study of triple gauge boson production processes within this model would also be phenomenologically important, as they could effectively participate in interesting new physics searches at the TeV scale. They have been studied in the SM at NLO [104–107] level. NLO results of the triple photon production in the SM have recently been presented including the effect of photon fragmentation [108] or matching them with different parton shower (PS) Monte Carlo programmes [109]. These SM processes also serve as potential backgrounds to a number of new physics signals coming from different BSM scenarios. For example, the SM $\gamma\gamma\gamma$ process is a background to single photon production, together with one techni-pion in technicolor model, whereas

$\gamma\gamma Z$ process in the SM is a background to the signal with di-photon plus missing energy in gauge-mediated supersymmetric theories.

In this chapter, we will consider the production of neutral triple electro-weak gauge bosons in warped extra dimension model at the LHC, *i.e.*, $PP \rightarrow VVV X$, where $V = \gamma, Z$ and X denotes some hadronic final states. Similar processes have been analyzed at LO in case of large extra dimensional models [110–112]. In fact, study of these processes in RS scenario bears equal importance, as their contributions in searching new physics using the triple gauge boson productions are undeniable in distinguishing physics arising from the potential BSM candidates like supersymmetry or technicolor.

4.2 Merging Matrix Element with Parton Shower

In LHC, additional jets are often produced from initial state radiation and can alter the LO predictions for relevant observables. Generally these additional jets are simulated using PS monte carlo. But these QCD radiations in the PS programs are generated in the soft and collinear approximation based on Sudakov form factors. The widely separated and hard emissions are not well-described in the PS approach, whereas the fixed order tree level amplitudes can provide reliable predictions in the hard region, but it fails in the collinear and soft limits. Therefore it is also essential to take into account the tree level amplitude containing additional jets. Both descriptions have to be combined in an appropriate matching method by avoiding double counting or gaps between samples with different multiplicity. Several algorithms have been proposed for this purpose, mainly based on the event re-weighting (eg. CKKW) [113,114] or event rejection (eg. MLM) [115].

4.2.1 CKKW

The naive approach to matrix element merging with parton shower at LO is done choosing a scale Q_{cut} . It is required that PS will fill the phase space below Q_{cut} whereas the ME describes the region above Q_{cut} . The idea is to use matrix element along with Sudakov form factor above the merging scale and the parton shower below the merging scale. Therefore the correction to the first emission is given by,

$$\begin{aligned} d\sigma^{\text{CKKW}} = & B(\Phi_B) \times \left[\Delta(Q^2, Q_0^2) + \int_{Q_0^2} \frac{dq^2}{q^2} \int dz \frac{\alpha_s}{2\pi} \mathcal{P}(z) \Delta(Q^2, q^2) \Theta(Q_{cut}^2 - q^2) \right] d\Phi_B \\ & + \left[\alpha_s R(\Phi_{B+1}) \Delta(Q^2, q^2) \Theta(q^2 - Q_{cut}^2) \right] d\Phi_{B+1} \end{aligned} \quad (4.1)$$

One important feature evident from Eq. 4.1 that it violates unitarity due to cut posed on the phase-space. But this will not have a large impact if this cut is chosen reasonably so that the total cross-section remains relatively stable with respect to the variations of the scale Q_{cut} . For more than one jet merging, the second term in Eq. 4.1 can be treated as the born for one extra emission process and the same expression as Eq. 4.1 can be repeated.

The implementation of CKKW algorithm follows as:

1. Different multiplicity events are generated with fixed strong coupling constant α_s using matrix element cut-off Q_{cut} defined by k_T jet measure. This will remove any divergences from the ME.
2. Merging scale Q_{ME} is chosen to the same as the matrix element cut off scale Q_{cut} .
3. Events are re-weighted using Sudakov form factors and running coupling constants.
4. Parton shower is introduced where the starting scale of the parton shower from each

parton is chosen according to the scale where the parton first appears and veto any shower emission above Q_{cut} .

The jet measure used in CKKW is the Durham k_\perp and the shower evolution variable is used to be the virtuality which somewhat constraints its applicability. Another variation of CKKW has been implemented named as the CKKW-L method which differs in calculating the Sudakov form factor (the Sudakov form factor factorizes unlike the original CKKW case). The shower veto algorithm also differs from the original CKKW.

4.2.2 MLM

MLM approach is the easiest to invoke the jet merging with parton shower since there is no need to change the PS program. In this scheme the ME is directly fed to the PS program. The final state partons are then clustered back to jets using a cone algorithm. If all the jets match with the ME partons then event is selected, otherwise it is rejected. The parton shower is restricted below the merging scale and Sudakov form factor is built to take care of no emission above the merging scale. The merging scale Q_{ME} and matrix element cuts of scale Q_{cut} are chosen such a way that $Q_{ME} > Q_{cut}$. This happens as the events slightly below the merging scale can end up above the shower. The choice of such scale depends on the process considered.

The algorithm follows as:

1. Generate the events with different jet multiplicity n and matrix element cut Q_{cut} .
2. The merging scale Q_{ME} is chosen such that $Q_{ME} > Q_{cut}$.
3. Shower is generated with a veto $Q_{ME} > Q_{cut}$. The starting scale of shower is chosen as $\sqrt{p_i \cdot p_j}$, where i and j are the color-connected partons.

4. The generated partons from shower are clustered back into N jets using a cone algorithm.
5. If $N < n$, where n is matrix element partons, the event is rejected otherwise if $N \geq n$ and each of the original n partons is uniquely contained within any reconstructed jets, then the event is accepted.

4.2.3 Shower- k_T

The shower- k_T scheme [116] is based on event rejection like MLM which is implemented in MADGRAPH5. Unlike the MLM cone algorithm here one uses K_T jet algorithm as jet measure. In this scheme the events are generated by MG with a minimum separation in the phase space Q_{cut} and $P_{T_{min}}$ between the final-state partons (ij) and between the final-state and initial-state partons (iB) respectively which is characterized by the k_T jet measure:

$$d_{ij}^2 = \min(p_{Ti}^2, p_{Tj}^2) \Delta R_{ij}^2 > Q_{cut}^2, \quad d_{iB}^2 = p_{Ti}^2 > p_{T_{min}}^2 \quad (4.2)$$

Here $\Delta R_{ij}^2 = 2[\cosh(\eta_i - \eta_j) - \cos(\phi_i - \phi_j)]$, where p_{Ti} , η_i , ϕ_i are the transverse momentum, pseudo-rapidity and azimuthal angle of the parton i . The k_T value is set as the renormalization scale at each QCD emission vertex. The events are then passed to PYTHIA [117] for showering. In shower- k_T scheme, pythia p_T -ordered shower is used for showering. PYTHIA reports the scale of the hardest emission ($Q_{hardest}^{PS}$) in the shower and vetoes events based on the k_T values of the hardest shower emission instead of performing a jet clustering and comparing to the ME. If $Q_{hardest}^{PS} > Q_{cut}$ for lower multiplicity samples, then the event is rejected, whereas for highest multiplicity sample an event is rejected if $Q_{hardest}^{PS} > Q_{softest}^{ME}$, the scale of the softest parton in the event from ME.

Note that all these merging procedures differ from each other in the definition of jet

measure and in determining the starting conditions and vetoing in shower. In this analysis however we have used the shower- k_T scheme for jet merging which is implemented in MADGRAPH5, where we choose to work with $Q_{cut} = p_{T_{min}}$.

4.3 Triple Neutral Gauge boson production in RS

The leading order neutral triple gauge boson production processes $PP \rightarrow VVV X$ at the LHC come from the subprocess,

$$q(p_1) + \bar{q}(p_2) \rightarrow V(p_3) + V(p_4) + V(p_5) \quad ,$$

where $V = \gamma, Z$ and X is any final state hadron. Typical Feynman diagrams for the SM are shown in Fig. (4.1). The contribution from RS case is shown in Fig. (4.2).

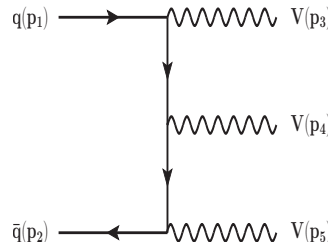


Figure 4.1: Typical SM Feynman diagrams for neutral tri-boson production.

This process has been merged with the 1-jet process $PP \rightarrow VVVj X$ in MADGRAPH5 (MG) [118] framework to have a better description of different distributions. Due to extra radiation emission, $q(\bar{q})g$ initiated subprocesses also come up. The merged events are then matched to a Parton Shower (PS). The Z bosons are let to decay to lepton pairs, thus accounting for the off-shell contributions.

The fixed order merging approach gives a better description of the region of hard and well separated jet whereas the parton shower takes care of the infrared region correctly.

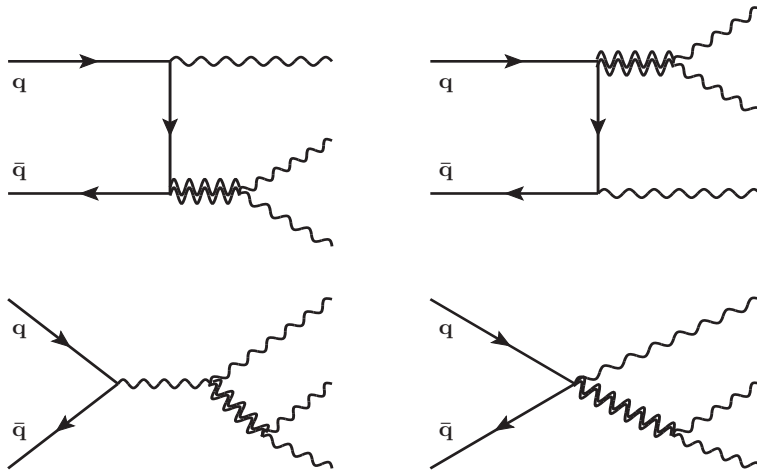


Figure 4.2: Typical RS contribution for neutral tri-boson production. The double-line represents RS graviton. For diagrams with one extra jet one can attach a gluon to any of the initial or internal lines.

These merged-matched events provide a realistic framework to be compared to the experimental outcomes. The Lagrangian of the RS model is written using FeynRules [119] and it is combined together with the SM Lagrangian. The universal FeynRules output (UFO) of the combined Lagrangian (*i.e.*, $\mathcal{L}_{\text{RS}} + \mathcal{L}_{\text{SM}}$) is then imported within MADGRAPH5 framework and used for the generation of events. The model parameters \bar{c}_0 and M_1 , the mass of the first excited KK mode have been set as external inputs and we choose to work with the following values: $M_1 = 1.7$ TeV and $\bar{c}_0 = 0.03$ which remain within the latest experimental bounds provided by ATLAS [84, 120] and CMS [85, 121] collaborations. In addition, we have systematically implemented the KK mode summation algorithm in the spin-2 HELAS routine [122]. Kinematical distributions of various observables have been recalculated for different di-final states such as, di-photon, Drell-Yan, ZZ , W^+W^- in fixed order NLO and NLO+PS using this present layout and they are found to be in excellent agreement with those results that are present in the literature [94, 100–103]. This essentially ensures the proper execution of the whole computational set-up. We have generated events for the following four neutral triple vector boson processes: (i) $\gamma\gamma\gamma$, (ii) $\gamma\gamma Z$, (iii) γZZ and (iv) ZZZ under the above mentioned arrangements. The

Z bosons are decayed to lepton-pair which will be discussed in the next section in detail. Each of these processes consists of three types of contributions coming from pure SM, pure RS and the interference between these two.

4.4 Numerical Result

In this section, we present numerical results of various kinematical distributions for the above four processes. All the results are presented for LHC with center of mass energy $\sqrt{S} = 13$ TeV. In our analysis, the following set of external parameters are used as input:

$$\begin{aligned} m_Z &= 91.188 \text{ GeV} , & \sin^2(\theta_W) &= 0.222 , \\ G_F &= 1.16639 \cdot 10^{-5} \text{ GeV}^{-2} , & \alpha^{-1} &= 132.507 . \end{aligned} \quad (4.3)$$

During the generation of events we let the Z bosons to decay to $\ell^+\ell^-$ pair. Events are generated with loose cuts on the transverse momentum (P_T) and rapidity (y) of the final state particles:

$$P_T^{\gamma,\ell} > 15 \text{ GeV} , \quad |y^{\gamma,\ell}| \leq 2.6 . \quad (4.4)$$

The factorization scale (μ_F) as well as the renormalization scale (μ_R) are chosen as the invariant mass of the final state particles and MSTW2008LO (68%CL) PDF has been used. Throughout this chapter, we have considered five massless quark flavors ($n_f = 5$) and neglected all top quark contributions. In case of processes containing two or three photons in final state, a photon separation cut $\Delta R_{\gamma\gamma} > 0.3$ is used during event generation. $\Delta R_{\gamma\gamma} = \sqrt{(\Delta y)^2 + (\Delta\phi)^2}$ is the separation of the two photons in the rapidity-azimuthal angle (y, ϕ) plane. For processes involving leptons and photons in final state, we have applied $\Delta R_{\gamma\ell} > 0.3$ and $\Delta R_{\ell^+\ell^-} > 0.3$. For consistently merging 0-jet sample with 1-jet sample we have followed the path prescribed in [116] and checked the stability of the cross-

section by varying the scale Q_{cut} . Additional checks on the smoothness of the distributions, for example the differential jet-rate (DJR) plots, in the ME and PS transition region have been done. For the four processes under consideration the choices of Q_{cut} are much the same around 90 - 95 GeV where we find best smooth DJR plots and also the matched cross-section remains within 13% of the unmatched cross-section. For $\gamma\gamma\gamma$, γZZ and ZZZ we choose $Q_{cut} = 95$ GeV whereas for $\gamma\gamma Z$ we took $Q_{cut} = 90$ GeV. Showering is done with PYTHIA P_T -ordered shower as described in the previous section. Different analysis cuts used on the final state particles at the time of analysis are described in the following subsections for each processes.

For the processes involving photons, the photons can come from the hard process or as a result of fragmentation which is a QED collinear effect. In order to get rid of such collinear divergences without involving additional non-perturbative effects, the smooth cone isolation criteria on the photons as proposed by Frixione [123], is used. A cone of radius $R = \sqrt{(y - y_\gamma)^2 + (\phi - \phi_\gamma)^2}$ is considered in the $(y - \phi)$ plane around a photon satisfying the condition that the total hadronic transverse energy $E(R)$ within $R < R_\gamma$ would be less than a maximum limit $E(R)_{max}$ given by,

$$E(R)_{max} = \epsilon_\gamma E_T^\gamma \left(\frac{1 - \cos R}{1 - \cos R_\gamma} \right)^n , \quad (4.5)$$

where E_T^γ is the transverse energy of the photon; $\epsilon_\gamma, R_\gamma, n$ are three parameters of the Frixione isolation. During event generation we choose $\epsilon_\gamma = 1, R_\gamma = 0.3, n = 1$.

For the reconstruction of Z bosons from opposite sign lepton-pair, events are selected based on the selection criterion:

$$|M_{\ell^+\ell^-} - M_Z| \leq 15 \text{ GeV} , \quad (4.6)$$

where $M_{\ell^+\ell^-}$ is the reconstructed invariant mass of the opposite sign lepton-pair. The

following transverse momentum and pseudo-rapidity cut on jets during analysis in all four processes are used

$$P_T^j > 50 \text{ GeV}, \quad \eta^j \leq 4.5 \quad (4.7)$$

For all four processes, an extra cut has been put on the final state particles invariant mass ($M > 600$ GeV) for transverse momentum distributions and rapidity distributions which are displayed in the respective figures. We have checked that the generated events give unbiased results with reference to the choices of generation and analysis cuts. Scale dependencies are obtained by varying the renormalization scale (μ_R) and the factorization scale (μ_F) [124] in the range $(\mu_R, \mu_F) = (\kappa_R \mu_0, \kappa_F \mu_0)$, where μ_0 is the invariant mass of the three vector boson final states or its decay products when Z s are involved. The scale factors κ_R, κ_F are in the range $(1/2, 2)$, we choose the combination $(\kappa_R, \kappa_F) = (1/2, 1/2), (1, 1), (1/2, 1), (1, 1/2), (1, 2), (2, 1), (2, 2)$ to study the scale variation. The scale uncertainty is represented by taking the envelope of all individual variations.

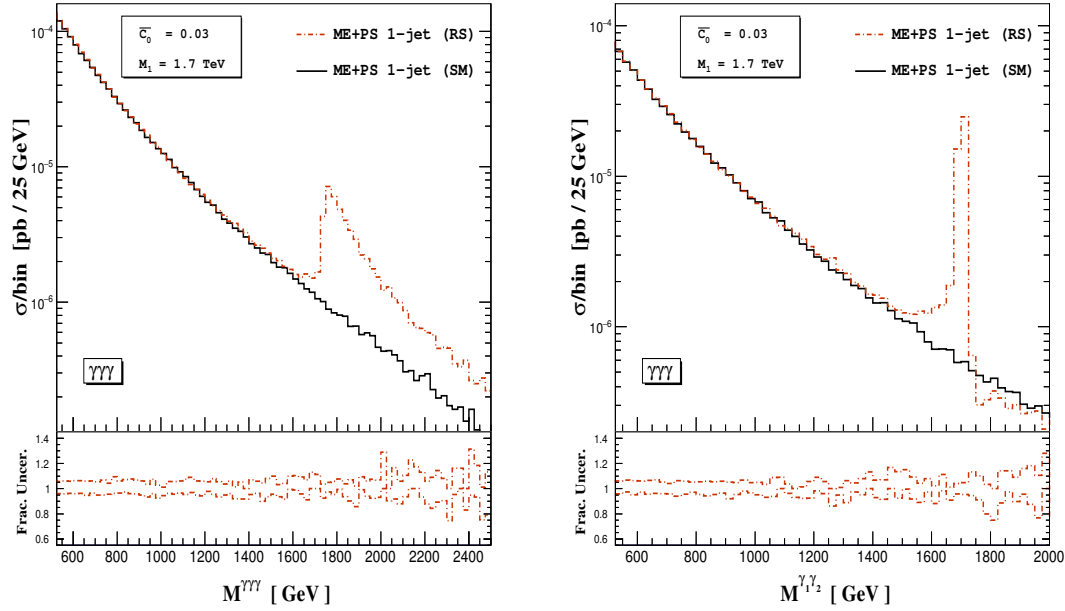


Figure 4.3: Invariant masses of $\gamma\gamma\gamma$ (left) and of two hardest photons (right) for $\gamma\gamma\gamma$ production.

Next we discuss and present our results for each of the neutral triple boson final states

separately presenting some select distribution that are of interest for the RS model. For all figures, we followed the following convention; we give the distributions corresponding to the SM and SM+RS that contribute to the observable for ME+PS merged to 1-jet for central scale choice $(\kappa_R, \kappa_F) = (1, 1)$. In the lower inset we put the fractional scale uncertainty for ME+PS with 1-jet for RS case.

4.4.1 $\gamma\gamma\gamma$

Observing the $\gamma\gamma\gamma$ channel has a great advantage over the other triple neutral channels, because experimentally it provides a cleaner signature. $\gamma\gamma\gamma$ production in the RS model has also been studied in [125]. Here we present the result merged with 1-jet as well as include showering thus improving the result, viable to the experimental search. During the analysis level we use more stringent cuts than that used at the generation level: (a) cuts on transverse momentum and pseudo-rapidity of final state photons used are $P_T^\gamma > 25$ GeV, $\eta^\gamma \leq 2.5$, (b) Frixione parameters used are $R_\gamma = 0.4$, $\epsilon_\gamma = 1$, $n = 2$ and (c) photon-photon separation cut $R_{\gamma\gamma} > 0.4$. Finally the photons are ordered according to their transverse momentum.

In the Fig. 4.3, we present the invariant mass distribution for tri-photon on the left panel and the invariant mass of the hardest di-photon state on the right panel. In the invariant mass distribution of the tri-photon the peak appears near 1.7 TeV. The peak is slightly shifted from 1.7 TeV towards higher invariant mass region. This is evident from the fact that the RS graviton is produced in association with a vector boson. In the expression for invariant mass there are dot products between all three momenta of the final state photons, thus shifting the peak slightly towards the higher invariant mass region. A cleaner signature of RS graviton can be found in the invariant mass distribution of the hardest two photon pairs where the RS peak appears at 1.7 TeV. From the transverse

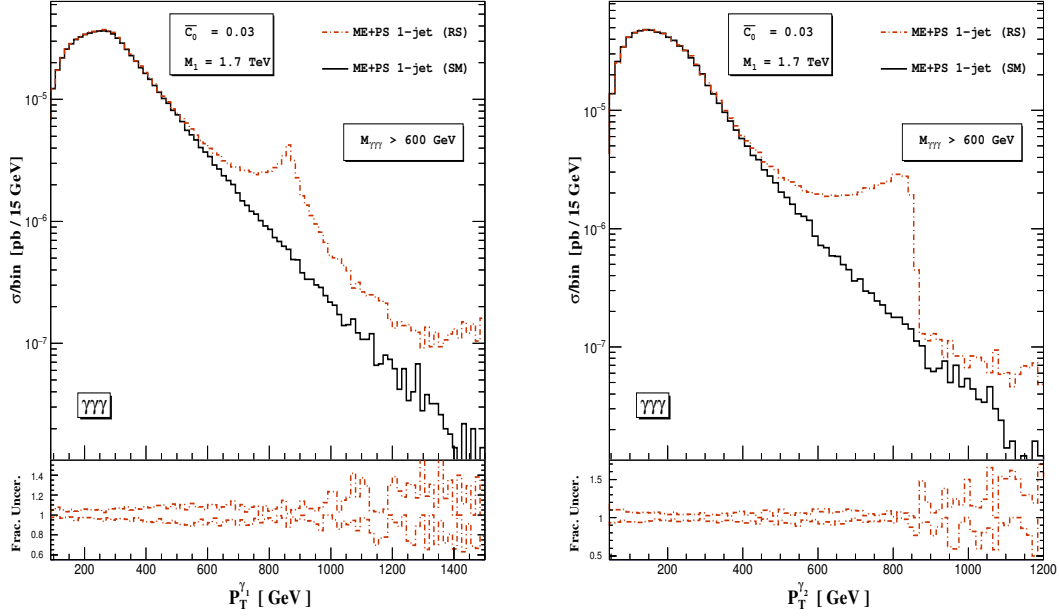


Figure 4.4: Transverse momentum distributions of hardest photon γ_1 (left) and next hard photon γ_2 (right) for $\gamma\gamma\gamma$ production.

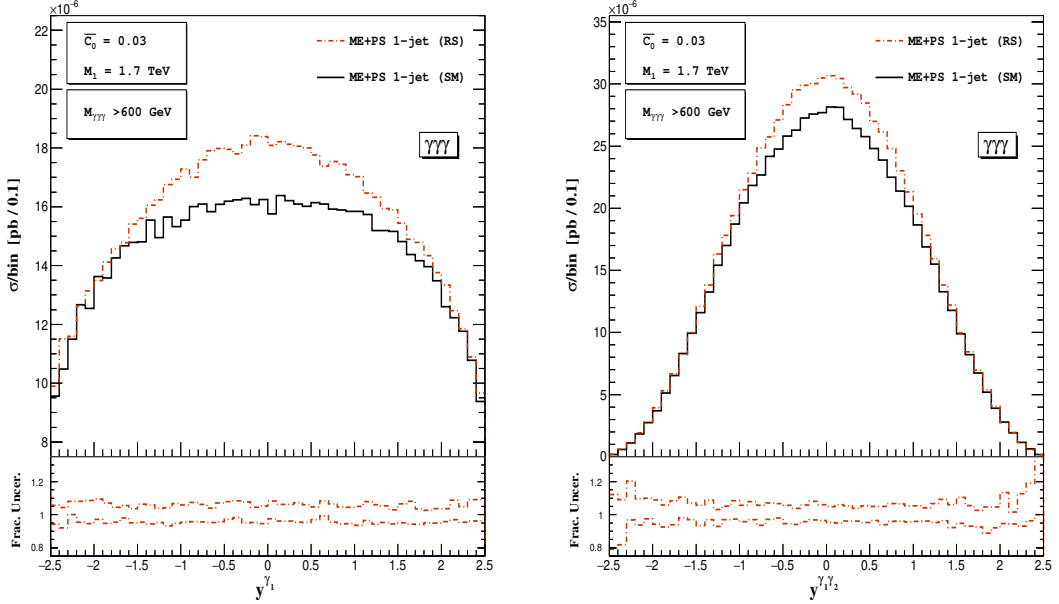


Figure 4.5: Rapidity distributions of hardest photon (left) and hardest pair (right) for $\gamma\gamma\gamma$ production.

momentum distributions (Fig. 4.4) as well as in the rapidity distributions (Fig. 4.5), significant deviation from SM results is observed. In general the 1-jet merged sample gives a harder distributions. For the Fig. 4.3 (left panel) the uncertainty at the RS peak

is about 7.7% and for the di-photon invariant mass (right panel) the uncertainty is about 10%. For the p_T distribution the uncertainties are larger, for the hardest photon (Fig. 4.4) it is about 15% and for the second hardest it is about 8.3% around the peaks in the P_T distribution which correspond to about half the RS resonance. For the rapidity plots (Fig. 4.5) the uncertainty is about 10% in the central rapidity region.

4.4.2 $\gamma\gamma Z$

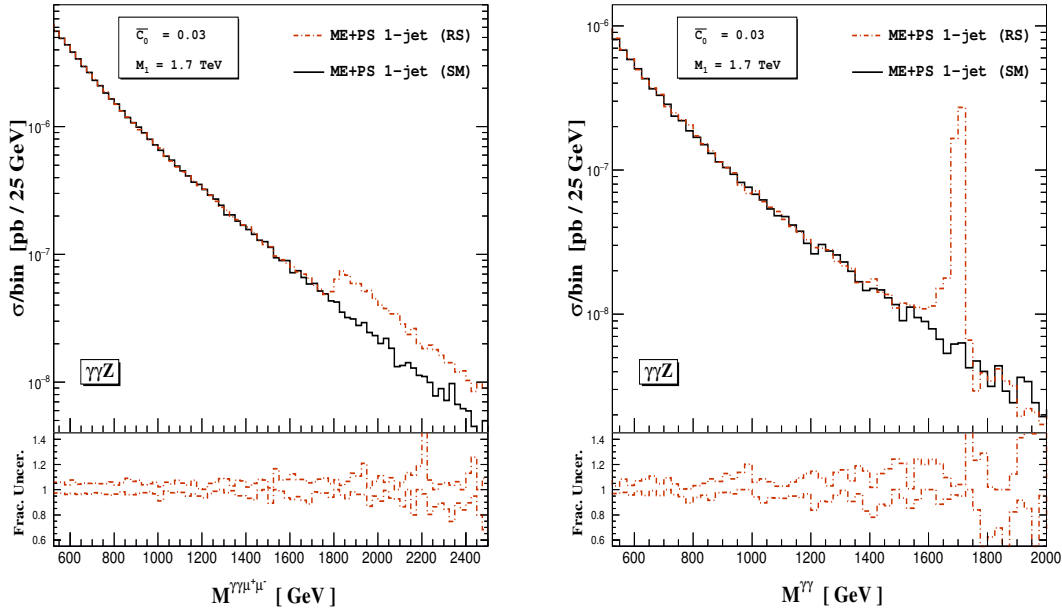


Figure 4.6: Invariant mass distributions of $\gamma\gamma\mu^+\mu^-$ (left) and $\gamma\gamma$ (right) for $\gamma\gamma Z$ production.

In $\gamma\gamma Z$ production the effect of the massive RS KK-modes can be observed in the $\gamma\gamma Z$ invariant mass as well as in the di-photon invariant mass (Fig. 4.6). The Z boson is allowed to decay to $\mu^+\mu^-$ pair. Minimal analysis level cuts on the final state leptons and photons transverse momentum $P_T^{\gamma,l} \geq 25 \text{ GeV}$ and pseudo-rapidity cut $\eta^{\gamma,l} \leq 2.5$ are put. In order to fulfill detector resolution, cuts on the separation of photon, lepton and

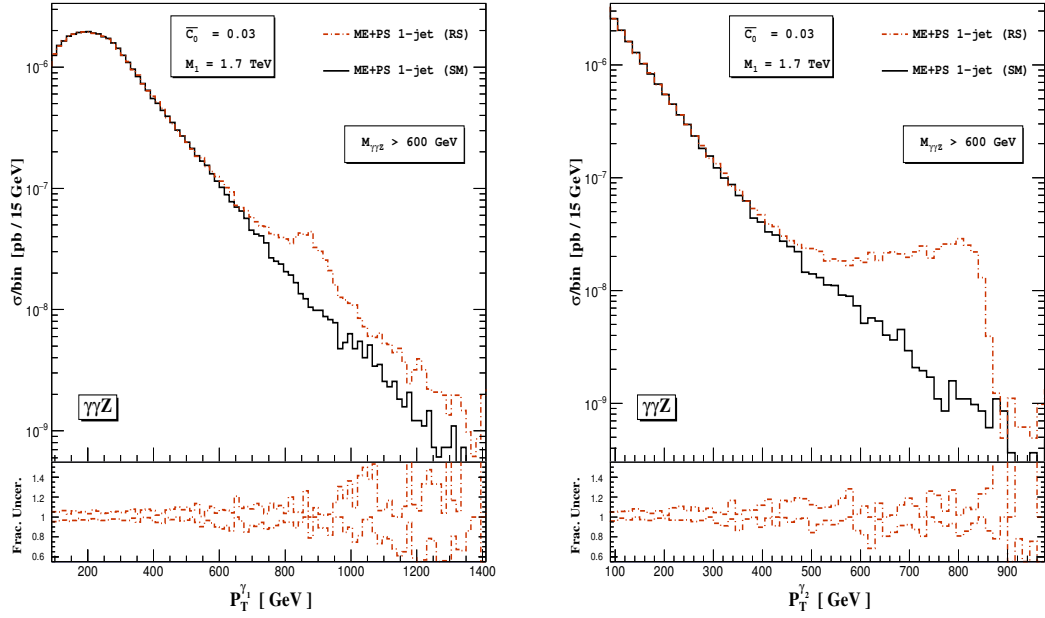


Figure 4.7: Transverse momentum distributions of hardest photon γ_1 (left) and second hard photon γ_1 (right) for $\gamma\gamma Z$ production.

jets are imposed:

$$R_{\gamma l} > 0.4, \quad R_{ll} > 0.4, \quad R_{lj} > 0.7 . \quad (4.8)$$

The invariant mass distribution of $\gamma\gamma\mu^+\mu^-$ system shows an enhancement at about the RS peak but is additionally shifted compared to the tri-photon case due to the mass of the Z boson. In this process the RS graviton can only decay into a photon-pair, hence the invariant mass distribution of di-photon pair shows the peak at the RS mass. The uncertainty in the enhanced region is about 8% for the $\gamma\gamma\mu^+\mu^-$ invariant mass distribution and for the di-photon invariant mass at the RS peak it is about 9.9%. The transverse momentum distributions (Fig. 4.7) of each photon clearly shows the RS signature appearing nearly at the half of the KK mass. The uncertainty for the transverse momentum distribution are much higher, at about 26%.

In the P_T distributions in Figs. 4.4, 4.7 the parton shower resums the large logarithms

in the collinear region which suppress the low P_T cross section. In this region the scale uncertainty is also low as the higher logarithms are resummed to all orders.

4.4.3 γZZ

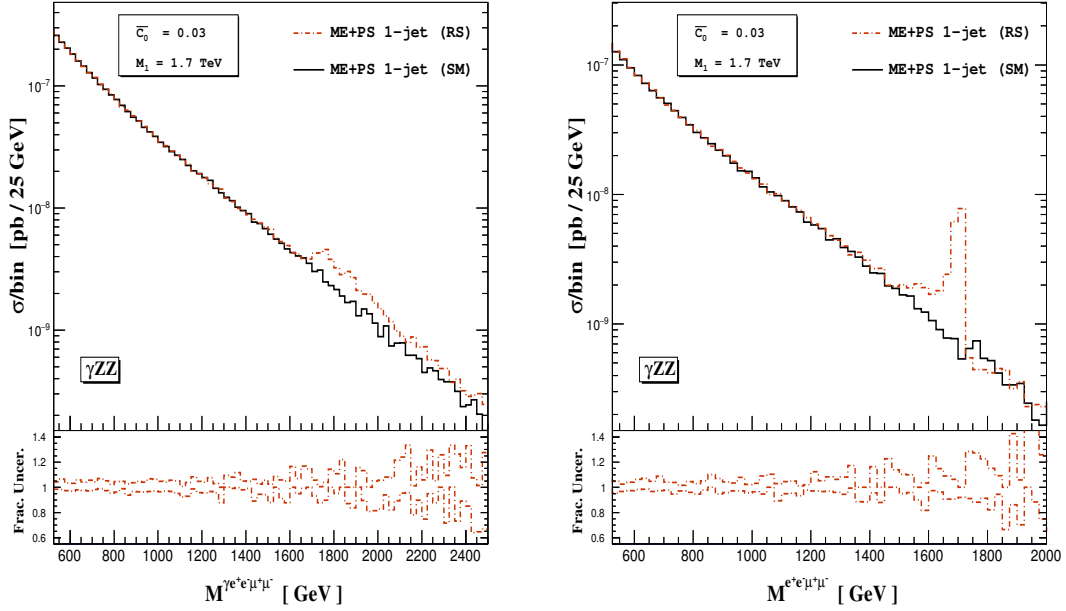


Figure 4.8: Invariant mass distributions of $\gamma e^+e^-\mu^+\mu^-$ (left) and $e^+e^-\mu^+\mu^-$ (right) for γZZ production.

The same set of analysis cuts are used here, as the $\gamma\gamma Z$ case. One Z -boson is decayed to a e^+e^- pair and the other Z -boson to a $\mu^+\mu^-$ pair during event generation. In the γZZ invariant mass distribution (Fig. 4.8) there is slight enhancement of RS contribution over the SM, around the invariant mass region (1.7 TeV). But the effect of massive KK state is best found on the di- Z boson invariant mass distribution (Fig. 4.8) and it peaks at 1.7 TeV as expected. The p_T distributions are not very useful to discriminating the RS signatures. The uncertainty for the invariant mass distribution of $\gamma e^+e^-\mu^+\mu^-$ system is about 15% and for the invariant mass of the $e^+e^-\mu^+\mu^-$ system which is as a result of the RS graviton decay is about 8.8%.

4.4.4 ZZZ

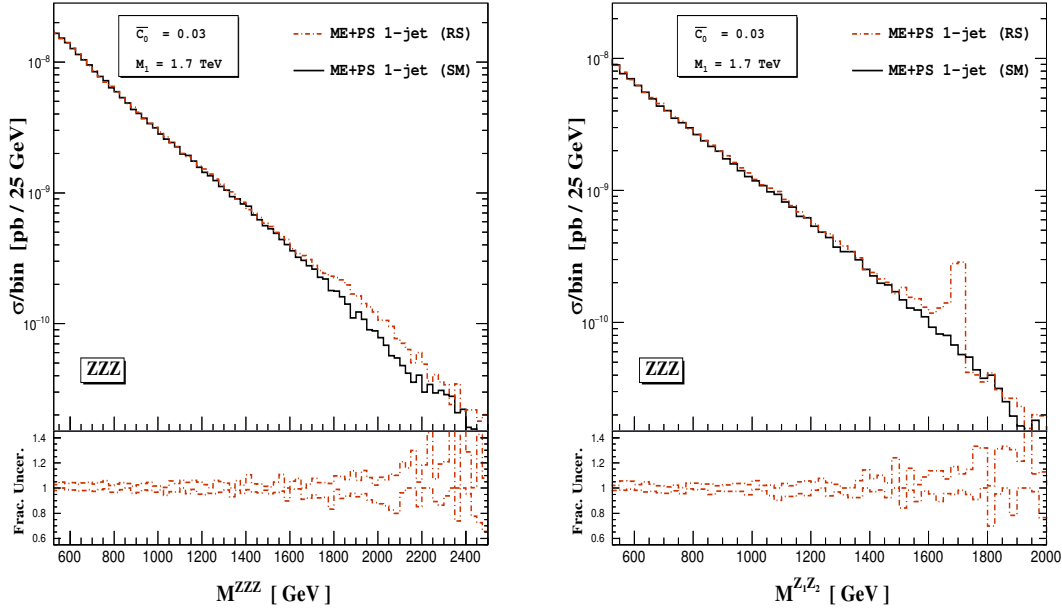


Figure 4.9: Invariant mass distributions of $e^+e^-\mu^+\mu^-\mu^+\mu^-$ (left) and hardest two lepton pairs (right) for ZZZ production.

For ZZZ production, we choose to decay two Z bosons to two $\mu^+\mu^-$ pairs whereas the other Z boson is decayed to a e^+e^- pair. For this process also same set of analysis cuts has been used, $P_T^l \geq 25 \text{ GeV}$, $\eta^l \leq 2.5$, where $l = e^+, e^-, \mu^+, \mu^-$. The Z bosons are reconstructed according to the criterion described at the beginning of this section (see Eq. (4.6)). The reconstructed Z bosons are then ordered according to their transverse momentum. Thus in the figures $Z_{1,2}$ represents transverse momentum ordered Z bosons. Small enhancement over the SM can be seen in the ZZZ invariant mass distribution (Fig. 4.9 left panel). The uncertainty in that region is found to be about 13-14%. In this case also the RS contribution is best found in the hardest two Z boson invariant mass distribution (Fig. 4.9 right panel). The uncertainty at the peak region is about 13.25%.

4.4.5 Event Estimation at the LHC

The invariant mass spectrum can be used to estimate the signal as well as background events at the LHC. We have taken the $\gamma\gamma\gamma$ process for this purpose. Here signal refers to the SM+RS events and background as SM only. From the invariant mass distributions (Fig. 4.3) an estimation of the signal and background events for the LHC Run-II with 13 TeV center-of-mass energy can be made. For this purpose we have considered the invariant mass distributions over 1500 GeV where the enhancement due to RS graviton signal is clearly visible over the SM background. We find that for 100 fb^{-1} luminosity there are 8 signal events over 3 background events from the $M^{\gamma\gamma\gamma}$ distribution (Fig. 4.3 left panel) and 6 signal events over 2 background events from $M^{\gamma_1\gamma_2}$ distribution (Fig. 4.3 right panel).

4.5 Conclusions

In the context of RS model, effects of the exchange of virtual KK graviton have been studied on the neutral triple gauge boson production processes at the 13 TeV LHC. This process could play a vital role in discriminating physics beyond the SM and in estimating the contribution coming from potential BSM scenarios in new physics searches. We have incorporated the RS model, using FeynRules in association with an algorithm that takes care of the KK mode summation of gravitons within MADGRAPH5 environment and performed a number of checks to ensure their proper implementation.

We have merged $P \ P \rightarrow VVV$ and $P \ P \rightarrow VVV + j$ event samples for better prediction of the distributions and observe that it gives harder distributions compared to the unmerged sample. To make theoretical prediction closer to the experimental situation, we have also matched the merged events with parton shower. Final state Z bosons are

allowed to decay to either of the following leptonic decay modes: (i) $Z \rightarrow e^+e^-$, (ii) $Z \rightarrow \mu^+\mu^-$ at the time of event generation, thus taking into account off-shell effects as well. For process with more than one stable photon, the photons are ordered according to their P_T and then the required number of photons are collected, based on their hardness. Likewise, for triple Z -boson production, Z bosons are reconstructed from their daughter particles and then ordered according to the hardness. Numerical results of some selective differential distributions for a set of kinematical variables have been presented for the merged samples. All these codes are flexible enough to incorporate the experimental cuts, different values for model parameters *etc.* and they can be used to obtain numerical results of any kind of distributions that would indeed help the experimental collaborations.

Of the neutral tri-gauge boson final states considered here, the tri-photon final state has the highest rate and can be used to look for signatures of the RS model. For the tri-photon process, the invariant mass, P_T distributions of various photons ordered in terms of the hardness and rapidity distributions are all good discriminators of the RS model. The scale uncertainties are by and large within 10% for the invariant mass distribution. In the tri-final invariant mass distribution the cross section is enhanced in the RS resonance peak region, which diminishes in going from the $\gamma\gamma\gamma$ to the ZZZ final state. The di-invariant mass distribution for all four processes is a clear indicator of the RS resonance peak. In the di-invariant mass distributions the peak of the RS resonance is most enhanced for the $\gamma\gamma\gamma$ and diminishes in going to the ZZZ production process.

Although the soft region is correctly described by parton shower and the hard region by extra jet merging, the cross-section is still LO accurate. It would be more convenient to have the cross-section with NLO accuracy as well. There are several methods like POWHEG, MC@NLO etc. which can achieve the NLO cross-section as well as the soft region is correctly described by parton shower. In the next chapter we will explore the production of di-final states in the RS model with MC@NLO matching.

DI-FINAL PRODUCTION AT NLO+PS ACCURACY IN RS MODEL

5.1 Introduction

Search of physics beyond the SM is an important objective of the LHC physics program and is motivated by the large hierarchy that exists between the gravitational Planck scale and the electro-weak symmetry breaking scale. Among various options, an interesting alternative that addressed the hierarchy problem was achieved by invoking extra spacial dimensions in TeV scale brane world scenarios [81, 82, 99]. Classification based on the geometry of extra spacial dimension leads to two classes of model *viz.* the factorizable [81, 82] and non-factorizable extra dimensions [99]. In both these models the SM particles are constrained in the 4-dimensional world and only gravity is allowed in the extra dimensional bulk. The ADD model with factorizable extra dimensions, has negligible curvature results in a tower of spin-2 Kaluza-Klein (KK) modes while the RS model with non-factorizable extra dimension has significant curvature leading to narrow spin-2 KK mode resonances. The phenomenology of these two models are quite distinct, with the ADD model leading to an enhancement of the tale of the invariant mass distribution as a result of the combined effect of the tower of KK modes. In contrast, the RS model leads to the production of

a narrow width RS KK mode resonances. The KK modes could be produced *via* the $q\bar{q}$ channel or the gg channel which would then decay to SM bosons or fermions leading to di-final states. These processes are being explored at the LHC leading to bounds on the model parameters [84, 85, 120, 126]. Of course, to put stringent bounds on the model parameters at a hadron collider like the LHC, it is essential to have the next-to-leading order (NLO) QCD corrections, as the leading order (LO) predictions suffer from large theoretical uncertainties. Presently the di-final state processes are available to NLO accuracy for DY [127, 128], di-photon [94, 129], ZZ [100, 130], W^+W^- [101, 131] and di-jet [132] for the extra dimension scenarios ADD and RS. This has been further extended to the NLO+PS accuracy for the ADD model for the di-final state processes [133, 134], excluding the jets.

In this chapter, we present the di-final state production processes (except those containing jet(s) in the LO) at hadron colliders which are interfaced with Parton Shower (PS) Monte Carlo to NLO accuracy using the MC@NLO formalism for the RS model. It should be pointed out that, the success to fully automatize the SM calculations to this accuracy is rather recent [118], but the status of BSM models to the same accuracy is still wanting. Precise theoretical predictions to NLO+PS accuracy are extremely desirable for the RS model and hence these codes are being made available for the LHC community. Various physical observables are studied, which are of relevance to future studies of these processes. These processes have been probed at the LHC Run I, in the SM, Higgs production and BSM searches and a more detailed study is expected in the Run II.

5.2 NLO with PS : MC@NLO

The fixed order NLO result is needed for better accuracy for the cross-section but it fails in the soft and collinear region whereas PSMC correctly describes the infrared region.

Therefore for better description of the observables it is needed to merge these two approach. The main problem in this procedure is that there could be double counting (or deficit) due to real emission (or non-emission) from MC as well as from fixed order NLO computation in some kinematical configurations. This happens in the soft and collinear region where both MC and fixed order (FO) NLO have contributions. Therefore the goal is to avoid any double counting or gap so that the full phase-space is correctly described.

The MC@NLO approach to match PS with fixed order NLO is mainly based on a modified subtraction method. The subtraction term $S(\Phi_1)$ is taken to be identical with the singular part from the real emission $R^s(\Phi_1)$ which in turn can be factorized in terms of universal subtraction terms containing parton shower splitting kernels,

$$S(\Phi_1) = B(\Phi_B) \otimes \mathcal{P}(\Phi_1) \quad (5.1)$$

The differential cross-section for the first emission can be written as,

$$\begin{aligned} d\sigma^{\text{NLO}} = & \left[B(\Phi_B) + \alpha_s V(\Phi_B) + \alpha_s B(\Phi_B) \otimes \int \mathcal{P}(\Phi_1) d\Phi_1 \right] d\Phi_B \\ & \times \left[\Delta(Q^2, Q_0^2) + \int_{Q_0^2} \frac{dq^2}{q^2} \int dz \frac{\alpha_s}{2\pi} \mathcal{P}(z) \Delta(Q^2, q^2) \right] \\ & + \left[\alpha_s R(\Phi_{B+1}) - \alpha_s B(\Phi_B) \otimes \mathcal{P}(\Phi_1) \right] d\Phi_{B+1} \end{aligned} \quad (5.2)$$

Naively in a parton shower monte carlo one adds shower approximations on the born configurations. But then the rate won't be NLO accurate and also the hard region will not be correctly described. So it needs to shower from NLO results, but in that case there will be double counting as shower also can add contributions which are already present in NLO. Through the MC@NLO formalism these double counting are avoided so that the soft and collinear is correctly described by parton shower and the hard region by NLO

result. The matched differential cross-section is given by

$$\begin{aligned} d\sigma^{\text{MC@NLO}} = & \left[B(\Phi_B) + \alpha_s V(\Phi_B) + \alpha_s B(\Phi_B) \otimes \int \mathcal{P}(\Phi_1) d\Phi_1 \right] d\Phi_B I_B^{MC} \\ & + \left[\alpha_s R(\Phi_{B+1}) - \alpha_s B(\Phi_B) \otimes \mathcal{P}(\Phi_1) \right] d\Phi_{B+1} I_{B+1}^{MC} \end{aligned} \quad (5.3)$$

where I^{MC} is so called the interface-to-MC. It can be seen from Eq. 5.3, two kinds of events can be generated, one with born configurations named as \mathbb{S} events and one with real emission configurations called \mathbb{H} events. Each of these terms are separately divergent free. It can be seen from Eq. 5.3 that the MC@NLO result is mostly dominated by the \mathbb{S} events except for the large p_T region. The \mathbb{H} events have minor contribution to the infrared region since it is almost vanishing at this region, whereas it is non-vanishing in the hard region and gives contribution to the cross-section and distributions. One important feature evident from Eq. 5.3 is that the weight of \mathbb{H} events can be negative for some cases where the counter term dominates. Note that this is necessary for correct prediction of NLO rate and we can't force to have positive events unlike generators like POWHEG. Needless to say that the fraction of such negative weights is small in order to get a physical NLO cross-section. There is no restriction put on the radiations from the shower emission from the \mathbb{H} events, *i.e.* the shower emission should be softer than the NLO real emission. The cross-section for producing events in the phase space region where shower can generate much harder radiations than in \mathbb{H} events are power suppressed as \mathbb{H} events being non-singular in the infrared region. The MC@NLO result correctly describes the soft and collinear region also more stable than the fixed order NLO result. This is due to the absence of divergences in the weights within the \mathbb{S} and the \mathbb{H} events separately, rather than cancellation of opposite divergences between two samples. The MC@NLO result correctly predicts the high- p_T region at NLO accuracy as well as the low-pt region the distributions are correctly described by parton shower dominated by the \mathbb{S} events.

5.3 Di-final State Production in RS Model

We have considered NLO QCD corrections to all the jet-exclusive tree level di-final state processes, namely Drell-Yan, di-photon, ZZ and W^+W^- production processes in the SM as well as in the RS scenario and these $\mathcal{O}(\alpha_s)$ corrected results are then matched with parton shower Monte Carlo using MC@NLO formalism [135]. The Feynman diagrams for the born process are shown in Fig. (5.1). The long-dash lines represent the colorless di-final states *viz.* $\gamma\gamma, \ell^+\ell^-, ZZ$ and W^+W^- . The RS graviton is shown as the double curly lines. The typical virtual corrections are shown in Fig. (5.2). The real correction Feynman diagrams are shown in Fig. (5.3) for $q\bar{q}$, Fig. (5.4) for qg and in Fig. (5.5) for gg channels. The total RS contribution represents both the signal and background



Figure 5.1: Born contribution for colorless di-final production through RS graviton. The long-dash line represents the di-final states *viz.* $\gamma\gamma, \ell^+\ell^-, ZZ$ and W^+W^- . The RS graviton is shown as double curly lines.

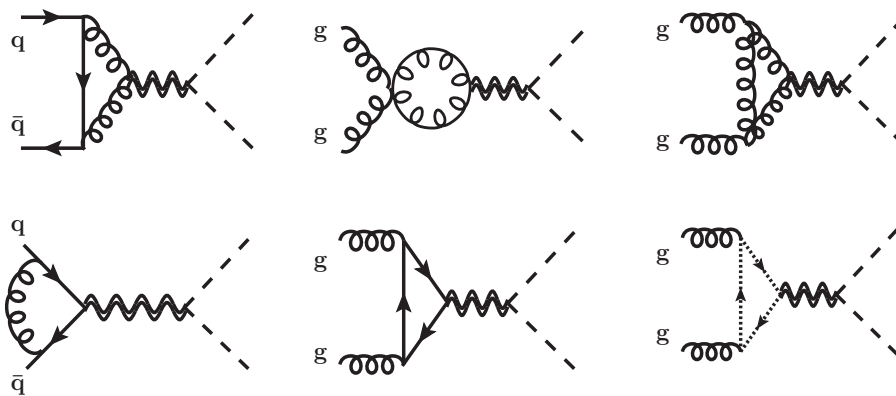


Figure 5.2: Virtual corrections for colorless di-final production through RS graviton. The last diagram involves ghost loop (dotted line) appearing due to the use of Feynman Gauge.

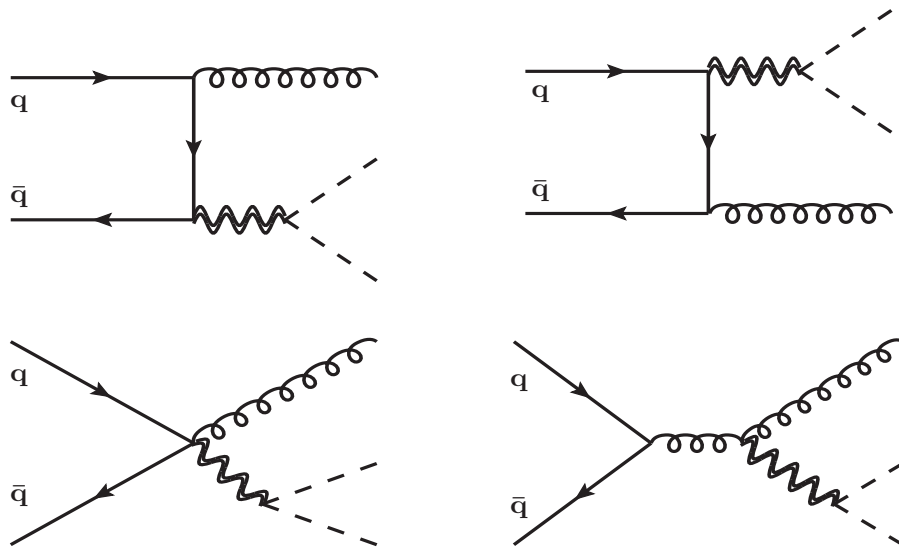


Figure 5.3: Real corrections ($q\bar{q}$ initiated) for colorless difinal production through RS graviton.

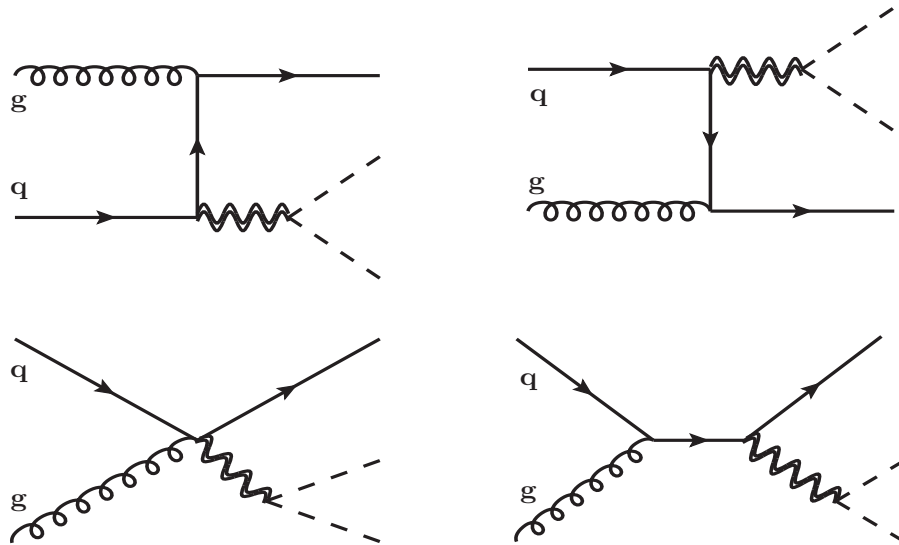


Figure 5.4: Real corrections (qg initiated) for colorless difinal production through RS graviton.

together consisting of pure SM, pure BSM and the interference between the two, whereas the SM contribution alone is treated as background.

For all the above mentioned processes, the parton level Born squared amplitude in the SM comes only from $q\bar{q}$ initiated Feynman diagrams, while in the RS model both $q\bar{q}$ and

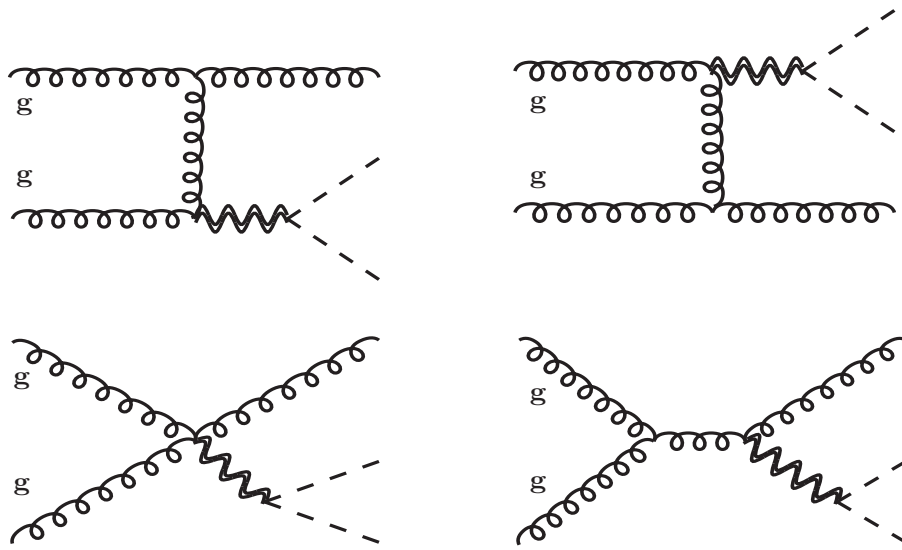


Figure 5.5: Real corrections (gg initiated) for colorless difinal production through RS graviton.

gg initiated Feynman diagrams contribute. In addition there is interference terms between the SM and RS model subprocesses. In the fixed order analysis, the $\mathcal{O}(\alpha_s)$ correction terms correspond to two categories of Feynman diagrams: (i) real emission and (ii) one-loop virtual correction. In the real emission part, $q\bar{q}$ or gg initiated subprocesses contribute leading to an extra gluon emission in addition to the desired final state. The $\bar{q}(q)g$ initiated partonic subprocesses begin to contribute at $\mathcal{O}(\alpha_s)$. Matrix elements coming from the one-loop virtual diagrams participate in the $\mathcal{O}(\alpha_s)$ correction, when multiplied by the corresponding Born amplitude. All these partonic subprocesses producing $\mathcal{O}(\alpha_s)$ correction terms behave alike for all of our processes of interest. Moreover, one additional $\mathcal{O}(\alpha_s)$ contribution shows up in the fixed order calculation for the di-boson final state processes due to the interference between gg initiated box diagrams in the SM and gg initiated Born diagrams in the RS scenario. We have taken care of all the aforesaid contributions in our present calculation.

While dealing with Drell-Yan process, we have only considered e^+e^- final state, as the other possible channel *i.e.* $PP \rightarrow \mu^+\mu^-X$ would be phenomenologically same with the

chosen one, apart from the experimental identification of the final state particles. In case of di-photon production, we have adopted smooth cone isolation technique [123] proposed by Frixione to get rid of using fragmentation contribution which are non-perturbative in nature which indicate the probability of fragmenting a parton into photon. We call it as Frixione isolation (FI) which ensures that soft radiation is not eliminated in any region of phase space and at the same time guarantees infra-red (IR) safety of the observable. In order to implement it, a cone of radius $r = \sqrt{(\eta - \eta_\gamma)^2 + (\phi - \phi_\gamma)^2}$ is to be defined centering around the direction of each photon in the pseudo-rapidity (η) and azimuthal angle (ϕ) plane. It is then demanded that in order to satisfy the isolation criteria, the sum of the hadronic transverse energy $H(r)$ has to be always less than $H(r)_{\max}$ for all cones with radius $r \leq r_0$. In the present analysis, we have taken following choice of $H(r)_{\max}$ defined as,

$$H(r)_{\max} = \epsilon_\gamma E_T^\gamma \left(\frac{1 - \cos r}{1 - \cos r_0} \right)^n , \quad (5.4)$$

where E_T^γ is the transverse energy of the photon and ϵ_γ , r_0 and n are three FI parameters that are to be specified while applying such isolation. On-shell Z and W^\pm have been produced while generating events for ZZ and W^+W^- production processes respectively. The two Z bosons are then leptonically decayed to e^+e^- and $\mu^+\mu^-$ respectively at the time of showering. The decay channels $W^+ \rightarrow e^+\nu_e$ and $W^- \rightarrow \mu^-\bar{\nu}_\mu$ have been taken into account while showering W^+W^- events.

Owing to the tremendous development in computation of NLO correction in the last few years, automation plays an important role throughout this work. The universal Feyn-Rules [119] output (UFO) of the RS model has been imported within the MADGRAPH5 (MG5) environment [136]. We choose to work in the MG5_AMC@NLO framework [118] in which the Born level square matrix elements are generated using MG5 and calculation of the real emission cross sections together with their singularities are overseen by

MADFKS [137] package which uses the FKS subtraction scheme [69] in an automated way. However, a set of external FORTRAN codes, that handle virtual contributions, have been prepared using the analytical results involving one-loop amplitudes for e^+e^- [102], $\gamma\gamma$ [94], ZZ [100], W^+W^- [101] in the SM & RS model and they have been systematically implemented into this framework. Nevertheless, another in-house FORTRAN code which takes care of the summation of KK-tower propagators, has suitably been fitted in this environment, thereby making essential and appropriate changes in the spin-2 HELAS routines [133]. We have explicitly checked numerical cancellation of double and single poles coming from the real and virtual parts for all these processes and thereafter used this complete set-up to generate corresponding events. The generated events are then matched with HERWIG6 [138] parton shower using AMC@NLO, where the MC@NLO formalism is being automatized. Uncertainties in renormalization (μ_R) and factorization (μ_F) scale and in parton distribution functions (PDF) are also estimated in an automated way with no extra CPU cost. Note that, instead of decaying a particle at the time of showering, it is also possible to decay it into its preferred decay channel at the event generation level itself by making the use of MADSPIN [139] that restrains nearly all spin correlations. However, to use the same for Z or W^\pm decay is beyond the current scope due to the significant complexity involved in including KK-tower summation and changing HELAS [140, 141] routines accordingly.

5.4 Numerical Results

In this section, we present a number of differential distributions of various kinematical observables at the NLO+PS accuracy for e^+e^- , $\gamma\gamma$, ZZ , W^+W^- production processes at the LHC with center of mass energy $\sqrt{S} = 14$ TeV. Following electro-weak input parameters have been used at the time of event generation: (i) $\alpha_{EW}^{-1} = 132.507$, (ii) $G_F =$

1.16639×10^{-5} GeV $^{-2}$, (iii) $M_Z = 91.188$ GeV and using them as input the mass of W boson $M_W = 80.419$ GeV and $\sin^2 \theta_w = 0.222$ are evaluated. We have considered $n_f = 5$ massless quark flavors in our present study. The central choices of μ_R and μ_F are always set equal to the invariant mass of the corresponding di-final state. MSTW(n)lo2008cl68 PDF sets [142] have been used throughout the analysis in order to generate (N)LO events and they determine the value of strong coupling α_s . (N)LO events are generated with very loose cuts on transverse momentum (P_T) and rapidity (y) of the final state particles and they are detailed here under: (a) Drell-Yan: $P_T^{e^+, e^-} \geq 15$ GeV, $|y^{e^+, e^-}| \leq 2.7$, $\Delta R^{e^+ e^-} > 0.3$, where $\Delta R = \sqrt{(\Delta y)^2 + (\Delta\phi)^2}$ denotes the separation between two particles in the rapidity-azimuthal angle plane, (b) Di-photon: $P_T^\gamma \geq 15$ GeV, $|y^\gamma| \leq 2.7$ with a set of particular FI parameters *i.e.*, $\epsilon_\gamma = 1$, $r_0 = 0.3$ and $n = 2$. However, no such kinematical cuts have been provided while generating events for ZZ and W^+W^- processes. Besides, for W^+W^- event generation we have taken diagonal unit CKM matrix and neglected top quark contribution in the whole analysis.

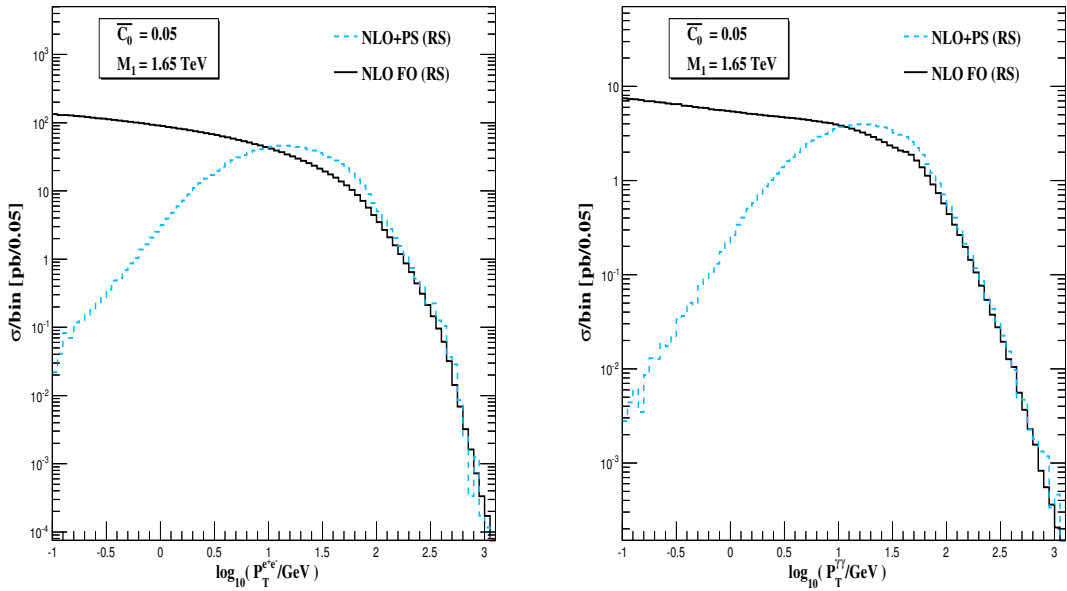


Figure 5.6: Transverse momentum distribution of RS contribution, shown in log-log scale at fixed order NLO and NLO+PS for the Drell-Yan (left) and di-photon (right) production processes.

The events thus generated are then matched with HERWIG6 [138] parton shower Monte Carlo using the MC@NLO formalism [135]. While showering di-lepton events, $P_T^l \geq 20$ GeV, $|y^l| \leq 2.5$, $\Delta R^{ll} > 0.4$ have been used for the analysis purpose, where $l = e^+, e^-$. In order to separate leptons from jets $\Delta R^{lj} > 0.7$ has also been applied at this stage and finally we have found out hardest e^+ and e^- to build several kinematical observables with them. In case of showering di-photon events, following analysis cuts are put on each photon with the following FI parameters: $P_T^\gamma \geq 20$ GeV, $|y^\gamma| \leq 2.5$, $\Delta R^{\gamma\gamma} > 0.4$ and $\epsilon_\gamma = 1$, $r_0 = 0.4$, $n = 2$ and we have collected two hardest photons γ_1 , γ_2 among many others. As described earlier, Z bosons are leptonically decayed at the time of showering ZZ events and the applied analysis cuts are as follows: $P_T^l \geq 20$ GeV, $|y^l| \leq 2.5$, $\Delta R^{ll} > 0.4$, $\Delta R^{lj} > 0.7$, where $l = e^+, e^-, \mu^+, \mu^-$. After that, all the final state stable leptons (*i.e.*, e^\pm, μ^\pm) are being collected to make pair of leptons that have equal flavor but opposite charge. Finally we have selected those leptons that are contributing as the hardest e^+e^- and $\mu^+\mu^-$ pairs with the condition that their invariant masses ($M^{l^+l^-}$) satisfy the criteria $|M^{l^+l^-} - M_Z| < 10$ GeV, to make sure that those leptons are actually decay products of the Z bosons. At the time of showering W^+W^- events with their corresponding decay modes, we have identified the final state stable lepton-neutrino pair whose mother is one of the W^\pm bosons and make them pass through the following set of analysis cuts: $P_T^l \geq 20$ GeV, $|y^l| \leq 2.5$, $\Delta R^{ll} > 0.4$, $\Delta R^{lj} > 0.7$ and $\cancel{E}_T > 30$ GeV. We have checked that all the above events generated in each processes produce completely unbiased results with the appliance of our present choices of generation and analysis cuts.

To show the effect of parton shower over the fixed order NLO results, we have presented in Fig. (6.3) the $\log_{10} P_T$ distributions of the e^+e^- (left) and $\gamma\gamma$ (right) pair at fixed order NLO (solid black) as well as in NLO+PS (dashed blue) accuracy for the RS case. Both the curves in each figure are plotted using respective analysis cuts and we have used the RS

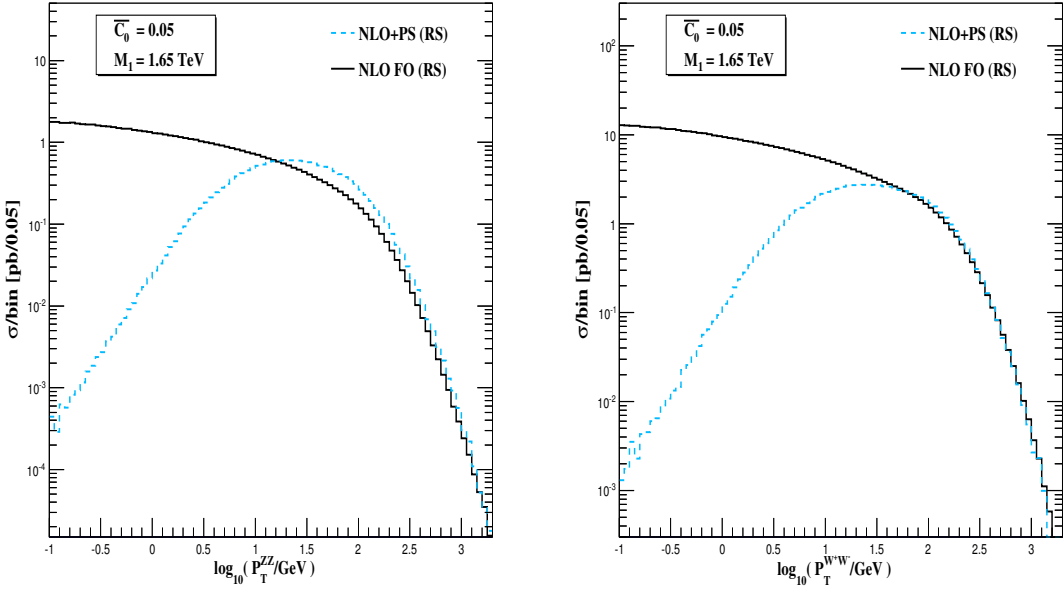


Figure 5.7: Transverse momentum distribution of RS contribution, shown in log-log scale at fixed order NLO and NLO+PS for the ZZ (left) and W^+W^- (right) production processes.

model parameter $\bar{C}_0 = 0.05$ and the corresponding M_1 value is taken as $M_1 = 1.65 \text{ TeV}$. Note that, by the label ‘RS’ in the figure, we mean the total contribution that consists of SM, RS and the interference between the two and we maintain the same convention in the rest of the figures as well. Likewise, Fig. (5.7) represents similar distributions for the ZZ (left) and W^+W^- (right) pairs. Each of these figures shows diverging nature of the fixed order NLO curve in the $P_T \rightarrow 0$ region, whereas the NLO+PS result gets convergent in that region ensuring the correct resummation of the Sudakov logarithms and thereby leading to a suppression in cross section in the low- P_T region. As expected, both the results are in good agreement with one another in the high- P_T region. Uncertainty calculations of various distributions have been performed automatically in the **AMC@NLO** framework by using its built-in re-weighting procedure that stores sufficient information in the parton level Les Houches event files. Independent variation of μ_R and μ_F scales are considered to calculate scale uncertainties. We have set $\mu_R = \xi_R M$ and $\mu_F = \xi_F M$, where M denotes the invariant mass of the di-final state (*i.e.*, $M^{e^+e^-}$, $M^{\gamma\gamma}$, M^{ZZ} or $M^{W^+W^-}$,

as applicable) and ξ_R , ξ_F can take any one of the values $(1, 1/2, 2)$ at a time. The scale uncertainty band would then be determined as the envelope [133] of the following (ξ_R, ξ_F) combinations: $(1, 1)$, $(1, 1/2)$, $(1, 2)$, $(1/2, 1/2)$, $(1/2, 1)$, $(2, 1)$, $(2, 2)$. On the other hand, PDF uncertainties are estimated using Hessian method as prescribed by the MSTW collaboration [142].

In all the subsequent figures, various distributions of kinematical observables are depicted using a consistent graphical representation. In the Figures the main frame, depicts distributions that are of outcome of both the RS (dash-dotted blue) and SM (solid black), are shown to NLO+PS accuracy, whereas the corresponding lower insets provide the estimation of the fractional scale (dashed red) and PDF (dash-double dotted green) uncertainties, which basically denote the variation of the central value (*i.e.*, the extremum value divided by the central value). Unless stated otherwise, $\bar{c}_0 = 0.05$ and $M_1 = 1.65$ TeV are used in all these plots.

5.4.1 $\ell^+ \ell^-$

Drell-Yan process is considered to be the standard candle which is both theoretically calculable and experimentally measurable with highest accuracy at the hadron colliders like the LHC. For the Drell-Yan production process, invariant mass distribution of the $e^+ e^-$ pair is shown in Fig. (5.8). The two peaks in the RS case indicate first (M_1) and second (M_2) excitations of the RS graviton and they perfectly match with the theoretical values (see Eq. ??). Fig. (5.9), (5.10) and (5.11) apprise the transverse momentum (left) and rapidity (right) distributions of the $e^+ e^-$ pair, e^+ and e^- respectively in the region $M_{e^+ e^-} > 600$ GeV. Such invariant mass cut, which is also applied consistently to the rest processes, is an optimal choice to reduce SM background effects, ensuring the influence of sufficient signal events at the same time. Individually, transverse momentum distributions

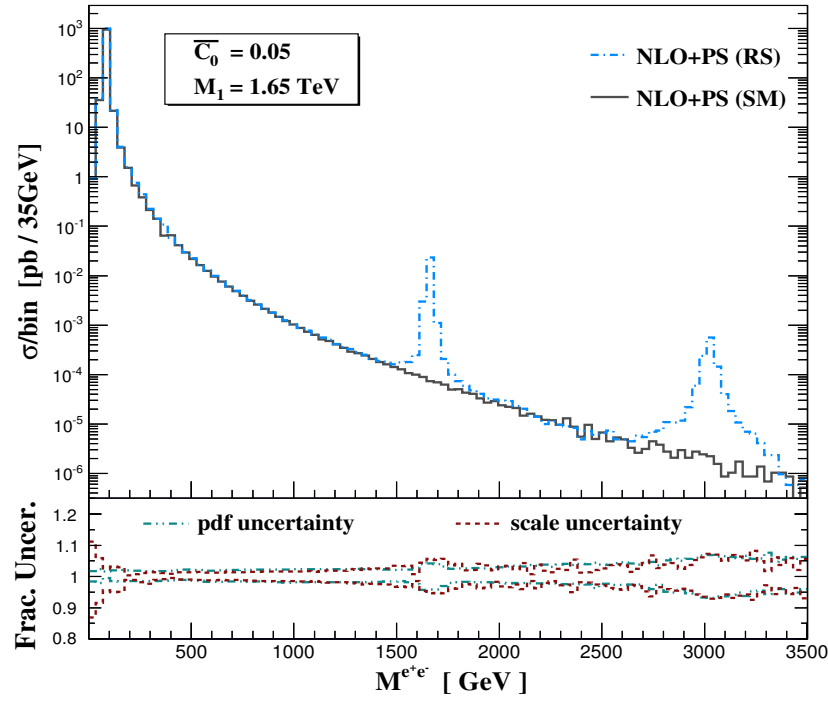


Figure 5.8: Invariant mass distribution of the di-lepton pair in Drell-Yan process for RS and SM.

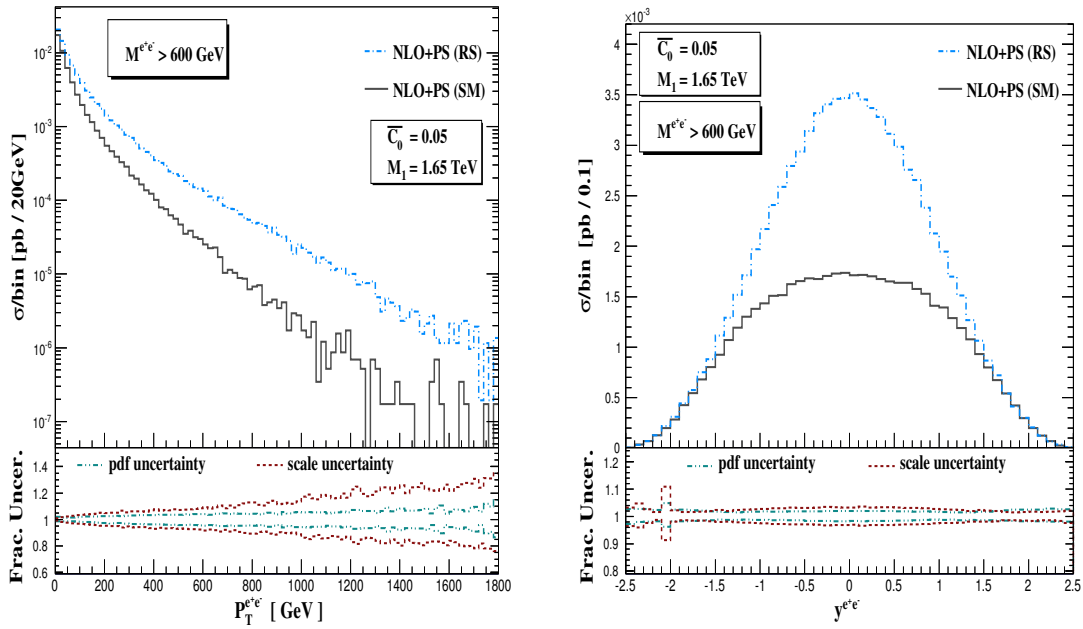


Figure 5.9: Transverse momentum (left) and rapidity (right) distribution of the di-lepton pair in both RS and SM.

of e^+ and e^- are of similar kind and two kinks are arising near the half of the M_1 and M_2 values. However, in the combined transverse momentum distribution of the e^+e^- pair,

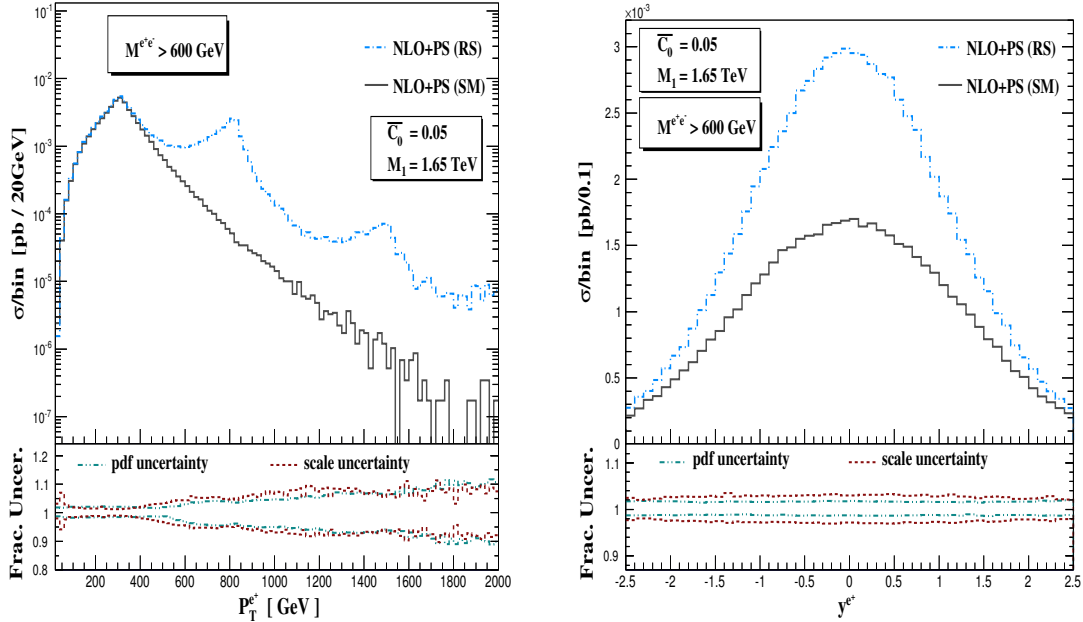


Figure 5.10: Transverse momentum (left) and rapidity (right) distribution of the positron for the Drell-Yan production process in SM and RS.

washing out of such kinks points out that the directions of outgoing e^+ and e^- are opposite to each other in the transverse plane of the beam direction. The fractional uncertainties associated with these P_T distributions are large in the high transverse momentum region, although they are quite minimal in the low- P_T region, where the higher order effects are included as a result of resummation. In the high- P_T region of e^+e^- pair, the large uncertainty is a reflection of the fact that it is in fact a leading order process. Note that, the rapidity distributions of e^+ and e^- are not similar because the high invariant mass cut is responsible in breaking the angular correlation between them. To estimate the improvement in the results while including NLO corrections, we find that the scale uncertainties in the central rapidity region of all these rapidity distributions in the RS case reduce to about 6-8% in NLO+PS, from about 10-12% at LO+PS. PDF uncertainties in NLO+PS are about 1-1.5% less compared to the LO+PS outcomes.

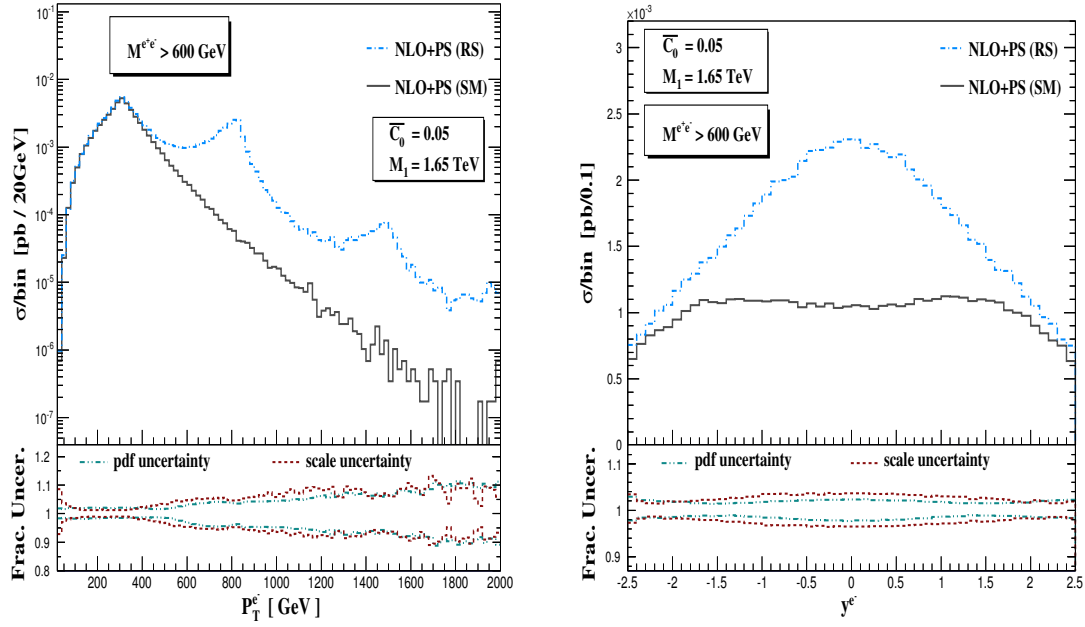


Figure 5.11: Transverse momentum (left) and rapidity (right) distribution of the electron for the Drell-Yan production process in SM and RS.

5.4.2 $\gamma\gamma$

Di-photon production is one important process to look for RS graviton resonance at the LHC. Distributions related to the di-photon production are shown in Fig. (5.12)-(5.14). In Fig. (5.12), we have presented invariant mass (left) distribution of the di-photon system and the separation (right) between the two hardest photons in the rapidity-azimuthal angle plane with the cut $M^{\gamma\gamma} > 600$ GeV. The invariant mass distribution clearly shows two peaks that correspond to the choice of M_1 value and the respective M_2 value derived from that. The $\Delta R^{\gamma\gamma}$ distributions are almost same for SM and RS and the peaks near the angle π (*i.e.*, 180°) in these distributions indicate the abundance of such two hardest photons that are mostly back-to-back and the associated scale uncertainty is becoming almost nil as the two photons are getting much away from one another. Fig. (5.13) and (5.14) represent the transverse momentum (left) and rapidity (right) distributions of the di-photon system and the hardest photon respectively in the region where the condition

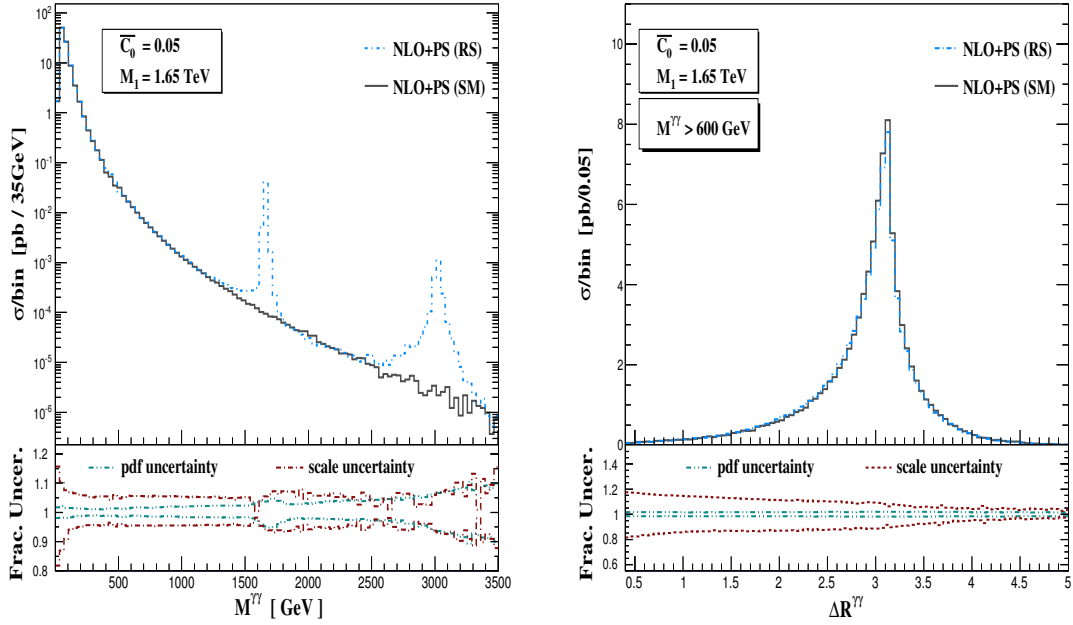


Figure 5.12: Invariant mass distribution of the di-photon pair (left) in RS and SM. The right panel shows the separation between two hardest photons in the rapidity-azimuthal angle plane.

$M^{\gamma\gamma} > 600$ GeV is satisfied. Here also, we are getting two kinks in the transverse momentum distribution of the individual hardest photon around the half of the first and second excitation values of the RS graviton. The scale uncertainties in the central rapidity regions in LO+PS were around 13-14% and they are as expected reduced to 10% in NLO+PS, although the reduction in PDF uncertainties is only about 0.2% between the NLO+PS and LO+PS results.

5.4.3 ZZ

In case of ZZ production, we have decayed the Z bosons into lepton pairs at the stage of showering. Then oppositely charged leptons are collected to form different observables like invariant mass of di- Z , transverse momentum, rapidity etc. Fig. (5.15)-(5.17) correspond to the distributions of decay products that are coming from the ZZ events. The invariant

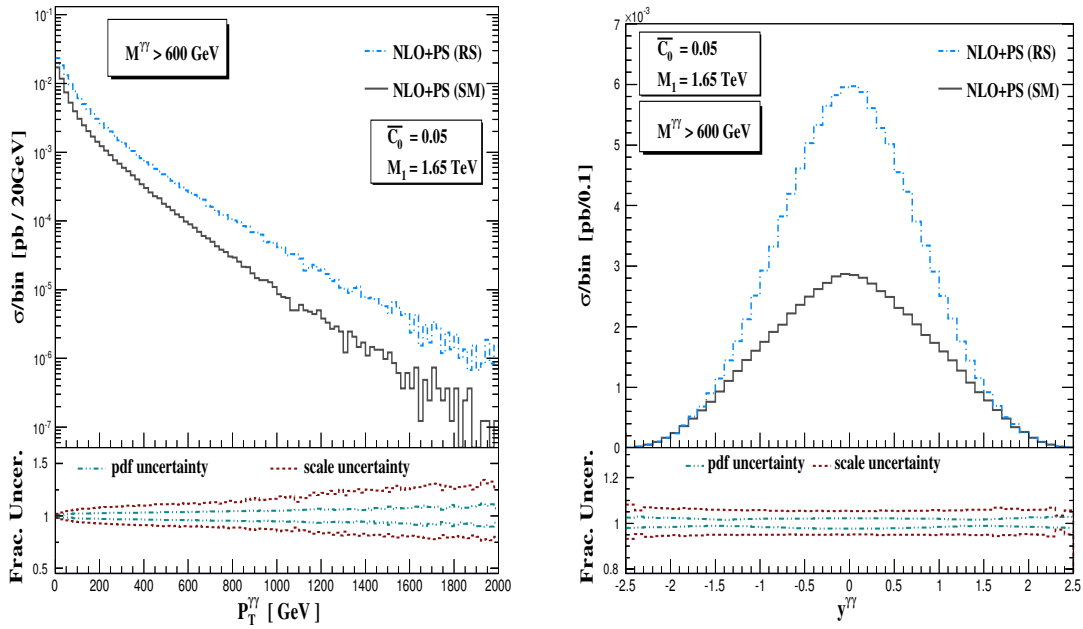


Figure 5.13: Di-photon transverse momentum (left) and rapidity (right) distribution in RS and SM.

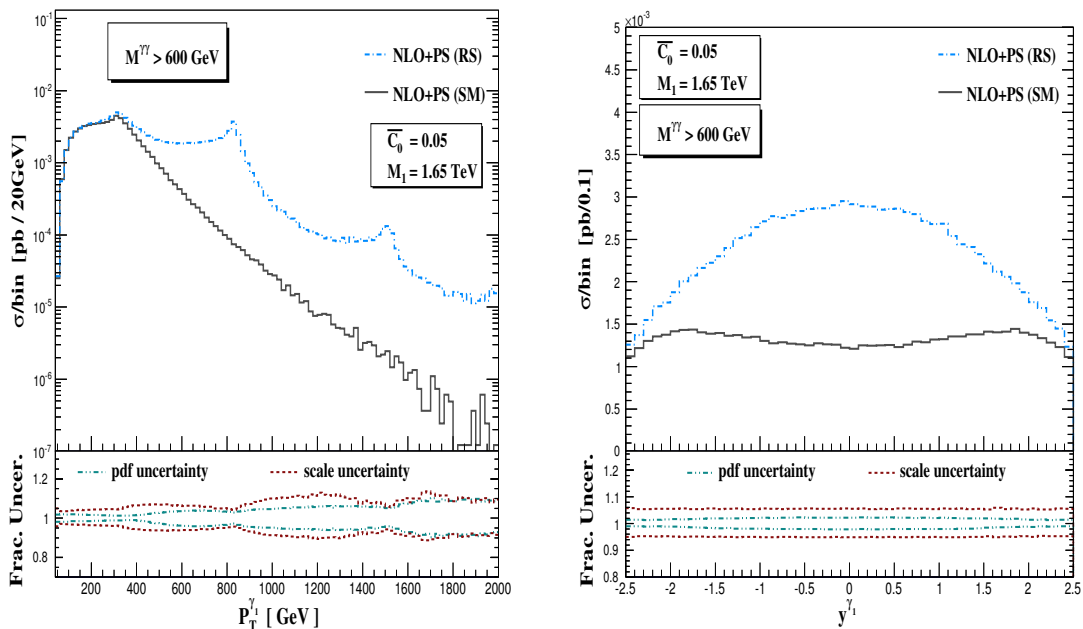


Figure 5.14: Transverse momentum (left) and rapidity (right) distribution of the hardest photon in di-photon production process in RS and SM.

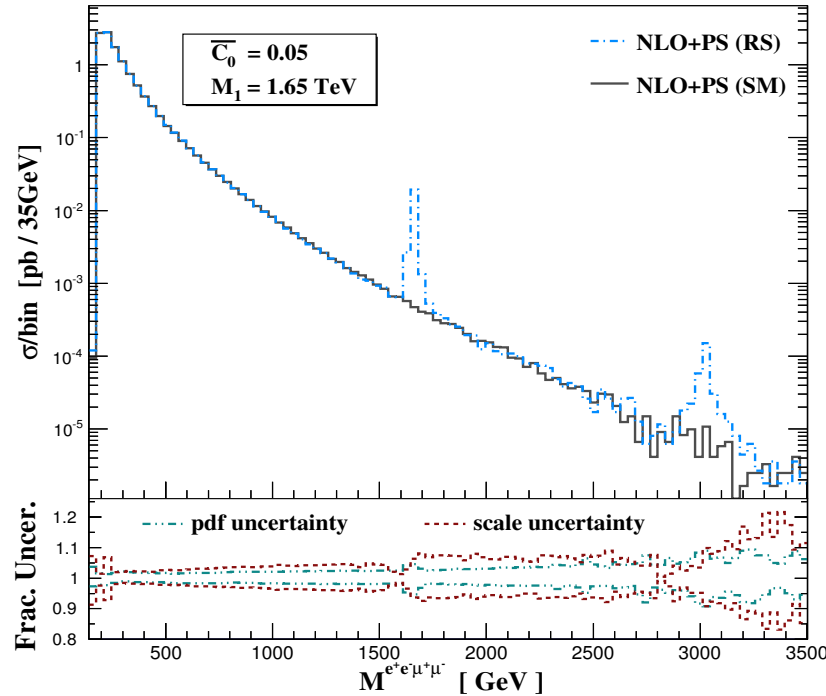


Figure 5.15: Four-lepton invariant mass ($M^{e^+e^-\mu^+\mu^-}$) distribution for RS and SM coming from the decay products of ZZ process.

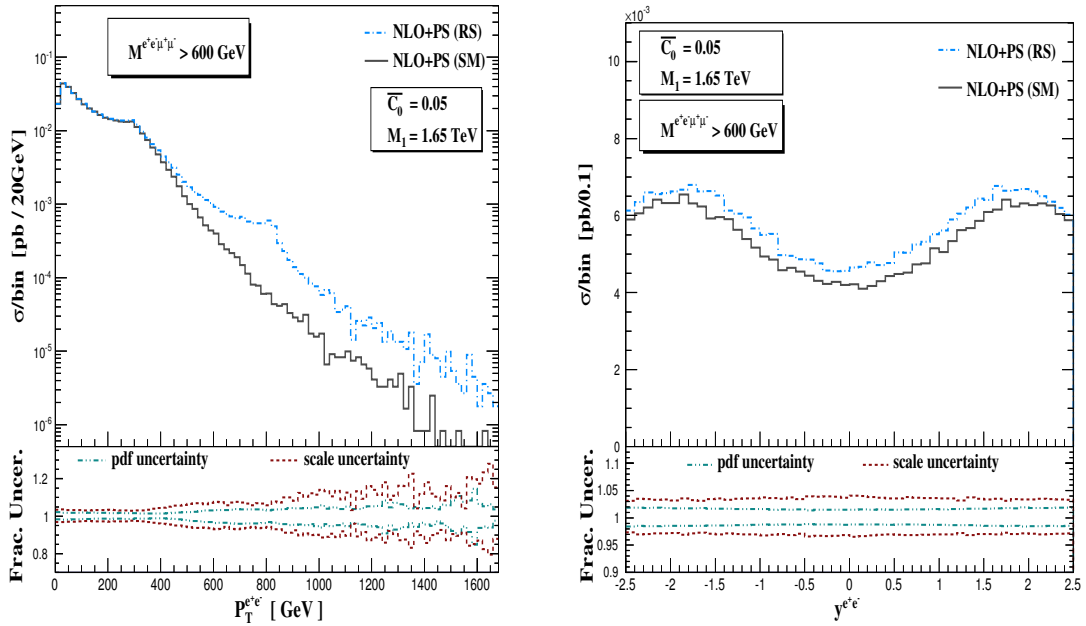


Figure 5.16: Transverse momentum (left) and rapidity (right) distribution of the e^+e^- pair coming from the decay products of ZZ process in RS and SM.

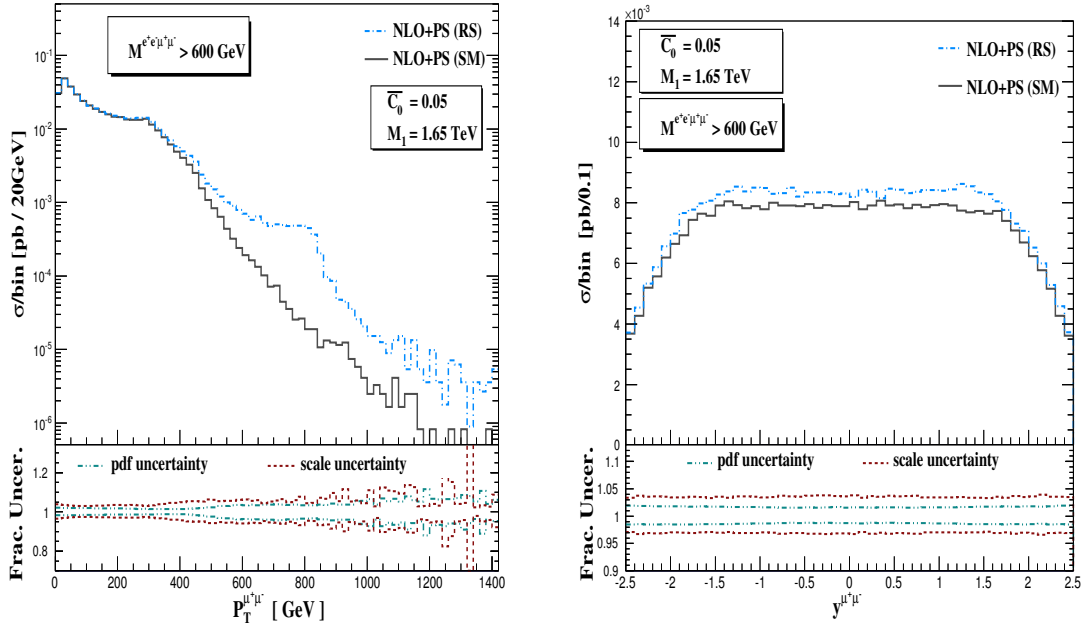


Figure 5.17: Transverse momentum (left) and rapidity (right) distribution of the $\mu^+\mu^-$ pair coming from ZZ decay for RS and SM.

mass ($M^{e^+e^-\mu^+\mu^-}$) distribution of all the final state leptons is depicted in Fig. (5.15). As expected, there are two peaks in this distribution indicating the first two excitations of the graviton considered in the RS model. The transverse momentum (left) and rapidity (right) distributions of the e^+e^- pair and $\mu^+\mu^-$ pair are respectively shown in Fig. (5.16) and (5.17) with the insertion of $M^{e^+e^-\mu^+\mu^-} > 600$ GeV cut. In these P_T distributions the first kink is visible at the half value of the first excitation. The rapidity distributions of those pairs are not alike because of the same reason of applying aforesaid high invariant mass cut for which the angular correlation between the decay products of the two Z bosons has been lost.

5.4.4 W^+W^-

Similar to the di-Z production, we have decayed the W bosons into leptonic channels. W^+ is decayed to e^+ and ν_e , whereas W^- is decayed into μ^- and $\bar{\nu}_\mu$. Few selective distributions

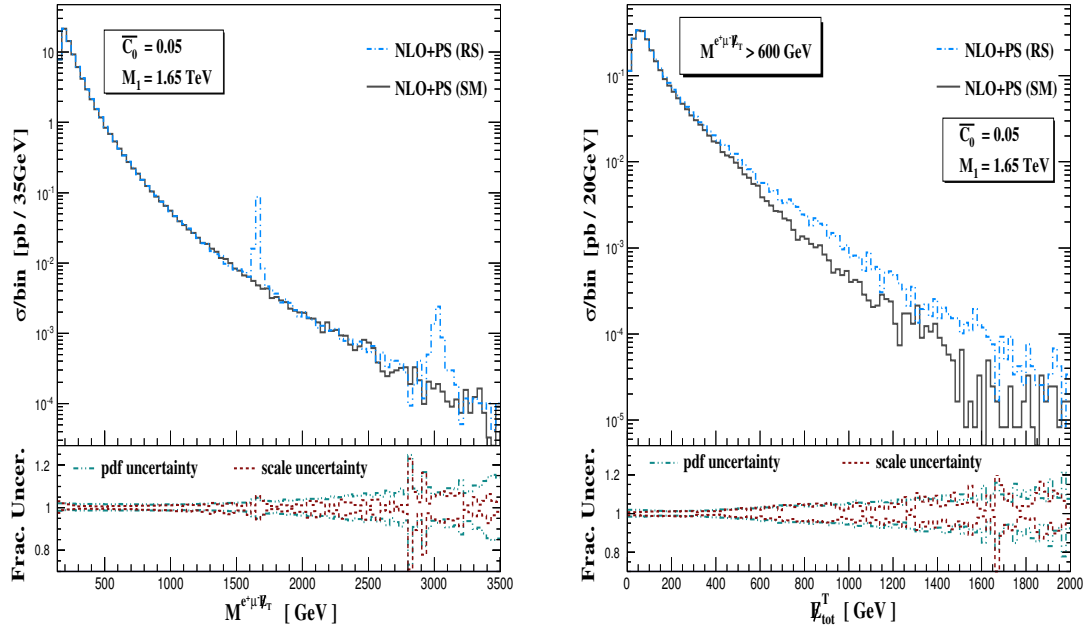


Figure 5.18: Invariant mass (left) distribution of the decay products of W^\pm and the total missing \cancel{E}_T distribution (right) in SM and RS.

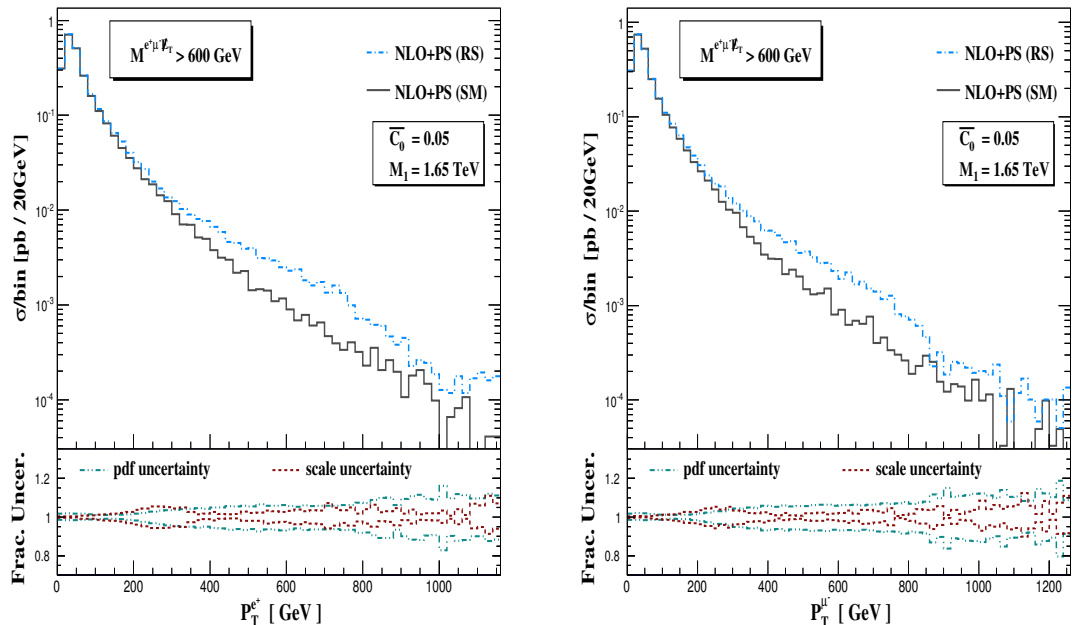


Figure 5.19: Transverse momentum distribution of e^+ (left) and μ^- (right) coming from W^\pm decay in RS and SM.

that are coming from W^+W^- events are given in Fig. (5.18) and (5.19). The left panel of Fig. (5.18) shows the invariant mass ($M^{e^+\mu^-\cancel{E}_T}$) distribution of the W^\pm decay products and in the right panel of this figure, we have presented the transverse missing energy (\cancel{E}_T) distribution that is coming from the electron neutrino and muon anti-neutrino which practically escape the experimental detection in the collider. $M^{e^+\mu^-\cancel{E}_T} > 600$ GeV cut is used for the later one to differentiate the missing \cancel{E}_T signal of the RS from the SM one. In Fig. (5.19), the transverse momentum distributions of the positron (left) and the muon (right) are shown in the region where $M^{e^+\mu^-\cancel{E}_T} > 600$ GeV and we find that the distribution in the RS case is comparatively harder than the SM distribution in this region.

\bar{c}_0	0.03	0.05	0.07	0.10
$M_1^{(3\sigma)}$ (TeV)	4.5	6.3	7.4	10.3
$M_1^{(5\sigma)}$ (TeV)	4.2	5.2	6.0	8.3

Table 5.1: Bounds on M_1 for various \bar{c}_0 values at the 14 TeV LHC with integrated luminosity of 50 fb^{-1} at 3-sigma and 5-sigma signal significance, coming from Drell-Yan process.

5.5 Search sensitivity at LHC-14

Di-photon and Drell-Yan channels are experimentally more favorable since these channels give clean signatures. Therefore these two channels can be used to investigate the search sensitivity of the RS model at the LHC. We have studied the search sensitivity of the RS model using these channels for the following \bar{c}_0 values at the 14 TeV LHC: $\bar{c}_0 = 0.03, 0.05, 0.07, 0.10$. We have calculated the total cross section for the signal plus background and the background alone using the invariant mass distribution of the e^+e^- ($\gamma\gamma$) pair in Drell-Yan (di-photon) production and estimated the minimum required luminosity that distinguishes the signal from the background at 3-sigma (3σ) and 5-sigma

(5σ) signal significance for various values of M_1 for a fixed \bar{c}_0 . The required minimum luminosity is defined as, $L_{\min} = \max\{L_{3\sigma(5\sigma)}, L_{3N_S(5N_S)}\}$, where $L_{3\sigma(5\sigma)}$ describes the integrated luminosity at 3-sigma (5-sigma) signal significance and $L_{3N_S(5N_S)}$ denotes the integrated luminosity to have at least 3(5) signal events. From the data set of M_1 vs. L_{\min} thus prepared, by inversion we find the M_1 value that corresponds to 50 fb^{-1} luminosity for each of the \bar{c}_0 values listed above and those bounds that are counted using Drell-Yan and di-photon processes are tabulated in Table 5.1 and 5.2 respectively. Of course, a full analysis including the effects of detector simulation, non-reducible backgrounds etc. would lead these bounds to their betterment.

\bar{c}_0	0.03	0.05	0.07	0.10
$M_1^{(3\sigma)} (\text{TeV})$	5.2	5.6	6.1	7.5
$M_1^{(5\sigma)} (\text{TeV})$	5.0	5.3	5.6	6.4

Table 5.2: Bounds on M_1 for various \bar{c}_0 values at the 14 TeV LHC with integrated luminosity of 50 fb^{-1} at 3-sigma and 5-sigma signal significance, coming from di-photon production process.

5.6 Conclusions

In this chapter, we have studied all the important di-final state processes ($\ell^+\ell^-$, $\gamma\gamma$, ZZ and W^+W^-) in the RS model to NLO+PS accuracy, implemented in the `AMC@NLO` framework. All the subprocesses to NLO in QCD have been taken into account for both the SM and RS model. For the di-final state processes under consideration, we demonstrate the importance of NLO+PS results over the fixed order NLO computations, by studying the p_T distribution of the di-final states. For suitable choice of RS model parameters, a selection of the results for various observables at the 14 TeV LHC are presented. PDF and scale uncertainties are presented for the various distributions which significantly reduce with the inclusion of NLO corrections. The di-lepton and di-photon

processes are used to study the search sensitivity of the RS model at 14 TeV LHC with 50 fb^{-1} luminosity. The stand-alone codes can be used to generate events with any choice of RS model parameters for di-final state processes discussed here to NLO+PS accuracy and are being made available on the website <http://amcatnlo.cern.ch> which would be useful in upcoming LHC runs at 13 and 14 TeV.

6

TWO-LOOP QCD CORRECTION TO MASSIVE GRAVITON DECAYING TO QUARK-ANTIQUARK-GLUON

6.1 Introduction

Since the early 1980s, the search for new physics using mono-jet events has attracted a lot of attention. This is a simple final state, with one jet of hadrons and nothing else, but it could be crucial to reveal the presence of new phenomena. Particularly search topology with missing transverse energy accompanied by a jet plays an important role in searches for new physics containing dark matter candidates. It is undeniable that the nature of dark matter is one of the big open questions in particle physics nowadays and despite years of searching, no one actually knows what dark matter actually is, the closest we've gotten to figuring that out is crossing off each potential candidate one by one. The mono-jet analysis has been always considered the golden channel for the search for dark matter at colliders. Dark matter particle can arise from various BSM scenarios, such as neutralinos from supersymmetric models could be one interesting example; a massive graviton from extra dimensional models also serves as potential dark matter candidate etc. Mono-jet

final states provide an unique access to the search for such exotic particles at the hadron colliders. But events with this kind of topology do not automatically point to new physics as the SM processes can give rise to similar signatures. For example, consider the production of a Z boson in association with a jet in the SM, where the Z boson decays to a pair of neutrinos. This also gives similar signature as neutrino escapes the detection. Therefore mono-jet searches require that we understand these backgrounds to a very good accuracy. The CDF and D \emptyset experiments at the Fermilab searched for such signature before the LHC era. At that time it was commonly believed that jet-related measurements at colliders could not achieve experimental precisions better than 10-20%. But the advancement of detector technology along with carefully designed event selection strategy, with the use of data-driven techniques in constraining the irreducible backgrounds, translates into extremely precise background predictions. As the background estimation is needed to a good accuracy for this process, one also needs precise knowledge for the signal to make any discovery of new physics.

The processes with hadronic final state such as *mono-jet*, *di-jet*, $t\bar{t}$ etc. suffer from large QCD corrections, as a result of QCD radiation from the initial legs as well as from the final legs. NLO corrections for these kind of processes fail to provide good accuracy, theory error at NLO often already larger than the experimental one. It is therefore important to evaluate the next order in perturbative expansion, since this is the only way to enhance the credibility of theoretical predictions. It has been seen that the precise theoretical predictions help a lot to make any discovery or to constraint parameter space of some models. For Example, for several years the $t\bar{t}$ forward-backward asymmetry measured at Tevatron was several standard deviations away from the LO SM prediction and for a long time it was thought to be signature of new physics beyond the SM; people thought there could be heavy axi-gluon or KK gluons or even new phenomena in the t -channel or u -channel. Even the NLO correction along with soft gluon resummation fails to address

the discrepancy measured at the D \emptyset and CDF. Whereas at the LHC with higher accuracy measurements show no such asymmetry [143]. Later with the full NNLO calculation [144], it has been seen that the correction is as large as 27% relative to the NLO correction and it is shown that the result agrees very well with the experimental results. Thus higher order correction becomes crucial to fully understand the experimental results or even to establish or rule out any new model beyond the SM. Another important example is the Higgs boson production via gluon fusion. NLO accuracy turned out to be insufficient for this process. The reason behind this is that the LO cross-section is proportional to α_s^2 and therefore exhibits a strong dependence on the choice of the scale. Including the NLO corrections decreases the scale dependence, but the cross-section increases by a very large amount, approximately 70%. Clearly NLO correction for this case fails miserably, the large size of the NLO corrections indicate potentially significant contributions from even higher perturbative orders, and it is essential to calculate the full NNLO corrections to this process. Even for this case it has been found that the cross-section increases less from NLO to NNLO than from LO to NLO, indicating a slow convergence of the perturbative expansion. This demands the N³LO calculation for this process which is done very recently [145].

The full NNLO calculation mainly consists of three parts: the virtual contributions from all the sub-processes, the real-virtual piece and the pure real corrections. The virtual contribution comes from the two-loop corrections to the basic $2 \rightarrow 2$ process, the real-virtual piece consists of one-loop virtual corrections to the single real radiation $2 \rightarrow 3$ process and the pure real corrections comes from the double real radiation $2 \rightarrow 4$ process at the tree-level (see Fig. 6.1). Each of these contributions is infrared divergent. In particular, the double-virtual piece contains all IR divergences explicitly at the level of the amplitude, in the real-virtual and in the double-real parts the divergences become explicit only after the integration over their respective phase-spaces. The phase-space integrals are

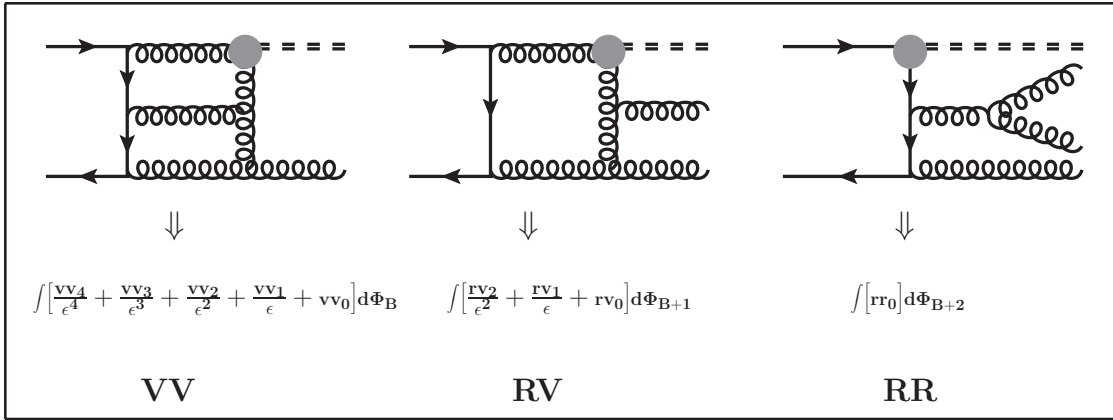


Figure 6.1: The different components of NNLO calculation (gravion+jet). VV is the double virtual piece which contains two-loop diagrams. RV is the one loop diagrams with one extra radiation. RR is the pure double radiation diagram.

typically extremely difficult to be computed analytically and the only possibility is that of resorting to numerical integration. There have been recent progress towards this direction and different methods have become available, like q_T -Subtraction [146, 147], Antenna Subtraction [148], Sector Decomposition [149–152] etc. After the ultraviolet renormalization, and performing the phase-space integrations, all the IR divergences become explicit and their sum yields finite result as a consequence of the KLN theorem [64, 65].

In this chapter we will discuss the calculation of the two-loop virtual QCD correction to massive spin-2 Graviton decaying to $q + \bar{q} + g$ considering a generic universal spin-2 coupling to the SM through the conserved energy-momentum tensor. Such a massive spin-2 particle can arise in extra-dimension models [99, 153]. We will discuss the ultraviolet and infrared structure of the QCD amplitudes in the presence of spin-2 field. Study of spin-2 production at NNLO level is not new. The quark and gluon form-factors for spin-2 production have been calculated at two-loop level [154] and at three-loop level [155] in perturbative QCD (pQCD). An attempt to consider the soft and collinear contribution at NNLO accuracy was made [156] in the context of spin-2. This reduces the unphysical scale uncertainties, thereby improving the predictions. The full NNLO correction has

been studied [157] for Drell-Yan process with spin-2 mediators in the context of ADD.

6.2 Method of Diagram Reduction

The most efficient procedure to calculate the two loop correction is the method of diagram reduction. In this section we will briefly describe this procedure with a toy example. The computational strategy is two-fold: First to convert the Feynman integrals into scalar integrals. Then exploiting the properties of dimensional regularization like IBP, LI to establish several relations among the scalar integrals associated to the original Feynman diagram thereby reducing the large number of scalar integrals into a smaller irreducible set of master integrals. Secondly, the actual evaluation of the MI's.

6.2.1 Reduction to Master Integrals

Classification to Topologies

Any Feynman diagram can be decomposed as a linear combination of scalar integrals times tensors. Consider the process $q\bar{q} \rightarrow ZZ$ at 1-loop. Typical Feynman diagram takes the form:

$$\mathcal{F}^{(1)}(p_1, p_2, p_3, p_4) = \bar{u}(p_2) \left\{ \sum_i C_i(p_1, p_2, p_3, p_4) \mathcal{T}^{\mu\nu}(p_i) \right\} u(p_1) \epsilon^\mu(p_3) \epsilon^\nu(p_4) \quad (6.1)$$

The functions C'_i 's contain all the different scalar integrals. For example consider a simple example for the expression inside the braces of Eq. 6.1 as,

$$\int \mathcal{D}^d k \frac{k^\mu k^\nu}{(k^2)((k-p)^2)} = C_1(p^2) g^{\mu\nu} + C_2(p^2) \frac{p^\mu p^\nu}{p^2} \quad (6.2)$$

We can find the expressions for $C_1(p^2)$ and $C_2(p^2)$ as a linear combinations of scalar integrals by multiplying Eq. 6.2 with $g^{\mu\nu}$ and $p^\mu p^\nu$ respectively. In d-dimension this is given by,

$$\begin{aligned} C_1(p^2) &= \frac{1}{(d-1)} \left(\int \mathcal{D}^d k \frac{k^2}{D_1 D_2} - \frac{1}{p^2} \int \mathcal{D}^d k \frac{(k.p)^2}{D_1 D_2} \right) \\ C_2(p^2) &= \frac{1}{(d-1)} \left(\frac{d}{p^2} \int \mathcal{D}^d k \frac{(k.p)^2}{D_1 D_2} - \int \mathcal{D}^d k \frac{k^2}{D_1 D_2} \right) \end{aligned} \quad (6.3)$$

The most general scalar integral for any loop can be written as,

$$J(p_i) = \int \prod_{j=1}^l \mathcal{D}^d k_j \frac{S_1^{a_1} \dots S_m^{a_m}}{D_1^{b_1} \dots D_n^{b_n}} \quad (6.4)$$

where $S_i = q_x \cdot q_y$ are different irreducible scalar products with $q_{x,y} = \{p_i, k_j\}$ i.e. the set of all internal (k_j) and independent external momenta (p_i) and $D_i = (q_i^2 + m_i^2)$ different propagators. The number of irreducible scalar products are completely determined by the number of external legs e , number of loops l and n number of different propagators and is given by,

$$m = l \left(e + \frac{l}{2} - \frac{1}{2} \right) - n \quad (6.5)$$

At 1-loop, there is no irreducible scalar products. At 1-loop, same number of denominators appear as the number of scalar products for any external leg diagram. Thus at 1-loop all scalar products are reducible and can be written in terms of denominators only. For example, 1-loop, 2-leg diagram has 2 scalar products *viz.* $k_1 \cdot k_1$ and $k_1 \cdot p$ which are written in terms of two denominators $D_1 = k_1^2$ and $D_2 = (k_1 - p)^2$. Similarly all 3-leg or 4-leg diagrams are also reducible in terms of 3 or 4 denominators respectively.

At higher loop, this is not the case. Let us consider a 2-loop massive Sunrise diagram (see Fig. 6.2) with denominators $D_1 = k_1^2 + m_1^2$, $D_2 = k_2^2 + m_2^2$ and $D_3 = (k_1 - k_2 - p)^2 + m_3^2$. For this topology, the number of scalar products are 5 (*viz.* $k_1 \cdot k_1$, $k_2 \cdot k_2$, $k_1 \cdot k_2$, $k_1 \cdot p$ and $k_2 \cdot p$) constructed out of internal momenta k_1 , k_2 and external momenta p . Therefore the number of irreducible scalar products are 2 according to Eq. 6.5. Thus the most general

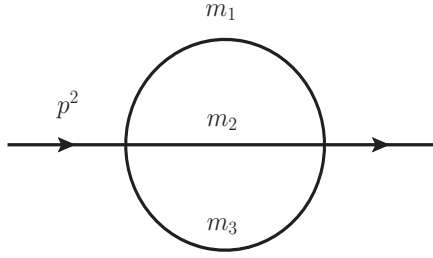


Figure 6.2: Two-loop massive Sunrise diagram.

scalar integral in 2-loop Sunrise diagram is according to Eq. 6.4,

$$J(b_1, b_2, b_3, a_4, a_5) = \int \prod_{j=1}^2 \mathcal{D}^d k_j \frac{S_4^{a_4} S_5^{a_5}}{D_1^{b_1} D_2^{b_2} D_3^{b_3}} \quad (6.6)$$

where $S_4 = k_1 \cdot p$ and $S_5 = k_2 \cdot p$. There is another way to characterize the most general scalar integrals coming out of Sunrise topology. Instead of irreducible scalar products one can introduce the same number of auxiliary propagators. For this case, let us introduce $D_4 = (k_1 - p)^2$ and $D_5 = (k_2 - p)^2$. Therefore the most general scalar integrals are written in the following form,

$$J(b_1, b_2, b_3, b_4, b_5) = \int \prod_{j=1}^2 \mathcal{D}^d k_j \frac{1}{D_1^{b_1} D_2^{b_2} D_3^{b_3} D_4^{b_4} D_5^{b_5}} \quad (6.7)$$

with $b_1, b_2, b_3 \geq 0$ and $b_3, b_4 \in \mathbb{Z}$. In this way all scalar products can be expressed in terms of 5 denominators only. Note that approach 6.6 and 6.7 are completely equivalent.

With Eq. 6.7, all scalar integrals can be classified as topologies, defined by the propagators regardless of their powers.

Integration-By-Parts Identities

The IBP identities are the most important class of identities that can be established among dimensionally regularized Feynman integrals. They are simply manifestation of

Gauss's law in d-dimension, which states that the total derivative with respect to the loop momenta vanishes in dimensional regularization.

$$\int \frac{d^d k_1}{(2\pi)^d} \cdots \int \frac{d^d k_l}{(2\pi)^d} \frac{\partial}{\partial k_i^\mu} \cdot \left(v_j^\mu \frac{1}{\Pi_p \mathcal{D}_p^{n_p}} \right) = 0 \quad (6.8)$$

where l is the number of loops, $n_p \in \mathbb{Z}$, \mathcal{D}_p are the propagators. v_j^μ is loop momenta (k_j^μ) or the external momenta (p_j^μ). Performing the differentiation on the left and rewriting the scalar products in terms of the \mathcal{D}_i 's, the IBP relations can be expressed in to more compact form as follows :

$$\sum_i a_i J(b_{i,1} + n_1, \dots, b_{i,N} + n_N) = 0 \quad (6.9)$$

where

$$J(m_1, \dots, m_N) = \int \frac{d^d k_1}{(2\pi)^d} \cdots \int \frac{d^d k_l}{(2\pi)^d} \frac{1}{\Pi_p \mathcal{D}_p^{m_p}} \quad (6.10)$$

Here a_i are polynomials in n_j , $b_{i,j} \in \{-1, 0, 1\}$. Let us consider a simple example,

$$J(1, 1, 1, 1, 1) = \int \frac{d^d k_1}{(2\pi)^d} \int \frac{d^d k_2}{(2\pi)^d} \frac{1}{\mathcal{D}_1 \mathcal{D}_2 \mathcal{D}_3 \mathcal{D}_4 \mathcal{D}_5} \quad (6.11)$$

One IBP relation yields (derivative w.r.t k_1^μ)

$$\begin{aligned} & \int \frac{d^d k_1}{(2\pi)^d} \int \frac{d^d k_2}{(2\pi)^d} \partial_{k_1^\mu} \left(\frac{p^\mu}{\mathcal{D}_1 \mathcal{D}_2 \mathcal{D}_3 \mathcal{D}_4 \mathcal{D}_5} \right) = 0 \\ & \Rightarrow \int \frac{d^d k_1}{(2\pi)^d} \int \frac{d^d k_2}{(2\pi)^d} \frac{1}{\mathcal{D}_1 \mathcal{D}_2 \mathcal{D}_3 \mathcal{D}_4 \mathcal{D}_5} \left(\frac{2k_1 \cdot p}{\mathcal{D}_1} + \frac{2(k_1 \cdot p - k_2 \cdot p - p^2)}{\mathcal{D}_3} + \frac{2(k_1 \cdot p - p^2)}{\mathcal{D}_4} \right) = 0 \end{aligned} \quad (6.12)$$

Now converting the scalar products $k_1.p$ and $k_2.p$ in terms of \mathcal{D}_i 's and taking $p^2 = 0$,

$$\int \frac{d^d k_1}{(2\pi)^d} \int \frac{d^d k_2}{(2\pi)^d} \left(-\frac{1}{\mathcal{D}_1^2 \mathcal{D}_2 \mathcal{D}_3 \mathcal{D}_5} + \frac{1}{\mathcal{D}_2 \mathcal{D}_3^2 \mathcal{D}_4 \mathcal{D}_5} - \frac{1}{\mathcal{D}_1 \mathcal{D}_3^2 \mathcal{D}_4 \mathcal{D}_5} - \frac{1}{\mathcal{D}_1 \mathcal{D}_2 \mathcal{D}_3^2 \mathcal{D}_5} + \frac{1}{\mathcal{D}_1 \mathcal{D}_2 \mathcal{D}_3^2 \mathcal{D}_4} + \frac{1}{\mathcal{D}_2 \mathcal{D}_3 \mathcal{D}_4^2 \mathcal{D}_5} \right) = 0 \quad (6.13)$$

In other way written in terms of J 's

$$\begin{aligned} & -J(2, 1, 1, 0, 1) + J(0, 1, 2, 1, 1) - J(1, 0, 2, 1, 1) - J(1, 1, 2, 0, 1) \\ & + J(1, 1, 2, 1, 0) + J(0, 1, 1, 2, 1) = 0 \end{aligned} \quad (6.14)$$

Note that each IBP identity may relate the original scalar integral with other scalar integrals with one power of any propagator raised or lowered. For each integrand, the number of IBP relations is given by $l(l+e-1)$. Thus IBP relation reduces the number of scalar integrals through these identities.

Lorentz Invariance Identities

LI identities are realized as a result of the invariance of loop integral under the Lorentz transformation of external momenta,

$$J(p_i + \delta p_i) = J(p_i) \quad (6.15)$$

This leads to the following scalar LI relation,

$$p_i^\mu p_j^\nu \left(\sum_k p_{k[\nu} \frac{\partial}{\partial p_{k]}^\mu} \right) J(n_1, \dots, n_N) = 0 \quad (6.16)$$

For box topologies *i.e.* topologies with 3 independent external momenta, one can have 3 LI identities corresponding to Eq. 6.16. The LI identities are not independent from

the IBP identities, in fact it is shown [158] that LI identities can always be represented as a linear combination of the IBP identities. Nevertheless, the inclusion of LI identities accelerates the solution of the system of equations.

Evaluation of Master Integrals

Using the IBP and LI identities, a scattering amplitude at a certain order in perturbation theory can be reduced to a small sub-set of scalar integrals known as the Master Integrals. There is no way out to reduce this set further. Therefore the issue remains to the computation of these MIs. There are different techniques developed for the analytical evaluation of these MIs, for example at 1-loop the Feynman parametrization, Mellin-Barnes representations etc. At higher loops, some alternatives have been developed. For example the dispersion relation [159, 160] approach to compute 3-loop QED correction to electron $g - 2$ [161]. The idea is to make use of the unitarity properties of the S-matrix in order to write a dispersion relation for a given Feynman diagram in terms of its imaginary part, whose computation is usually easier than that of the entire Feynman graph.

One more efficient procedure is to consider differential equations for the MIs [162, 163]. The method consists in using IBPs in order to derive linear first order differential equations in the external invariants satisfied by the master integrals. Although there is an issue of fixing the boundary conditions. This can be done for example, by explicitly calculating the integrals in a specific kinematical point, either attempting a direct integration or using for example asymptotic expansions [164–166].

6.3 Spin-2 in association with a jet

The processes with missing energy associated with a SM particle can also give significant information about new physics predicting spin-2 particle. Particularly, jet + missing energy is one important process studied at the LHC to look for BSM signature like dark matter in simplified models. A massive spin-2 particle which goes undetected could be an important dark matter candidate. The NLO correction for this process in large extra dimension has been considered in [167] and it is shown that the QCD corrections for this process could be as large as 50% and suffer from large scale uncertainties. Therefore a full NNLO correction is important for such process to have accurate prediction of cross-section and distributions and also to have the scale uncertainties under control. An attempt has been made towards this direction in [168], where the virtual NNLO QCD correction has been studied for massive spin-2 $\rightarrow g + g + g$. Although the gg initiated sub-process is the dominant contribution at the LHC, as the perturbative order increases the other sub-processes like $q\bar{q}$, $q(\bar{q})g$ begin to contribute significantly. In this chapter we present the analytical result for the two loop virtual QCD correction to the process massive spin-2 $\rightarrow q + \bar{q} + g$. After appropriate analytical continuation of the kinematical variables to the respective regions [169], the result presented here can be used for other scattering sub-processes *viz.* $q + \bar{q} \rightarrow G + g$ and $q(\bar{q}) + g \rightarrow G + q(\bar{q})$, where G denotes the spin-2 field. This computation along with the $G \rightarrow g + g + g$ [168] to two-loop completes the full two-loop QCD corrections to the production of spin-2+jet at a hadron collider.

Our main motivation here is two-fold; first to probe the structure of Quantum Field Theory in the presence of a spin-2 field, to check the universality of infrared (IR) pole structure in QCD [170]. The correct IR pole structure has been realized in the case of spin-2 $\rightarrow g + g + g$ [168]. Here we demonstrate the same for spin-2 $\rightarrow q + \bar{q} + g$. Secondly, we present one of the important ingredients for full two-loop QCD correction for real

graviton production associated with a jet. The rank-2 nature of spin-2 increases the complexity of the calculation. Using state-of-the-art techniques like Integration-By-Parts (IBP) identities [171, 172] and Lorentz Invariance (LI) identities [163], we are able to reduce all the scalar integrals to a fewer set of Master Integrals (MI). These MIs are available in [163, 173–177]. Finally we observe the universality of infrared factorization of QCD amplitudes as predicted by Catani [170] (see also [178]).

6.3.1 Effective Action

We consider a generic spin-2 particle minimally coupled to the SM fields through the conserved SM energy-momentum tensor. The effective action which describes a spin-2 particle ($G^{\mu\nu}(x)$) interacting with colored particles is given by [81–83, 88, 90, 99]

$$\mathcal{S}_{int} = -\frac{\kappa}{2} \int d^4x \ T_{\mu\nu}^{QCD}(x) \ G^{\mu\nu}(x), \quad (6.17)$$

where κ is a dimensionful universal coupling which determines the strength of graviton coupling to the SM. $T_{\mu\nu}^{QCD}$ is given by

$$\begin{aligned} T_{\mu\nu}^{QCD} = & -g_{\mu\nu}\mathcal{L}_{QCD} - F_{\mu\rho}^a F_{\nu}^{a\rho} - \frac{1}{\xi}g_{\mu\nu}\partial^\rho(A_\rho^a\partial^\sigma A_\sigma^a) + \frac{1}{\xi}(A_\nu^a\partial_\mu(\partial^\sigma A_\sigma^a) + A_\mu^a\partial_\nu(\partial^\sigma A_\sigma^a)) \\ & + \frac{i}{4}\left[\bar{\psi}\gamma_\mu(\partial_\nu - ig_s T^a A_\nu^a)\psi - \bar{\psi}(\partial_\nu + ig_s T^a A_\nu^a)\gamma_\mu\psi + (\mu \leftrightarrow \nu)\right] \\ & + \left[\partial_\mu\bar{\omega}^a(\partial_\nu\omega^a - g_s f^{ARC} A_\nu^c\omega^b) + (\mu \leftrightarrow \nu)\right], \end{aligned} \quad (6.18)$$

where g_s is the strong coupling constant and ξ is gauge fixing parameter. Here \mathcal{L}_{QCD} is the QCD Lagrangian, given by,

$$\begin{aligned}\mathcal{L}_{QCD} = & -\frac{1}{4}F_{\mu\nu}^a(x)F^{a,\mu\nu}(x) + \bar{\psi}(x)\left(i\cancel{D} + g_sT^a\cancel{A}^a - m_\psi\right)\psi(x) - \frac{1}{2\xi}\left(\partial^\mu A_\mu^a(x)\right)^2 \\ & + \partial^\mu\bar{\omega}^a(x)\left(\partial_\mu\omega^a(x) - g_sf^{abc}A_\mu^c(x)\omega^b(x)\right)\end{aligned}\quad (6.19)$$

Here ω^a is the ghost field introduced in order to cancel the unphysical degrees of freedom associated with the gluon fields (A_μ^a). T^a and f^{abc} represent the generator and structure constants of $SU(N)$ gauge group, respectively. Throughout the computation, we consider $SU(N)$ as our gauge group and the QCD corresponds to $N = 3$.

6.3.2 Notations

The decay process considered is

$$G(Q) \rightarrow q(p_1) + \bar{q}(p_2) + g(p_3). \quad (6.20)$$

The corresponding Mandelstam variables for this process are defined as

$$s \equiv (p_1 + p_2)^2, \quad t \equiv (p_2 + p_3)^2, \quad u \equiv (p_3 + p_1)^2. \quad (6.21)$$

They satisfy the following relation

$$s + t + u = M_G^2 \equiv Q^2. \quad (6.22)$$

Here M_G is the mass of the spin-2 field. The following dimensionless invariants which appear in the argument of harmonic polylogarithms (HPL) [179] and two-dimensional

HPLs [176] are also defined:

$$x \equiv s/Q^2, \quad y \equiv u/Q^2, \quad z \equiv t/Q^2. \quad (6.23)$$

Accordingly, Eq. (6.22) becomes

$$x + y + z = 1. \quad (6.24)$$

6.3.3 Ultraviolet Renormalization

Beyond leading order in perturbation theory, the on-shell QCD amplitudes develop both ultraviolet and infrared divergences. The spin-2 coupling to the SM particles κ is free from such ultraviolet renormalization, which is due to the fact that spin-2 couples universally to the SM through conserved current. So the only UV renormalization required is for the strong coupling constant \hat{g}_s . Before performing the renormalization, we need to regularize the theory in order to identify the true nature of the divergences. We regularize the theory under dimensional regularization where the space-time dimension is chosen to be $d = 4 + \epsilon$. Expanding the scattering amplitude in powers of $\hat{a}_s = \hat{g}_s^2/16\pi^2$, the matrix element (ME) is given by:

$$|\mathcal{M}\rangle = \left(\frac{\hat{a}_s}{\mu_0^\epsilon} S_\epsilon\right)^{\frac{1}{2}} \left(|\hat{\mathcal{M}}^{(0)}\rangle + \left(\frac{\hat{a}_s}{\mu_0^\epsilon} S_\epsilon\right) |\hat{\mathcal{M}}^{(1)}\rangle + \left(\frac{\hat{a}_s}{\mu_0^\epsilon} S_\epsilon\right)^2 |\hat{\mathcal{M}}^{(2)}\rangle + \mathcal{O}(\hat{a}_s^3)\right) \quad (6.25)$$

where \hat{g}_s is the unrenormalized strong coupling constant, $S_\epsilon = \exp[-\frac{\epsilon}{2}(\gamma_E - \ln 4\pi)]$ and $\gamma_E = 0.5772 \dots$ is the Euler constant. $|\hat{\mathcal{M}}^{(i)}\rangle$ is the unrenormalized color-space vector representing the i^{th} loop-amplitude. μ_0 is a mass scale introduced to make the strong coupling constant (\hat{g}_s) dimensionless in d -dimension. We work within the $\overline{\text{MS}}$ scheme for performing the UV renormalization, in which the renormalized coupling constant $a_s \equiv a_s(\mu_R^2)$ is defined at the renormalization scale μ_R and is related to the unrenormalized

\hat{a}_s by

$$\begin{aligned} \frac{\hat{a}_s}{\mu_0^\epsilon} S_\epsilon &= \frac{a_s}{\mu_R^\epsilon} Z(\mu_R^2), \\ &= \frac{a_s}{\mu_R^\epsilon} \left[1 + a_s \frac{2\beta_0}{\epsilon} + a_s^2 \left(\frac{4\beta_0^2}{\epsilon} + \frac{\beta_1}{\epsilon} \right) + \mathcal{O}(a_s^3) \right], \end{aligned} \quad (6.26)$$

where

$$\beta_0 = \left(\frac{11}{3} C_A - \frac{4}{3} T_F n_f \right), \quad \beta_1 = \left(\frac{34}{3} C_A^2 - \frac{20}{3} C_A T_F n_f - 4 C_F T_F n_f \right). \quad (6.27)$$

Here $C_A = N$ and $C_F = (N^2 - 1)/2N$ are the quadratic Casimir of the SU(N) group. $T_F = 1/2$ and n_f is the number of light active quark flavors.

The matrix element can also be expressed as a power series of renormalized strong coupling constant with UV finite matrix elements $|\mathcal{M}^{(i)}\rangle$,

$$|\mathcal{M}\rangle = (a_s)^{\frac{1}{2}} \left(|\mathcal{M}^{(0)}\rangle + a_s |\mathcal{M}^{(1)}\rangle + a_s^2 |\mathcal{M}^{(2)}\rangle + \mathcal{O}(a_s^3) \right) \quad (6.28)$$

where

$$\begin{aligned} |\mathcal{M}^{(0)}\rangle &= \left(\frac{1}{\mu_R^\epsilon} \right)^{\frac{1}{2}} |\hat{\mathcal{M}}^{(0)}\rangle, \\ |\mathcal{M}^{(1)}\rangle &= \left(\frac{1}{\mu_R^\epsilon} \right)^{\frac{3}{2}} \left[|\hat{\mathcal{M}}^{(1)}\rangle + \mu_R^\epsilon \frac{r_1}{2} |\hat{\mathcal{M}}^{(0)}\rangle \right], \\ |\mathcal{M}^{(2)}\rangle &= \left(\frac{1}{\mu_R^\epsilon} \right)^{\frac{5}{2}} \left[|\hat{\mathcal{M}}^{(2)}\rangle + \mu_R^\epsilon \frac{3r_1}{2} |\hat{\mathcal{M}}^{(1)}\rangle + \mu_R^{2\epsilon} \left(\frac{r_2}{2} - \frac{r_1^2}{8} \right) |\hat{\mathcal{M}}^{(0)}\rangle \right] \end{aligned} \quad (6.29)$$

with

$$r_1 = \frac{2\beta_0}{\epsilon}, \quad r_2 = \left(\frac{4\beta_0^2}{\epsilon^2} + \frac{\beta_1}{\epsilon} \right) \quad (6.30)$$

6.3.4 Infrared Factorization

In higher order calculation, the UV renormalized matrix elements contain singularities of infrared origin. Generally two kinds of singularities arise – the soft and collinear while working with massless QCD. According to the KLN theorem, these singularities get canceled against the similar contribution from real emission Feynman diagrams, resulting in infrared safe observables. The IR divergences have a universal structure in dimensional regularization, which was predicted in [170] to two loop, except the two loop single pole in ϵ . In [178, 180, 181] the infrared structure of scattering amplitudes are studied and connection of the single pole to soft anomalous dimension matrix is predicted. The factorization of the single pole in quark and gluon form factors in terms of soft and collinear anomalous dimensions was demonstrated to two-loop level [182] whose validity at three-loop was later established in [183]. The proposal by Catani was generalized beyond two loops using soft collinear effective field theory by Becher and Neubert in [184]. Gardi and Magnea have arrived at the same conclusion [185] using Wilson lines for hard partons and soft and eikonal jet functions in dimensional regularization.

According to Catani's prediction [170], the renormalized amplitude factorizes in dimensional regularization. The ME at a given order $|\mathcal{M}^{(i)}\rangle$ can be expressed as the sum of the lower order MEs times appropriate insertion operators ($\mathbf{I}_q^{(i)}(\epsilon)$) and a finite piece $|\mathcal{M}^{(i)fin}\rangle$. These insertion operators contain the infrared pole structure which are universal. For the present case, we have two external massless quarks and a gluon, for which the one-loop and the two-loop ME can be written in the following form,

$$\begin{aligned} |\mathcal{M}^{(1)}\rangle &= 2 \mathbf{I}_q^{(1)}(\epsilon) |\mathcal{M}^{(0)}\rangle + |\mathcal{M}^{(1)fin}\rangle, \\ |\mathcal{M}^{(2)}\rangle &= 2 \mathbf{I}_q^{(1)}(\epsilon) |\mathcal{M}^{(1)}\rangle + 4 \mathbf{I}_q^{(2)}(\epsilon) |\mathcal{M}^{(0)}\rangle + |\mathcal{M}^{(2)fin}\rangle \end{aligned} \quad (6.31)$$

where the one-loop and two-loop insertion operators are given by

$$\begin{aligned}\mathbf{I}_q^{(1)}(\epsilon) &= \frac{1}{2} \frac{e^{-\frac{\epsilon}{2}\gamma_E}}{\Gamma(1+\frac{\epsilon}{2})} \left\{ \left(\frac{4}{\epsilon^2} - \frac{3}{\epsilon} \right) (C_A - 2C_F) \left[\left(-\frac{s}{\mu_R^2} \right)^{\frac{\epsilon}{2}} \right] \right. \\ &\quad \left. + \left(-\frac{4C_A}{\epsilon^2} + \frac{3C_A}{2\epsilon} + \frac{\beta_0}{2\epsilon} \right) \left[\left(-\frac{t}{\mu_R^2} \right)^{\frac{\epsilon}{2}} + \left(-\frac{u}{\mu_R^2} \right)^{\frac{\epsilon}{2}} \right] \right\}, \\ \mathbf{I}_q^{(2)}(\epsilon) &= \frac{1}{2} \mathbf{I}_q^{(1)}(\epsilon) \left[\mathbf{I}_q^{(1)}(\epsilon) - \frac{2\beta_0}{\epsilon} \right] + \frac{e^{\frac{\epsilon}{2}\gamma_E}}{\Gamma(1+\frac{\epsilon}{2})} \left[-\frac{\beta_0}{\epsilon} + K \right] \mathbf{I}_q^{(1)}(2\epsilon) \\ &\quad + \left(2\mathbf{H}_q^{(2)}(\epsilon) + \mathbf{H}_g^{(2)}(\epsilon) \right)\end{aligned}\tag{6.32}$$

where

$$K = \left(\frac{67}{18} - \frac{\pi^2}{6} \right) C_A - \frac{10}{9} T_F n_f.\tag{6.33}$$

The functions $\mathbf{H}_q^{(2)}(\epsilon)$, $\mathbf{H}_g^{(2)}(\epsilon)$ are dependent on the renormalization scheme. In the $\overline{\text{MS}}$ scheme these are given by

$$\begin{aligned}\mathbf{H}_q^{(2)}(\epsilon) &= \frac{1}{\epsilon} \left\{ C_A C_F \left(-\frac{245}{432} + \frac{23}{16} \zeta_2 - \frac{13}{4} \zeta_3 \right) + C_F^2 \left(\frac{3}{16} - \frac{3}{2} \zeta_2 + 3 \zeta_3 \right) \right. \\ &\quad \left. + C_F n_f \left(\frac{25}{216} - \frac{1}{8} \zeta_2 \right) \right\}, \\ \mathbf{H}_g^{(2)}(\epsilon) &= \frac{1}{\epsilon} \left\{ C_A^2 \left(-\frac{5}{24} - \frac{11}{48} \zeta_2 - \frac{1}{4} \zeta_3 \right) + C_A n_f \left(\frac{29}{54} + \frac{1}{24} \zeta_2 \right) + \frac{1}{4} C_F n_f - \frac{5}{54} n_f^2 \right\}.\end{aligned}\tag{6.34}$$

Here ζ_i is the Riemann Zeta function, some of them are listed below,

$$\zeta_0 = -\frac{1}{2}, \quad \zeta_1 = \infty, \quad \zeta_2 = \frac{\pi^2}{6}, \quad \zeta_3 = 1.20205\dots, \quad \zeta_4 = \frac{\pi^4}{90}\tag{6.35}$$

6.4 Calculation of Amplitudes

In this section we discuss the calculational details of the amplitudes $|\hat{\mathcal{M}}^{(i)}\rangle$ for the process $G \rightarrow q + \bar{q} + g$ to two-loop level in pQCD. Particularly we calculate the squared matrix elements $\langle \mathcal{M}^{(0)} | \mathcal{M}^{(1)} \rangle$ and $\langle \mathcal{M}^{(0)} | \mathcal{M}^{(2)} \rangle$. Due to the tensorial coupling of spin-2 with the SM, the computational procedure becomes tedious. Starting from the generation of Feynman amplitudes, we systematically automatize the calculational procedure using in-house codes based on FORM [186], Mathematica, Reduze 2 [187] and LiteRed [188, 189].

6.4.1 Generation of Feynman Diagrams and Simplification

QGRAF [190] is used to generate all the Feynman amplitudes in terms of symbolic expressions. For the process under consideration, we have 4 Feynman diagrams in the Born, 43 in the one-loop and 847 in the two-loop level; where all the tadpoles and self-energy corrections to the external legs have been excluded. The raw QGRAF output is then manipulated using in-house FORM routines to incorporate the Feynman rules [88, 90] and to take care of the color and Dirac matrix ordering. For the internal gluons Feynman gauge is used and the ghost-graviton interactions [191] are introduced in the Lagrangian (see Eq. (6.18)) as is necessary for higher order computations. For the external gluon the physical polarisations are summed using

$$\sum_{\lambda=\pm 1} \epsilon^\mu(p_3, \lambda) \epsilon^{\nu*}(p_3, \lambda) = -g^{\mu\nu} + \frac{p_3^\mu n^\nu + n^\mu p_3^\nu}{p_3 \cdot n}. \quad (6.36)$$

Here λ is the helicity which takes the value ± 1 for massless gluons, p_3 is the momentum of the external gluon. n is an arbitrary light-like 4-vector. We choose $n = p_1$, one of the external fermion momenta without loss of generality. The spin-2 polarisation sum in

d-dimension is given by [88, 191]:

$$\begin{aligned} B^{\mu\nu;\rho\sigma}(q) &= \left(g^{\mu\rho} - \frac{q^\mu q^\sigma}{q \cdot q}\right) \left(g^{\nu\sigma} - \frac{q^\nu q^\sigma}{q \cdot q}\right) + \left(g^{\mu\sigma} - \frac{q^\mu q^\sigma}{q \cdot q}\right) \left(g^{\nu\rho} - \frac{q^\nu q^\rho}{q \cdot q}\right) \\ &\quad - \frac{2}{d-1} \left(g^{\mu\nu} - \frac{q^\mu q^\nu}{q \cdot q}\right) \left(g^{\rho\sigma} - \frac{q^\rho q^\sigma}{q \cdot q}\right). \end{aligned} \quad (6.37)$$

where the metric $g_{\mu\nu} = \text{diag}(1, -1, -1, -1)$. The squared matrix elements are further processed using in-house codes based on LiteRed and Mathematica.

6.4.2 Reduction of Tensor Integrals

Two loop calculation involves a large number of higher rank Feynman integrals, particularly in the present case it contains tensorial integrals. The conventional approach is to convert the different Feynman integrals into scalar integrals. This generates thousands of scalar integrals which need to be properly classified. The idea is to connect all the scalar integrals to belong to a particular basis. The basis is chosen keeping in mind that any scalar products of loop momenta and external momenta can be expressed only in terms of linear combinations of the propagators. In the case of one-loop there are four different scalar products which are written in terms of four propagators. It is straight forward to choose the following set as the basis for the one-loop case,

$$\begin{aligned} B_{11} &= \{\mathcal{D}_1, \mathcal{D}_{1;1}, \mathcal{D}_{1;12}, \mathcal{D}_{1;123}\}, \\ B_{12} &= \{\mathcal{D}_1, \mathcal{D}_{1;2}, \mathcal{D}_{1;23}, \mathcal{D}_{1;123}\}, \\ B_{13} &= \{\mathcal{D}_1, \mathcal{D}_{1;3}, \mathcal{D}_{1;31}, \mathcal{D}_{1;123}\} \end{aligned} \quad (6.38)$$

where

$$\mathcal{D}_1 = k_1^2, \quad \mathcal{D}_{1;i} = (k_1 - p_i)^2, \quad \mathcal{D}_{1;ij} = (k_1 - p_i - p_j)^2, \quad \mathcal{D}_{1;ijk} = (k_1 - p_i - p_j - p_k)^2 \quad (6.39)$$

with $i, j, k = 1, 2, 3$. At two-loop case, the choice of basis is not trivial. At two-loop one has 9 independent scalar products of loop momenta and external momenta, *viz.* $\{(k_\alpha \cdot k_\beta), (k_\alpha \cdot p_i)\}; \alpha, \beta = 1, 2$ and $i = 1, 2, 3$. whereas the physical diagrams contain at most 7 different propagators. At this stage we have two choices: either we can express 7 out of 9 scalar products in terms of 7 different propagators and remaining 2 as irreducible scalar products, otherwise we can invoke two extra auxiliary propagators so that all 9 scalar products can be expressed in terms of denominators only. We choose the later and hence we need to increase the number of propagators to 9. With the help of Reduze 2, all the two-loop diagrams are classified into six different auxiliary topologies presented below:

$$\begin{aligned} B_{21} &= \{\mathcal{D}_0, \mathcal{D}_1, \mathcal{D}_2, \mathcal{D}_{1;1}, \mathcal{D}_{2;1}, \mathcal{D}_{1;12}, \mathcal{D}_{2;12}, \mathcal{D}_{1;123}, \mathcal{D}_{2;123}\}, \\ B_{22} &= \{\mathcal{D}_0, \mathcal{D}_1, \mathcal{D}_2, \mathcal{D}_{1;2}, \mathcal{D}_{2;2}, \mathcal{D}_{1;23}, \mathcal{D}_{2;23}, \mathcal{D}_{1;123}, \mathcal{D}_{2;123}\}, \\ B_{23} &= \{\mathcal{D}_0, \mathcal{D}_1, \mathcal{D}_2, \mathcal{D}_{1;3}, \mathcal{D}_{2;3}, \mathcal{D}_{1;31}, \mathcal{D}_{2;31}, \mathcal{D}_{1;123}, \mathcal{D}_{2;123}\}, \\ B_{24} &= \{\mathcal{D}_0, \mathcal{D}_1, \mathcal{D}_2, \mathcal{D}_{1;1}, \mathcal{D}_{2;1}, \mathcal{D}_{0;3}, \mathcal{D}_{1;12}, \mathcal{D}_{2;12}, \mathcal{D}_{1;123}\}, \\ B_{25} &= \{\mathcal{D}_0, \mathcal{D}_1, \mathcal{D}_2, \mathcal{D}_{1;2}, \mathcal{D}_{2;2}, \mathcal{D}_{0;1}, \mathcal{D}_{1;23}, \mathcal{D}_{2;23}, \mathcal{D}_{1;123}\}, \\ B_{26} &= \{\mathcal{D}_0, \mathcal{D}_1, \mathcal{D}_2, \mathcal{D}_{1;3}, \mathcal{D}_{2;3}, \mathcal{D}_{0;2}, \mathcal{D}_{1;31}, \mathcal{D}_{2;31}, \mathcal{D}_{1;123}\} \end{aligned} \tag{6.40}$$

where

$$\begin{aligned} \mathcal{D}_0 &= (k_1 - k_2)^2, \quad \mathcal{D}_\alpha = k_\alpha^2, \quad \mathcal{D}_{\alpha;i} = (k_\alpha - p_i)^2, \quad \mathcal{D}_{\alpha;ij} = (k_\alpha - p_i - p_j)^2, \\ \mathcal{D}_{0;i} &= (k_1 - k_2 - p_i)^2, \quad \mathcal{D}_{\alpha;ijk} = (k_\alpha - p_i - p_j - p_k)^2. \end{aligned} \tag{6.41}$$

Although properly classified, these large number of scalar integrals are not all independent. In fact they are related by the IBP identities [171, 172] and LI identities [163] which follow from the Poincare invariance. At a fixed order, IBP and LI identities result in a large linear system of equations for the integrals. The inclusion of LI identities accelerates the solution of the system of equations, although they are not independent from the IBP identities [158]. We generate the IBP relations and LI identities using Laporta

algorithm [192] as implemented in LiteRed. Using LiteRed along with Mint [193, 194] we reduce all different scalar integrals to a fewer set of irreducible scalar integrals *i.e.* the MIs.

6.4.3 Master Integrals

After the application of IBP and LI identities, a small number of remaining integrals which are not reducible further *i.e.* the MIs, must be evaluated explicitly. There are powerful techniques such as the differential equation method [162, 163, 195] or the Mellin-Barnes integral representation [196, 197] which can then be employed to derive an expansion of the master integrals in ϵ . For the current case, the topologies consist of one off-shell and three massless external legs with all internal propagators being massless. At one-loop, two kinds of MIs appear, *viz.* the *Bubble*- two-propagator MI and *Box*- four-propagator MI. In case of two-loop we find a total of 24 topologies, out of which 8 are non-planar topologies and 16 planar topologies. All the two-loop MIs topologies in our calculation can be related to the MI computed in [176, 177]. At this point we would like to note that some of the MIs in our case do not appear as given in [176, 177]. The reason behind this is the different convention in the basis in LiteRed and in [176, 177] (see the difference between Eq. 6.6 and Eq. 6.7 in section 6.2.1). Thus we found topologies containing higher power of propagators instead of the irreducible numerator in [176, 177]. Nevertheless those can be related by properly using the IBP and LI identities. In this way we reduce all the scalar integrals to the known set of MIs. We also found two extra topologies for the MI [168], *viz.* *Kite* and *GlassS* which are basically product of two one-loop MIs. *GlassS* is found to be the product of two *Bubbles*. *Kite* is the product of one *Bubble* and one *Box* one-loop MIs. In the Appendix ?? we present these extra MIs. Using all the MIs we finally find the unrenormalized one-loop $\langle \hat{\mathcal{M}}^{(0)} | \hat{\mathcal{M}}^{(1)} \rangle$ and two-loop $\langle \hat{\mathcal{M}}^{(0)} | \hat{\mathcal{M}}^{(2)} \rangle$ matrix elements which are presented in the next section.

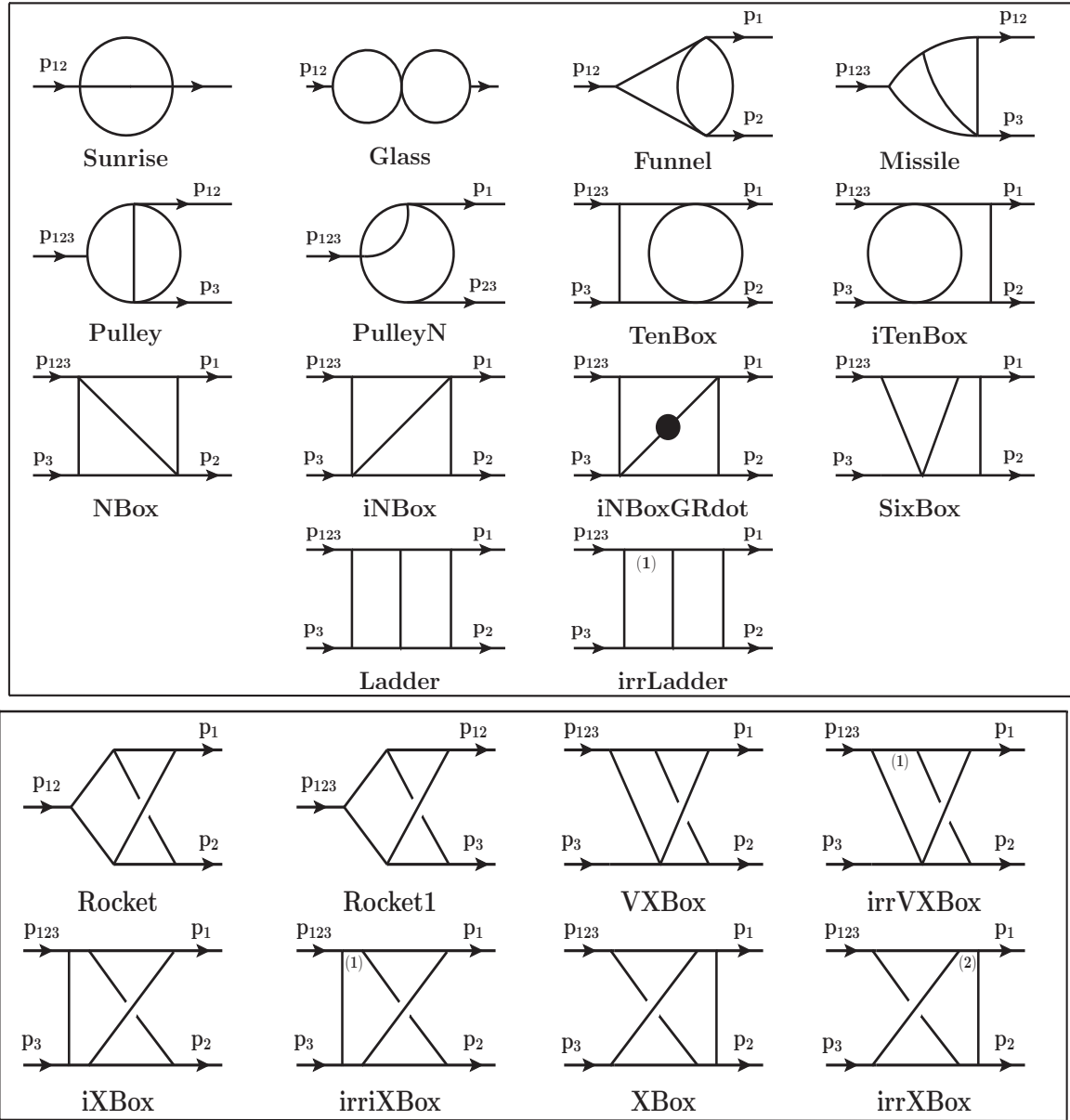


Figure 6.3: Planar and non-planar topologies for the master integrals.

6.5 Results

We have checked that the gauge fixing term appearing at the g-g-G vertex cancels against the contributions coming from ghost-ghost-G and ghost-ghost-gluon-G vertices. This cancellation of gauge dependent terms involving spin-2 serves a crucial check on our computation. Following the renormalization prescription in section (6.3.3), we compute the

UV renormalized matrix elements $\langle \mathcal{M}^{(0)} | \mathcal{M}^{(1)} \rangle$ and $\langle \mathcal{M}^{(0)} | \mathcal{M}^{(2)} \rangle$ in terms of the unrenormalized ones,

$$\begin{aligned}\langle \mathcal{M}^{(0)} | \mathcal{M}^{(1)} \rangle &= \left(\frac{1}{\mu_R^\epsilon}\right)^2 \left[\langle \hat{\mathcal{M}}^{(0)} | \hat{\mathcal{M}}^{(1)} \rangle + \mu_R^\epsilon \frac{r_1}{2} \langle \hat{\mathcal{M}}^{(0)} | \hat{\mathcal{M}}^{(0)} \rangle \right] \\ \langle \mathcal{M}^{(0)} | \mathcal{M}^{(2)} \rangle &= \left(\frac{1}{\mu_R^\epsilon}\right)^3 \left[\langle \hat{\mathcal{M}}^{(0)} | \hat{\mathcal{M}}^{(2)} \rangle + \mu_R^\epsilon \frac{3r_1}{2} \langle \hat{\mathcal{M}}^{(0)} | \hat{\mathcal{M}}^{(1)} \rangle \right. \\ &\quad \left. + \mu_R^{2\epsilon} \left(\frac{r_2}{2} - \frac{r_1^2}{8}\right) \langle \hat{\mathcal{M}}^{(0)} | \hat{\mathcal{M}}^{(0)} \rangle \right].\end{aligned}\quad (6.42)$$

Similarly the renormalized matrix elements according to Catani's prescription can be written as

$$\begin{aligned}\langle \mathcal{M}^{(0)} | \mathcal{M}^{(1)} \rangle &= 2 \mathbf{I}_q^{(1)}(\epsilon) \langle \mathcal{M}^{(0)} | \mathcal{M}^{(0)} \rangle + \langle \mathcal{M}^{(0)} | \mathcal{M}^{(1)fin} \rangle \\ \langle \mathcal{M}^{(0)} | \mathcal{M}^{(2)} \rangle &= 2 \mathbf{I}_q^{(1)}(\epsilon) \langle \mathcal{M}^{(0)} | \mathcal{M}^{(1)} \rangle + 4 \mathbf{I}_q^{(2)}(\epsilon) \langle \mathcal{M}^{(0)} | \mathcal{M}^{(0)} \rangle + \langle \mathcal{M}^{(0)} | \mathcal{M}^{(2)fin} \rangle.\end{aligned}\quad (6.43)$$

From Eq. (6.42) we extract the coefficients of different poles *viz.* the $1/\epsilon^4, 1/\epsilon^3, 1/\epsilon^2, 1/\epsilon$ and we find that they exactly agree with the respective poles coming from Eq. (6.43). By comparing the $\mathcal{O}(\epsilon^0)$ terms from these two sets of equations (Eq. (6.42)) and (Eq. (6.43)), we obtain the unknown pieces $\langle \mathcal{M}^{(0)} | \mathcal{M}^{(1)fin} \rangle$ and $\langle \mathcal{M}^{(0)} | \mathcal{M}^{(2)fin} \rangle$.

The final result is written in the following form:

$$\begin{aligned}\langle \mathcal{M}^{(0)} | \mathcal{M}^{(0)} \rangle &= \mathcal{F}_b \mathcal{A}^{(0)}, \\ \langle \mathcal{M}^{(0)} | \mathcal{M}^{(1)fin} \rangle &= \mathcal{F}_b \left\{ \mathcal{A}_0^{(1)} \ln\left(-\frac{Q^2}{\mu_R^2}\right) + \left(\mathcal{A}_1^{(1)} \zeta_2 + \mathcal{A}_2^{(1)}\right) \right\}, \\ \langle \mathcal{M}^{(0)} | \mathcal{M}^{(2)fin} \rangle &= \mathcal{F}_b \left\{ \mathcal{A}_0^{(2)} \ln^2\left(-\frac{Q^2}{\mu_R^2}\right) \right. \\ &\quad \left. + \left(\mathcal{A}_1^{(2)} \zeta_3 + \mathcal{A}_2^{(2)} \zeta_2 + \mathcal{A}_3^{(2)}\right) \ln\left(-\frac{Q^2}{\mu_R^2}\right) \right. \\ &\quad \left. + \left(\mathcal{A}_4^{(2)} \zeta_2^2 + \mathcal{A}_5^{(2)} \zeta_3 + \mathcal{A}_6^{(2)} \zeta_2 + \mathcal{A}_7^{(2)}\right) \right\}\end{aligned}\quad (6.44)$$

where

$$\mathcal{F}_b = 16\pi^2 \kappa^2 (N^2 - 1) Q^2, \quad (6.45)$$

$$\mathcal{A}^{(0)} = \frac{\left(2 + y^2(3 - 9z) - 4z + 3z^2 - z^3 + y^3(-1 + 4z) + y(-4 + 12z - 9z^2 + 4z^3) \right)}{4yz(1 - y - z)}, \quad (6.46)$$

$$\begin{aligned} \mathcal{A}_i^{(1)} &= \mathcal{A}_{i;C_A}^{(1)} C_A + \mathcal{A}_{i;C_F}^{(1)} C_F + \mathcal{A}_{i;n_f}^{(1)} n_f, \\ \mathcal{A}_i^{(2)} &= \mathcal{A}_{i;C_A^2}^{(2)} C_A^2 + \mathcal{A}_{i;C_F^2}^{(2)} C_F^2 + \mathcal{A}_{i;n_f^2}^{(2)} n_f^2 + \mathcal{A}_{i;C_A C_F}^{(2)} C_A C_F + \mathcal{A}_{i;C_A n_f}^{(2)} C_A n_f + \mathcal{A}_{i;C_F n_f}^{(2)} C_F n_f. \end{aligned} \quad (6.47)$$

$$\begin{aligned}
\mathcal{A}_0^{(1)} &= -\frac{\beta_0}{2} \mathcal{A}_0; \\
\mathcal{A}_{1;CA}^{(1)} &= -C_A \mathcal{A}_0; \quad \mathcal{A}_{1;CF}^{(1)} = 0; \quad \mathcal{A}_{1;n_f}^{(1)} = 0; \\
\mathcal{A}_{2;CA}^{(1)} &= \left\{ -6(-1+y)y^4(-1+z)(y+z) + 6(-1+y)y^5(-1+z)(y+z) + 84(-1+y)y^3(-1+z)(y+z) - 54(-1+y)y^4(-1+z)(y+z) + 44(-1+y)y^5(-1+z)(y+z) + 132(-1+y)y^2(-1+z)(z^2(y+z)) - 152(-1+y)y^3(-1+z)(z^2(y+z)) + 48(-1+y)y^5(-1+z)(z^2(y+z)) + 84(-1+y)y(-1+z)(z^3(y+z)) - 152(-1+y)y^2(-1+z)(z^3(y+z)) - 88(-1+y)y^3(-1+z)(z^3(y+z)) + 144(-1+y)y^4(-1+z)(z^3(y+z)) - 6(-1+y)(-1+z)(z^4(y+z)) - 54(-1+y)y(-1+z)(z^4(y+z)) + 144(-1+y)y^3(-1+z)(z^4(y+z)) + 6(-1+y)(-1+z)(z^5(y+z)) + 44(-1+y)y(-1+z)(z^5(y+z)) + 48(-1+y)y^2(-1+z)(z^5(y+z)) + 3(-1+y)y(-1+z)(y+z)^4(16y^3 + y^2(-41+12z)) - 2(7-6z+3z^2) + 3y(13-9z+4z^2)H(0,y)^2 + 3(-1+y)(-1+z)(y+z)^4(-14+39z-41z^2+16z^3+6y^2(-1+2z)) + 3y(4-9z+4z^2)H(0,z)^2 + 3(-1+y)(-1+z)(y+z)^4(4+16y^4-22z+45z^2-43z^3+16z^4+y^3(-43+20z)) + 3y^2(15-17z+8z^2) + y(-22+48z-51z^2+20z^3)H(1,z)^2 + 2(-1+z)(y+z)^4H(0,y)(-10+30y-35y^2) + 20y^3-5y^4+20z-80yz+132y^2z-116y^3z+44y^4z-15z^2+60yz^2-72y^2z^2+24y^3z^2+5z^3 - 25yz^3+20y^2z^3+3(-1+y)(2+y^2(3-9z)-4z+3z^2-z^3+y^3(-1+4z))+y(-4+12z-9z^2)+4z^3)H(0,z) + 3(-1+y)(2+16y^4-4z+3z^2-z^3+2y^3(-21+8z))+6y^2(7-6z+2z^2)+y(-18+24z-15z^2+4z^3)H(1,z)) + (-1+y)(-1+z)(y^7(-9+84z))+3y^6(9-83z+144z^2)-9z^4(-2+4z-3z^2+z^3) + 3y^5(-12+92z-373z^2+324z^3)+yz^3(-36-136z+276z^2-249z^3+84z^4)+y^2z^2(-60-292z+1053z^2-1119z^3+432z^4)+y^3z(-36-292z+1608z^2-2175z^3+972z^4)+y^4(18-136z+1053z^2-2175z^3+1248z^4))H(2,y) + 3(-1+y)(-1+z)(y+z)^4(4+16y^4-22z+45z^2-43z^3+16z^4+y^3(-43+20z))+3y^2(15-17z+8z^2) - 17z+8z^2)+y(-22+48z-51z^2)H(2,y)^2 + 2(-1+y)(y+z)^4H(0,z)(-5(-1+z)^2(2-2z+z^2) + 5y^3(1-5z+4z^2)+3y^2(-5+20z-24z^2+8z^3)+4y(5-20z+33z^2-29z^3+11z^4)+3(-1+z)(y^3(-1+4z))+4y(-1+z)^2(-1+4z)+3y^2(1-5z+4z^2)+2(1-9z+21z^2-21z^3+8z^4))H(2,y)) + (-1+y)(-1+z)H(1,z)(3y^7(-3+28z))+3y^6(9-83z+144z^2)-9z^4(-2+4z-3z^2+z^3)+3y^5(-12+92z-373z^2+324z^3)+yz^3(-36-136z+276z^2-249z^3+84z^4)+y^2z^2(-60-292z+1053z^2-1119z^3+432z^4)+y^3z(-36-292z+1608z^2-2175z^3+972z^4)+y^4(18-136z+1053z^2-2175z^3+1248z^4)-6(y+z)^4(4+16y^4-22z+45z^2-43z^3+16z^4+y^3(-43+20z))+3y^2(15-17z+8z^2)+y(-22+48z-51z^2+20z^3))H(3,y)) - 6(-1+y)y(-1+z)(y+z)^4(16y^3+y^2(-41+12z))-2(7-6z+3z^2)+3y(13-9z+4z^2)H(0,0,y) - 6(-1+y)(-1+z)(y+z)^4(-14+39z-41z^2+16z^3+6y^2(-1+2z))+3y(4-9z+4z^2)H(0,0,z) - 6(-1+y)(-1+z)(y+z)^4(2+16y^4-4z+3z^2-z^3+2y^3(-21+8z))+6y^2(7-6z+2z^2)+y(-18+24z-15z^2+4z^3)H(0,1,z) + 6(-1+y)(-1+z)(y+z)^4(2+16y^4-4z+3z^2-z^3+2y^3(-21+8z))+6y^2(7-6z+2z^2)+y(-18+24z-15z^2+4z^3)H(0,2,y) - 6(-1+y)y(-1+z)(y+z)^4(16y^3+y^2(-41+12z))-2(7-6z+3z^2)+3y(13-9z+4z^2)H(1,0,y) + 6(-1+y)(-1+z)(y+z)^4(2+y^2(3-9z)-4z+3z^2-z^3+y^3(-1+4z))+y(-4+12z-9z^2+4z^3)H(1,0,z) - 6(-1+y)(-1+z)(y+z)^4(4+16y^4-22z+45z^2-43z^3+16z^4+y^3(-43+20z))+3y^2(15-17z+8z^2)+y(-22+48z-51z^2+20z^3))H(1,1,z) + 6(-1+y)(-1+z)(y+z)^4(2+16y^4-4z+3z^2-z^3+2y^3(-21+8z))+6y^2(7-6z+2z^2)+y(-18+24z-15z^2+4z^3)H(2,0,y) - 6(-1+y)(-1+z)(y+z)^4(4+16y^4-22z+45z^2-43z^3+16z^4+y^3(-43+20z))+3y^2(15-17z+8z^2)+y(-22+48z-51z^2+20z^3))H(2,2,y) - 6(-1+y)(-1+z)(y+z)^4(4+16y^4-22z+45z^2-43z^3+16z^4+y^3(-43+20z))+3y^2(15-17z+8z^2)+y(-22+48z-51z^2+20z^3))H(3,2,y) \right\} / \left(24(-1+y)y(-1+z)(y+z)^4 \right);
\end{aligned}$$

$$\begin{aligned}
\mathcal{A}_{2;CF}^{(1)} &= \left\{ 20(-1+y)y(-1+z)(y+z) - 59(-1+y)y^2(-1+z)(y+z) + 68(-1+y)y^3(-1+z)(y+z) - 39(-1+y)y^4(-1+z)(y+z) + 10(-1+y)y^5(-1+z)(y+z) + 20(-1+y)(-1+z)(y+z) - 138(-1+y)y(-1+z)(y+z) + 316(-1+y)y^2(-1+z)(y+z) - 318(-1+y)y^3(-1+z)(y+z) + 161(-1+y)y^4(-1+z)(y+z) - 41(-1+y)y^5(-1+z)(y+z) - 59(-1+y)(-1+z)(z^2(y+z)) + 316(-1+y)y(-1+z)(z^2(y+z)) - 578(-1+y)y^2(-1+z)(z^2(y+z)) + 435(-1+y)y^3(-1+z)(z^2(y+z)) - 142(-1+y)y^4(-1+z)(z^2(y+z)) + 28(-1+y)y^5(-1+z)(z^2(y+z)) + 68(-1+y)(-1+z)(z^3(y+z)) - 318(-1+y)y(-1+z)(z^3(y+z)) + 435(-1+y)y^2(-1+z)(z^3(y+z)) - 202(-1+y)y^3(-1+z)(z^3(y+z)) \right\};
\end{aligned}$$

$$\begin{aligned}
& + z)z^3(y+z) + 20(-1+y)y^4(-1+z)z^3(y+z) - 39(-1+y)(-1+z)z^4(y+z) + 161(-1+y)y(-1+z)z^4(y+z) \\
& - 142(-1+y)y^2(-1+z)z^4(y+z) + 20(-1+y)y^3(-1+z)z^4(y+z) + 10(-1+y)(-1+z)z^5(y+z) - 41(-1 \\
& + y)y(-1+z)z^5(y+z) + 28(-1+y)y^2(-1+z)z^5(y+z) - (-1+y)^2(-1+4y)(-1+z)^2(y+z)^2(-2+2y^3+4z \\
& - 3z^2+z^3+y^2(-6+4z)+y(6-8z+3z^2))H(0,y)^2+(1-y)(-1+y)(y^3+3y^2(-1+z)+4y(-1+z)^2+2(-1 \\
& + z)^3)(-1+z)^2(y+z)^2(-1+4z)H(0,z)^2+(1-y)(-1+y)(-1+z)^2(y+z)^2(4+8y^4-18z+33z^2-27z^3 \\
& + 8z^4+y^3(-27+20z)+3y^2(11-17z+8z^2)+y(-18+48z-51z^2+20z^3))H(1,z)^2+(-1+z)^2(-1+y+z)(y \\
& + z)^2H(0,y)(-yz(8y^3+y(30-27z)+12(-1+z)+2y^2(-13+6z))) - 2(-1+y)^2(-1+4y)(2+2y^2+2y(-2 \\
& + z)-2z+z^2)H(1,z))+(1-y)(-1+y)(-1+z)^2(y^5(-3+20z)+y^4(9-73z+80z^2)-3z^2(-2+4z-3z^2) \\
& + z^3)+6y^3(-2+15z-34z^2+20z^3)+yz(-8-32z+90z^2-73z^3+20z^4)+2y^2(3-16z+81z^2-102z^3 \\
& + 40z^4))H(2,y)+(1-y)(-1+y)(-1+z)^2(y+z)^2(4+8y^4-18z+33z^2-27z^3+8z^4+y^3(-27+20z) \\
& + 3y^2(11-17z+8z^2)+y(-18+48z-51z^2+20z^3))H(2,y)^2+(1-y)(-1+y)(-1+y+z)(y \\
& + z)^2H(0,z)(yz(-12+30z-26z^2+8z^3+3y(4-9z+4z^2))+2(y^2+2y(-1+z)+2(-1+z)^2)(-1+z)^2(-1 \\
& + 4z)H(2,y))+(-1+y+z)(-1+y+z-yz)^2H(1,z)(y^4(3-20z)+y^3(-6+50z-60z^2)+3z^2(2-2z+z^2) \\
& + y^2(6-34z+94z^2-60z^3)-2yz(4+17z-25z^2+10z^3)+2(y+z)^2(-4+8y^3+14z-19z^2+8z^3 \\
& + y^2(-19+12z)+2y(7-10z+6z^2))H(3,y))+2(1-y)(1-5y+4y^2)(-y-z)(-1+z)^2(2y^4+6y^3(-1+z) \\
& + y^2(6-14z+7z^2)+z(-2+4z-3z^2+z^3)+y(-2+10z-11z^2+4z^3))H(0,0,y)+2(1-y)(-1+y)(-y \\
& - z)(-1+z)(1-5z+4z^2)(y^4+2(-1+z)^3z+2y(-1+z)^2(-1+3z)+y^3(-3+4z)+y^2(4-11z \\
& + 7z^2))H(0,0,z)+2(-1+y)^2(-1+4y)(-1+z)^2(y+z)^2(-2+2y^3+4z-3z^2+z^3+y^2(-6+4z)+y(6-8z \\
& + 3z^2))H(0,1,z)-2(-1+y)^2(-1+4y)(-1+z)^2(y+z)^2(-2+2y^3+4z-3z^2+z^3+y^2(-6+4z)+y(6-8z \\
& + 3z^2))H(0,2,y)+2(-1+y)^2(-1+4y)(-1+z)^2(y+z)^2(-2+2y^3+4z-3z^2+z^3+y^2(-6+4z)+y(6-8z \\
& + 3z^2))H(1,0,y)+2(-1+y)^2(-1+z)^2(y+z)^2(4+8y^4-18z+33z^2-27z^3+8z^4+y^3(-27+20z) \\
& + 3y^2(11-17z+8z^2)+y(-18+48z-51z^2+20z^3))H(1,1,z)-2(-1+y)^2(-1+4y)(-1+z)^2(y+z)^2(-2 \\
& + 2y^3+4z-3z^2+z^3+y^2(-6+4z)+y(6-8z+3z^2))H(2,0,y)+2(-1+y)^2(-1+z)^2(y+z)^2(4+8y^4 \\
& - 18z+33z^2-27z^3+8z^4+y^3(-27+20z)+3y^2(11-17z+8z^2)+y(-18+48z-51z^2+20z^3))H(2,2,y) \\
& + 2(-1+y)^2(-1+z)^2(y+z)^2(4+8y^4-18z+33z^2-27z^3+8z^4+y^3(-27+20z)+3y^2(11-17z+8z^2) \\
& + y(-18+48z-51z^2+20z^3))H(3,2,y)\Big\}\Big/\Big(4(-1+y)^2y(-1+z)^2z(-1+y+z)(y+z)^2\Big);
\end{aligned}$$

$$\begin{aligned}
\mathcal{A}_{2;n_f}^{(1)} = & \Big\{ -24y^4z + 12y^5z - 8y^6z - 24y^3z^2 + 8y^4z^2 - 8y^5z^2 - 24y^2z^3 - 8y^3z^3 + 16y^4z^3 - 24yz^4 \\
& + 8y^2z^4 + 16y^3z^4 + 12yz^5 - 8y^2z^5 - 8yz^6 - (y+z)^4(2+y^2(3-9z)-4z+3z^2-z^3+y^3(-1+4z) \\
& + y(-4+12z-9z^2+4z^3))H(0,y) - (y+z)^4(2+y^2(3-9z)-4z+3z^2-z^3+y^3(-1+4z)+y(-4+12z \\
& - 9z^2+4z^3))H(0,z) + 4yz(-5y^3+3y^4+yz^2+y^2(6+z-6z^2)+z^2(6-5z+3z^2))H(1,z) + 4yz(-5y^3 \\
& + 3y^4+yz^2+y^2(6+z-6z^2)+z^2(6-5z+3z^2))H(2,y)\Big\}\Big/\Big(24yz(-1+y+z)(y+z)^4\Big).
\end{aligned}$$

We notice that unlike the Higgs decay *i.e.* $H \rightarrow b + \bar{b} + g$ [198], there is no C_F term in the $\mathcal{A}_0^{(1)}$, which is due to the absence of Yukawa-like term in spin-2 case. All the two-loop coefficients are presented in the Appendix C.2, except for the $\mathcal{A}_7^{(2)}$ coefficients which are available in the arXiv submission as ascillary file in Mathematica format [199].

6.6 Conclusion

In this chapter, we present the two-loop virtual QCD correction to massive $G \rightarrow q + \bar{q} + g$ considering the minimal and universal coupling between spin-2 and the SM particles. We confine ourselves within the framework of massless QCD where only the light quark degrees of freedom are taken into account. We employ the Feynman diagrammatic approach to achieve our goal. As expected, the computation becomes very tedious not only due to the presence of a large number of Feynman diagrams but also due to the involvement of a tensorial coupling. In-house codes and state-of-the-art techniques, in particular, IBP and LI identities, are employed extensively to execute the computation successfully. The bare matrix elements contain UV as well as IR divergences. The strong coupling constant renormalization is sufficient to make it UV finite. No extra UV renormalization is required for the spin-2 coupling as a consequence of the conserved SM energy-momentum tensor through which it couples universally to the SM fields. The UV finite matrix elements exhibit poles of infrared origin in dimensional regularization. The resulting infrared pole structures are in exact agreement with the Catani's prescription which ensures the universal factorization property of QCD amplitudes even in the presence of spin-2 field. This serves a crucial check on the correctness of our computation. The result presented here is an important piece, which now completes the full two-loop calculation of real graviton production associated with a jet. The full NNLO computation to this process needs additional inputs like the real-virtual piece and double real emission piece, with all these pieces together we will be able to predict precisely the mono-jet cross-section and distributions at the NNLO level.

CONCLUSION

Precision study is very important in searching for new physics as well as to provide reliable theoretical predictions. In hadron collider like the LHC, scattering processes greatly suffer from the QCD corrections thereby necessitate the inclusion of NLO, NNLO or even N^3LO corrections. From theoretical point of view, the calculation of scattering amplitudes become more and more complex with the inclusion of more and more particle in the final state as well as to achieve higher accuracy in the perturbation theory.

To this aim, we have studied at LO the triple neutral vector bosons *viz.* $\gamma\gamma\gamma$, $\gamma\gamma Z$, γZZ and ZZZ productions in the context of RS scenario. To get more realistic distributions we have taken into account effect of extra hard jet for these processes through the merging procedure. Moreover, the effect of soft radiations can not be neglected in hadron collider like the LHC. We have also taken those into account through the PYTHIA-6.4 matching program. This enables our results to be directly compared with the experiments and to search for RS signature in those channels.

To estimate the higher order effect in RS model, we have considered four important scattering channels $\gamma\gamma$, $\ell^+\ell^-$, ZZ , W^+W^- at the NLO. Theoretical scale uncertainties which are very large at the LO order are reduced with the inclusion of NLO calculation, thereby predicting high accuracy for cross-section and distributions. However this NLO

accuracy is not sufficient to describe the infrared region in some observable like transverse momentum. The reason is QCD radiation from the initial legs in this region leaves large logarithms which need to be taken into account. This necessitates the inclusion of a parton shower program. However care should be taken as the parton shower and the hard process both might contribute in the infrared region which might lead to double counting or gaps in those phase space region. Several methods like MC@NLO, POWHEG etc. are available to systematically address those issues. We have used the MC@NLO method as implemented in MG5_AMC@NLO framework. Using Herwig6 parton shower, we are able to provide NLO+PS accuracy for these di-final processes. We have systematically automatized the procedure and provide UFO model and codes for those processes so that they can be used in the search of RS signature at the LHC. These codes are publicly available in the website <http://amcatnlo.cern.ch> and can be used for any parameters and energies at the LHC.

NLO corrections provide reliable results for many processes. However it is always interesting to check the convergence of the perturbation theory by going beyond the NLO. In hadron colliders, scattering processes which involves more number of jets suffer greatly from large QCD correction. For example jet with missing energy is one such process which is used in the search for Dark Matter or any other BSM physics. It is found that the NLO correction for this process is very large. Therefore NLO accuracy is not sufficient for such processes and we have to think about the NNLO order. Whereas a full automation is possible at the NLO level for all SM processes and many BSM processes, automation at the NNLO level is still not possible. Not only the multi-loop calculations make the job difficult, but also the real emissions corrections are difficult to calculate. However, development are in progress towards these directions. Several methods are being proposed to achieve NNLO accuracy for different type of scattering processes. Towards this direction we have computed the full two-loop QCD corrections

for a massive spin-2 decaying to quark-anti-quark-gluon. This is one of the important subprocesses contributing in the calculation of jet+missing energy, where the missing energy is a massive graviton. Using state-of-the-art techniques we are able to show the universal infrared behavior of QCD. We have systematically automatized the procedure using several tools like FORM, Mathematica, LiteRed etc. This result can be used in the full NNLO correction to this process.



A.1 Color algebra

Below we present some important relations followed by the generators (T_{ij}^a) and structure constants (f^{abc}) of $SU(3)_c$.

$$\begin{aligned}
\text{Tr}(T^a T^b) &= \frac{1}{2} \delta^{ab}, \\
\text{Tr}(T^a T^b T^c) &= \frac{1}{4} (d^{abc} + i f^{abc}), \\
\text{Tr}(T^a T^b T^a T^c) &= -\frac{1}{4N} \delta^{bc}, \\
T_{ij}^a T_{kl}^a &= \frac{1}{2} \left(\delta_{il} \delta_{jk} - \frac{1}{N} \delta_{ij} \delta_{kl} \right), \\
T_{ij}^a T_{jk}^a &= \frac{N^2 - 1}{2N} \delta_{ik}, \\
f^{abc} &= -2i \text{Tr}(T^a [T^b, T^c]), \\
f^{acd} f^{bcd} &= N \delta^{ab}, \\
f^{ade} f^{bef} f^{cf d} &= \frac{N}{2} f^{abc}, \\
d^{abc} &= 2 \text{Tr}(T^a [T^b, T^c]), \\
\{T^a, T^b\} &= \frac{1}{N} \delta^{ab} + d^{abc} T^c, \\
T^a T^b &= \frac{1}{2} \left(\frac{1}{N} \delta^{ab} + (d^{abc} + i f^{abc}) T^c \right),
\end{aligned}$$

$$\text{Tr}(T^a T^b T^c) = \frac{1}{4} (d^{abc} + i f^{abc}),$$

$$f^{acd} d^{bcd} = 0 .$$

d^{abc} is known as the symmetric structure constant and for QCD $N = 3$.

In the fundamental representation of $SU(3)$, $T^a T^a$ is a Casimir operator which commutes with all the generators of $SU(3)$. It is easy to prove that $T^a T^a = \frac{N^2 - 1}{2N} = C_F$.

$$(T^a T^a)_{ij} = T_{ik}^a T_{kj}^a = \frac{1}{2} \left(\delta_{ij} \delta_{kk} - \frac{1}{N} \delta_{ik} \delta_{kj} \right)$$

$$= \frac{N^2 - 1}{2N} \delta_{ij}$$

$$= C_F \delta_{ij} \quad (\text{A.1})$$

where we define,

$$C_F = \frac{N^2 - 1}{2N} \quad (\text{A.2})$$

Therefore $T^a T^a = C_F I$, a multiple of the unit matrix and thus commutes with all the generators of $SU(3)$.

In similar fashion, the Casimir in the adjoint representation can be found to be $C_A = N$. Note that in the adjoint representation the structure constants can be written as $(N^2 - 1) \times (N^2 - 1)$ matrices as,

$$A_{bc}^a \equiv -i f^{abc} \quad (\text{A.3})$$

Therefore the Jacobi identity (Eq. 2.14) reflects as

$$[F^a, F^b] = i f^{abc} F^c \quad (\text{A.4})$$

Thus in the adjoint representation $F^c F^c$ represents a Casimir operator.

$$\begin{aligned}
 (F^c F^c)_{ab} &= F_{ad}^c F_{db}^c \\
 &= i^2 f^{cad} f^{cdb} \\
 &= f^{acd} f^{bcd} \\
 &= N \delta_{ab} \\
 &= C_A \delta_{ab}
 \end{aligned} \tag{A.5}$$

where $C_A = N$ is the Casimir in the adjoint representation. Therefore in the case of QCD, we have

$$C_F = \frac{4}{3}, \quad C_A = 3 \tag{A.6}$$

A.2 Dirac Algebra in D-dimension

The anti-commutation relation among the gamma matrices are defined same as the 4-dimensional case. Thus

$$\{\gamma_\mu, \gamma_\nu\} \equiv \gamma_\mu \gamma_\nu + \gamma_\nu \gamma_\mu = 2g_{\mu\nu} \mathbb{1} \tag{A.7}$$

where $\mu, \nu = 0, 1, 2, \dots, D - 1$.

$$\begin{aligned}
 g_{\mu\nu} g^{\mu\nu} &= D \\
 \gamma_\mu \gamma^\mu &= D \mathbb{1}
 \end{aligned} \tag{A.8}$$

In the D dimension, for simplicity the following is taken,

$$\text{Tr}(\mathbb{1}) = 4 \tag{A.9}$$

With this choice, the trace relations among the gamma matrices do not get affected in

D -dimension. Note that one can also choose

$$\text{Tr}(\mathbb{1}) = 2^{D/2} \quad (\text{A.10})$$

with even D . However, this choice differs by one ε term which when multiplied with the divergent term gives constant term. This constant term can be absorbed in renormalisation and provides the renormalisation scheme.

In D dimension however, there is now an ambiguity with the definition of γ_5 matrix. In 4-dimensions γ_5 is defined as

$$\gamma_5 = \frac{i}{4!} \varepsilon_{\mu\nu\rho\sigma} \gamma^\mu \gamma^\nu \gamma^\rho \gamma^\sigma \quad (\text{A.11})$$

with the properties,

$$\{\gamma_5, \gamma_\mu\} = 0, \quad \gamma_5^2 = \mathbb{1}, \quad \text{Tr}(\gamma_5 \gamma_\mu \gamma_\nu \gamma_\rho \gamma_\sigma) = 4i \varepsilon_{\mu\nu\rho\sigma} \quad (\text{A.12})$$

However this definition can't be used in D -dimension as this will lead to inconsistencies. For example, in D -dimension,

$$\text{Tr}(\gamma_\mu \gamma_5 \gamma^\mu) = -\text{Tr}(\gamma_\mu \gamma^\mu \gamma_5) = D \text{Tr}(\gamma_5) \quad (\text{A.13})$$

This implies that

$$D \text{Tr}(\gamma_5) = 0 \quad (\text{A.14})$$

Now since $D \neq 0$, we must have $\text{Tr}(\gamma_5) = 0$. In a similar way it can be proved that

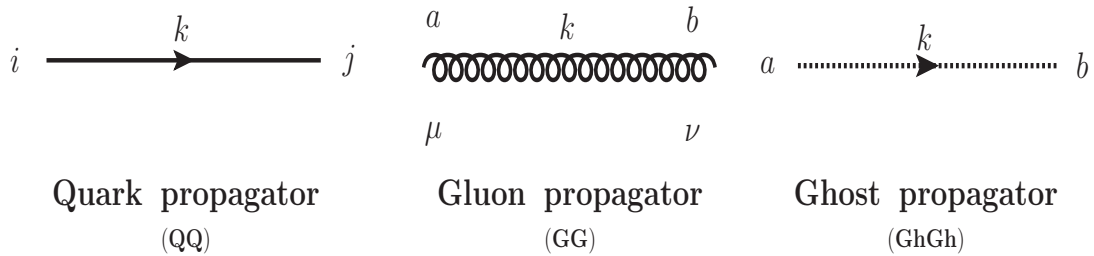
$$\text{Tr}(\gamma_5 \gamma_\mu \gamma_\nu \gamma_\rho \gamma_\sigma) = 0 \quad (\text{A.15})$$

which actually contradicts with the 4-dimensional result. In fact if we demand that our

expressions can be analytically continued from the D -dimensions to the 4-dimesnions, then we can not choose that γ_5 matrix anticommutes with all other gamma matrices in D -dimensions. Several way out are possible to this problem. For example 't Hooft and Veltman suggested to define γ_5 such that it anti-commutes with the 4-dimensional subset of gamma matrices but it commutes with the rest $D - 4$ gamma matrices. More details can be found on this problem in [200] and references therein.

A.3 QCD Feynman rules

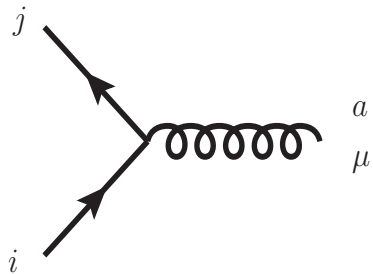
A.3.1 Propagators



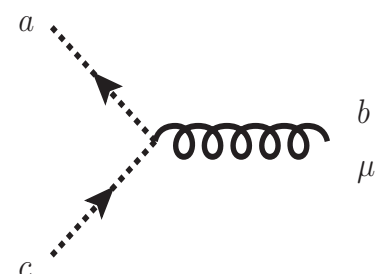
$$\begin{aligned}
 \mathbf{QQ} &\equiv \frac{i\delta_{ij}(\not{k} + m_q)}{(k^2 - m_q^2 + i\epsilon)}, \\
 \mathbf{GG} &\equiv \frac{-i\delta_{ab}}{k^2 + i\epsilon} \left[g_{\mu\nu} - (1 - \xi) \frac{k_\mu k_\nu}{k^2} \right], \\
 \mathbf{GhGh} &\equiv \frac{-i\delta_{ab}}{k^2 + i\epsilon}.
 \end{aligned} \tag{A.16}$$

$$\xi \text{ is the gauge parameter, } \xi = \begin{cases} 1, & \text{Feynman Gauge} \\ 0, & \text{Landau Gauge} \end{cases}$$

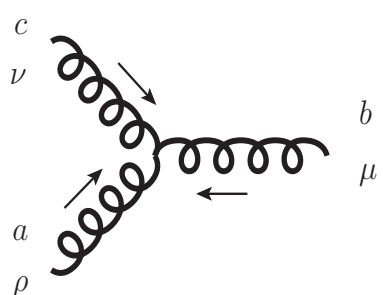
A.3.2 Vertices



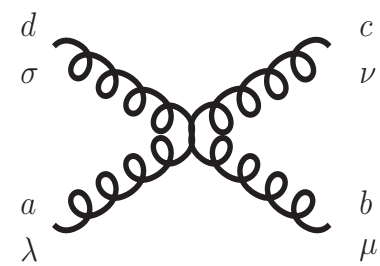
Quark – gluon vertex
(QQG)



Ghost – gluon vertex
(GhGhG)



Three – gluon vertex
(GGG)



Four – gluon vertex
(GGGG)

$$\text{QQG} \equiv -ig_s \gamma_\mu T_{ij}^a ,$$

$$\text{GhGhG} \equiv g_s f^{abc} q_\mu ,$$

$$\text{GGG} \equiv -g_s f^{abc} \left[(q_1 - q_2)_\nu g_{\mu\rho} + (q_2 - q_3)_\rho g_{\mu\nu} + (q_3 - q_1)_\mu g_{\nu\rho} \right], \quad (\text{A.17})$$

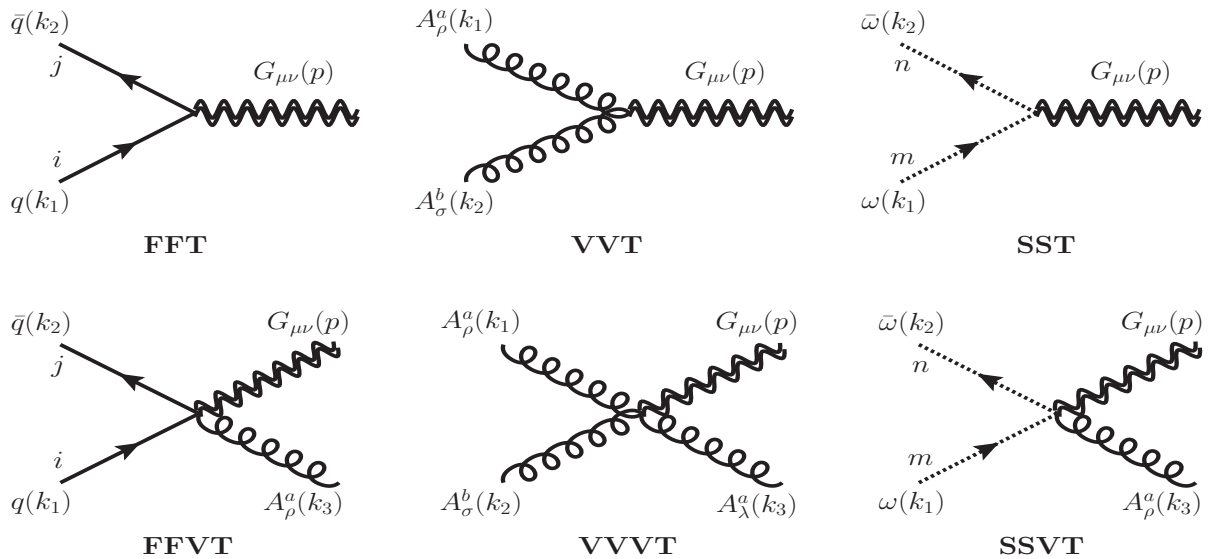
$$\text{GGGG} \equiv -ig_s^2 \left[f^{abe} f^{cde} (g_{\nu\rho} g_{\mu\sigma} - g_{\rho\sigma} g_{\mu\nu}) \right.$$

$$+ f^{ace} f^{bde} (g_{\mu\rho} g_{\nu\sigma} - g_{\rho\sigma} g_{\mu\nu})$$

$$\left. + f^{ade} f^{cbe} (g_{\nu\rho} g_{\mu\sigma} - g_{\rho\mu} g_{\sigma\nu}) \right].$$

B.1 Feynman rules for SM-graviton interactions

Feynman rules for a spin-2 graviton interacting with the SM with tensorial couplings are summarized below.



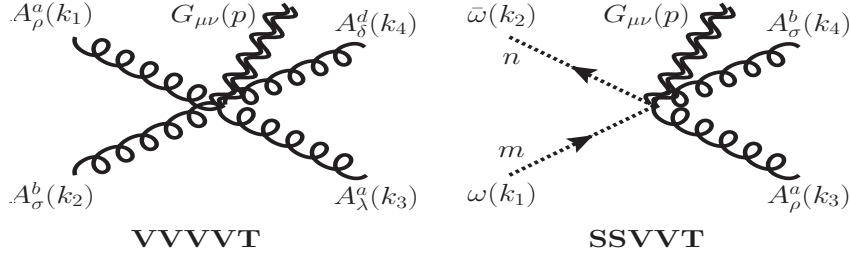


Figure B.1: Feynman rules for graviton interaction with scalar, vector and fermions.

$$\begin{aligned}
\text{FFT} &\equiv -\frac{i\kappa}{8}\delta_{ij}\left[\gamma_\mu(k_1-k_2)_\nu + \gamma_\nu(k_1-k_2)_\mu - 2\eta_{\mu\nu}(\not{k}_1 - \not{k}_2 - 2m_q)\right], \\
\text{VVT} &\equiv -\frac{i\kappa}{2}\delta^{ab}\left[(k_1 \cdot k_2 + m_A^2)C_{\mu\nu\rho\sigma} + D_{\mu\nu\rho\sigma} + \xi^{-1}E_{\mu\nu\rho\sigma}\right], \\
\text{SST} &\equiv -\frac{i\kappa}{2}\delta_{mn}\left[m_\phi^2\eta_{\mu\nu} + C_{\mu\nu\rho\sigma}k_1^\rho k_2^\sigma\right], \\
\text{FFVT} &\equiv \frac{ig\kappa}{4}T_{ij}^a\left[C_{\mu\nu\rho\sigma} - \eta_{\mu\nu}\eta_{\rho\sigma}\right]\gamma^\sigma, \\
\text{VVVT} &\equiv \frac{g\kappa}{2}f^{abc}\left[C_{\mu\nu\rho\sigma}(k_1 - k_2)_\lambda + C_{\mu\nu\rho\lambda}(k_3 - k_1)_\sigma + C_{\mu\nu\sigma\lambda}(k_2 - k_3)_\rho + F_{\mu\nu\rho\sigma\lambda}\right], \\
\text{SSVT} &\equiv \frac{ig\kappa}{2}\left[C_{\mu\nu\rho\sigma}(k_1 + k_2)^\sigma\right]T_{mn}^a, \\
\text{VVVVT} &\equiv -\frac{ig^2\kappa}{2}\left[f^{eac}f^{ebd}G_{\mu\nu\rho\sigma\lambda\delta} + f^{eab}f^{ecd}G_{\mu\nu\rho\lambda\sigma\delta} + f^{ead}f^{ebc}G_{\mu\nu\rho\sigma\delta\lambda}\right], \\
\text{SSVVT} &\equiv -\frac{ig^2\kappa}{2}[C_{\mu\nu\rho\sigma}\{T^a, T^b\}_{mn}].
\end{aligned}$$

The parameters C, D, E, F, G are defined as,

$$\begin{aligned}
C_{\mu\nu\rho\sigma} &= \eta_{\mu\rho}\eta_{\nu\sigma} + \eta_{\mu\sigma}\eta_{\nu\rho} - \eta_{\mu\nu}\eta_{\rho\sigma}, \\
D_{\mu\nu\rho\sigma}(k_1, k_2) &= \eta_{\mu\nu}k_{1\sigma}k_{2\rho} - \left[\eta_{\mu\sigma}k_{1\nu}k_{2\rho} + \eta_{\mu\rho}k_{1\nu}k_{2\sigma} - \eta_{\rho\sigma}k_{1\mu}k_{2\nu} + (\mu \leftrightarrow \nu)\right], \\
E_{\mu\nu\rho\sigma}(k_1, k_2) &= \eta_{\mu\nu}(k_{1\rho}k_{1\sigma} + k_{2\rho}k_{2\sigma} + k_{1\sigma}k_{2\rho}) - \left[\eta_{\nu\sigma}k_{1\mu}k_{1\rho} + \eta_{\nu\rho}k_{2\mu}k_{2\sigma} + (\mu \leftrightarrow \nu)\right], \\
F_{\mu\nu\rho\sigma\lambda}(k_1, k_2, k_3) &= \eta_{\mu\rho}\eta_{\sigma\lambda}(k_2 - k_3)_\nu + \eta_{\mu\sigma}\eta_{\rho\lambda}(k_3 - k_1)_\nu + \eta_{\mu\lambda}\eta_{\rho\sigma}(k_1 - k_2)_\nu + (\mu \leftrightarrow \nu), \\
G_{\mu\nu\rho\sigma\lambda\delta} &= \eta_{\mu\nu}(\eta_{\rho\sigma}\eta_{\lambda\delta} - \eta_{\rho\delta}\eta_{\sigma\lambda}) + \left[\eta_{\mu\rho}\eta_{\nu\delta}\eta_{\lambda\sigma} + \eta_{\mu\lambda}\eta_{\nu\sigma}\eta_{\rho\delta}\right. \\
&\quad \left.- \eta_{\mu\rho}\eta_{\nu\sigma}\eta_{\lambda\delta} - \eta_{\mu\lambda}\eta_{\nu\delta}\eta_{\rho\sigma} + (\mu \leftrightarrow \nu)\right].
\end{aligned} \tag{B.1}$$

C

C.1 Harmonic polylogarithms

Harmonic polylogarithms (HPLs) play a central role in the analytic evaluation of integrals arising in perturbative quantum field theory. They are generalisation of Neilson's polylogarithms and are defined as one-variable functions depending, besides the argument, on a set of indices, grouped for convenience into a vector. Here we briefly discuss some important properties of HPLs. For more details one can see [176, 179]. The HPLs are represented by $H(\vec{m}_\omega; y)$; \vec{m}_ω being a ω -dimensional vector which belongs to the set $\{-1, 0, 1\}$ through which we define the following rational functions

$$f(1; y) \equiv \frac{1}{1-y}, \quad f(0; y) \equiv \frac{1}{y}, \quad f(-1; y) \equiv \frac{1}{1+y}. \quad (\text{C.1})$$

The weight-1 ($\omega = 1$) HPLs are then defined as

$$H(1, y) \equiv -\ln(1-y), \quad H(0, y) \equiv \ln(y), \quad H(-1, y) \equiv \ln(1+y). \quad (\text{C.2})$$

For $\omega > 1$ HPLs are defined as

$$H(m, \vec{m}_\omega; y) \equiv \int_0^y dx f(m, x) H(\vec{m}_\omega; x), \quad m \in 0, \pm 1. \quad (\text{C.3})$$

Moreover the higher dimensional HPLs are defined following the Eq. (C.3) for the new elements 2,3 in \vec{m}_ω , representing a new class of rational functions

$$f(2; y) \equiv f(1 - z; y) \equiv \frac{1}{1 - y - z}, \quad f(3; y) \equiv f(z; y) \equiv \frac{1}{y + z}; \quad (\text{C.4})$$

correspondingly the weight-1 ($\omega = 1$) two-dimensional HPLs are given by

$$H(2, y) \equiv -\ln\left(1 - \frac{y}{1 - z}\right), \quad H(3, y) \equiv \ln\left(\frac{y + z}{z}\right). \quad (\text{C.5})$$

Properties

HPLs follow some important properties,

Shuffle algebra: Product of two HPLs with weights ω_1 and ω_2 of same argument y is a HPL of weight $(\omega_1 + \omega_2)$ and argument y . This way all possible permutations of the elements of \vec{m}_{ω_1} and \vec{m}_{ω_2} are considered preserving the relative orders of the element of \vec{m}_{ω_1} and \vec{m}_{ω_2} ,

$$H(\vec{m}_{\omega_1}; y) H(\vec{m}_{\omega_2}; y) = \sum_{\vec{m}_\omega = \vec{m}_{\omega_1} \uplus \vec{m}_{\omega_2}} H(\vec{m}_\omega; y) \quad (\text{C.6})$$

Integration-by-parts identities: Using the integration-by-parts identities the ordering of the elements of \vec{m}_ω inside the HPL can be reversed and in this process some products of

two HPLs can be generated.

$$\begin{aligned}
 H(\vec{m}_\omega; y) &\equiv H(m_1, m_2, \dots, m_\omega; y) = H(m_1; y) H(m_2, \dots, m_\omega; y) \\
 &\quad - H(m_2, m_1; y) H(m_3, \dots, m_\omega; y) \\
 &\quad + \dots + (-1)^{\omega+1} H(m_\omega, \dots, m_2, m_1; y).
 \end{aligned} \tag{C.7}$$

Equations C.6 and C.7 are very useful in writing the higher-weight HPLs in terms of lower-weight HPLs or products of HPLs, which have been used in the checks of the different poles in chapter 6. Below we provide the necessary relations of HPLs used in our computation.

$$\begin{aligned}
 H(0, 2, 0, y) &= H(0, y)H(0, 2, y) - 2H(0, 0, 2, y), \\
 H(1, 0, 2, y) &= H(1, y)H(0, 2, y) - H(0, 1, 2, y) - H(0, 2, 1, y), \\
 H(1, 2, 0, y) &= H(1, y)H(2, 0, y) - H(2, 1, y)H(0, y) + H(0, 2, 1, y), \\
 H(2, 0, 0, y) &= H(2, y)H(0, 0, y) - H(0, 2, y)H(0, y) + H(0, 0, 2, y), \\
 H(2, 0, 2, y) &= H(2, y)H(0, 2, y) - 2H(0, 2, 2, y), \\
 H(2, 2, 2, y) &= \frac{1}{3}H(2, y)H(2, 2, y), \\
 H(2, 2, 0, y) &= H(2, y)H(2, 0, y) - H(2, 2, y)H(0, y) + H(0, 2, 2, y), \\
 H(3, 0, 2, y) &= H(3, y)H(0, 2, y) - H(0, 3, 2, y) - H(0, 2, 3, y), \\
 H(3, 2, 0, y) &= H(3, y)H(2, 0, y) - H(2, 3, y)H(0, y) + H(0, 2, 3, y), \\
 H(3, 3, 2, y) &= H(3, y)H(3, 2, y) - H(3, 3, y)H(2, y) + H(2, 3, 3, y), \\
 H(2, 1, 0, y) &= H(2, y)H(1, 0, y) - H(1, 2, y)H(0, y) + H(0, 1, 2, y), \\
 H(2, 3, 2, y) &= H(2, y)H(3, 2, y) - 2H(3, 2, 2, y)
 \end{aligned} \tag{C.8}$$

C.2 Two-loop coefficients

$$\begin{aligned}
\mathcal{A}_0^{(2)} &= -\frac{3\beta_0^2}{8} \mathcal{A}_0; \\
\mathcal{A}_{1;C_A^2}^{(2)} &= -\mathcal{A}_0; \quad \mathcal{A}_{1;C_F^2}^{(2)} = 24 \mathcal{A}_0; \quad \mathcal{A}_{1;n_f^2}^{(2)} = 0; \quad \mathcal{A}_{1;C_A C_F}^{(2)} = -26 \mathcal{A}_0; \quad \mathcal{A}_{1;C_A n_f}^{(2)} = 0; \quad \mathcal{A}_{1;C_F n_f}^{(2)} = 0; \\
\mathcal{A}_{2;C_A^2}^{(2)} &= \frac{55}{12} \mathcal{A}_0; \quad \mathcal{A}_{2;C_F^2}^{(2)} = -12 \mathcal{A}_0; \quad \mathcal{A}_{2;n_f^2}^{(2)} = 0; \quad \mathcal{A}_{2;C_A C_F}^{(2)} = \frac{23}{2} \mathcal{A}_0; \quad \mathcal{A}_{2;C_A n_f}^{(2)} = -\frac{5}{6} \mathcal{A}_0; \quad \mathcal{A}_{2;C_F n_f}^{(2)} = -\mathcal{A}_0; \\
\mathcal{A}_{3;C_A^2}^{(2)} &= \left\{ 8(-1+y)^2 y(-1+z)^2 z(y+z)(39y^6(-1+4z) + y^5(84-710z+204z^2) + 3z^3(26-41z+28z^2-13z^3) \right. \\
&\quad - 3y^4(41-372z+507z^2+56z^3) + 2yz^2(117-543z+558z^2-355z^3+78z^4) - 2y^3(-39+543z-1354z^2 \\
&\quad + 850z^3+84z^4) + y^2z(234-1662z+2708z^2-1521z^3+204z^4)) - 8(-1+y)^2 y(-1+z)^2 z(y+z)^4(56+500y^4 \\
&\quad + 34z-396z^2+550z^3-244z^4+y^3(-1415+1348z)+3y^2(433-715z+180z^2)-4y(110-219z+42z^2 \\
&\quad + 38z^3))H(0,y)^3 + 8(-1+y)^2 y(-1+z)^2 z(y+z)^4(-56+244y^4+440z-1299z^2+1415z^3-500z^4+2y^3(-275 \\
&\quad + 76z)+y^2(396+168z-540z^2)-y(34+876z-2145z^2+1348z^3))H(0,z)^3 - 32(-1+y)^2 y(-1+z)^2 z(y+z)^4(9 \\
&\quad + 364y^4-203z+702z^2-872z^3+364z^4+y^3(-872+564z)+6y^2(117-167z+92z^2)+y(-203+606z-1002z^2 \\
&\quad + 564z^3))H(1,z)^3 + (-1728y^{12}(-1+z)^2+216(-1+z)^5z^6(-1+4z)+24y^{11}(-1+z)^2(375+718z)+y^{10}(-19080 \\
&\quad - 28289z+250122z^2-338949z^3+136304z^4)-y(-1+z)^2 z^5(-8082+36428z-80967z^2+91745z^3-40992z^4+1728z^5) \\
&\quad + y^9(20808+63133z-748547z^2+1624467z^3-1359901z^4+400256z^5)+y^2(-1+z)^2 z^4(25944-171016z+438304z^2 \\
&\quad - 585767z^3+364650z^4-73560z^5+864z^6)+y^8(-12024-69787z+1130000z^2-3636494z^3+4922656z^4-3035579z^5 \\
&\quad + 701120z^6)+y^7(3312+52501z-1005911z^2+4577790z^3-9135618z^4+9138769z^5-4491307z^6+860032z^7) \\
&\quad + y^3z^3(32844-401168z+1810731z^2-4338377z^3+6108582z^4-5103134z^5+2392815z^6-537669z^7+35376z^8) \\
&\quad + y^4z^2(23424-374888z+2225864z^2-6614805z^3+11116384z^4-10963698z^5+6184528z^6-1787581z^7+190880z^8) \\
&\quad + y^5z(6066-175600z+1559775z^2-6176973z^3+12917254z^4-15269476z^5+10196989z^6-3546779z^7+488960z^8) \\
&\quad + y^6(-288-26312z+553704z^2-3461777z^3+9763000z^4-14401588z^5+11527644z^6-4728907z^7+774416z^8))H(2,y)^2 \\
&\quad - 32(-1+y)^2 y(-1+z)^2 z(y+z)^4(9+364y^4-203z+702z^2-872z^3+364z^4+y^3(-872+564z)+6y^2(117-167z \\
&\quad + 92z^2)+y(-203+606z-1002z^2+564z^3))H(2,y)^3 + H(0,y)^2((y+z)^2(1728y^{10}(-1+z)^2+216(-1+z)^5z^3(-1 \\
&\quad + 4z)-72y^9(-1+z)^2(149+87z)+y^8(28080-43945z-17990z^2+55603z^3-21640z^4)+y(-1+z)^2 z^2(144-3573z \\
&\quad + 10219z^2-12168z^3+4234z^4+864z^5)-y^7(39888-94511z+2851z^2+137595z^3-104887z^4+19064z^5)+y^6(32832 \\
&\quad - 125478z+90408z^2+113163z^3-158918z^4+46681z^5+1096z^6)-y^2(-1+z)^2 z(360-2430z-10125z^2+18134z^3 \\
&\quad - 1460z^4-13140z^5+4320z^6)+y^5(-15336+94486z-141904z^2+19649z^3+66045z^4+13557z^5-53601z^6+17104z^7) \\
&\quad + y^4(3600-38177z+94480z^2-70947z^3+25180z^4-94718z^5+142546z^6-75040z^7+13184z^8)+y^3(-288+7227z \\
&\quad - 28965z^2+25131z^3+4151z^4+35390z^5-108748z^6+97128z^7-33618z^8+2592z^9))+48(-1+y)^2 y(-1+z)^2 z(y \\
&\quad + z)^4(16y^4+4y^3(-11+6z)+6y^2(8-9z+2z^2)-3(-2+4z-3z^2+z^3)+y(-26+48z-33z^2+12z^3))H(0,z) \\
&\quad + 144(-1+y)^2 y(-1+z)^2 z(y+z)^4(2+16y^4-4z+3z^2-z^3+2y^3(-21+8z)+6y^2(7-6z+2z^2)+y(-18 \\
&\quad + 24z-15z^2+4z^3))H(1,z) + 48(-1+y)^2 y(-1+z)^2 z(y+z)^4(2+16y^4-4z+3z^2-z^3+2y^3(-21+8z) \\
&\quad + 6y^2(7-6z+2z^2)+y(-18+24z-15z^2+4z^3))H(2,y)) + H(0,z)^2((y+z)^2(1728y^9(-1+z)^2(-1+3z) \\
&\quad - 216(-1+z)^6z^3(-1+4z)+y^8(9000-48470z+93492z^2-78258z^3+23552z^4)+4y^7(-4770+28897z-69529z^2 \\
&\quad + 79974z^3-42772z^4+8200z^5)+y(-1+z)^2 z^2(144-3501z+19081z^2-43239z^3+50375z^4-23976z^5+1728z^6) \\
&\quad + y^6(20808-148735z+427794z^2-614728z^3+447358z^4-140145z^5+9016z^6)+y^5(-12024+107821z-367983z^2 \\
&\quad + 619778z^3-507386z^4+132177z^5+54601z^6-26984z^7)-y^2(-1+z)^2 z(360-2934z-12651z^2+74708z^3-142537z^4 \\
&\quad + 119942z^5-36936z^6+864z^7)+y^4(3312-41639z+174106z^2-315241z^3+188404z^4+184665z^5-356162z^6 \\
&\quad + 199207z^7-37336z^8)+y^3(-288+7155z-40995z^2+60519z^3+92277z^4-437623z^5+633399z^6-444135z^7+146323z^8 \\
&\quad - 16632z^9))+48(-1+y)^2 y(-1+z)^2 z(y+z)^4(y^3(-1+4z)+4y(-1+z)^2(-1+4z)+3y^2(1-5z+4z^2)+2(1 \\
&\quad - 9z+21z^2-21z^3+8z^4))H(1,z) + 144(-1+y)^2 y(-1+z)^2 z(y+z)^4(y^3(-1+4z)+4y(-1+z)^2(-1+4z) \\
&\quad + 3y^2(1-5z+4z^2)+2(1-9z+21z^2-21z^3+8z^4))H(2,y)) + H(1,z)^2(-1728y^{12}(-1+z)^2+216(-1 \\
&\quad + z)^5z^6(-1+4z)+24y^{11}(-1+z)^2(375+718z)+y^{10}(-19080-28289z+250122z^2-338949z^3+136304z^4)-y(-1 \\
&\quad + z)^2z^5(-8082+36428z-80967z^2+91745z^3-40992z^4+1728z^5)+y^9(20808+63133z-748547z^2+1624467z^3 \\
&\quad - 1359901z^4+400256z^5)+y^2(-1+z)^2 z^4(25944-171016z+438304z^2-585767z^3+364650z^4-73560z^5+864z^6) \\
&\quad + y^8(-12024-69787z+1130000z^2-3636494z^3+4922656z^4-3035579z^5+701120z^6)+y^7(3312+52501z-1005911z^2 \\
&\quad + 4577790z^3-9135618z^4+9138769z^5-4491307z^6+860032z^7)+y^3z^3(32844-401168z+1810731z^2-4338377z^3
\end{aligned}$$

$$\begin{aligned}
& + 6108582z^4 - 5103134z^5 + 2392815z^6 - 537669z^7 + 35376z^8) + y^4z^2(23424 - 374888z + 2225864z^2 - 6614805z^3 \\
& + 11116384z^4 - 10963698z^5 + 6184528z^6 - 1787581z^7 + 190880z^8) + y^5z(6066 - 175600z + 1559775z^2 - 6176973z^3 \\
& + 12917254z^4 - 15269476z^5 + 10196989z^6 - 3546779z^7 + 488960z^8) + y^6(-288 - 26312z + 553704z^2 - 3461777z^3 \\
& + 9763000z^4 - 14401588z^5 + 11527644z^6 - 4728907z^7 + 774416z^8) - 96(-1 + y)^2y(-1 + z)^2z(y + z)^4(13 + 380y^4 - 225z \\
& + 747z^2 - 915z^3 + 380z^4 + y^3(-915 + 584z) + 9y^2(83 - 117z + 64z^2) + y(-225 + 654z - 1053z^2 + 584z^3))H(2, y) \\
& - 96(-1 + y)^2y(-1 + z)^2z(y + z)^4(4 + 16y^4 - 22z + 45z^2 - 43z^3 + 16z^4 + y^3(-43 + 20z) + 3y^2(15 - 17z + 8z^2) \\
& + y(-22 + 48z - 51z^2 + 20z^3))H(3, y) - 2(y + z)^2(1728y^{10}(-1 + z)^2 + 216(-1 + z)^5z^3(-1 + 4z) - 72y^9(-1 \\
& + z)^2(149 + 87z) + y^8(28080 - 43945z - 17990z^2 + 55603z^3 - 21640z^4) + y(-1 + z)^2z^2(144 - 3573z + 10219z^2 \\
& - 12168z^3 + 4234z^4 + 864z^5) - y^7(39888 - 94511z + 2851z^2 + 137595z^3 - 104887z^4 + 19064z^5) + y^6(32832 - 125478z \\
& + 90408z^2 + 113163z^3 - 158918z^4 + 46681z^5 + 1096z^6) - y^2(-1 + z)^2z(360 - 2430z - 10125z^2 + 18134z^3 - 1460z^4 \\
& - 13140z^5 + 4320z^6) + y^5(-15336 + 94486z - 141904z^2 + 19649z^3 + 66045z^4 + 13557z^5 - 53601z^6 + 17104z^7) + y^4(3600 \\
& - 38177z + 94480z^2 - 70947z^3 + 25180z^4 - 94718z^5 + 142546z^6 - 75040z^7 + 13184z^8) + y^3(-288 + 7227z - 28965z^2 \\
& + 25131z^3 + 4151z^4 + 35390z^5 - 108748z^6 + 97128z^7 - 33618z^8 + 2592z^9))H(0, 0, y) - 2(y + z)^2(1728y^9(-1 + z)^2(-1 \\
& + 3z) - 216(-1 + z)^6z^3(-1 + 4z) + y^8(9000 - 48470z + 93492z^2 - 78258z^3 + 23552z^4) + 4y^7(-4770 + 28897z - 69529z^2 \\
& + 79974z^3 - 42772z^4 + 8200z^5) + y(-1 + z)^2z^2(144 - 3501z + 19081z^2 - 43239z^3 + 50375z^4 - 23976z^5 + 1728z^6) \\
& + y^6(20808 - 148735z + 427794z^2 - 614728z^3 + 447358z^4 - 140145z^5 + 9016z^6) + y^5(-12024 + 107821z - 367983z^2 \\
& + 619778z^3 - 507386z^4 + 132177z^5 + 54601z^6 - 26984z^7) - y^2(-1 + z)^2z(360 - 2934z - 12651z^2 + 74708z^3 - 142537z^4 \\
& + 119942z^5 - 36936z^6 + 864z^7) + y^4(3312 - 41639z + 174106z^2 - 315241z^3 + 188404z^4 + 184665z^5 - 356162z^6 \\
& + 199207z^7 - 37336z^8) + y^3(-288 + 7155z - 40995z^2 + 60519z^3 + 92277z^4 - 437623z^5 + 633399z^6 - 444135z^7 + 146323z^8 \\
& - 16632z^9))H(0, 0, z) + 8(-1 + y)^2y(-1 + z)z(528y^8(-1 + z) - 3(-1 + z)^2z^4(14 - 14z + 3z^2) + 6y^7(227 - 631z \\
& + 404z^2) + 6y^6(-223 + 1245z - 1758z^2 + 738z^3) + 3y^5(182 - 2102z + 5517z^2 - 4865z^3 + 1284z^4) + 2y^2z^2(-294 \\
& + 1706z - 2858z^2 + 1581z^3 + 225z^4 - 354z^5) + yz^3(-384 + 1354z - 1582z^2 + 531z^3 + 261z^4 - 180z^5) - 4y^3z(96 \\
& - 1033z + 2746z^2 - 2667z^3 + 666z^4 + 180z^5) + y^4(-42 + 2398z - 11683z^2 + 18420z^3 - 10149z^4 + 1128z^5))H(0, 1, z) \\
& - 8(-1 + y)y(-1 + z)^2z(528y^9 + 6y^8(-323 + 492z) + 12y^7(237 - 866z + 609z^2) + 3z^4(-30 + 60z - 49z^2 + 19z^3) \\
& + 3y^6(-692 + 4784z - 7993z^2 + 3540z^3) + yz^3(-144 + 1364z - 1944z^2 + 1374z^3 - 405z^4) + y^5(732 - 9572z + 30498z^2 \\
& - 31161z^3 + 9960z^4) + y^2z^2(-204 + 3656z - 8678z^2 + 7902z^3 - 3411z^4 + 348z^5) + 2y^3z(-72 + 2320z - 8830z^2 \\
& + 11118z^3 - 6117z^4 + 1086z^5) + y^4(-90 + 2804z - 18275z^2 + 34641z^3 - 24864z^4 + 6048z^5))H(0, 2, y) + 264(-1 \\
& + y)^2y^2(-1 + z)^2z(y + z)^4(16y^3 + y^2(-41 + 12z) - 2(7 - 6z + 3z^2) + 3y(13 - 9z + 4z^2))H(1, 0, y) - 8(-1 \\
& + y)^2y(-1 + z)z(-3(-1 + z)^2z^4(30 - 30z + 19z^2) + y^7(57 - 405z + 348z^2) + 3y^6(-49 + 392z - 939z^2 + 592z^3) \\
& + 3y^5(60 - 516z + 1941z^2 - 2857z^3 + 1356z^4) + yz^3(-144 + 956z - 2180z^2 + 2505z^3 - 1581z^4 + 444z^5) \\
& + y^2z^2(-204 + 1868z - 6197z^2 + 9312z^3 - 6951z^4 + 2160z^5) + y^3z(-144 + 1808z - 8288z^2 + 15567z^3 - 13539z^4 \\
& + 4548z^5) + y^4(-90 + 902z - 5345z^2 + 13260z^3 - 14271z^4 + 5472z^5))H(1, 0, z) + 2(1728y^{12}(-1 + z)^2 - 216(-1 \\
& + z)^5z^6(-1 + 4z) - 24y^{11}(-1 + z)^2(375 + 718z) + y^{10}(19080 + 28289z - 250122z^2 + 338949z^3 - 136304z^4) + y(-1 \\
& + z)^2z^5(-8082 + 36428z - 80967z^2 + 91745z^3 - 40992z^4 + 1728z^5) - y^9(20808 + 63133z - 748547z^2 + 1624467z^3 \\
& - 1359901z^4 + 400256z^5) + y^8(12024 + 69787z - 113000z^2 + 3636494z^3 - 4922656z^4 + 3035579z^5 - 701120z^6) - y^2(-1 \\
& + z)^2z^4(25944 - 171016z + 438304z^2 - 585767z^3 + 364650z^4 - 73560z^5 + 864z^6) - y^7(3312 + 52501z - 1005911z^2 \\
& + 4577790z^3 - 9135618z^4 + 9138769z^5 - 4491307z^6 + 860032z^7) + y^6(288 + 26312z - 553704z^2 + 3461777z^3 - 9763000z^4 \\
& + 14401588z^5 - 11527644z^6 + 4728907z^7 - 774416z^8) + y^5z(-6066 + 175600z - 1559775z^2 + 6176973z^3 - 12917254z^4 \\
& + 15269476z^5 - 10196989z^6 + 3546779z^7 - 488960z^8) + y^4z^2(-23424 + 374888z - 2225864z^2 + 6614805z^3 - 11116384z^4 \\
& + 10963698z^5 - 6184528z^6 + 1787581z^7 - 190880z^8) + y^3z^3(-32844 + 401168z - 1810731z^2 + 4338377z^3 - 6108582z^4 \\
& + 5103134z^5 - 2392815z^6 + 537669z^7 - 35376z^8))H(1, 1, z) + H(3, y)(96(-1 + y)^2y(-1 + z)^2z(y + z)^4(4 + 16y^4 - 22z \\
& + 45z^2 - 43z^3 + 16z^4 + y^3(-43 + 20z) + 3y^2(15 - 17z + 8z^2) + y(-22 + 48z - 51z^2 + 20z^3))H(0, 1, z) + 96(-1 \\
& + y)^2y(-1 + z)^2z(y + z)^4(4 + 16y^4 - 22z + 45z^2 - 43z^3 + 16z^4 + y^3(-43 + 20z) + 3y^2(15 - 17z + 8z^2) + y(-22 \\
& + 48z - 51z^2 + 20z^3))H(1, 0, z) + 192(-1 + y)^2y(-1 + z)^2z(y + z)^4(4 + 16y^4 - 22z + 45z^2 - 43z^3 + 16z^4 \\
& + y^3(-43 + 20z) + 3y^2(15 - 17z + 8z^2) + y(-22 + 48z - 51z^2 + 20z^3))H(1, 1, z)) - 8(-1 + y)y(-1 + z)^2z(528y^9 \\
& + 6y^8(-323 + 492z) + 12y^7(237 - 866z + 609z^2) + 3z^4(-30 + 60z - 49z^2 + 19z^3) + 3y^6(-692 + 4784z - 7993z^2 \\
& + 3540z^3) + yz^3(-144 + 1364z - 1944z^2 + 1374z^3 - 405z^4) + y^5(732 - 9572z + 30498z^2 - 31161z^3 + 9960z^4) \\
& + y^2z^2(-204 + 3656z - 8678z^2 + 7902z^3 - 3411z^4 + 348z^5) + 2y^3z(-72 + 2320z - 8830z^2 + 11118z^3 - 6117z^4 \\
& + 1086z^5) + y^4(-90 + 2804z - 18275z^2 + 34641z^3 - 24864z^4 + 6048z^5))H(2, 0, y) + 2(1728y^{12}(-1 + z)^2 - 216(-1 \\
& + z)^5z^6(-1 + 4z) - 24y^{11}(-1 + z)^2(375 + 718z) + y^{10}(19080 + 28289z - 250122z^2 + 338949z^3 - 136304z^4) + y(-1
\end{aligned}$$

$$\begin{aligned}
& + z)^2 z^5 (-8082 + 36428 z - 80967 z^2 + 91745 z^3 - 40992 z^4 + 1728 z^5) - y^9 (20808 + 63133 z - 748547 z^2 + 1624467 z^3 \\
& - 1359901 z^4 + 400256 z^5) + y^8 (12024 + 69787 z - 1130000 z^2 + 3636494 z^3 - 4922656 z^4 + 3035579 z^5 - 701120 z^6) - y^2 (-1 \\
& + z)^2 z^4 (25944 - 171016 z + 438304 z^2 - 585767 z^3 + 364650 z^4 - 73560 z^5 + 864 z^6) - y^7 (3312 + 52501 z - 1005911 z^2 \\
& + 4577790 z^3 - 9135618 z^4 + 9138769 z^5 - 4491307 z^6 + 860032 z^7) + y^6 (288 + 26312 z - 553704 z^2 + 3461777 z^3 - 9763000 z^4 \\
& + 14401588 z^5 - 11527644 z^6 + 4728907 z^7 - 774416 z^8) + y^5 z (-6066 + 175600 z - 1559775 z^2 + 6176973 z^3 - 12917254 z^4 \\
& + 15269476 z^5 - 10196989 z^6 + 3546779 z^7 - 488960 z^8) + y^4 z^2 (-23424 + 374888 z - 2225864 z^2 + 6614805 z^3 - 11116384 z^4 \\
& + 10963698 z^5 - 6184528 z^6 + 1787581 z^7 - 190880 z^8) + y^3 z^3 (-32844 + 401168 z - 1810731 z^2 + 4338377 z^3 - 6108582 z^4 \\
& + 5103134 z^5 - 2392815 z^6 + 537669 z^7 - 35376 z^8) H(2, 2, y) + H(0, z) (-88 (-1 + y)^2 y (-1 + z) z (y + z)^4 (-5 (-1 + z)^2 \\
& - 2 z + z^2) + 5 y^3 (1 - 5 z + 4 z^2) + 3 y^2 (-5 + 20 z - 24 z^2 + 8 z^3) + 4 y (-5 - 20 z + 33 z^2 - 29 z^3 + 11 z^4)) + 96 (-1 \\
& + y)^2 y (-1 + z)^2 z (y + z)^4 (1 + 8 y^4 - 9 z + 21 z^2 - 21 z^3 + 8 z^4 + y^3 (-21 + 8 z) + 3 y^2 (7 - 7 z + 4 z^2) + y (-9 + 18 z \\
& - 21 z^2 + 8 z^3)) H(1, z)^2 - 264 (-1 + y)^2 y (-1 + z)^2 z (y + z)^4 (y^3 (-1 + 4 z) + 4 y (-1 + z)^2 (-1 + 4 z) + 3 y^2 (1 - 5 z \\
& + 4 z^2) + 2 (1 - 9 z + 21 z^2 - 21 z^3 + 8 z^4)) H(2, y) + 96 (-1 + y)^2 y (-1 + z)^2 z (y + z)^4 (8 y^4 + 2 y^3 (-11 + 6 z) \\
& + 12 y^2 (2 - 3 z + 2 z^2) + y (-13 + 42 z - 57 z^2 + 24 z^3) + 3 (1 - 9 z + 21 z^2 - 21 z^3 + 8 z^4)) H(2, y)^2 + H(1, z) (32 (-1 \\
& + y)^2 y (-1 + z) z (-6 (-1 + z)^2 z^4 (1 - z + z^2) + 6 y^7 (1 - 10 z + 9 z^2) + 3 y^6 (-4 + 54 z - 155 z^2 + 104 z^3) + 3 y^5 (4 \\
& - 52 z + 279 z^2 - 497 z^3 + 262 z^4) + y z^3 (30 + 8 z - 182 z^2 + 321 z^3 - 255 z^4 + 78 z^5) + y^2 z^2 (48 + 38 z - 650 z^2 \\
& + 1338 z^3 - 1185 z^4 + 408 z^5) + 2 y^3 z (15 + 28 z - 475 z^2 + 1158 z^3 - 1185 z^4 + 453 z^5) + 2 y^4 (-3 + 22 z - 301 z^2 \\
& + 981 z^3 - 1260 z^4 + 552 z^5)) + 96 (-1 + y)^2 y (-1 + z)^2 z^2 (y + z)^4 (-14 + 39 z - 41 z^2 + 16 z^3 + 6 y^2 (-1 + 2 z) + 3 y (4 \\
& - 9 z + 4 z^2)) H(2, y) - 96 (-1 + y)^2 y (-1 + z)^2 z (y + z)^4 (4 + 16 y^4 - 22 z + 45 z^2 - 43 z^3 + 16 z^4 + y^3 (-43 + 20 z) \\
& + 3 y^2 (15 - 17 z + 8 z^2) + y (-22 + 48 z - 51 z^2 + 20 z^3)) H(3, y)) - 96 (-1 + y)^2 y (-1 + z)^2 z (y + z)^4 (16 y^4 + 4 y^3 (-11 \\
& + 6 z) + 6 y^2 (8 - 9 z + 2 z^2) - 3 (-2 + 4 z - 3 z^2 + z^3) + y (-26 + 48 z - 33 z^2 + 12 z^3)) H(0, 0, y) - 96 (-1 + y)^2 y (-1 \\
& + z)^2 z (y + z)^4 (-14 + 39 z - 41 z^2 + 16 z^3 + 6 y^2 (-1 + 2 z) + 3 y (4 - 9 z + 4 z^2)) H(0, 0, z) - 96 (-1 + y)^2 y (-1 \\
& + z)^2 z (y + z)^4 (2 + 16 y^4 - 4 z + 3 z^2 - z^3 + 2 y^3 (-21 + 8 z) + 6 y^2 (7 - 6 z + 2 z^2) + y (-18 + 24 z - 15 z^2 \\
& + 4 z^3)) H(0, 1, z) - 96 (-1 + y)^2 y (-1 + z)^2 z (-1 + y + z) (y + z)^4 (-4 + 18 z - 27 z^2 + 16 z^3 + y^2 (-2 + 8 z) + 2 y (2 \\
& - 7 z + 2 z^2)) H(0, 2, y) + 96 (-1 + y)^2 y (-1 + z)^2 z (y + z)^4 (2 + y^2 (3 - 9 z) - 4 z + 3 z^2 - z^3 + y^3 (-1 + 4 z) + y (-4 \\
& + 12 z - 9 z^2 + 4 z^3)) H(1, 0, z) - 96 (-1 + y)^2 y (-1 + z)^2 z (y + z)^4 (4 + 16 y^4 - 22 z + 45 z^2 - 43 z^3 + 16 z^4 + y^3 (-43 \\
& + 20 z) + 3 y^2 (15 - 17 z + 8 z^2) + y (-22 + 48 z - 51 z^2 + 20 z^3)) H(1, 1, z) - 96 (-1 + y)^2 y (-1 + z)^2 z (-1 + y + z) (y \\
& + z)^4 (-4 + 18 z - 27 z^2 + 16 z^3 + y^2 (-2 + 8 z) + 2 y (2 - 7 z + 2 z^2)) H(2, 0, y) - 192 (-1 + y)^2 y (-1 + z)^2 z (y \\
& + z)^4 (8 y^4 + 2 y^3 (-11 + 6 z) + 12 y^2 (2 - 3 z + 2 z^2) + y (-13 + 42 z - 57 z^2 + 24 z^3) + 3 (1 - 9 z + 21 z^2 - 21 z^3 \\
& + 8 z^4)) H(2, 2, y) + 264 (-1 + y)^2 y (-1 + z)^2 z (y + z)^4 (4 + 16 y^4 - 22 z + 45 z^2 - 43 z^3 + 16 z^4 + y^3 (-43 + 20 z) \\
& + 3 y^2 (15 - 17 z + 8 z^2) + y (-22 + 48 z - 51 z^2 + 20 z^3)) H(3, 2, y) + H(0, y) (-88 (-1 + y) y (-1 + z)^2 z (y + z)^4 (y^4 (-5 \\
& + 44 z) + 4 y^3 (5 - 29 z + 6 z^2) + 5 (-2 + 4 z - 3 z^2 + z^3) - 5 y (-6 + 16 z - 12 z^2 + 5 z^3) + y^2 (-35 + 132 z - 72 z^2 \\
& + 20 z^3)) + 48 (-1 + y)^2 y (-1 + z)^2 z (y + z)^4 (6 - 26 z + 48 z^2 - 44 z^3 + 16 z^4 + 3 y^3 (-1 + 4 z) + 3 y^2 (3 - 11 z + 4 z^2) \\
& + 6 y (-2 + 8 z - 9 z^2 + 4 z^3)) H(0, 0, z)^2 + 96 (-1 + y)^2 y (-1 + z)^2 z (y + z)^4 (3 + 24 y^4 - 13 z + 24 z^2 - 22 z^3 + 8 z^4 \\
& + 3 y^3 (-21 + 8 z) + 3 y^2 (21 - 19 z + 8 z^2) + 3 y (-9 + 14 z - 12 z^2 + 4 z^3)) H(1, z)^2 + 32 (-1 + y) y (-1 + z)^2 z (y^8 (-6 \\
& + 78 z) + 3 y^7 (6 - 85 z + 136 z^2) + 6 z^4 (-1 + 2 z - 2 z^2 + z^3) + 3 y^6 (-8 + 107 z - 395 z^2 + 302 z^3) + 2 y z^3 (15 + 22 z \\
& - 78 z^2 + 81 z^3 - 30 z^4) + 2 y^5 (9 - 91 z + 669 z^2 - 1185 z^3 + 552 z^4) + y^2 z^2 (48 + 56 z - 602 z^2 + 837 z^3 - 465 z^4 \\
& + 54 z^5) + y^3 z (30 + 38 z - 950 z^2 + 1962 z^3 - 1491 z^4 + 312 z^5) + y^4 (-6 + 8 z - 650 z^2 + 2316 z^3 - 2520 z^4 \\
& + 786 z^5)) H(2, y) + 96 (-1 + y)^2 y (-1 + z)^2 z (y + z)^4 (1 + 8 y^4 - 9 z + 21 z^2 - 21 z^3 + 8 z^4 + y^3 (-21 + 8 z) + 3 y^2 (7 \\
& - 7 z + 4 z^2) + y (-9 + 18 z - 21 z^2 + 8 z^3)) H(2, y)^2 + H(0, z) (-264 (-1 + y)^2 y (-1 + z)^2 z (y + z)^4 (2 + y^2 (3 - 9 z) \\
& - 4 z + 3 z^2 - z^3 + y^3 (-1 + 4 z) + y (-4 + 12 z - 9 z^2 + 4 z^3)) + 96 (-1 + y)^2 y (-1 + z)^2 z (-1 + y + z) (y + z)^4 (16 y^3 \\
& + y^2 (-27 + 4 z) - 2 (2 - 2 z + z^2) + 2 y (9 - 7 z + 4 z^2)) H(1, z) + 96 (-1 + y)^2 y (-1 + z)^2 z (-1 + y + z) (y + z)^4 (-4 \\
& + 18 z - 27 z^2 + 16 z^3 + y^2 (-2 + 8 z) + 2 y (2 - 7 z + 2 z^2)) H(2, y)) + H(1, z) (-264 (-1 + y)^2 y (-1 + z)^2 z (y + z)^4 (2 \\
& + 16 y^4 - 4 z + 3 z^2 - z^3 + 2 y^3 (-21 + 8 z) + 6 y^2 (7 - 6 z + 2 z^2) + y (-18 + 24 z - 15 z^2 + 4 z^3)) + 96 (-1 + y)^2 y^2 (-1 \\
& + z)^2 z (y + z)^4 (16 y^3 + y^2 (-41 + 12 z) - 2 (7 - 6 z + 3 z^2) + 3 y (13 - 9 z + 4 z^2)) H(2, y) - 96 (-1 + y)^2 y (-1 \\
& + z)^2 z (y + z)^4 (4 + 16 y^4 - 22 z + 45 z^2 - 43 z^3 + 16 z^4 + y^3 (-43 + 20 z) + 3 y^2 (15 - 17 z + 8 z^2) + y (-22 + 48 z \\
& - 51 z^2 + 20 z^3)) H(3, y)) - 96 (-1 + y)^2 y (-1 + z)^2 z (y + z)^4 (16 y^3 + y^2 (-41 + 12 z) - 2 (7 - 6 z + 3 z^2) + 3 y (13 \\
& - 9 z + 4 z^2)) H(0, 0, y) - 96 (-1 + y)^2 y (-1 + z)^2 z (y + z)^4 (6 - 26 z + 48 z^2 - 44 z^3 + 16 z^4 + 3 y^3 (-1 + 4 z) + 3 y^2 (3 \\
& - 11 z + 4 z^2) + 6 y (-2 + 8 z - 9 z^2 + 4 z^3)) H(0, 0, z) - 96 (-1 + y)^2 y (-1 + z)^2 z (-1 + y + z) (y + z)^4 (16 y^3 + y^2 (-27 \\
& + 4 z) - 2 (2 - 2 z + z^2) + 2 y (9 - 7 z + 4 z^2)) H(0, 1, z) + 96 (-1 + y)^2 y (-1 + z)^2 z (y + z)^4 (2 + 16 y^4 - 4 z + 3 z^2 \\
& - z^3 + 2 y^3 (-21 + 8 z) + 6 y^2 (7 - 6 z + 2 z^2) + y (-18 + 24 z - 15 z^2 + 4 z^3)) H(0, 2, y) - 96 (-1 + y)^2 y (-1 + z)^2 z (y
\end{aligned}$$

$$\begin{aligned}
& + z)^4(16y^3 + y^2(-41 + 12z) - 2(7 - 6z + 3z^2) + 3y(13 - 9z + 4z^2))H(1, 0, y) - 96(-1 + y)^2y(-1 + z)^2z(-1 + y \\
& + z)(y + z)^4(16y^3 + y^2(-27 + 4z) - 2(2 - 2z + z^2) + 2y(9 - 7z + 4z^2))H(1, 0, z) - 192(-1 + y)^2y(-1 + z)^2z(y \\
& + z)^4(3 + 24y^4 - 13z + 24z^2 - 22z^3 + 8z^4 + 3y^3(-21 + 8z) + 3y^2(21 - 19z + 8z^2) + 3y(-9 + 14z - 12z^2 \\
& + 4z^3))H(1, 1, z) + 96(-1 + y)^2y(-1 + z)^2z(y + z)^4(2 + 16y^4 - 4z + 3z^2 - z^3 + 2y^3(-21 + 8z) + 6y^2(7 - 6z \\
& + 2z^2) + y(-18 + 24z - 15z^2 + 4z^3))H(2, 0, y) - 96(-1 + y)^2y(-1 + z)^2z(y + z)^4(4 + 16y^4 - 22z + 45z^2 - 43z^3 \\
& + 16z^4 + y^3(-43 + 20z) + 3y^2(15 - 17z + 8z^2) + y(-22 + 48z - 51z^2 + 20z^3))H(2, 2, y) - 96(-1 + y)^2y(-1 \\
& + z)^2z(y + z)^4(4 + 16y^4 - 22z + 45z^2 - 43z^3 + 16z^4 + y^3(-43 + 20z) + 3y^2(15 - 17z + 8z^2) + y(-22 + 48z \\
& - 51z^2 + 20z^3))H(3, 2, y) + H(2, y)(-44(-1 + y)^2y(-1 + z)^2z(y^7(-9 + 84z) + 3y^6(9 - 83z + 144z^2) - 9z^4(-2 \\
& + 4z - 3z^2 + z^3) + 3y^5(-12 + 92z - 373z^2 + 324z^3) + yz^3(-36 - 136z + 276z^2 - 249z^3 + 84z^4) + y^2z^2(-60 \\
& - 292z + 1053z^2 - 1119z^3 + 432z^4) + y^3z(-36 - 292z + 1608z^2 - 2175z^3 + 972z^4) + y^4(18 - 136z + 1053z^2 - 2175z^3 \\
& + 1248z^4)) - 96(-1 + y)^2y^2(-1 + z)^2z(y + z)^4(16y^3 + y^2(-41 + 12z) - 2(7 - 6z + 3z^2) + 3y(13 - 9z \\
& + 4z^2))H(0, 0, y) - 288(-1 + y)^2y(-1 + z)^2z(y + z)^4(y^3(-1 + 4z) + 4y(-1 + z)^2(-1 + 4z) + 3y^2(1 - 5z + 4z^2) \\
& + 2(1 - 9z + 21z^2 - 21z^3 + 8z^4))H(0, 0, z) - 96(-1 + y)^2y(-1 + z)^2z^2(y + z)^4(-14 + 39z - 41z^2 + 16z^3 \\
& + 6y^2(-1 + 2z) + 3y(4 - 9z + 4z^2))H(0, 1, z) + 96(-1 + y)^2y(-1 + z)^2z(y + z)^4(2 + 16y^4 - 4z + 3z^2 - z^3 \\
& + 2y^3(-21 + 8z) + 6y^2(7 - 6z + 2z^2) + y(-18 + 24z - 15z^2 + 4z^3))H(0, 2, y) - 96(-1 + y)^2y^2(-1 + z)^2z(y \\
& + z)^4(16y^3 + y^2(-41 + 12z) - 2(7 - 6z + 3z^2) + 3y(13 - 9z + 4z^2))H(1, 0, y) - 96(-1 + y)^2y(-1 + z)^2z^2(y \\
& + z)^4(-14 + 39z - 41z^2 + 16z^3 + 6y^2(-1 + 2z) + 3y(4 - 9z + 4z^2))H(1, 0, z) + 192(-1 + y)^2y(-1 + z)^2z(y \\
& + z)^4(13 + 380y^4 - 225z + 747z^2 - 915z^3 + 380z^4 + y^3(-915 + 584z) + 9y^2(83 - 117z + 64z^2) + y(-225 + 654z \\
& - 1053z^2 + 584z^3))H(1, 1, z) + 96(-1 + y)^2y(-1 + z)^2z(y + z)^4(2 + 16y^4 - 4z + 3z^2 - z^3 + 2y^3(-21 + 8z) \\
& + 6y^2(7 - 6z + 2z^2) + y(-18 + 24z - 15z^2 + 4z^3))H(2, 0, y) - 96(-1 + y)^2y(-1 + z)^2z(y + z)^4(4 + 16y^4 - 22z \\
& + 45z^2 - 43z^3 + 16z^4 + y^3(-43 + 20z) + 3y^2(15 - 17z + 8z^2) + y(-22 + 48z - 51z^2 + 20z^3))H(2, 2, y) - 96(-1 \\
& + y)^2y(-1 + z)^2z(y + z)^4(4 + 16y^4 - 22z + 45z^2 - 43z^3 + 16z^4 + y^3(-43 + 20z) + 3y^2(15 - 17z + 8z^2) + y(-22 \\
& + 48z - 51z^2 + 20z^3))H(3, 2, y) + H(1, z)(-44(-1 + y)^2y(-1 + z)^2z(y^7(-9 + 84z) + 3y^6(9 - 83z + 144z^2) \\
& - 9z^4(-2 + 4z - 3z^2 + z^3) + 3y^5(-12 + 92z - 373z^2 + 324z^3) + yz^3(-36 - 136z + 276z^2 - 249z^3 + 84z^4) \\
& + y^2z^2(-60 - 292z + 1053z^2 - 1119z^3 + 432z^4) + y^3z(-36 - 292z + 1608z^2 - 2175z^3 + 972z^4) + y^4(18 - 136z \\
& + 1053z^2 - 2175z^3 + 1248z^4)) - 96(-1 + y)^2y(-1 + z)^2z(y + z)^4(13 + 380y^4 - 225z + 747z^2 - 915z^3 + 380z^4 \\
& + y^3(-915 + 584z) + 9y^2(83 - 117z + 64z^2) + y(-225 + 654z - 1053z^2 + 584z^3))H(2, y)^2 + 264(-1 + y)^2y(-1 \\
& + z)^2z(y + z)^4(4 + 16y^4 - 22z + 45z^2 - 43z^3 + 16z^4 + y^3(-43 + 20z) + 3y^2(15 - 17z + 8z^2) + y(-22 + 48z \\
& - 51z^2 + 20z^3))H(3, y) - 96(-1 + y)^2y(-1 + z)^2z(y + z)^4(4 + 16y^4 - 22z + 45z^2 - 43z^3 + 16z^4 + y^3(-43 + 20z) \\
& + 3y^2(15 - 17z + 8z^2) + y(-22 + 48z - 51z^2 + 20z^3))H(2, y)H(3, y) - 288(-1 + y)^2y(-1 + z)^2z(y + z)^4(2 + 16y^4 \\
& - 4z + 3z^2 - z^3 + 2y^3(-21 + 8z) + 6y^2(7 - 6z + 2z^2) + y(-18 + 24z - 15z^2 + 4z^3))H(0, 0, y) - 96(-1 + y)^2y(-1 \\
& + z)^2z^2(y + z)^4(-14 + 39z - 41z^2 + 16z^3 + 6y^2(-1 + 2z) + 3y(4 - 9z + 4z^2))H(0, 0, z) - 96(-1 + y)^2y(-1 \\
& + z)^2z(y + z)^4(2 + 16y^4 - 4z + 3z^2 - z^3 + 2y^3(-21 + 8z) + 6y^2(7 - 6z + 2z^2) + y(-18 + 24z - 15z^2 \\
& + 4z^3))H(0, 1, z) - 96(-1 + y)^2y^2(-1 + z)^2z(y + z)^4(16y^3 + y^2(-41 + 12z) - 2(7 - 6z + 3z^2) + 3y(13 - 9z \\
& + 4z^2))H(0, 2, y) + 96(-1 + y)^2y(-1 + z)^2z(y + z)^4(4 + 16y^4 - 22z + 45z^2 - 43z^3 + 16z^4 + y^3(-43 + 20z) \\
& + 3y^2(15 - 17z + 8z^2) + y(-22 + 48z - 51z^2 + 20z^3))H(0, 3, y) + 96(-1 + y)^2y(-1 + z)^2z(y + z)^4(2 + y^2(3 - 9z) \\
& - 4z + 3z^2 - z^3 + y^3(-1 + 4z) + y(-4 + 12z - 9z^2 + 4z^3))H(1, 0, z) - 96(-1 + y)^2y(-1 + z)^2z(y + z)^4(4 + 16y^4 \\
& - 22z + 45z^2 - 43z^3 + 16z^4 + y^3(-43 + 20z) + 3y^2(15 - 17z + 8z^2) + y(-22 + 48z - 51z^2 + 20z^3))H(1, 1, z) \\
& - 96(-1 + y)^2y^2(-1 + z)^2z(y + z)^4(16y^3 + y^2(-41 + 12z) - 2(7 - 6z + 3z^2) + 3y(13 - 9z + 4z^2))H(2, 0, y) \\
& + 192(-1 + y)^2y(-1 + z)^2z(y + z)^4(13 + 380y^4 - 225z + 747z^2 - 915z^3 + 380z^4 + y^3(-915 + 584z) + 9y^2(83 - 117z \\
& + 64z^2) + y(-225 + 654z - 1053z^2 + 584z^3))H(2, 2, y) + 96(-1 + y)^2y(-1 + z)^2z(y + z)^4(4 + 16y^4 - 22z + 45z^2 \\
& - 43z^3 + 16z^4 + y^3(-43 + 20z) + 3y^2(15 - 17z + 8z^2) + y(-22 + 48z - 51z^2 + 20z^3))H(2, 3, y) + 96(-1 + y)^2y(-1 \\
& + z)^2z(y + z)^4(4 + 16y^4 - 22z + 45z^2 - 43z^3 + 16z^4 + y^3(-43 + 20z) + 3y^2(15 - 17z + 8z^2) + y(-22 + 48z \\
& - 51z^2 + 20z^3))H(3, 0, y) + 96(-1 + y)^2y(-1 + z)^2z(y + z)^4(4 + 16y^4 - 22z + 45z^2 - 43z^3 + 16z^4 + y^3(-43 \\
& + 20z) + 3y^2(15 - 17z + 8z^2) + y(-22 + 48z - 51z^2 + 20z^3))H(3, 2, y) + 48(-1 + y)^2y(-1 + z)^2z(y + z)^4(56 \\
& + 596y^4 + 34z - 396z^2 + 550z^3 - 244z^4 + y^3(-1661 + 1420z) + 3y^2(511 - 769z + 204z^2) - 4y(131 - 237z + 51z^2 \\
& + 38z^3))H(0, 0, 0, y) - 48(-1 + y)^2y(-1 + z)^2z(y + z)^4(-56 + 244y^4 + 524z - 1533z^2 + 1661z^3 - 596z^4 \\
& + 2y^3(-275 + 76z) + y^2(396 + 204z - 612z^2) - y(34 + 948z - 2307z^2 + 1420z^3))H(0, 0, 0, z) + 96(-1 + y)^2y(-1 \\
& + z)^2z(y + z)^4(2 + 32y^4 - 4z + 3z^2 - z^3 + y^3(-83 + 28z) + 3y^2(27 - 21z + 8z^2) + y(-32 + 36z - 21z^2 \\
& + 4z^3))H(0, 0, 1, z) - 96(-1 + y)^2y(-1 + z)^2z(y + z)^4(32y^4 + y^3(-85 + 36z) + 3y^2(29 - 27z + 8z^2) - 3(-2 + 4z
\end{aligned}$$

$$\begin{aligned}
& -3z^2 + z^3) + y(-40 + 60z - 39z^2 + 12z^3))H(0, 0, 2, y) + 96(-1 + y)^2y^2(-1 + z)^2z(y + z)^4(16y^3 + y^2(-41 + 12z) \\
& - 2(7 - 6z + 3z^2) + 3y(13 - 9z + 4z^2))H(0, 1, 0, y) + 96(-1 + y)^2y(-1 + z)^2z(y + z)^4(-2 + 16y^4 + 8y^3(-5 + z) \\
& + 4z - 3z^2 + z^3 + 6y^2(6 - 3z + 2z^2) + y(-10 + 3z^2 - 4z^3))H(0, 1, 0, z) + 96(-1 + y)^2y(-1 + z)^2z(y \\
& + z)^4(32y^4 + y^3(-85 + 36z) + 3y^2(29 - 27z + 8z^2) - 3(-2 + 4z - 3z^2 + z^3) + y(-40 + 60z - 39z^2 \\
& + 12z^3))H(0, 1, 1, z) - 96(-1 + y)^2y(-1 + z)^2z(y + z)^4(32y^4 + y^3(-85 + 36z) + 3y^2(29 - 27z + 8z^2) - 3(-2 \\
& + 4z - 3z^2 + z^3) + y(-40 + 60z - 39z^2 + 12z^3))H(0, 2, 0, y) - 96(-1 + y)^2y(-1 + z)^2z(y + z)^4(2 + 32y^4 - 4z \\
& + 3z^2 - z^3 + y^3(-83 + 28z) + 3y^2(27 - 21z + 8z^2) + y(-32 + 36z - 21z^2 + 4z^3))H(0, 2, 2, y) + 96(-1 + y)^2y(-1 \\
& + z)^2z(y + z)^4(4 + 16y^4 - 22z + 45z^2 - 43z^3 + 16z^4 + y^3(-43 + 20z) + 3y^2(15 - 17z + 8z^2) + y(-22 + 48z \\
& - 51z^2 + 20z^3))H(0, 3, 2, y) + 192(-1 + y)^2y^2(-1 + z)^2z(y + z)^4(16y^3 + y^2(-41 + 12z) - 2(7 - 6z + 3z^2) \\
& + 3y(13 - 9z + 4z^2))H(1, 0, 0, y) - 288(-1 + y)^2y(-1 + z)^2z(y + z)^4(2 + y^2(3 - 9z) - 4z + 3z^2 - z^3 + y^3(-1 \\
& + 4z) + y(-4 + 12z - 9z^2 + 4z^3))H(1, 0, 0, z) + 96(-1 + y)^2y(-1 + z)^2z(y + z)^4(2 + 16y^4 - 4z + 3z^2 - z^3 \\
& + 2y^3(-21 + 8z) + 6y^2(7 - 6z + 2z^2) + y(-18 + 24z - 15z^2 + 4z^3))H(1, 0, 1, z) + 96(-1 + y)^2y^2(-1 + z)^2z(y \\
& + z)^4(16y^3 + y^2(-41 + 12z) - 2(7 - 6z + 3z^2) + 3y(13 - 9z + 4z^2))H(1, 0, 2, y) - 96(-1 + y)^2y(-1 + z)^2z(y \\
& + z)^4(2 + y^2(3 - 9z) - 4z + 3z^2 - z^3 + y^3(-1 + 4z) + y(-4 + 12z - 9z^2 + 4z^3))H(1, 1, 0, z) + 96(-1 + y)^2y(-1 \\
& + z)^2z(y + z)^4(30 + 776y^4 - 472z + 1539z^2 - 1873z^3 + 776z^4 + y^3(-1873 + 1188z) + 3y^2(513 - 719z + 392z^2) \\
& + y(-472 + 1356z - 2157z^2 + 1188z^3))H(1, 1, 1, z) + 96(-1 + y)^2y^2(-1 + z)^2z(y + z)^4(16y^3 + y^2(-41 + 12z) - 2(7 \\
& - 6z + 3z^2) + 3y(13 - 9z + 4z^2))H(1, 2, 0, y) - 96(-1 + y)^2y(-1 + z)^2z(y + z)^4(32y^4 + y^3(-85 + 36z) + 3y^2(29 \\
& - 27z + 8z^2) - 3(-2 + 4z - 3z^2 + z^3) + y(-40 + 60z - 39z^2 + 12z^3))H(2, 0, 0, y) - 96(-1 + y)^2y(-1 + z)^2z(y \\
& + z)^4(2 + 32y^4 - 4z + 3z^2 - z^3 + y^3(-83 + 28z) + 3y^2(27 - 21z + 8z^2) + y(-32 + 36z - 21z^2 \\
& + 4z^3))H(2, 0, 2, y) + 96(-1 + y)^2y^2(-1 + z)^2z(y + z)^4(16y^3 + y^2(-41 + 12z) - 2(7 - 6z + 3z^2) + 3y(13 - 9z \\
& + 4z^2))H(2, 1, 0, y) - 96(-1 + y)^2y(-1 + z)^2z(y + z)^4(2 + 32y^4 - 4z + 3z^2 - z^3 + y^3(-83 + 28z) + 3y^2(27 \\
& - 21z + 8z^2) + y(-32 + 36z - 21z^2 + 4z^3))H(2, 2, 0, y) + 96(-1 + y)^2y(-1 + z)^2z(y + z)^4(30 + 776y^4 - 472z \\
& + 1539z^2 - 1873z^3 + 776z^4 + y^3(-1873 + 1188z) + 3y^2(513 - 719z + 392z^2) + y(-472 + 1356z - 2157z^2 \\
& + 1188z^3))H(2, 2, 2, y) + 96(-1 + y)^2y(-1 + z)^2z(y + z)^4(4 + 16y^4 - 22z + 45z^2 - 43z^3 + 16z^4 + y^3(-43 + 20z) \\
& + 3y^2(15 - 17z + 8z^2) + y(-22 + 48z - 51z^2 + 20z^3))H(2, 3, 2, y) + 96(-1 + y)^2y(-1 + z)^2z(y + z)^4(4 + 16y^4 \\
& - 22z + 45z^2 - 43z^3 + 16z^4 + y^3(-43 + 20z) + 3y^2(15 - 17z + 8z^2) + y(-22 + 48z - 51z^2 + 20z^3))H(3, 0, 2, y) \\
& + 96(-1 + y)^2y(-1 + z)^2z(y + z)^4(4 + 16y^4 - 22z + 45z^2 - 43z^3 + 16z^4 + y^3(-43 + 20z) + 3y^2(15 - 17z + 8z^2) \\
& + y(-22 + 48z - 51z^2 + 20z^3))H(3, 2, 0, y) + 192(-1 + y)^2y(-1 + z)^2z(y + z)^4(4 + 16y^4 - 22z + 45z^2 - 43z^3 \\
& + 16z^4 + y^3(-43 + 20z) + 3y^2(15 - 17z + 8z^2) + y(-22 + 48z - 51z^2 + 20z^3))H(3, 2, 2, y) \Big\} / \Big(192(-1 + y)^2y^2(-1 \\
& + z)^2z^2(-1 + y + z)(y + z)^4 \Big);
\end{aligned}$$

$$\begin{aligned}
\mathcal{A}_{3;C_F^2}^{(2)} = & \Big\{ -18(-1 + y)^2y(-1 + z)^2z(y + z)^2(2 + y^2(3 - 9z) - 4z + 3z^2 - z^3 + y^3(-1 + 4z) + y(-4 + 12z - 9z^2 + 4z^3)) \\
& - 12(-1 + y)^2y(-1 + z)^2z(-1 + y + z)(y + z)^2(-44 + 528y^3 + 66z - 99z^2 + 64z^3 + y^2(-829 + 412z) + 2y(187 - 176z \\
& + 58z^2))H(0, y)^3 - 12(-1 + y)^2y(-1 + z)^2z(-1 + y + z)(y + z)^2(-44 + 64y^3 + 374z - 829z^2 + 528z^3 + y^2(-99 \\
& + 116z) + y(66 - 352z + 412z^2))H(0, z)^3 - 12(-1 + y)^2y(-1 + z)^2z(-1 + y + z)(y + z)^2(4 + 72y^3 + 46z - 131z^2 \\
& + 72z^3 + y^2(-131 + 108z) + 2y(23 - 50z + 54z^2))H(1, z)^3 - 2(432y^{10}(-1 + z)^2 - 54(-1 + z)^5z^4(-1 + 4z) \\
& + 2y^9(-1 + z)^2(-1125 + 1321z) + 3y^8(1590 - 7130z + 10312z^2 - 5603z^3 + 822z^4) + y^7(-5202 + 29970z - 47113z^2 \\
& + 16349z^3 + 14834z^4 - 8838z^5) + y(-1 + z)^2z^3(-1653 + 4845z - 5811z^2 + 4198z^3 - 2002z^4 + 432z^5) + y^6(3006 \\
& - 18611z + 14103z^2 + 65692z^3 - 134393z^4 + 90425z^5 - 20168z^6) - y^2(-1 + z)^2z^2(792 - 14109z + 32355z^2 - 27545z^3 \\
& + 10016z^4 - 1898z^5 + 216z^6) + y^5(-828 + 945z + 35948z^2 - 178242z^3 + 329525z^4 - 282687z^5 + 110081z^6 - 14742z^7) \\
& + y^4(72 + 4209z - 39045z^2 + 174583z^3 - 372816z^4 + 403037z^5 - 220595z^6 + 54578z^7 - 4050z^8) + y^3z(-1401 + 13065z \\
& - 78255z^2 + 213625z^3 - 291633z^4 + 209152z^5 - 75802z^6 + 11847z^7 - 598z^8))H(2, y)^2 - 12(-1 + y)^2y(-1 + z)^2z(-1 \\
& + y + z)(y + z)^2(4 + 72y^3 + 46z - 131z^2 + 72z^3 + y^2(-131 + 108z) + 2y(23 - 50z + 54z^2))H(2, y)^3 \\
& + H(0, z)^2(-108(-1 + z)^6z^3(-1 + 4z) - 4y^9(-1 + z)^2(216 + 215z) + y^8(4500 - 8947z - 426z^2 + 9495z^3 - 4692z^4) \\
& + y(-1 + z)^3z^2(-72 + 2469z - 8130z^2 + 15633z^3 - 12928z^4 + 864z^5) - y^7(9540 - 30281z + 21427z^2 + 17363z^3 \\
& - 25789z^4 + 7740z^5) - 2y^6(-5202 + 24062z - 33217z^2 + 1427z^3 + 33635z^4 - 28049z^5 + 7274z^6) - y^2(-1 + z)^2z(180 \\
& + 114z - 13297z^2 + 48726z^3 - 88199z^4 + 76698z^5 - 22076z^6 + 432z^7) - 4y^5(1503 - 9820z + 19651z^2 - 5048z^3 \\
& - 33560z^4 + 51210z^5 - 31336z^6 + 7400z^7) + y^4(1656 - 15965z + 40998z^2 + 3632z^3 - 193426z^4 + 388782z^5 - 361522z^6 \\
& + 164423z^7 - 28648z^8) - y^3(144 - 2787z + 8149z^2 + 23010z^3 - 166174z^4 + 387958z^5 - 474394z^6 + 314077z^7 - 100103z^8
\end{aligned}$$

$$\begin{aligned}
& + 10120z^9 + 48(-1+y)^2y(y^2 + 2y(-1+z) + 2(-1+z)^2)(-1+z)^2z(-1+y+z)(y+z)^2(-1+4z)H(1,z) + 48(-1 \\
& + y)^2y(y^2 + 2y(-1+z) + 2(-1+z)^2)(-1+z)^2z(-1+y+z)(y+z)^2(-1+4z)H(2,y)) + H(0,y)^2(864y^{10}(-1+z)^2 \\
& + 108(-1+z)^5z^3(-1+4z) - 4y^9(-1+z)^2(1341 + 1234z) + y^8(14040 - 14991z - 32938z^2 + 54743z^3 - 20800z^4) \\
& + y^7(-19944 + 36561z + 52567z^2 - 160807z^3 + 117263z^4 - 25640z^5) - y(-1+z)^2z^2(-72 + 2577z - 8383z^2 + 13377z^3 \\
& - 10501z^4 + 3020z^5) - 4y^6(-4104 + 13505z + 4189z^2 - 53569z^3 + 65725z^4 - 30346z^5 + 4627z^6) + y^2(-1+z)^2z(-180 \\
& - 366z + 14249z^2 - 35168z^3 + 44729z^4 - 26794z^5 + 4744z^6) - 2y^5(3834 - 21096z + 12153z^2 + 79661z^3 - 164736z^4 \\
& + 132075z^5 - 49685z^6 + 7794z^7) + y^4(1800 - 16449z + 20344z^2 + 84562z^3 - 275038z^4 + 340574z^5 - 219676z^6 + 73813z^7 \\
& - 9876z^8) - y^3(144 - 2823z + 4349z^2 + 40704z^3 - 163328z^4 + 272002z^5 - 250136z^6 + 128747z^7 - 31815z^8 + 2156z^9) \\
& + 48(-1+y)^2y(-1+4y)(-1+z)^2z(-1+y+z)(y+z)^2(2+2y^2 + 2y(-2+z) - 2z+z^2)H(1,z) + 48(-1+y)^2y(-1 \\
& + 4y)(-1+z)^2z(-1+y+z)(y+z)^2(2+2y^2 + 2y(-2+z) - 2z+z^2)H(2,y)) + H(1,z)^2(-2(432y^{10}(-1+z)^2 \\
& - 54(-1+z)^5z^4(-1+4z) + 2y^9(-1+z)^2(-1125 + 1321z) + 3y^8(1590 - 7130z + 10312z^2 - 5603z^3 + 822z^4) \\
& + y^7(-5202 + 29970z - 47113z^2 + 16349z^3 + 14834z^4 - 8838z^5) + y(-1+z)^2z^3(-1653 + 4845z - 5811z^2 + 4198z^3 \\
& - 2002z^4 + 432z^5) + y^6(3006 - 18611z + 14103z^2 + 65692z^3 - 134393z^4 + 90425z^5 - 20168z^6) - y^2(-1+z)^2z^2(792 \\
& - 14109z + 32355z^2 - 27545z^3 + 10016z^4 - 1898z^5 + 216z^6) + y^5(-828 + 945z + 35948z^2 - 178242z^3 + 329525z^4 \\
& - 282687z^5 + 110081z^6 - 14742z^7) + y^4(72 + 4209z - 39045z^2 + 174583z^3 - 372816z^4 + 403037z^5 - 220595z^6 + 54578z^7 \\
& - 4050z^8) + y^3z(-1401 + 13065z - 78255z^2 + 213625z^3 - 291633z^4 + 209152z^5 - 75802z^6 + 11847z^7 - 598z^8)) - 60(-1 \\
& + y)^2y(-1+z)^2z(-1+y+z)(y+z)^2(-4+56y^3 + 50z - 109z^2 + 56z^3 + y^2(-109 + 84z) + y(50 - 92z \\
& + 84z^2))H(2,y) - 96(-1+y)^2y(-1+z)^2z(-1+y+z)(y+z)^2(-4+8y^3 + 14z - 19z^2 + 8z^3 + y^2(-19 + 12z) \\
& + 2y(7 - 10z + 6z^2))H(3,y)) - 2(864y^{10}(-1+z)^2 + 108(-1+z)^5z^3(-1+4z) - 4y^9(-1+z)^2(1341 + 1234z) \\
& + y^8(14040 - 14991z - 32938z^2 + 54743z^3 - 20800z^4) + y^7(-19944 + 36561z + 52567z^2 - 160807z^3 + 117263z^4 - 25640z^5) \\
& - y(-1+z)^2z^2(-72 + 2577z - 8383z^2 + 13377z^3 - 10501z^4 + 3020z^5) - 4y^6(-4104 + 13505z + 4189z^2 - 53569z^3 \\
& + 65725z^4 - 30346z^5 + 4627z^6) + y^2(-1+z)^2z(-180 - 366z + 14249z^2 - 35168z^3 + 44729z^4 - 26794z^5 + 4744z^6) \\
& - 2y^5(3834 - 21096z + 12153z^2 + 79661z^3 - 164736z^4 + 132075z^5 - 49685z^6 + 7794z^7) + y^4(1800 - 16449z + 20344z^2 \\
& + 84562z^3 - 275038z^4 + 340574z^5 - 219676z^6 + 73813z^7 - 9876z^8) - y^3(144 - 2823z + 4349z^2 + 40704z^3 - 163328z^4 \\
& + 272002z^5 - 250136z^6 + 128747z^7 - 31815z^8 + 2156z^9))H(0,0,y) + 2(108(-1+z)^6z^3(-1+4z) + 4y^9(-1+z)^2(216 \\
& + 215z) + y^8(-4500 + 8947z + 426z^2 - 9495z^3 + 4692z^4) - y(-1+z)^3z^2(-72 + 2469z - 8130z^2 + 15633z^3 - 12928z^4 \\
& + 864z^5) + y^7(9540 - 30281z + 21427z^2 + 17363z^3 - 25789z^4 + 7740z^5) + 2y^6(-5202 + 24062z - 33217z^2 + 1427z^3 \\
& + 33635z^4 - 28049z^5 + 7274z^6) + y^2(-1+z)^2z(180 + 114z - 13297z^2 + 48726z^3 - 88199z^4 + 76698z^5 - 22076z^6 \\
& + 432z^7) + 4y^5(1503 - 9820z + 19651z^2 - 5048z^3 - 33560z^4 + 51210z^5 - 31336z^6 + 7400z^7) + y^4(-1656 + 15965z \\
& - 40998z^2 - 3632z^3 + 193426z^4 - 388782z^5 + 361522z^6 - 164423z^7 + 28648z^8) + y^3(144 - 2787z + 8149z^2 + 23010z^3 \\
& - 166174z^4 + 387958z^5 - 474394z^6 + 314077z^7 - 100103z^8 + 10120z^9))H(0,0,z) - 48(-1+y)^2y^2z^2(-1+y+z)(y \\
& + z)^2(-12 + 30z - 26z^2 + 8z^3 + 3y(4 - 9z + 4z^2))H(0,1,z) - 48y^2(-1+z)^2z^2(-1+y+z)(y+z)^2(8y^3 + y(30 \\
& - 27z) + 12(-1+z) + 2y^2(-13 + 6z))H(0,2,y) - 48(-1+y)^2y^2z^2(-1+y+z)(y+z)^2(-12 + 30z - 26z^2 + 8z^3 \\
& + 3y(4 - 9z + 4z^2))H(1,0,z) + 4(432y^{10}(-1+z)^2 - 54(-1+z)^5z^4(-1+4z) + 2y^9(-1+z)^2(-1125 + 1321z) \\
& + 3y^8(1590 - 7130z + 10312z^2 - 5603z^3 + 822z^4) + y^7(-5202 + 29970z - 47113z^2 + 16349z^3 + 14834z^4 - 8838z^5) \\
& + y(-1+z)^2z^3(-1653 + 4845z - 5811z^2 + 4198z^3 - 2002z^4 + 432z^5) + y^6(3006 - 18611z + 14103z^2 + 65692z^3 \\
& - 134393z^4 + 90425z^5 - 20168z^6) - y^2(-1+z)^2z^2(792 - 14109z + 32355z^2 - 27545z^3 + 10016z^4 - 1898z^5 + 216z^6) \\
& + y^5(-828 + 945z + 35948z^2 - 178242z^3 + 329525z^4 - 282687z^5 + 110081z^6 - 14742z^7) + y^4(72 + 4209z - 39045z^2 \\
& + 174583z^3 - 372816z^4 + 403037z^5 - 220595z^6 + 54578z^7 - 4050z^8) + y^3z(-1401 + 13065z - 78255z^2 + 213625z^3 \\
& - 291633z^4 + 209152z^5 - 75802z^6 + 11847z^7 - 598z^8))H(1,1,z) + 192(-1+y)^2y(-1+z)^2z(-1+y+z)(y+z)^2(-4 \\
& + 8y^3 + 14z - 19z^2 + 8z^3 + y^2(-19 + 12z) + 2y(7 - 10z + 6z^2))H(3,y)H(1,1,z) + H(0,y)(96(-1+y)^2y(-1 \\
& + 4y)(-1+z)^2z(-1+y+z)(y+z)^2(2+2y^2 + 2y(-2+z) - 2z+z^2)H(1,z)^2 + 48y^2(-1+z)^2z^2(-1+y+z)(y+z)^2 \\
& + z^2(8y^3 + y(30 - 27z) + 12(-1+z) + 2y^2(-13 + 6z))H(2,y) + 96(-1+y)^2y(-1+4y)(-1+z)^2z(-1+y+z)(y+z)^2(2 \\
& + 2y^2 + 2y(-2+z) - 2z+z^2)H(1,1,z)) - 48y^2(-1+z)^2z^2(-1+y+z)(y+z)^2(8y^3 + y(30 - 27z) + 12(-1+z) \\
& + 2y^2(-13 + 6z))H(2,0,y) + 4(432y^{10}(-1+z)^2 - 54(-1+z)^5z^4(-1+4z) + 2y^9(-1+z)^2(-1125 + 1321z) \\
& + 3y^8(1590 - 7130z + 10312z^2 - 5603z^3 + 822z^4) + y^7(-5202 + 29970z - 47113z^2 + 16349z^3 + 14834z^4 - 8838z^5) \\
& + y(-1+z)^2z^3(-1653 + 4845z - 5811z^2 + 4198z^3 - 2002z^4 + 432z^5) + y^6(3006 - 18611z + 14103z^2 + 65692z^3 \\
& - 134393z^4 + 90425z^5 - 20168z^6) - y^2(-1+z)^2z^2(792 - 14109z + 32355z^2 - 27545z^3 + 10016z^4 - 1898z^5 + 216z^6) \\
& + y^5(-828 + 945z + 35948z^2 - 178242z^3 + 329525z^4 - 282687z^5 + 110081z^6 - 14742z^7) + y^4(72 + 4209z - 39045z^2
\end{aligned}$$

$$\begin{aligned}
& + 174583z^3 - 372816z^4 + 403037z^5 - 220595z^6 + 54578z^7 - 4050z^8) + y^3 z (-1401 + 13065z - 78255z^2 + 213625z^3 \\
& - 291633z^4 + 209152z^5 - 75802z^6 + 11847z^7 - 598z^8)) H(2, 2, y) + H(0, z) (96(-1 + y)^2 y (y^2 + 2y(-1 + z) + 2(-1 \\
& + z)^2)(-1 + z)^2 z (-1 + y + z) (y + z)^2 (-1 + 4z) H(2, y)^2 + H(1, z) (48(-1 + y)^2 y^2 z^2 (-1 + y + z) (y + z)^2 (-12 + 30z \\
& - 26z^2 + 8z^3 + 3y(4 - 9z + 4z^2)) + 96(-1 + y)^2 y (y^2 + 2y(-1 + z) + 2(-1 + z)^2)(-1 + z)^2 z (-1 + y + z) (y \\
& + z)^2 (-1 + 4z) H(2, y)) - 192(-1 + y)^2 y (y^2 + 2y(-1 + z) + 2(-1 + z)^2)(-1 + z)^2 z (-1 + y + z) (y + z)^2 (-1 \\
& + 4z) H(2, 2, y)) + H(2, y) (-96(-1 + y)^2 y (-1 + 4y)(-1 + z)^2 z (-1 + y + z) (y + z)^2 (2 + 2y^2 + 2y(-2 + z) - 2z \\
& + z^2) H(0, 0, y) - 96(-1 + y)^2 y (y^2 + 2y(-1 + z) + 2(-1 + z)^2)(-1 + z)^2 z (-1 + y + z) (y + z)^2 (-1 + 4z) H(0, 0, z) \\
& - 96(-1 + y)^2 y (y^2 + 2y(-1 + z) + 2(-1 + z)^2)(-1 + z)^2 z (-1 + y + z) (y + z)^2 (-1 + 4z) H(0, 1, z) + 96(-1 + y)^2 y (-1 \\
& + 4y)(-1 + z)^2 z (-1 + y + z) (y + z)^2 (2 + 2y^2 + 2y(-2 + z) - 2z + z^2) H(0, 2, y) - 96(-1 + y)^2 y (-1 + 4y)(-1 \\
& + z)^2 z (-1 + y + z) (y + z)^2 (2 + 2y^2 + 2y(-2 + z) - 2z + z^2) H(1, 0, y) - 96(-1 + y)^2 y (y^2 + 2y(-1 + z) + 2(-1 \\
& + z)^2)(-1 + z)^2 z (-1 + y + z) (y + z)^2 (-1 + 4z) H(1, 0, z) + 120(-1 + y)^2 y (-1 + z)^2 z (-1 + y + z) (y + z)^2 (-4 + 56y^3 \\
& + 50z - 109z^2 + 56z^3 + y^2(-109 + 84z) + y(50 - 92z + 84z^2)) H(1, 1, z) + 96(-1 + y)^2 y (-1 + 4y)(-1 + z)^2 z (-1 + y \\
& + z) (y + z)^2 (2 + 2y^2 + 2y(-2 + z) - 2z + z^2) H(2, 0, y) - 96(-1 + y)^2 y (-1 + z)^2 z (-1 + y + z) (y + z)^2 (-4 + 8y^3 \\
& + 14z - 19z^2 + 8z^3 + y^2(-19 + 12z) + 2y(7 - 10z + 6z^2)) H(2, 2, y) - 96(-1 + y)^2 y (-1 + z)^2 z (-1 + y + z) (y \\
& + z)^2 (-4 + 8y^3 + 14z - 19z^2 + 8z^3 + y^2(-19 + 12z) + 2y(7 - 10z + 6z^2)) H(3, 2, y)) + H(1, z) (-60(-1 + y)^2 y (-1 \\
& + z)^2 z (-1 + y + z) (y + z)^2 (-4 + 56y^3 + 50z - 109z^2 + 56z^3 + y^2(-109 + 84z) + y(50 - 92z + 84z^2)) H(2, y)^2 \\
& - 96(-1 + y)^2 y (-1 + z)^2 z (-1 + y + z) (y + z)^2 (-4 + 8y^3 + 14z - 19z^2 + 8z^3 + y^2(-19 + 12z) + 2y(7 - 10z \\
& + 6z^2)) H(2, y) H(3, y) - 96(-1 + y)^2 y (-1 + 4y)(-1 + z)^2 z (-1 + y + z) (y + z)^2 (2 + 2y^2 + 2y(-2 + z) - 2z \\
& + z^2) H(0, 0, y) - 96(-1 + y)^2 y (y^2 + 2y(-1 + z) + 2(-1 + z)^2)(-1 + z)^2 z (-1 + y + z) (y + z)^2 (-1 + 4z) H(0, 0, z) \\
& - 96(-1 + y)^2 y (-1 + 4y)(-1 + z)^2 z (-1 + y + z) (y + z)^2 (2 + 2y^2 + 2y(-2 + z) - 2z + z^2) H(0, 1, z) - 96(-1 \\
& + y)^2 y (-1 + 4y)(-1 + z)^2 z (-1 + y + z) (y + z)^2 (2 + 2y^2 + 2y(-2 + z) - 2z + z^2) H(0, 2, y) - 96(-1 + y)^2 y (-1 \\
& + z)^2 z (-1 + y + z) (y + z)^2 (-4 + 8y^3 + 14z - 19z^2 + 8z^3 + y^2(-19 + 12z) + 2y(7 - 10z + 6z^2)) H(1, 1, z) - 96(-1 \\
& + y)^2 y (-1 + 4y)(-1 + z)^2 z (-1 + y + z) (y + z)^2 (2 + 2y^2 + 2y(-2 + z) - 2z + z^2) H(2, 0, y) + 120(-1 + y)^2 y (-1 \\
& + z)^2 z (-1 + y + z) (y + z)^2 (-4 + 56y^3 + 50z - 109z^2 + 56z^3 + y^2(-109 + 84z) + y(50 - 92z + 84z^2)) H(2, 2, y) \\
& + 96(-1 + y)^2 y (-1 + z)^2 z (-1 + y + z) (y + z)^2 (-4 + 8y^3 + 14z - 19z^2 + 8z^3 + y^2(-19 + 12z) + 2y(7 - 10z \\
& + 6z^2)) H(2, 3, y) + 96(-1 + y)^2 y (-1 + z)^2 z (-1 + y + z) (y + z)^2 (-4 + 8y^3 + 14z - 19z^2 + 8z^3 + y^2(-19 + 12z) \\
& + 2y(7 - 10z + 6z^2)) H(3, 2, y)) + 72(-1 + y)^2 y (-1 + z)^2 z (-1 + y + z) (y + z)^2 (-44 + 528y^3 + 66z - 99z^2 + 64z^3 \\
& + y^2(-829 + 412z) + 2y(187 - 176z + 58z^2)) H(0, 0, 0, y) + 72(-1 + y)^2 y (-1 + z)^2 z (-1 + y + z) (y + z)^2 (-44 + 64y^3 \\
& + 374z - 829z^2 + 528z^3 + y^2(-99 + 116z) + y(66 - 352z + 412z^2)) H(0, 0, 0, z) + 192(-1 + y)^2 y (-1 + 4y)(-1 \\
& + z)^2 z (-1 + y + z) (y + z)^2 (2 + 2y^2 + 2y(-2 + z) - 2z + z^2) H(0, 1, 1, z) - 192(-1 + y)^2 y (-1 + 4y)(-1 + z)^2 z (-1 + y \\
& + z) (y + z)^2 (2 + 2y^2 + 2y(-2 + z) - 2z + z^2) H(0, 2, 2, y) + 96(-1 + y)^2 y (-1 + 4y)(-1 + z)^2 z (-1 + y + z) (y \\
& + z)^2 (2 + 2y^2 + 2y(-2 + z) - 2z + z^2) H(1, 0, 1, z) + 96(-1 + y)^2 y (-1 + 4y)(-1 + z)^2 z (-1 + y + z) (y + z)^2 (2 \\
& + 2y^2 + 2y(-2 + z) - 2z + z^2) H(1, 0, 2, y) + 72(-1 + y)^2 y (-1 + z)^2 z (-1 + y + z) (y + z)^2 (-12 + 104y^3 + 102z \\
& - 207z^2 + 104z^3 + 3y^2(-69 + 52z) + 6y(17 - 30z + 26z^2)) H(1, 1, 1, z) + 96(-1 + y)^2 y (-1 + 4y)(-1 + z)^2 z (-1 + y \\
& + z) (y + z)^2 (2 + 2y^2 + 2y(-2 + z) - 2z + z^2) H(1, 2, 0, y) - 192(-1 + y)^2 y (-1 + 4y)(-1 + z)^2 z (-1 + y + z) (y \\
& + z)^2 (2 + 2y^2 + 2y(-2 + z) - 2z + z^2) H(2, 0, 2, y) + 96(-1 + y)^2 y (-1 + 4y)(-1 + z)^2 z (-1 + y + z) (y + z)^2 (2 \\
& + 2y^2 + 2y(-2 + z) - 2z + z^2) H(2, 1, 0, y) - 192(-1 + y)^2 y (-1 + 4y)(-1 + z)^2 z (-1 + y + z) (y + z)^2 (2 + 2y^2 \\
& + 2y(-2 + z) - 2z + z^2) H(2, 2, 0, y) + 72(-1 + y)^2 y (-1 + z)^2 z (-1 + y + z) (y + z)^2 (-12 + 104y^3 + 102z - 207z^2 \\
& + 104z^3 + 3y^2(-69 + 52z) + 6y(17 - 30z + 26z^2)) H(2, 2, 2, y) + 96(-1 + y)^2 y (-1 + z)^2 z (-1 + y + z) (y + z)^2 (-4 \\
& + 8y^3 + 14z - 19z^2 + 8z^3 + y^2(-19 + 12z) + 2y(7 - 10z + 6z^2)) H(2, 3, 2, y) + 192(-1 + y)^2 y (-1 + z)^2 z (-1 + y \\
& + z) (y + z)^2 (-4 + 8y^3 + 14z - 19z^2 + 8z^3 + y^2(-19 + 12z) + 2y(7 - 10z + 6z^2)) H(3, 2, 2, y) \Big\} / \Big(48(-1 + y)^2 y^2 (-1 \\
& + z)^2 z^2 (-1 + y + z) (y + z)^2 \Big);
\end{aligned}$$

$$\begin{aligned}
A_{3;n_f^2}^{(2)} = & \left\{ 4(5y^7(-1 + 4z) + y^6(15 - 83z + 80z^2) - 5z^4(-2 + 4z - 3z^2 + z^3) + y^5(-20 + 147z - 273z^2 + 140z^3) + yz^3(40 \right. \\
& - 154z + 147z^2 - 83z^3 + 20z^4) + y^2 z^2(60 - 254z + 363z^2 - 273z^3 + 80z^4) + y^3 z(40 - 254z + 462z^2 - 439z^3 \\
& + 140z^4) + y^4(10 - 154z + 363z^2 - 439z^3 + 160z^4)) - 9(y + z)^4(2 + y^2(3 - 9z) - 4z + 3z^2 - z^3 + y^3(-1 + 4z) \\
& + y(-4 + 12z - 9z^2 + 4z^3)) H(0, y) - 9(y + z)^4(2 + y^2(3 - 9z) - 4z + 3z^2 - z^3 + y^3(-1 + 4z) + y(-4 + 12z - 9z^2 \\
& + 4z^3)) H(0, z) + 36yz(-5y^3 + 3y^4 + yz^2 + y^2(6 + z - 6z^2) + z^2(6 - 5z + 3z^2)) H(1, z) + 36yz(-5y^3 + 3y^4 \\
& + yz^2 + y^2(6 + z - 6z^2) + z^2(6 - 5z + 3z^2)) H(2, y) \Big\} / \Big(216yz(-1 + y + z) (y + z)^4 \Big);
\end{aligned}$$

$$\begin{aligned}
\mathcal{A}_{3;CACF}^{(2)} = & \left\{ -4(-1+y)y(-1+z)z(y+z)((-1+z)^2z(5450 - 5153z + 2725z^2) + y^5(2725 - 10952z + 7336z^2) + y^4(-10603 \right. \\
& + 43407z - 37764z^2 + 4960z^3) + y^3(18481 - 86606z + 117680z^2 - 53624z^3 + 4960z^4) + y(5450 - 38046z + 86747z^2 \\
& - 86606z^3 + 43407z^4 - 10952z^5) + y^2(-16053 + 86747z - 157946z^2 + 117680z^3 - 37764z^4 + 7336z^5)) + 36(-1 \\
& + y)^2y(-1+z)^2z(y+z)^2(272 + 3128y^4 - 470z + 417z^2 - 419z^3 + 200z^4 + y^3(-8003 + 5572z) + 3y^2(2355 - 3089z \\
& + 936z^2) + y(-2462 + 4440z - 2739z^2 + 772z^3))H(0, y)^3 + 36(-1+y)^2y(-1+z)^2z(y+z)^2(272 + 200y^4 - 2462z \\
& + 7065z^2 - 8003z^3 + 3128z^4 + y^3(-419 + 772z) + 3y^2(139 - 913z + 936z^2) + y(-470 + 4440z - 9267z^2 \\
& + 5572z^3))H(0, z)^3 + 36(-1+y)^2y(-1+z)^2z(y+z)^2(60 + 1048y^4 - 1190z + 3387z^2 - 3305z^3 + 1048z^4 \\
& + y^3(-3305 + 2652z) + y^2(3387 - 5793z + 3624z^2) + y(-1190 + 3984z - 5793z^2 + 2652z^3))H(1, z)^3 + 9(2592y^{10}(-1 \\
& + z)^2 - 324(-1+z)^5z^4(-1+4z) + 4y^9(-1+z)^2(-3375 + 1232z) + y^8(28620 - 84611z + 64366z^2 + 10459z^3 \\
& - 18996z^4) + y(-1+z)^2z^3(-10284 + 31286z - 47769z^2 + 47069z^3 - 22936z^4 + 2592z^5) - y^7(31212 - 112231z \\
& + 31885z^2 + 231313z^3 - 265795z^4 + 83616z^5) + y^6(18036 - 61763z - 163792z^2 + 837127z^3 - 1162130z^4 + 669294z^5 \\
& - 136448z^6) - y^2(-1+z)^2z^2(8364 - 92610z + 217312z^2 - 239107z^3 + 137650z^4 - 33236z^5 + 1296z^6) - y^5(4968 \\
& + 12031z - 343845z^2 + 1384321z^3 - 2358789z^4 + 1969504z^5 - 787230z^6 + 119040z^7) + y^4(432 + 28202z - 276976z^2 \\
& + 1189366z^3 - 2507872z^4 + 2799861z^5 - 1679342z^6 + 504259z^7 - 58092z^8) + y^3z(-8772 + 93570z - 525300z^2 \\
& + 1423618z^3 - 2064667z^4 + 1697887z^5 - 784219z^6 + 182395z^7 - 14512z^8))H(2, y)^2 + 36(-1+y)^2y(-1+z)^2z(y \\
& + z)^2(60 + 1048y^4 - 1190z + 3387z^2 - 3305z^3 + 1048z^4 + y^3(-3305 + 2652z) + y^2(3387 - 5793z + 3624z^2) + y(-1190 \\
& + 3984z - 5793z^2 + 2652z^3))H(2, y)^3 + H(0, z)^2(9(324(-1+z)^6z^3(-1+4z) + 16y^9(-1+z)^2(162 + 73z) \\
& + y^8(-13500 + 34093z - 26250z^2 + 5391z^3 + 1180z^4) + y^7(28620 - 106481z + 143631z^2 - 77501z^3 + 5003z^4 + 6728z^5) \\
& - 2y(-1+z)^2z^2(108 - 3068z + 15065z^2 - 37089z^3 + 46088z^4 - 22256z^5 + 1296z^6) + y^6(-31212 + 163509z \\
& - 312112z^2 + 240300z^3 - 456z^4 - 105981z^5 + 44124z^6) + 2y^2(-1+z)^2z(270 - 1316z - 14807z^2 + 70951z^3 \\
& - 142240z^4 + 124888z^5 - 36250z^6 + 648z^7) + y^5(18036 - 132635z + 331953z^2 - 300344z^3 - 147828z^4 + 523715z^5 \\
& - 390745z^6 + 97848z^7) + y^4(-4968 + 54838z - 176524z^2 + 144129z^3 + 393770z^4 - 1110625z^5 + 1146516z^6 - 538862z^7 \\
& + 92640z^8) + y^3(432 - 9848z + 42974z^2 + 4423z^3 - 410951z^4 + 1156123z^5 - 1515467z^6 + 1025284z^7 - 326466z^8 \\
& + 33496z^9)) - 864(-1+y)^2y(-1+z)^2z(y+z)^2(y^3(-1+4z) + 4y(-1+z)^2(-1+4z) + 3y^2(1-5z+4z^2) \\
& + 2(1-8z+18z^2-17z^3+6z^4))H(1, z) - 1728(-1+y)^2y(-1+z)^2z(y+z)^2(2-15z+33z^2-30z^3+10z^4 \\
& + y^3(-1+4z) + 4y(-1+z)^2(-1+4z) + 3y^2(1-5z+4z^2))H(2, y)) + H(0, y)^2(-9(2592y^{10}(-1+z)^2 + 324(-1 \\
& + z)^5z^3(-1+4z) - 4y^9(-1+z)^2(4023 + 4486z) - 6y^8(-7020 + 5368z + 21840z^2 - 31731z^3 + 11516z^4) + y^7(-59832 \\
& + 90672z + 223220z^2 - 565474z^3 + 397382z^4 - 85968z^5) - y(-1+z)^2z^2(-216 + 6244z - 21180z^2 + 34761z^3 - 27075z^4 \\
& + 7648z^5) + y^6(49248 - 151456z - 105440z^2 + 735113z^3 - 850650z^4 + 378865z^5 - 56004z^6) + y^2(-1+z)^2z(-540 \\
& + 1876z + 30168z^2 - 80106z^3 + 101421z^4 - 58502z^5 + 11408z^6) - y^5(23004 - 128508z + 71864z^2 + 470215z^3 \\
& - 932695z^4 + 701645z^5 - 235797z^6 + 30272z^7) + y^4(5400 - 53988z + 88836z^2 + 166115z^3 - 638606z^4 + 766830z^5 \\
& - 456762z^6 + 139069z^7 - 16732z^8) - y^3(432 - 9956z + 29272z^2 + 57505z^3 - 334959z^4 + 576238z^5 - 518670z^6 \\
& + 256651z^7 - 61569z^8 + 5056z^9)) - 432(-1+y)^2y(-1+z)^2z(-1+y+z)(y+z)^2(2+2y^2+2y(-2+z) \\
& - 2z+z^2)H(0, z) - 1728(-1+y)^2y(-1+z)^2z(y+z)^2(2+10y^4-4z+3z^2-z^3+2y^3(-15+8z)+3y^2(11 \\
& - 12z+4z^2)+y(-15+24z-15z^2+4z^3))H(1, z) - 864(-1+y)^2y(-1+z)^2z(y+z)^2(2+12y^4-4z+3z^2 \\
& - z^3+2y^3(-17+8z)+12y^2(3-3z+z^2)+y(-16+24z-15z^2+4z^3))H(2, y)) + H(1, z)^2(9(2592y^{10}(-1+z)^2 \\
& - 324(-1+z)^5z^4(-1+4z) + 4y^9(-1+z)^2(-3375 + 1232z) + y^8(28620 - 84611z + 64366z^2 + 10459z^3 - 18996z^4) \\
& + y(-1+z)^2z^3(-10284 + 31286z - 47769z^2 + 47069z^3 - 22936z^4 + 2592z^5) - y^7(31212 - 112231z + 31885z^2) \\
& + 231313z^3 - 265795z^4 + 83616z^5) + y^6(18036 - 61763z - 163792z^2 + 837127z^3 - 1162130z^4 + 669294z^5 - 136448z^6) \\
& - y^2(-1+z)^2z^2(8364 - 92610z + 217312z^2 - 239107z^3 + 137650z^4 - 33236z^5 + 1296z^6) - y^5(4968 + 12031z \\
& - 343845z^2 + 1384321z^3 - 2358789z^4 + 1969504z^5 - 787230z^6 + 119040z^7) + y^4(432 + 28202z - 276976z^2 + 1189366z^3 \\
& - 2507872z^4 + 2799861z^5 - 1679342z^6 + 504259z^7 - 58092z^8) + y^3z(-8772 + 93570z - 525300z^2 + 1423618z^3 \\
& - 2064667z^4 + 1697887z^5 - 784219z^6 + 182395z^7 - 14512z^8)) + 108(-1+y)^2y(-1+z)^2z(y+z)^2(124 + 1240y^4 \\
& - 1510z + 4011z^2 - 3865z^3 + 1240z^4 + y^3(-3865 + 2972z) + y^2(4011 - 6609z + 4008z^2) + y(-1510 + 4752z - 6609z^2 \\
& + 2972z^3))H(2, y) + 1728(-1+y)^2y(-1+z)^2z(y+z)^2(4+12y^4-20z+39z^2-35z^3+12z^4+5y^3(-7+4z) \\
& + 3y^2(13-17z+8z^2)+y(-20+48z-51z^2+20z^3))H(3, y)) + 18(2592y^{10}(-1+z)^2 + 324(-1+z)^5z^3(-1+4z) \\
& - 4y^9(-1+z)^2(4023 + 4486z) - 6y^8(-7020 + 5368z + 21840z^2 - 31731z^3 + 11516z^4) + y^7(-59832 + 90672z \\
& + 223220z^2 - 565474z^3 + 397382z^4 - 85968z^5) - y(-1+z)^2z^2(-216 + 6244z - 21180z^2 + 34761z^3 - 27075z^4 \\
& + 7648z^5) + y^6(49248 - 151456z - 105440z^2 + 735113z^3 - 850650z^4 + 378865z^5 - 56004z^6) + y^2(-1+z)^2z(-540 \\
& + 1876z + 30168z^2 - 80106z^3 + 101421z^4 - 58502z^5 + 11408z^6) - y^5(23004 - 128508z + 71864z^2 + 470215z^3
\end{aligned}$$

$$\begin{aligned}
& - 932695z^4 + 701645z^5 - 235797z^6 + 30272z^7) + y^4(5400 - 53988z + 88836z^2 + 166115z^3 - 638606z^4 + 766830z^5 \\
& - 456762z^6 + 139069z^7 - 16732z^8) - y^3(432 - 9956z + 29272z^2 + 57505z^3 - 334959z^4 + 576238z^5 - 518670z^6 \\
& + 256651z^7 - 61569z^8 + 5056z^9))H(0, 0, y) - 18(324(-1+z)^6z^3(-1+4z) + 16y^9(-1+z)^2(162+73z) + y^8(-13500 \\
& + 34093z - 26250z^2 + 5391z^3 + 1180z^4) + y^7(28620 - 106481z + 143631z^2 - 77501z^3 + 5003z^4 + 6728z^5) - 2y(-1 \\
& + z)^2z^2(108 - 3068z + 15065z^2 - 37089z^3 + 46088z^4 - 22256z^5 + 1296z^6) + y^6(-31212 + 163509z - 312112z^2 \\
& + 240300z^3 - 456z^4 - 105981z^5 + 44124z^6) + 2y^2(-1+z)^2z(270 - 1316z - 14807z^2 + 70951z^3 - 142240z^4 \\
& + 124888z^5 - 36250z^6 + 648z^7) + y^5(18036 - 132635z + 331953z^2 - 300344z^3 - 147828z^4 + 523715z^5 - 390745z^6 \\
& + 97848z^7) + y^4(-4968 + 54838z - 176524z^2 + 144129z^3 + 393770z^4 - 1110625z^5 + 1146516z^6 - 538862z^7 + 92640z^8) \\
& + y^3(432 - 9848z + 42974z^2 + 4423z^3 - 410951z^4 + 1156123z^5 - 1515467z^6 + 1025284z^7 - 326466z^8 \\
& + 33496z^9))H(0, 0, z) - 216(-1+y)^2yz(88y^6(-1+z)^2 - (-1+z)^3z^2(14 - 14z + 3z^2) + y^5(-278 + 828z - 816z^2 \\
& + 272z^3) - y(-1+z)^2z(-68 + 202z - 114z^2 - 61z^3 + 60z^4) + 2y^4(157 - 686z + 1012z^2 - 591z^3 + 114z^4) \\
& - y^3(138 - 984z + 2141z^2 - 1802z^3 + 433z^4 + 68z^5) + y^2(14 - 340z + 1129z^2 - 1351z^3 + 427z^4 + 293z^5 \\
& - 172z^6))H(0, 1, z) + 216y(-1+z)^2z(88y^8 + y^7(-470 + 456z) + 2y^6(511 - 1064z + 482z^2) + z^2(30 - 60z + 49z^2 \\
& - 19z^3) + y^5(-1156 + 4028z - 3857z^2 + 1036z^3) + yz(20 - 342z + 666z^2 - 509z^3 + 162z^4) + y^4(716 - 3888z \\
& + 6107z^2 - 3483z^3 + 564z^4) + y^2(30 - 432z + 1885z^2 - 2545z^3 + 1441z^4 - 273z^5) + y^3(-230 + 1944z - 4787z^2 \\
& + 4380z^3 - 1557z^4 + 124z^5))H(0, 2, y) - 2376(-1+y)^2y(-1+4y)(-1+z)^2z(-1+y+z)(y+z)^2(2+2y^2 \\
& + 2y(-2+z) - 2z+z^2)H(1, 0, y) + 432(-1+y)^2yz(-4(-1+z)^3z^2(1-z+z^2) + y^5(-4+48z - 87z^2 + 40z^3) \\
& + 4y(-1+z)^2z(-3 - 5z + 27z^2 - 31z^3 + 13z^4) + y^4(8 - 128z + 407z^2 - 465z^3 + 172z^4) + y^3(-8 + 124z \\
& - 552z^2 + 1046z^3 - 889z^4 + 276z^5) + y^2(4 - 28z + 244z^2 - 760z^3 + 1079z^4 - 735z^5 + 196z^6))H(1, 0, z) \\
& - 18(2592y^{10}(-1+z)^2 - 324(-1+z)^5z^4(-1+4z) + 4y^9(-1+z)^2(-3375 + 1232z) + y^8(28620 - 84611z + 64366z^2 \\
& + 10459z^3 - 18996z^4) + y(-1+z)^2z^3(-10284 + 31286z - 47769z^2 + 47069z^3 - 22936z^4 + 2592z^5) - y^7(31212 \\
& - 112231z + 31885z^2 + 231313z^3 - 265795z^4 + 83616z^5) + y^6(18036 - 61763z - 163792z^2 + 837127z^3 - 1162130z^4 \\
& + 669294z^5 - 136448z^6) - y^2(-1+z)^2z^2(8364 - 92610z + 217312z^2 - 239107z^3 + 137650z^4 - 33236z^5 + 1296z^6) \\
& - y^5(4968 + 12031z - 343845z^2 + 1384321z^3 - 2358789z^4 + 1969504z^5 - 787230z^6 + 119040z^7) + y^4(432 + 28202z \\
& - 276976z^2 + 1189366z^3 - 2507872z^4 + 2799861z^5 - 1679342z^6 + 504259z^7 - 58092z^8) + y^3z(-8772 + 93570z \\
& - 525300z^2 + 1423618z^3 - 2064667z^4 + 1697887z^5 - 784219z^6 + 182395z^7 - 14512z^8))H(1, 1, z) + H(3, y)(-864(-1 \\
& + y)^2y(-1+z)^2z(-1+y+z)(y+z)^2(-4 + 8y^3 + 14z - 19z^2 + 8z^3 + y^2(-19 + 12z) + 2y(7 - 10z \\
& + 6z^2))H(0, 1, z) - 864(-1+y)^2y(-1+z)^2z(-1+y+z)(y+z)^2(-4 + 8y^3 + 14z - 19z^2 + 8z^3 + y^2(-19 + 12z) \\
& + 2y(7 - 10z + 6z^2))H(1, 0, z) - 3456(-1+y)^2y(-1+z)^2z(y+z)^2(4 + 12y^4 - 20z + 39z^2 - 35z^3 + 12z^4 \\
& + 5y^3(-7 + 4z) + 3y^2(13 - 17z + 8z^2) + y(-20 + 48z - 51z^2 + 20z^3))H(1, 1, z) + 216y(-1+z)^2z(88y^8 \\
& + y^7(-470 + 456z) + 2y^6(511 - 1064z + 482z^2) + z^2(30 - 60z + 49z^2 - 19z^3) + y^5(-1156 + 4028z - 3857z^2 \\
& + 1036z^3) + yz(20 - 342z + 666z^2 - 509z^3 + 162z^4) + y^4(716 - 3888z + 6107z^2 - 3483z^3 + 564z^4) + y^2(30 \\
& - 432z + 1885z^2 - 2545z^3 + 1441z^4 - 273z^5) + y^3(-230 + 1944z - 4787z^2 + 4380z^3 - 1557z^4 + 124z^5))H(2, 0, y) \\
& - 18(2592y^{10}(-1+z)^2 - 324(-1+z)^5z^4(-1+4z) + 4y^9(-1+z)^2(-3375 + 1232z) + y^8(28620 - 84611z + 64366z^2 \\
& + 10459z^3 - 18996z^4) + y(-1+z)^2z^3(-10284 + 31286z - 47769z^2 + 47069z^3 - 22936z^4 + 2592z^5) - y^7(31212 \\
& - 112231z + 31885z^2 + 231313z^3 - 265795z^4 + 83616z^5) + y^6(18036 - 61763z - 163792z^2 + 837127z^3 - 1162130z^4 \\
& + 669294z^5 - 136448z^6) - y^2(-1+z)^2z^2(8364 - 92610z + 217312z^2 - 239107z^3 + 137650z^4 - 33236z^5 + 1296z^6) \\
& - y^5(4968 + 12031z - 343845z^2 + 1384321z^3 - 2358789z^4 + 1969504z^5 - 787230z^6 + 119040z^7) + y^4(432 + 28202z \\
& - 276976z^2 + 1189366z^3 - 2507872z^4 + 2799861z^5 - 1679342z^6 + 504259z^7 - 58092z^8) + y^3z(-8772 + 93570z \\
& - 525300z^2 + 1423618z^3 - 2064667z^4 + 1697887z^5 - 784219z^6 + 182395z^7 - 14512z^8))H(2, 2, y) + H(0, z)(1188(-1 \\
& + y)^2y^2z^2(-1+y+z)(y+z)^2(-12 + 30z - 26z^2 + 8z^3 + 3y(4 - 9z + 4z^2)) - 864(-1+y)^2y(-1+z)^2z(y \\
& + z)^2(4y^4 + (-1+z)^3(-1+4z) + y^3(-13 + 8z) + 3y^2(5 - 7z + 4z^2) + y(-7 + 18z - 21z^2 + 8z^3))H(1, z)^2 \\
& + 2376(-1+y)^2y(y^2 + 2y(-1+z) + 2(-1+z)^2)(-1+z)^2z(-1+y+z)(y+z)^2(-1+4z)H(2, y) - 864(-1 \\
& + y)^2y(-1+z)^2z(y+z)^2(5 + 4y^4 - 39z + 87z^2 - 81z^3 + 28z^4 + y^3(-15 + 16z) + 3y^2(7 - 17z + 12z^2) \\
& + y(-15 + 66z - 93z^2 + 40z^3))H(2, y)^2 + H(1, z)(-432(-1+y)^2yz(-4(-1+z)^3z^2(1-z+z^2) + y^5(-4 + 48z \\
& - 87z^2 + 40z^3) + 4y(-1+z)^2z(-3 - 5z + 27z^2 - 31z^3 + 13z^4) + y^4(8 - 128z + 407z^2 - 465z^3 + 172z^4) \\
& + y^3(-8 + 124z - 552z^2 + 1046z^3 - 889z^4 + 276z^5) + y^2(4 - 28z + 244z^2 - 760z^3 + 1079z^4 - 735z^5 + 196z^6)) \\
& - 864(-1+y)^2y(-1+z)^2z(y+z)^2(2 - 28z + 69z^2 - 67z^3 + 24z^4 + y^3(-1 + 4z) + 3y^2(1 - 7z + 8z^2) + y(-4 \\
& + 36z - 63z^2 + 28z^3))H(2, y) + 864(-1+y)^2y(-1+z)^2z(-1+y+z)(y+z)^2(-4 + 8y^3 + 14z - 19z^2 + 8z^3 \\
& + y^2(-19 + 12z) + 2y(7 - 10z + 6z^2))H(3, y) + 864(-1+y)^2y(-1+4y)(-1+z)^2z(-1+y+z)(y+z)^2(2 + 2y^2
\end{aligned}$$

$$\begin{aligned}
& + 2y(-2+z) - 2z + z^2)H(0, 0, y) + 864(-1+y)^2y(y^2 + 2y(-1+z) + 2(-1+z)^2)(-1+z)^2z(-1+y+z)(y \\
& + z)^2(-1+4z)H(0, 0, z) + 864(-1+y)^2y(-1+4y)(-1+z)^2z(-1+y+z)(y+z)^2(2+2y^2 + 2y(-2+z) - 2z \\
& + z^2)H(0, 1, z) + 864(-1+y)^2y(-1+z)^2z(y+z)^2(4-18z + 33z^2 - 27z^3 + 8z^4 + y^3(-2+8z) + 6y^2(1-4z \\
& + 2z^2) + y(-8+36z - 45z^2 + 20z^3))H(0, 2, y) + 864(-1+y)^2y(-1+z)^2z(-1+y+z)(y+z)^2(-4+8y^3 + 14z \\
& - 19z^2 + 8z^3 + y^2(-19+12z) + 2y(7-10z+6z^2))H(1, 1, z) + 864(-1+y)^2y(-1+z)^2z(y+z)^2(4-18z \\
& + 33z^2 - 27z^3 + 8z^4 + y^3(-2+8z) + 6y^2(1-4z+2z^2) + y(-8+36z - 45z^2 + 20z^3))H(2, 0, y) + 1728(-1 \\
& + y)^2y(-1+z)^2z(y+z)^2(5+4y^4 - 39z + 87z^2 - 81z^3 + 28z^4 + y^3(-15+16z) + 3y^2(7-17z+12z^2) \\
& + y(-15+66z - 93z^2 + 40z^3))H(2, 2, y)) - 2376(-1+y)^2y(-1+z)^2z(-1+y+z)(y+z)^2(-4+8y^3 + 14z \\
& - 19z^2 + 8z^3 + y^2(-19+12z) + 2y(7-10z+6z^2))H(3, 2, y) + H(0, y)(1188y^2(-1+z)^2z^2(-1+y+z)(y \\
& + z)^2(8y^3 + y(30-27z) + 12(-1+z) + 2y^2(-13+6z)) - 432(-1+y)^2y(y^2 + 2y(-1+z) + 2(-1+z)^2)(-1 \\
& + z)^2z(-1+y+z)(y+z)^2(-1+4z)H(0, z)^2 - 864(-1+y)^2y(-1+z)^2z(y+z)^2(5+28y^4 - 15z + 21z^2 \\
& - 15z^3 + 4z^4 + y^3(-81+40z) + y^2(87-93z+36z^2) + y(-39+66z - 51z^2 + 16z^3))H(1, z)^2 - 432y(-1 \\
& + z)^2z(y^7(-4+52z) + 4y^6(4-57z+49z^2) - 4z^2(-1+2z-2z^2+z^3) + y^5(-28+408z - 735z^2 + 276z^3) \\
& + 4yz(-3-7z+31z^2 - 32z^3 + 12z^4) + y^4(28-360z+1079z^2 - 889z^3 + 172z^4) + y^2(4+4z+244z^2 - 552z^3 \\
& + 407z^4 - 87z^5) + y^3(-16+136z - 760z^2 + 1046z^3 - 465z^4 + 40z^5))H(2, y) - 864(-1+y)^2y(-1+z)^2z(y \\
& + z)^2(4y^4 + (-1+z)^3(-1+4z) + y^3(-13+8z) + 3y^2(5-7z+4z^2) + y(-7+18z - 21z^2 + 8z^3))H(2, y)^2 \\
& + H(0, z)(-864(-1+y)^2y(-1+z)^2z(y+z)^2(4+8y^4 - 8z + 6z^2 - 2z^3 + y^3(-27+20z) + 3y^2(11-15z \\
& + 4z^2) + 2y(-9+18z - 12z^2 + 4z^3))H(1, z) - 864(-1+y)^2y(-1+z)^2z(y+z)^2(4-18z + 33z^2 - 27z^3 + 8z^4 \\
& + y^3(-2+8z) + 6y^2(1-4z+2z^2) + y(-8+36z - 45z^2 + 20z^3))H(2, y)) + H(1, z)(2376(-1+y)^2y(-1+4y)(-1 \\
& + z)^2z(-1+y+z)(y+z)^2(2+2y^2 + 2y(-2+z) - 2z + z^2) - 864(-1+y)^2y(-1+z)^2z(y+z)^2(2+24y^4 - 4z \\
& + 3z^2 - z^3 + y^3(-67+28z) + 3y^2(23-21z+8z^2) + y(-28+36z - 21z^2 + 4z^3))H(2, y) + 864(-1+y)^2y(-1 \\
& + z)^2z(-1+y+z)(y+z)^2(-4+8y^3 + 14z - 19z^2 + 8z^3 + y^2(-19+12z) + 2y(7-10z+6z^2))H(3, y)) + 864(-1 \\
& + y)^2y(-1+4y)(-1+z)^2z(-1+y+z)(y+z)^2(2+2y^2 + 2y(-2+z) - 2z + z^2)H(0, 0, y) + 864(-1+y)^2y(y^2 \\
& + 2y(-1+z) + 2(-1+z)^2)(-1+z)^2z(-1+y+z)(y+z)^2(-1+4z)H(0, 0, z) + 864(-1+y)^2y(-1+z)^2z(y \\
& + z)^2(4+8y^4 - 8z + 6z^2 - 2z^3 + y^3(-27+20z) + 3y^2(11-15z+4z^2) + 2y(-9+18z - 12z^2 \\
& + 4z^3))H(0, 1, z) - 864(-1+y)^2y(-1+4y)(-1+z)^2z(-1+y+z)(y+z)^2(2+2y^2 + 2y(-2+z) - 2z \\
& + z^2)H(0, 2, y) + 864(-1+y)^2y(-1+4y)(-1+z)^2z(-1+y+z)(y+z)^2(2+2y^2 + 2y(-2+z) - 2z \\
& + z^2)H(1, 0, y) + 864(-1+y)^2y(-1+z)^2z(y+z)^2(4+8y^4 - 8z + 6z^2 - 2z^3 + y^3(-27+20z) + 3y^2(11-15z \\
& + 4z^2) + 2y(-9+18z - 12z^2 + 4z^3))H(1, 0, z) + 1728(-1+y)^2y(-1+z)^2z(y+z)^2(5+28y^4 - 15z + 21z^2 \\
& - 15z^3 + 4z^4 + y^3(-81+40z) + y^2(87-93z+36z^2) + y(-39+66z - 51z^2 + 16z^3))H(1, 1, z) - 864(-1 \\
& + y)^2y(-1+4y)(-1+z)^2z(-1+y+z)(y+z)^2(2+2y^2 + 2y(-2+z) - 2z + z^2)H(2, 0, y) + 864(-1+y)^2y(-1 \\
& + z)^2z(-1+y+z)(y+z)^2(-4+8y^3 + 14z - 19z^2 + 8z^3 + y^2(-19+12z) + 2y(7-10z \\
& + 6z^2))H(3, 2, y)) + H(1, z)(1188(-1+y)^2y(-1+z)^2z(-1+y+z)(y^4(-3+20z) - 3z^2(2-2z+z^2) + y^3(6 \\
& - 50z + 60z^2) + 2yz(4+17z - 25z^2 + 10z^3) + y^2(-6+34z - 94z^2 + 60z^3)) + 108(-1+y)^2y(-1+z)^2z(y \\
& + z)^2(124 + 1240y^4 - 1510z + 4011z^2 - 3865z^3 + 1240z^4 + y^3(-3865 + 2972z) + y^2(4011 - 6609z + 4008z^2) + y(-1510 \\
& + 4752z - 6609z^2 + 2972z^3))H(2, y)^2 - 2376(-1+y)^2y(-1+z)^2z(-1+y+z)(y+z)^2(-4+8y^3 + 14z - 19z^2 \\
& + 8z^3 + y^2(-19+12z) + 2y(7-10z+6z^2))H(3, y) + 1728(-1+y)^2y(-1+z)^2z(y+z)^2(4+12y^4 - 20z + 39z^2 \\
& - 35z^3 + 12z^4 + 5y^3(-7+4z) + 3y^2(13-17z+8z^2) + y(-20+48z - 51z^2 + 20z^3))H(2, y)H(3, y) + 3456(-1 \\
& + y)^2y(-1+z)^2z(y+z)^2(2+10y^4 - 4z + 3z^2 - z^3 + 2y^3(-15+8z) + 3y^2(11-12z+4z^2) + y(-15+24z \\
& - 15z^2 + 4z^3))H(0, 0, y) + 864(-1+y)^2y(-1+z)^2z(y+z)^2(2-28z + 69z^2 - 67z^3 + 24z^4 + y^3(-1+4z) \\
& + 3y^2(1-7z+8z^2) + y(-4+36z - 63z^2 + 28z^3))H(0, 0, z) + 1728(-1+y)^2y(-1+z)^2z(y+z)^2(2+12y^4 \\
& - 4z + 3z^2 - z^3 + 2y^3(-17+8z) + 12y^2(3-3z+z^2) + y(-16+24z - 15z^2 + 4z^3))H(0, 1, z) + 864(-1 \\
& + y)^2y(-1+z)^2z(y+z)^2(2+24y^4 - 4z + 3z^2 - z^3 + y^3(-67+28z) + 3y^2(23-21z+8z^2) + y(-28+36z \\
& - 21z^2 + 4z^3))H(0, 2, y) - 864(-1+y)^2y(-1+z)^2z(-1+y+z)(y+z)^2(-4+8y^3 + 14z - 19z^2 + 8z^3 + y^2(-19 \\
& + 12z) + 2y(7-10z+6z^2))H(0, 3, y) - 864(-1+y)^2y(-1+z)^2z(y+z)^2(2+y^2(3-9z) - 4z + 3z^2 - z^3 \\
& + y^3(-1+4z) + y(-4+12z - 9z^2 + 4z^3))H(1, 0, z) + 1728(-1+y)^2y(-1+z)^2z(y+z)^2(4+12y^4 - 20z + 39z^2 \\
& - 35z^3 + 12z^4 + 5y^3(-7+4z) + 3y^2(13-17z+8z^2) + y(-20+48z - 51z^2 + 20z^3))H(1, 1, z) + 864(-1 \\
& + y)^2y(-1+z)^2z(y+z)^2(2+24y^4 - 4z + 3z^2 - z^3 + y^3(-67+28z) + 3y^2(23-21z+8z^2) + y(-28+36z \\
& - 21z^2 + 4z^3))H(2, 0, y) - 216(-1+y)^2y(-1+z)^2z(y+z)^2(124 + 1240y^4 - 1510z + 4011z^2 - 3865z^3 + 1240z^4
\end{aligned}$$

$$\begin{aligned}
& + y^3(-3865 + 2972z) + y^2(4011 - 6609z + 4008z^2) + y(-1510 + 4752z - 6609z^2 + 2972z^3))H(2, 2, y) - 1728(-1 \\
& + y)^2y(-1 + z)^2z(y + z)^2(4 + 12y^4 - 20z + 39z^2 - 35z^3 + 12z^4 + 5y^3(-7 + 4z) + 3y^2(13 - 17z + 8z^2) \\
& + y(-20 + 48z - 51z^2 + 20z^3))H(2, 3, y) - 864(-1 + y)^2y(-1 + z)^2z(-1 + y + z)(y + z)^2(-4 + 8y^3 + 14z - 19z^2 \\
& + 8z^3 + y^2(-19 + 12z) + 2y(7 - 10z + 6z^2))H(3, 0, y) - 1728(-1 + y)^2y(-1 + z)^2z(y + z)^2(4 + 12y^4 - 20z \\
& + 39z^2 - 35z^3 + 12z^4 + 5y^3(-7 + 4z) + 3y^2(13 - 17z + 8z^2) + y(-20 + 48z - 51z^2 + 20z^3))H(3, 2, y)) \\
& + H(2, y)(1188(-1 + y)^2y(-1 + z)^2z(-1 + y + z)(y^4(-3 + 20z) - 3z^2(2 - 2z + z^2) + y^3(6 - 50z + 60z^2) \\
& + 2yz(4 + 17z - 25z^2 + 10z^3) + y^2(-6 + 34z - 94z^2 + 60z^3)) + 864(-1 + y)^2y(-1 + z)^2z(y + z)^2(2 + 24y^4 \\
& - 4z + 3z^2 - z^3 + y^3(-67 + 28z) + 3y^2(23 - 21z + 8z^2) + y(-28 + 36z - 21z^2 + 4z^3))H(0, 0, y) + 3456(-1 \\
& + y)^2y(-1 + z)^2z(y + z)^2(2 - 15z + 33z^2 - 30z^3 + 10z^4 + y^3(-1 + 4z) + 4y(-1 + z)^2(-1 + 4z) + 3y^2(1 - 5z \\
& + 4z^2))H(0, 0, z) + 864(-1 + y)^2y(-1 + z)^2z(y + z)^2(2 - 28z + 69z^2 - 67z^3 + 24z^4 + y^3(-1 + 4z) + 3y^2(1 \\
& - 7z + 8z^2) + y(-4 + 36z - 63z^2 + 28z^3))H(0, 1, z) - 1728(-1 + y)^2y(-1 + z)^2z(y + z)^2(2 + 12y^4 - 4z + 3z^2 \\
& - z^3 + 2y^3(-17 + 8z) + 12y^2(3 - 3z + z^2) + y(-16 + 24z - 15z^2 + 4z^3))H(0, 2, y) + 864(-1 + y)^2y(-1 \\
& + z)^2z(y + z)^2(2 + 24y^4 - 4z + 3z^2 - z^3 + y^3(-67 + 28z) + 3y^2(23 - 21z + 8z^2) + y(-28 + 36z - 21z^2 \\
& + 4z^3))H(1, 0, y) + 864(-1 + y)^2y(-1 + z)^2z(y + z)^2(2 - 28z + 69z^2 - 67z^3 + 24z^4 + y^3(-1 + 4z) + 3y^2(1 \\
& - 7z + 8z^2) + y(-4 + 36z - 63z^2 + 28z^3))H(1, 0, z) - 216(-1 + y)^2y(-1 + z)^2z(y + z)^2(124 + 1240y^4 - 1510z \\
& + 4011z^2 - 3865z^3 + 1240z^4 + y^3(-3865 + 2972z) + y^2(4011 - 6609z + 4008z^2) + y(-1510 + 4752z - 6609z^2 \\
& + 2972z^3))H(1, 1, z) - 1728(-1 + y)^2y(-1 + z)^2z(y + z)^2(2 + 12y^4 - 4z + 3z^2 - z^3 + 2y^3(-17 + 8z) + 12y^2(3 \\
& - 3z + z^2) + y(-16 + 24z - 15z^2 + 4z^3))H(2, 0, y) + 1728(-1 + y)^2y(-1 + z)^2z(y + z)^2(4 + 12y^4 - 20z + 39z^2 \\
& - 35z^3 + 12z^4 + 5y^3(-7 + 4z) + 3y^2(13 - 17z + 8z^2) + y(-20 + 48z - 51z^2 + 20z^3))H(2, 2, y) + 1728(-1 \\
& + y)^2y(-1 + z)^2z(y + z)^2(4 + 12y^4 - 20z + 39z^2 - 35z^3 + 12z^4 + 5y^3(-7 + 4z) + 3y^2(13 - 17z + 8z^2) \\
& + y(-20 + 48z - 51z^2 + 20z^3))H(3, 2, y)) - 216(-1 + y)^2y(-1 + z)^2z(y + z)^2(296 + 3224y^4 - 518z + 453z^2 \\
& - 431z^3 + 200z^4 + y^3(-8315 + 5764z) + 3y^2(2475 - 3233z + 984z^2) + y(-2630 + 4728z - 2919z^2 \\
& + 820z^3))H(0, 0, 0, y) - 216(-1 + y)^2y(-1 + z)^2z(y + z)^2(296 + 200y^4 - 2630z + 7425z^2 - 8315z^3 + 3224z^4 \\
& + y^3(-431 + 820z) + 3y^2(151 - 973z + 984z^2) + y(-518 + 4728z - 9699z^2 + 5764z^3))H(0, 0, 0, z) - 864(-1 \\
& + y)^2y(-1 + z)^2z(y + z)^2(2 + 16y^4 - 4z + 3z^2 - z^3 + y^3(-51 + 28z) + 3y^2(19 - 21z + 8z^2) + y(-24 + 36z \\
& - 21z^2 + 4z^3))H(0, 0, 1, z) + 864(-1 + y)^2y(-1 + z)^2z(y + z)^2(16y^4 + y^3(-53 + 36z) + 3y^2(21 - 27z + 8z^2) \\
& - 3(-2 + 4z - 3z^2 + z^3) + y(-32 + 60z - 39z^2 + 12z^3))H(0, 0, 2, y) - 864(-1 + y)^2y(-1 + 4y)(-1 + z)^2z(-1 + y \\
& + z)(y + z)^2(2 + 2y^2 + 2y(-2 + z) - 2z + z^2)H(0, 1, 0, y) - 864(-1 + y)^2y^2(-1 + z)^2z(y + z)^2(8y^3 + y^2(-25 \\
& + 12z) - 2(5 - 6z + 3z^2) + 3y(9 - 9z + 4z^2))H(0, 1, 0, z) - 864(-1 + y)^2y(-1 + z)^2z(y + z)^2(48y^4 + y^3(-137 \\
& + 68z) + 3y^2(49 - 51z + 16z^2) - 5(-2 + 4z - 3z^2 + z^3) + y(-68 + 108z - 69z^2 + 20z^3))H(0, 1, 1, z) + 864(-1 \\
& + y)^2y(-1 + z)^2z(y + z)^2(16y^4 + y^3(-53 + 36z) + 3y^2(21 - 27z + 8z^2) - 3(-2 + 4z - 3z^2 + z^3) + y(-32 + 60z \\
& - 39z^2 + 12z^3))H(0, 2, 0, y) + 2592(-1 + y)^2y(-1 + z)^2z(y + z)^2(2 + 16y^4 - 4z + 3z^2 - z^3 + 5y^3(-9 + 4z) \\
& + y^2(47 - 45z + 16z^2) + y(-20 + 28z - 17z^2 + 4z^3))H(0, 2, 2, y) - 864(-1 + y)^2y(-1 + z)^2z(-1 + y + z)(y \\
& + z)^2(-4 + 8y^3 + 14z - 19z^2 + 8z^3 + y^2(-19 + 12z) + 2y(7 - 10z + 6z^2))H(0, 3, 2, y) - 1728(-1 + y)^2y(-1 \\
& + 4y)(-1 + z)^2z(-1 + y + z)(y + z)^2(2 + 2y^2 + 2y(-2 + z) - 2z + z^2)H(1, 0, 0, y) + 864(-1 + y)^2y(-1 + z)^2z(y \\
& + z)^2(2 + y^2(3 - 9z) - 4z + 3z^2 - z^3 + y^3(-1 + 4z) + y(-4 + 12z - 9z^2 + 4z^3))H(1, 0, 0, z) - 1728(-1 \\
& + y)^2y(-1 + z)^2z(y + z)^2(2 + 12y^4 - 4z + 3z^2 - z^3 + 2y^3(-17 + 8z) + 12y^2(3 - 3z + z^2) + y(-16 + 24z \\
& - 15z^2 + 4z^3))H(1, 0, 1, z) - 864(-1 + y)^2y(-1 + z)^2z(y + z)^2(2 + 24y^4 - 4z + 3z^2 - z^3 + y^3(-67 + 28z) \\
& + 3y^2(23 - 21z + 8z^2) + y(-28 + 36z - 21z^2 + 4z^3))H(1, 0, 2, y) + 864(-1 + y)^2y(-1 + z)^2z(y + z)^2(2 + y^2(3 \\
& - 9z) - 4z + 3z^2 - z^3 + y^3(-1 + 4z) + y(-4 + 12z - 9z^2 + 4z^3))H(1, 1, 0, z) - 216(-1 + y)^2y(-1 + z)^2z(y \\
& + z)^2(156 + 1336y^4 - 1670z + 4323z^2 - 4145z^3 + 1336z^4 + y^3(-4145 + 3132z) + y^2(4323 - 7017z + 4200z^2) + y(-1670 \\
& + 5136z - 7017z^2 + 3132z^3))H(1, 1, 1, z) - 864(-1 + y)^2y(-1 + z)^2z(y + z)^2(2 + 24y^4 - 4z + 3z^2 - z^3 + y^3(-67 \\
& + 28z) + 3y^2(23 - 21z + 8z^2) + y(-28 + 36z - 21z^2 + 4z^3))H(1, 2, 0, y) + 864(-1 + y)^2y(-1 + z)^2z(y \\
& + z)^2(16y^4 + y^3(-53 + 36z) + 3y^2(21 - 27z + 8z^2) - 3(-2 + 4z - 3z^2 + z^3) + y(-32 + 60z - 39z^2 \\
& + 12z^3))H(2, 0, 0, y) + 2592(-1 + y)^2y(-1 + z)^2z(y + z)^2(2 + 16y^4 - 4z + 3z^2 - z^3 + 5y^3(-9 + 4z) + y^2(47 \\
& - 45z + 16z^2) + y(-20 + 28z - 17z^2 + 4z^3))H(2, 0, 2, y) - 864(-1 + y)^2y(-1 + z)^2z(y + z)^2(2 + 24y^4 - 4z \\
& + 3z^2 - z^3 + y^3(-67 + 28z) + 3y^2(23 - 21z + 8z^2) + y(-28 + 36z - 21z^2 + 4z^3))H(2, 1, 0, y) + 2592(-1 \\
& + y)^2y(-1 + z)^2z(y + z)^2(2 + 16y^4 - 4z + 3z^2 - z^3 + 5y^3(-9 + 4z) + y^2(47 - 45z + 16z^2) + y(-20 + 28z \\
& - 17z^2 + 4z^3))H(2, 2, 0, y) - 216(-1 + y)^2y(-1 + z)^2z(y + z)^2(156 + 1336y^4 - 1670z + 4323z^2 - 4145z^3 \\
& + 1336z^4 + y^3(-4145 + 3132z) + y^2(4323 - 7017z + 4200z^2) + y(-1670 + 5136z - 7017z^2 + 3132z^3))H(2, 2, 2, y)
\end{aligned}$$

$$\begin{aligned}
& -1728(-1+y)^2y(-1+z)^2z(y+z)^2(4+12y^4-20z+39z^2-35z^3+12z^4+5y^3(-7+4z)+3y^2(13-17z \\
& +8z^2)+y(-20+48z-51z^2+20z^3))H(2,3,2,y)-864(-1+y)^2y(-1+z)^2z(-1+y+z)(y+z)^2(-4+8y^3 \\
& +14z-19z^2+8z^3+y^2(-19+12z)+2y(7-10z+6z^2))H(3,0,2,y)-864(-1+y)^2y(-1+z)^2z(-1+y+z)(y \\
& +z)^2(-4+8y^3+14z-19z^2+8z^3+y^2(-19+12z)+2y(7-10z+6z^2))H(3,2,0,y)-3456(-1+y)^2y(-1 \\
& +z)^2z(y+z)^2(4+12y^4-20z+39z^2-35z^3+12z^4+5y^3(-7+4z)+3y^2(13-17z+8z^2)+y(-20+48z \\
& -51z^2+20z^3))H(3,2,2,y) \Big\} \Big/ \Big(864(-1+y)^2y^2(-1+z)^2z^2(-1+y+z)(y+z)^2 \Big);
\end{aligned}$$

$$\begin{aligned}
\mathcal{A}_{3;CA}^{(2)} n_f = & \Big\{ -8(-1+y)(-1+z)(y+z)(103y^6(-1+4z)+6y^5(47-272z+170z^2)+z^3(206-385z+282z^2-103z^3)+y^4(-385 \\
& +2703z-4017z^2+1000z^3)+3y^2z(206-1022z+1843z^2-1339z^3+340z^4)+yz^2(618-2620z+2703z^2-1632z^3 \\
& +412z^4)+y^3(206-2620z+5529z^2-4976z^3+1000z^4))+9(-1+y)(-1+z)(y+z)^4(-56+72y^4+529z-1569z^2 \\
& +1834z^3-744z^4-4y^3(31+12z)-3y^2(5-182z+216z^2)+y(105-1020z+2160z^2-1336z^3))H(0,y)^2-216(-1 \\
& +y)(-1+z)z(-1+y+z)(y+z)^4(3-12z+10z^2+y(-3+6z))H(0,y)^3-9(-1+y)(-1+z)(y+z)^4(56+744y^4 \\
& -105z+15z^2+124z^3-72z^4+2y^3(-917+668z)+3y^2(523-720z+216z^2)+y(-529+1020z-546z^2 \\
& +48z^3))H(0,z)^2-216(-1+y)y(3+10y^2+6y(-2+z)-3z)(-1+z)(-1+y+z)(y+z)^4H(0,z)^3+1080(-1+y)(-1 \\
& +z)(-1+y+z)(y+z)^4(10y^3+6y^2(-2+z)+y(3-6z+6z^2)+z(3-12z+10z^2))H(1,z)^3-72(-1+y)(-1 \\
& +z)(358y^8+14y^7(-63+152z)+y^6(732-4821z+5640z^2)+y^5(-223+3798z-11757z^2+9136z^3)+z^4(14-223z \\
& +732z^2-882z^3+358z^4)+yz^3(128-1175z+3798z^2-4821z^3+2128z^4)+2y^3z(64-1109z+5394z^2-8670z^3 \\
& +4568z^4)+y^2z^2(84-2218z+8460z^2-11757z^3+5640z^4)+y^4(14-1175z+8460z^2-17340z^3 \\
& +10532z^4))H(2,y)^2+1080(-1+y)(-1+z)(-1+y+z)(y+z)^4(10y^3+6y^2(-2+z)+y(3-6z+6z^2)+z(3-12z \\
& +10z^2))H(2,y)^3+H(0,y)(18(-1+z)(y+z)^4(y^4(-31+220z)+y^3(124-607z+96z^2)+31(-2+4z-3z^2+z^3) \\
& -31y(-6+16z-12z^2+5z^3)+y^2(-217+759z-387z^2+124z^3))+216(-1+y)(-1+z)(y+z)^4(2+y^2(3-9z) \\
& -4z+3z^2-z^3+y^3(-1+4z)+y(-4+12z-9z^2+4z^3))H(0,z)+216(-1+y)(-1+z)(y+z)^4(2+16y^4-4z \\
& +3z^2-z^3+2y^3(-21+8z)+6y^2(7-6z+2z^2)+y(-18+24z-15z^2+4z^3))H(1,z)+288(-1+y)y(-1 \\
& +z)(-5y^3+3y^4+yz^2+y^2(6+z-6z^2)+z^2(6-5z+3z^2))H(2,y))+H(1,z)^2(-72(-1+y)(-1+z)(358y^8 \\
& +14y^7(-63+152z)+y^6(732-4821z+5640z^2)+y^5(-223+3798z-11757z^2+9136z^3)+z^4(14-223z+732z^2 \\
& -882z^3+358z^4)+yz^3(128-1175z+3798z^2-4821z^3+2128z^4)+2y^3z(64-1109z+5394z^2-8670z^3+4568z^4) \\
& +y^2z^2(84-2218z+8460z^2-11757z^3+5640z^4)+y^4(14-1175z+8460z^2-17340z^3+10532z^4))+3240(-1+y)(-1 \\
& +z)(-1+y+z)(y+z)^4(10y^3+6y^2(-2+z)+y(3-6z+6z^2)+z(3-12z+10z^2))H(2,y))+H(0,z)(18(-1+y)(y \\
& +z)^4(-31(-1+z)^2(2-2z+z^2)+31y^3(1-5z+4z^2)+y^2(-93+372z-387z^2+96z^3)+y(124-496z+759z^2 \\
& -607z^3+220z^4))+288(-1+y)y(-1+z)z(-5y^3+3y^4+yz^2+y^2(6+z-6z^2)+z^2(6-5z+3z^2))H(1,z) \\
& +216(-1+y)(-1+z)(y+z)^4(y^3(-1+4z)+4y(-1+z)^2(-1+4z)+3y^2(1-5z+4z^2)+2(1-9z+21z^2-21z^3 \\
& +8z^4))H(2,y))-18(-1+y)(-1+z)(y+z)^4(-56+72y^4+529z-1569z^2+1834z^3-744z^4-4y^3(31+12z) \\
& -3y^2(5-18z+216z^2)+y(105-1020z+2160z^2-1336z^3))H(0,0,y)+18(-1+y)(-1+z)(y+z)^4(56+744y^4 \\
& -105z+15z^2+124z^3-72z^4+2y^3(-917+668z)+3y^2(523-720z+216z^2)+y(-529+1020z-546z^2 \\
& +48z^3))H(0,0,z)-72(-1+y)(-1+z)(48y^8+6y^7(-21+40z)+6y^6(21-102z+86z^2)-3z^4(-2+4z-3z^2 \\
& +z^3)+3y^5(-18+196z-411z^2+212z^3)+yz^3(48-122z+120z^2-57z^3+12z^4)+2y^2z^2(18-142z+234z^2 \\
& -153z^3+42z^4)+4y^3z(12-92z+237z^2-210z^3+66z^4)+y^4(6-248z+1053z^2-1335z^3+504z^4))H(0,1,z) \\
& +72(-1+y)(-1+z)(48y^8+6y^7(-21+40z)+6y^6(21-102z+86z^2)-3z^4(-2+4z-3z^2+z^3)+yz^4(-82 \\
& +96z-57z^2+12z^3)+4y^3z^2(-94+249z-210z^2+66z^3)+3y^5(-18+188z-411z^2+212z^3)+2y^2z^2(18 \\
& -146z+234z^2-153z^3+42z^4)+y^4(6-208z+1053z^2-1335z^3+504z^4))H(0,2,y)-216(-1+y)y(-1+z)(y \\
& +z)^4(16y^3+y^2(-41+12z)-2(7-6z+3z^2)+3y(13-9z+4z^2))H(1,0,y)+72(-1+y)(-1+z)(3y^7(-1+4z) \\
& +y^6(9-39z+48z^2)-3z^4(-2+4z-3z^2+z^3)+yz^4(-40+60z-39z^2+12z^3)+3y^5(-4+20z-51z^2 \\
& +28z^3)+y^3z^2(-124+312z-285z^2+84z^3)+y^2z^2(36-124z+207z^2-153z^3+48z^4)+y^4(6-40z+207z^2 \\
& -285z^3+96z^4))H(1,0,z)+144(-1+y)(-1+z)(358y^8+14y^7(-63+152z)+y^6(732-4821z+5640z^2)+y^5(-223 \\
& +3798z-11757z^2+9136z^3)+z^4(14-223z+732z^2-882z^3+358z^4)+yz^3(128-1175z+3798z^2-4821z^3 \\
& +2128z^4)+2y^3z(64-1109z+5394z^2-8670z^3+4568z^4)+y^2z^2(84-2218z+8460z^2-11757z^3+5640z^4) \\
& +y^4(14-1175z+8460z^2-17340z^3+10532z^4))H(1,1,z)+H(2,y)(36(-1+y)(-1+z)(y^7(-9+84z)+3y^6(9-83z \\
& +144z^2)-9z^4(-2+4z-3z^2+z^3)+3y^5(-12+70z-373z^2+324z^3))+yz^3(-168-26z+210z^2-249z^3 \\
& +84z^4)+y^2z^2(-60-314z+1053z^2-1119z^3+432z^4)+y^3z(-168-314z+1740z^2-2175z^3+972z^4)+y^4(18
\end{aligned}$$

$$\begin{aligned}
& -26z + 1053z^2 - 2175z^3 + 1248z^4)) - 6480(-1+y)(-1+z)(-1+y+z)(y+z)^4(10y^3 + 6y^2(-2+z) + y(3-6z \\
& + 6z^2) + z(3-12z+10z^2))H(1,1,z)) + 72(-1+y)(-1+z)(48y^8 + 6y^7(-21+40z) + 6y^6(21-102z+86z^2) \\
& - 3z^4(-2+4z-3z^2+z^3) + yz^4(-82+96z-57z^2+12z^3) + 4y^3z^2(-94+249z-210z^2+66z^3) + 3y^5(-18 \\
& + 188z-411z^2+212z^3) + 2y^2z^2(18-146z+234z^2-153z^3+42z^4) + y^4(6-208z+1053z^2-1335z^3 \\
& + 504z^4))H(2,0,y) + 144(-1+y)(-1+z)(358y^8 + 14y^7(-63+152z) + y^6(732-4821z+5640z^2) + y^5(-223+3798z \\
& - 11757z^2+9136z^3) + z^4(14-223z+732z^2-882z^3+358z^4) + yz^3(128-1175z+3798z^2-4821z^3+2128z^4) \\
& + 2y^3z(64-1109z+5394z^2-8670z^3+4568z^4) + y^2z^2(84-2218z+8460z^2-11757z^3+5640z^4) + y^4(14-1175z \\
& + 8460z^2-17340z^3+10532z^4))H(2,2,y) + H(1,z)(36(-1+y)(-1+z)(y^7(-9+84z) + 3y^6(9-83z+144z^2) \\
& - 9z^4(-2+4z-3z^2+z^3) + 3y^5(-12+70z-373z^2+324z^3) + yz^3(-168-26z+210z^2-249z^3+84z^4) \\
& + y^2z^2(-60-314z+1053z^2-1119z^3+432z^4) + y^3z(-168-314z+1740z^2-2175z^3+972z^4) + y^4(18-26z \\
& + 1053z^2-2175z^3+1248z^4)) + 3240(-1+y)(-1+z)(-1+y+z)(y+z)^4(10y^3 + 6y^2(-2+z) + y(3-6z+6z^2) \\
& + z(3-12z+10z^2))H(2,y)^2 - 216(-1+y)(-1+z)(y+z)^4(4+16y^4-22z+45z^2-43z^3+16z^4+y^3(-43+20z) \\
& + 3y^2(15-17z+8z^2) + y(-22+48z-51z^2+20z^3))H(3,y) - 6480(-1+y)(-1+z)(-1+y+z)(y+z)^4(4+16y^4-22z \\
& + 45z^2-43z^3+16z^4+y^3(-43+20z) + 3y^2(15-17z+8z^2) + y(-22+48z-51z^2+20z^3))H(3,2,y) + 1296(-1 \\
& + y)(-1+z)(-1+y+z)(y+z)^4(3-12z+10z^2+y(-3+6z))H(0,0,0,y) + 1296(-1+y)y(3+10y^2+6y(-2+z) \\
& - 3z)(-1+y)(-1+y+z)(y+z)^4H(0,0,0,z) - 6480(-1+y)(-1+z)(-1+y+z)(y+z)^4(10y^3 + 6y^2(-2+z) + y(3 \\
& - 6z+6z^2) + z(3-12z+10z^2))H(1,1,z) - 6480(-1+y)(-1+z)(-1+y+z)(y+z)^4(10y^3 + 6y^2(-2+z) + y(3 \\
& - 6z+6z^2) + z(3-12z+10z^2))H(2,2,2,y) \Big\} / \Big(864(-1+y)(-1+z)(-1+y+z)(y+z)^4 \Big);
\end{aligned}$$

$$\begin{aligned}
\mathcal{A}_{3;C_F n_f}^{(2)} = & \Big\{ (-1+y)(-1+z)((-1+z)^2z^2(490-463z+245z^2) + y^6(245-982z+656z^2) + y^5(-953+4142z-4366z^2 \\
& + 1096z^3) + y^4(1661-8739z+14467z^2-8188z^3+880z^4) + yz(980-4869z+9468z^2-8739z^3+4142z^4-982z^5) \\
& + y^3(-1443+9468z-21992z^2+21140z^3-8188z^4+1096z^5) + y^2(490-4869z+15614z^2-21992z^3+14467z^4 \\
& - 4366z^5+656z^6)) + 9(-1+y)^2(-1+4y)(-1+z)^2(y+z)^2(-2+2y^3+4z-3z^2+z^3+y^2(-6+4z)+y(6-8z \\
& + 3z^2))H(0,y)^2 - 9(1-y)(-1+y)(y^3+3y^2(-1+z)+4y(-1+z)^2+2(-1+z)^3)(-1+z)^2(y+z)^2(-1 \\
& + 4z)H(0,z)^2 + 63(1-y)(-1+z)^2(y+z)^2(4+8y^4-18z+33z^2-27z^3+8z^4+y^3(-27+20z)+3y^2(11 \\
& - 17z+8z^2)+y(-18+48z-51z^2+20z^3))H(1,z)^2 + H(0,y)(-27y(-1+z)^2z(-1+y+z)(y+z)^2(8y^3+y(30 \\
& - 27z)+12(-1+z)+2y^2(-13+6z))-54(-1+y)^2(-1+4y)(-1+z)^2(-1+y+z)(y+z)^2(2+2y^2+2y(-2+z) \\
& - 2z+z^2)H(1,z))+27(1-y)(-1+y)(-1+z)^2(y^5(-3+20z)+y^4(9-73z+80z^2)-3z^2(-2+4z-3z^2+z^3) \\
& + 6y^3(-2+15z-34z^2+20z^3)+yz(-8-32z+90z^2-73z^3+20z^4)+2y^2(3-16z+81z^2-102z^3 \\
& + 40z^4))H(2,y) + 63(1-y)(-1+y)(-1+z)^2(y+z)^2(4+8y^4-18z+33z^2-27z^3+8z^4+y^3(-27+20z) \\
& + 3y^2(11-17z+8z^2)+y(-18+48z-51z^2+20z^3))H(2,y)^2 + H(0,z)(-27(-1+y)^2yz(-1+y+z)(y+z)^2(-12 \\
& + 30z-26z^2+8z^3+3y(4-9z+4z^2))-54(-1+y)^2(y^2+2y(-1+z)+2(-1+z)^2)(-1+z)^2(-1+y+z)(y \\
& + z)^2(-1+4z)H(2,y))+H(1,z)(27(1-y)(-1+y)(-1+z)^2(-1+y+z)(y^4(-3+20z)-3z^2(2-2z+z^2)+y^3(6 \\
& - 50z+60z^2)+2yz(4+17z-25z^2+10z^3)+y^2(-6+34z-94z^2+60z^3))+54(-1+y)^2(-1+z)^2(-1+y+z)(y \\
& + z)^2(-4+8y^3+14z-19z^2+8z^3+y^2(-19+12z)+2y(7-10z+6z^2))H(3,y))+18(1-y)(1-5y+4y^2)(-1 \\
& + z)^2(y+z)(2y^4+6y^3(-1+z)+y^2(6-14z+7z^2)+z(-2+4z-3z^2+z^3)+y(-2+10z-11z^2) \\
& + 4z^3))H(0,0,y) + 18(1-y)(-1+y)(-1+z)(y+z)(1-5z+4z^2)(y^4+2(-1+z)^3z+2y(-1+z)^2(-1+3z) \\
& + y^3(-3+4z)+y^2(4-11z+7z^2))H(0,0,z) + 54(-1+y)^2(-1+4y)(-1+z)^2(y+z)^2(-2+2y^3+4z-3z^2+z^3) \\
& + y^2(-6+4z)+y(6-8z+3z^2))H(0,1,z) - 54(-1+y)^2(-1+4y)(-1+z)^2(y+z)^2(-2+2y^3+4z-3z^2+z^3) \\
& + y^2(-6+4z)+y(6-8z+3z^2))H(0,2,y) + 54(-1+y)^2(-1+4y)(-1+z)^2(y+z)^2(-2+2y^3+4z-3z^2+z^3) \\
& + y^2(-6+4z)+y(6-8z+3z^2))H(1,0,y) + 126(-1+y)^2(-1+z)^2(y+z)^2(4+8y^4-18z+33z^2-27z^3+8z^4 \\
& + y^3(-27+20z)+3y^2(11-17z+8z^2)+y(-18+48z-51z^2+20z^3))H(1,1,z) - 54(-1+y)^2(-1+4y)(-1+z)^2(y \\
& + z)^2(-2+2y^3+4z-3z^2+z^3+y^2(-6+4z)+y(6-8z+3z^2))H(2,0,y) + 126(-1+y)^2(-1+z)^2(y+z)^2(4 \\
& + 8y^4-18z+33z^2-27z^3+8z^4+y^3(-27+20z)+3y^2(11-17z+8z^2)+y(-18+48z-51z^2+20z^3))H(2,2,y) \\
& + 54(-1+y)^2(-1+z)^2(y+z)^2(4+8y^4-18z+33z^2-27z^3+8z^4+y^3(-27+20z)+3y^2(11-17z+8z^2) \\
& + y(-18+48z-51z^2+20z^3))H(3,2,y) \Big\} / \Big(108(-1+y)^2y(-1+z)^2z(-1+y+z)(y+z)^2 \Big);
\end{aligned}$$

$$\mathcal{A}_{4;C_A^2}^{(2)} = \frac{39}{20}\mathcal{A}_0; \quad \mathcal{A}_{4;C_F^2}^{(2)} = -\frac{44}{5}\mathcal{A}_0; \quad \mathcal{A}_{4;n_f^2}^{(2)} = 0; \quad \mathcal{A}_{4;C_A C_F}^{(2)} = \frac{93}{10}\mathcal{A}_0; \quad \mathcal{A}_{4;C_A n_f}^{(2)} = 0; \quad \mathcal{A}_{4;C_F n_f}^{(2)} = 0;$$

$$\begin{aligned}
\mathcal{A}_{5;C_A^2}^{(2)} &= \left\{ 6048y^9z + (-1+z)^5(814 - 814z + 83z^2) + 216y^8z(-177 + 74z - 12z^2 + 3z^3) + y(-1+z)^4(4884 - 4916z - 10029z^2 \right. \\
&\quad + 20360z^3 - 14040z^4 + 6048z^5) + y^7(83 + 112808z - 124552z^2 + 79000z^3 - 39863z^4 + 8812z^5) + y^2(-1+z)^3(12293 \\
&\quad - 2060z - 65043z^2 + 119980z^3 - 76600z^4 + 15984z^5) - y^3(-1+z)^2(-16695 - 44834z + 223663z^2 - 364320z^3 + 263636z^4 \\
&\quad - 73816z^5 + 2592z^6) + y^6(-1229 - 199901z + 397732z^2 - 413860z^3 + 281873z^4 - 103639z^5 + 14832z^6) + y^5(5714 \\
&\quad + 219568z - 670767z^2 + 965408z^3 - 836204z^4 + 417156z^5 - 103639z^6 + 8812z^7) + y^4(-13040 - 131106z + 629609z^2 \\
&\quad - 1215939z^3 + 1324022z^4 - 836204z^5 + 281873z^6 - 39863z^7 + 648z^8) + 36(-1+y)^4(-1+z)^4(2 + y^2(3 - 9z) - 4z \\
&\quad + 3z^2 - z^3 + y^3(-1 + 4z) + y(-4 + 12z - 9z^2 + 4z^3))H(0, y) + 36(-1+y)^4(-1+z)^4(2 + y^2(3 - 9z) - 4z + 3z^2 \\
&\quad - z^3 + y^3(-1 + 4z) + y(-4 + 12z - 9z^2 + 4z^3))H(0, z) - 36(-1+y)^4(-1+z)^4(220y^4 + y^3(-443 + 324z) + 3y^2(81 \\
&\quad - 117z + 32z^2) + y(-8 + 24z + 6z^2 - 24z^3) + 6(-2 + 4z - 3z^2 + z^3))H(1, y) + 36(-1+y)^4(-1+z)^4(220y^4 \\
&\quad + 4y^3(-111 + 82z) + 6y^2(41 - 60z + 16z^2) + 5(-2 + 4z - 3z^2 + z^3) - y(12 - 36z + 3z^2 + 20z^3))H(1, z) + 72(-1 \\
&\quad + y)^4(-1+z)^4(-11 + 110y^4 + 6z + 114z^2 - 219z^3 + 110z^4 + y^3(-219 + 152z) + 3y^2(38 - 59z + 32z^2) + y(6 + 30z \\
&\quad - 177z^2 + 152z^3))H(2, y) \Big\} / \left(144(-1+y)^4y(-1+z)^4z(-1+y+z) \right); \\
\mathcal{A}_{5;C_F^2}^{(2)} &= \left\{ -432y^9z - 6(-1+z)^5(31 - 30z + 20z^2) - 12y^8z(-261 + 147z - 40z^2 + 10z^3) - 6y(-1+z)^4(185 - 354z + 224z^2 \right. \\
&\quad + 102z^3 - 234z^4 + 72z^5) + y^7(-120 - 8820z + 8139z^2 - 1414z^3 - 733z^4 + 356z^5) - 3y^2(-1+z)^3(960 - 2620z \\
&\quad + 2922z^2 - 754z^3 - 949z^4 + 588z^5) + y^3(-1+z)^2(-4260 + 13428z - 23904z^2 + 19624z^3 - 6031z^4 - 454z^5 + 480z^6) \\
&\quad + y^6(780 + 11256z - 11571z^2 - 4643z^3 + 9499z^4 - 4121z^5 + 528z^6) + y^5(-2286 - 2220z - 5247z^2 + 31232z^3 - 36206z^4 \\
&\quad + 18060z^5 - 4121z^6 + 356z^7) + y^4(3930 - 13818z + 38097z^2 - 69183z^3 + 68534z^4 - 36206z^5 + 9499z^6 - 733z^7 \\
&\quad - 120z^8) - 12(-1+y)^4(-1+z)^4(14y^4 + 6y^2(-3 + z)z + y^3(-23 + 28z) + y(13 - 18z + 15z^2 - 8z^3) + 2(-2 + 4z \\
&\quad - 3z^2 + z^3))H(1, y) + 12(-1+y)^4(-1+z)^4(2 + 14y^4 - 4z + 3z^2 - z^3 + y^3(-26 + 40z) + y^2(9 - 45z + 6z^2) + y(1 \\
&\quad + 18z - 12z^2 + 4z^3))H(1, z) + 12(-1+y)^4(-1+z)^4(-2 + 14y^4 + 9z + 3z^2 - 24z^3 + 14z^4 + 8y^3(-3 + 4z) \\
&\quad + 3y^2(1 - 10z + 4z^2) + y(9 - 30z^2 + 32z^3))H(2, y) \Big\} / \left(6(-1+y)^4y(-1+z)^4z(-1+y+z) \right); \\
\mathcal{A}_{5;n_f^2}^{(2)} &= 0; \\
\mathcal{A}_{5;C_A C_F}^{(2)} &= \left\{ 3456y^9z + (-1+z)^5(2470 - 2290z + 1613z^2) + 72y^8z(-351 + 207z - 64z^2 + 16z^3) + y^7(1613 + 64136z - 47008z^2 \right. \\
&\quad - 12968z^3 + 21871z^4 - 6908z^5) + y(-1+z)^4(14640 - 32276z + 25053z^2 - 2392z^3 - 11448z^4 + 3456z^5) + y^2(-1 \\
&\quad + z)^3(37763 - 128708z + 163755z^2 - 83348z^3 - 2296z^4 + 14904z^5) - y^3(-1+z)^2(-55665 + 243490z - 455855z^2 \\
&\quad + 399648z^3 - 166612z^4 + 22184z^5 + 4608z^6) - y^6(10355 + 47891z + 31748z^2 - 206372z^3 + 191809z^4 - 69095z^5 \\
&\quad + 7488z^6) + y^5(30050 - 97592z + 392007z^2 - 755056z^3 + 679888z^4 - 308028z^5 + 69095z^6 - 6908z^7) + y^4(-51380 \\
&\quad + 292182z - 867721z^2 + 1421763z^3 - 1305946z^4 + 679888z^5 - 191809z^6 + 21871z^7 + 1152z^8) + 36(-1+y)^4(-1 \\
&\quad + z)^4(64y^4 + 18y^2z(-5 + 2z) + 4y^3(-27 + 34z) + y(66 - 96z + 81z^2 - 44z^3) + 11(-2 + 4z - 3z^2 + z^3))H(1, y) \\
&\quad - 36(-1+y)^4(-1+z)^4(4 + 64y^4 - 8z + 6z^2 - 2z^3 + y^3(-121 + 188z) + 3y^2(13 - 69z + 12z^2) + 2y(7 + 30z \\
&\quad - 18z^2 + 4z^3))H(1, z) - 72(-1+y)^4(-1+z)^4(-9 + 32y^4 + 29z + 3z^2 - 55z^3 + 32z^4 + y^3(-55 + 72z) + y^2(3 - 63z \\
&\quad + 36z^2) + y(29 - 18z - 63z^2 + 72z^3))H(2, y) \Big\} / \left(72(-1+y)^4y(-1+z)^4z(-1+y+z) \right); \\
\mathcal{A}_{5;C_A n_f}^{(2)} &= \left\{ -1296y^9z - 37(-1+z)^5(2 - 2z + z^2) - 18y^8z(-459 + 177z - 8z^2 + 2z^3) - y^7(37 + 23464z - 21866z^2 + 9620z^3 \right. \\
&\quad - 4555z^4 + 1076z^5) - y(-1+z)^4(444 - 388z - 1653z^2 + 3376z^3 - 3078z^4 + 1296z^5) - y^2(-1+z)^3(1147 + 878z \\
&\quad - 10719z^2 + 18518z^3 - 12308z^4 + 3186z^5) + y^6(259 + 38809z - 65000z^2 + 56576z^3 - 38287z^4 + 15203z^5 - 2376z^6) \\
&\quad + y^3(-1+z)^2(-1665 - 9214z + 35399z^2 - 55404z^3 + 37768z^4 - 9332z^5 + 144z^6) - y^5(814 + 40088z - 106383z^2 \\
&\quad + 140272z^3 - 121660z^4 + 62292z^5 - 15203z^6 + 1076z^7) + y^4(1480 + 24504z - 100897z^2 + 183975z^3 - 196954z^4 \\
&\quad + 121660z^5 - 38287z^6 + 4555z^7 - 36z^8) + 108(-1+y)^4y(-1+z)^4(10y^3 - 3(-1+z)^2 + 2y^2(-11 + 8z) + 3y(5 - 7z \\
&\quad + 2z^2))H(1, y) - 108(-1+y)^4y(-1+z)^4(10y^3 - 3(-1+z)^2 + 2y^2(-11 + 8z) + 3y(5 - 7z + 2z^2))H(1, z) - 108(-1 \\
&\quad + y)^4(-1+z)^4(-1 + y + z)(10y^3 + 6y^2(-2 + z) + y(3 - 6z + 6z^2) + z(3 - 12z + 10z^2))H(2, y) \Big\} / \left(72(-1+y)^4y(-1 \right. \\
&\quad \left. + z)^4z(-1+y+z) \right); \\
\mathcal{A}_{5;C_F n_f}^{(2)} &= -\frac{1}{9}\mathcal{A}_0;
\end{aligned}$$

$$\begin{aligned}
\mathcal{A}_{6;C_A^2}^{(2)} = & \left\{ 8(-1+y)(-1+z)(y+z)(-1008y^{12}z + 4(-1+z)^4z^5(10-z+5z^2) + 4y^{11}(5+622z-51z^2-1631z^3+551z^4) \right. \\
& - y(-1+z)^3z^4(200-96z+1182z^2-2503z^3+536z^4+1008z^5) + y^{10}(-84+1087z-12868z^2+50961z^3-50902z^4 \\
& + 13822z^5) - y^2(-1+z)^2z^3(-400+3298z-10431z^2+24380z^3-31260z^4+13276z^5+204z^6) + y^9(176-9291z \\
& + 57608z^2-186114z^3+279822z^4-174455z^5+38302z^6) + y^8(-264+11687z-100176z^2+374314z^3-739622z^4 \\
& + 736539z^5-343702z^6+61224z^7) + y^7(276-6537z+90451z^2-436329z^3+1100987z^4-1543684z^5+1154814z^6 \\
& - 427250z^7+61224z^8) + y^3z^2(400-4252z+32055z^2-129393z^3+304882z^4-436329z^5+374314z^6-186114z^7 \\
& + 50961z^8-6524z^9) + 2y^6(-82+1035z-24270z^2+152441z^3-484929z^4+903470z^5-973380z^6+577407z^7 \\
& - 171851z^8+19151z^9) + y^4z(200-4098z+32055z^2-165612z^3+515832z^4-969858z^5+1100987z^6-739622z^7 \\
& + 279822z^8-50902z^9+2204z^{10}) + y^5(40-696z+17427z^2-129393z^3+515832z^4-1240356z^5+1806940z^6 \\
& - 1543684z^7+736539z^8-174455z^9+13822z^{10})) - 9(-1+y)^4(-1+z)^4(y+z)^6(496y^4+y^3(-1129+1244z) \\
& + 3y^2(213-557z+284z^2) + y(62+444z-870z^2+416z^3) + 4(-17-46z+234z^2-301z^3+130z^4))H(0,y)^2 \\
& - 9(-1+y)^4(-1+z)^4(y+z)^6(-68+520y^4+62z+639z^2-1129z^3+496z^4+y^3(-301+104z) + y^2(936-870z \\
& + 852z^2) + y(-184+444z-1671z^2+1244z^3))H(0,z)^2 + 9(-1+y)^4(-1+z)^4(y+z)^6(-104+992y^4+246z+861z^2 \\
& - 1995z^3+992z^4+5y^3(-399+436z) + 3y^2(287-881z+440z^2) + y(246+696z-2643z^2+2180z^3))H(1,z)^2 \\
& + H(1,y)(-48(-1+y)^3(-1+z)^4(y+z)^6(-98+160y^5+247z-279z^2+96z^3+y^4(-697+232z)+y^3(1221-871z \\
& + 318z^2) + y(503-856z+768z^2-192z^3) + 3y^2(-363+416z-270z^2+32z^3)) + 144(-1+y)^4(-1+z)^4(y \\
& + z)^6(84y^4+y^3(-193+76z) + 3y^2(51-39z+16z^2) + 2(-2+4z-3z^2+z^3) - 2y(20-12z+3z^2 \\
& + 4z^3))H(1,z) - 12(672y^{15}z - (-1+z)^5z^6(-306+1094z-1417z^2+640z^3) - 8y^{14}(80+211z-246z^2-284z^3 \\
& + 71z^4) - 3y^{13}(-1539+3624z-2740z^2+6256z^3-6117z^4+1188z^5) + y^{12}(-14579+71063z-127704z^2+152312z^3 \\
& - 144029z^4+67593z^5-10032z^6) + y(-1+z)^4z^5(-1644+10824z-23462z^2+24135z^3-10904z^4+1000z^5+672z^6) \\
& + 6y^2(-1+z)^3z^4(947-7217z+22516z^2-36737z^3+33102z^4-15206z^5+2354z^6+328z^7) - 2y^{11}(-13173+94377z \\
& - 256362z^2+378172z^3-374314z^4+238281z^5-76309z^6+8656z^7) - 2y^{10}(14920-147049z+552045z^2-1083308z^3 \\
& + 1307983z^4-1034540z^5+496204z^6-121179z^7+10892z^8) + y^9(21725-293156z+1483434z^2-3858986z^3+5967465z^4 \\
& - 5942620z^5+3826296z^6-1476766z^7+296968z^8-23016z^9) + 2y^3(-1+z)^2z^3(-3384+44062z-198605z^2+462415z^3 \\
& - 632873z^4+523576z^5-249468z^6+60796z^7-7112z^8+1136z^9) + y^8(-9947+189503z-1308468z^2+4503474z^3 \\
& - 8996757z^4+11383863z^5-9480686z^6+5112368z^7-1673910z^8+296968z^9-21784z^{10}) - 2y^7(-1312+38311z \\
& - 380649z^2+1756308z^3-4551510z^4+7339866z^5-7783882z^6+5514200z^7-2556184z^8+738383z^9-121179z^{10} \\
& + 8656z^{11}) + y^5z(-1644+60348z-580226z^2+2711300z^3-7384344z^4+12777180z^5-14679732z^6+11383863z^7 \\
& - 5942620z^8+2069080z^9-476562z^{10}+67593z^{11}-3564z^{12}) + y^4z^2(-5682+101660z-722026z^2+2711300z^3 \\
& - 6165396z^4+910320z^5-8996757z^6+5967465z^7-2615966z^8+748628z^9-144029z^{10}+18351z^{11}-568z^{12}) \\
& - 2y^6(153-8700z+141024z^2-903687z^3+3082698z^4-6388590z^5+8608206z^6-7783882z^7+4740343z^8-1913148z^9 \\
& + 496204z^{10}-76309z^{11}+5016z^{12}))H(2,y) + 9(-1+y)^4(-1+z)^4(y+z)^6(-104+992y^4+246z+861z^2-1995z^3 \\
& + 992z^4+5y^3(-399+436z) + 3y^2(287-881z+440z^2) + y(246+696z-2643z^2+2180z^3))H(2,y)^2 + H(0,y)(-12(-1 \\
& + y)^3(y+z)^6(672y^6z+49(-1+z)^5(2-2z+z^2)+24y^5z(-93+74z-12z^2+3z^3)-y(-1+z)^4(-306+1096z \\
& - 1680z^2+1205z^3)+y^3(-1+z)^2(304-3453z+4062z^2-2983z^3+984z^4)+y^2(-1+z)^3(415-2620z+4200z^2 \\
& - 3661z^3+1156z^4)+y^4(-97+3488z-6112z^2+3784z^3-1283z^4+220z^5))-432(-1+y)^4(-1+z)^4(y+z)^6(2 \\
& + y^2(3-9z)-4z+3z^2-z^3+y^3(-1+4z)+y(-4+12z-9z^2+4z^3))H(0,z) + 144(-1+y)^4(-1+z)^4(y \\
& + z)^6(22y^3+4y^4-6y^2(10-9z+4z^2)+y(40-60z+39z^2-12z^3)+3(-2+4z-3z^2+z^3))H(1,z) + 144(-1 \\
& + y)^4(-1+z)^4(y+z)^6(2+y^2(3-9z)-4z+3z^2-z^3+y^3(-1+4z)+y(-4+12z-9z^2+4z^3))H(2,y) \\
& + H(0,z)(-12(-1+z)^3(y+z)^6(-((-1+z)^2(98-110z+97z^2))+y^7(49-1205z+1156z^2)+y^6(-343+6500z \\
& - 7129z^2+984z^3)+y^5(1078-15046z+18651z^2-4951z^3+220z^4)+y^3(2205-15725z+24536z^2-14560z^3+3784z^4 \\
& - 288z^5)+y^4(-1960+19590z-27359z^2+11012z^3-1283z^4+72z^5)+y^2(-1519+7900z-13305z^2+11272z^3 \\
& - 6112z^4+1776z^5)+y(588-2320z+3865z^2-4061z^3+3488z^4-2232z^5+672z^6))+144(-1+y)^4(-1+z)^4(y \\
& + z)^6(88y^4+y^3(-201+124z)+3y^2(49-57z+20z^2)+2(-2+4z-3z^2+z^3)-2y(15-18z+6z^2 \\
& + 4z^3))H(1,y) + 144(-1+y)^4(-1+z)^4(y+z)^6(2+y^2(3-9z)-4z+3z^2-z^3+y^3(-1+4z)+y(-4+12z-9z^2 \\
& + 4z^3))H(1,z) - 288(-1+y)^4(-1+z)^4(y+z)^6(44y^4+34y^3(-3+2z)-(-1+z)^2(-1+14z+2z^2)+3y^2(26 \\
& - 35z+14z^2)-y(21-48z+33z^2+4z^3))H(2,y)) + H(1,z)(-12(672y^{15}z - (-1+z)^5z^6(86-134z+91z^2) \\
& - 8y^{14}(80+211z-246z^2-284z^3+71z^4) - 3y^{13}(-1411+2984z-1460z^2+4976z^3-5477z^4+1060z^5) \\
& + y^{12}(-11927+54659z-85020z^2+92588z^3-96701z^4+47481z^5-6456z^6)+y(-1+z)^4z^5(708-1452z+1870z^2 \\
& - 2253z^3+2456z^4-1560z^5+672z^6) - 2y^{11}(-9295+64627z-158940z^2+201252z^3-181596z^4+112239z^5-30455z^6)
\end{aligned}$$

$$\begin{aligned}
& + 1496z^7) + 2y^2(-1+z)^3z^4(-99 + 1107z - 3248z^2 + 8087z^3 - 15336z^4 + 17678z^5 - 10838z^6 + 2904z^7) + 2y^{10}(-8632 \\
& + 86311z - 304059z^2 + 516984z^3 - 511401z^4 + 325416z^5 - 105440z^6 - 739z^7 + 5592z^8) - 2y^3(-1+z)^2z^3(-536 - 852z \\
& + 7455z^2 - 903z^3 - 46165z^4 + 106706z^5 - 114712z^6 + 62368z^7 - 14048z^8 + 144z^9) + 3y^9(3127 - 46340z + 231586z^2 \\
& - 539722z^3 + 671983z^4 - 471956z^5 + 148964z^6 + 36522z^7 - 42364z^8 + 8648z^9) + y^8(-2527 + 64339z - 489624z^2 \\
& + 1601594z^3 - 2644553z^4 + 2271207z^5 - 738570z^6 - 439680z^7 + 556890z^8 - 212212z^9 + 27760z^{10}) + 2y^7(34 - 6481z \\
& + 102519z^2 - 502456z^3 + 1134338z^4 - 1263358z^5 + 486190z^6 + 442468z^7 - 684158z^8 + 375311z^9 - 94127z^{10} + 8712z^{11}) \\
& + y^4z^2(198 + 2720z - 54406z^2 + 215036z^3 - 276280z^4 - 222736z^5 + 1183523z^6 - 1711791z^7 + 1308226z^8 - 546976z^9 \\
& + 107843z^{10} - 5429z^{11} + 72z^{12}) + y^5z(708 + 2880z - 75318z^2 + 390360z^3 - 862488z^4 + 683692z^5 + 668588z^6 \\
& - 2089833z^7 + 2146884z^8 - 1135548z^9 + 302226z^{10} - 32683z^{11} + 1204z^{12}) + 2y^6(43 - 562z - 22170z^2 + 191307z^3 \\
& - 617668z^4 + 934096z^5 - 486604z^6 - 520444z^7 + 1071647z^8 - 795420z^9 + 294048z^{10} - 50805z^{11} + 3204z^{12})) - 144(-1 \\
& + y)^4(-1+z)^4(y+z)^6(100y^4 + 2y^3(-127 + 60z) + 6y^2(38 - 41z + 24z^2) + z(-38 + 153z - 203z^2 + 88z^3) + y(-74 \\
& + 144z - 231z^2 + 132z^3))H(2, y) - 144(-1+y)^4(-1+z)^4(y+z)^6(-4 + 36y^4 - 4z + 51z^2 - 79z^3 + 36z^4 + y^3(-79 \\
& + 52z) + y^2(51 - 75z + 48z^2) + y(-4 + 24z - 75z^2 + 52z^3))H(3, y)) + 18(-1+y)^4(-1+z)^4(y+z)^6(496y^4 \\
& + y^3(-1129 + 1244z) + 3y^2(213 - 557z + 284z^2) + y(62 + 444z - 870z^2 + 416z^3) + 4(-17 - 46z + 234z^2 - 301z^3 \\
& + 130z^4))H(0, 0, y) + 18(-1+y)^4(-1+z)^4(y+z)^6(-68 + 520y^4 + 62z + 639z^2 - 1129z^3 + 496z^4 + 4y^3(-301 \\
& + 104z) + y^2(936 - 870z + 852z^2) + y(-184 + 444z - 1671z^2 + 1244z^3))H(0, 0, z) - 288(-1+y)^4(-1+z)^4(y+z)^6(2 \\
& + 10y^4 - 4z + 3z^2 - z^3 + 7y^3(-3 + 4z) + 6y^2(2 - 6z + z^2) + y(-3 + 18z - 12z^2 + 4z^3))H(0, 1, z) + 144(-1 \\
& + y)^4(-1+z)^4(y+z)^6(-8 + 36y^4 + 2z + 27z^2 - 37z^3 + 16z^4 + 11y^3(-7 + 4z) + y^2(45 - 51z + 36z^2) - y(-4 \\
& + 12z + 3z^2 + 4z^3))H(0, 2, y) - 144(-1+y)^4y(-1+z)^4(y+z)^6(4y^3 + y^2(19 + 12z) + 4(7 - 6z + 3z^2) - 3y(17 \\
& - 9z + 8z^2))H(1, 0, y) - 144(-1+y)^4(-1+z)^4(-1+y+z)(y+z)^6(88y^3 + 13y^2(-9 + 4z) - 2(2 - 2z + z^2) + y(42 \\
& - 38z + 8z^2))H(1, 0, z) + 288(-1+y)^4y(-1+z)^4(y+z)^6(5 + 2y^3 + 6z - 3z^2 + 4y^2(-1 + 6z) + 3y(-1 - 9z \\
& + 2z^2))H(1, 1, y) - 18(-1+y)^4(-1+z)^4(y+z)^6(-72 + 1792y^4 + 182z + 909z^2 - 2011z^3 + 992z^4 + y^3(-4043 \\
& + 3204z) + 3y^2(911 - 1505z + 664z^2) + y(-410 + 1560z - 3123z^2 + 2244z^3))H(1, 1, z) + 144(-1+y)^4(-1+z)^4(y \\
& + z)^6(84y^4 + y^3(-193 + 76z) + 3y^2(51 - 39z + 16z^2) + 2(-2 + 4z - 3z^2 + z^3) - 2y(20 - 12z + 3z^2 \\
& + 4z^3))H(1, 2, y) + 144(-1+y)^4(-1+z)^4(y+z)^6(-4 + 4y^4 + 46z - 159z^2 + 205z^3 - 88z^4 + y^3(21 + 4z) + y^2(-57 \\
& + 75z - 84z^2) + y(36 - 108z + 219z^2 - 140z^3))H(2, 0, y) - 144(-1+y)^4(-1+z)^4(y+z)^6(20y^4 + y^3(-49 + 60z) \\
& + 3y^2(11 - 35z + 24z^2) + 4z(-10 + 27z - 25z^2 + 8z^3) + 4y(-1 + 18z - 30z^2 + 12z^3))H(2, 1, y) - 18(-1+y)^4(-1 \\
& + z)^4(y+z)^6(-104 + 1536y^4 - 26z + 1821z^2 - 3227z^3 + 1536z^4 + y^3(-3227 + 2756z) + 3y^2(607 - 1217z + 632z^2) \\
& + y(-26 + 1272z - 3651z^2 + 2756z^3))H(2, 2, y) - 144(-1+y)^4(-1+z)^4(y+z)^6(-4 + 36y^4 - 4z + 51z^2 - 79z^3 \\
& + 36z^4 + y^3(-79 + 52z) + y^2(51 - 75z + 48z^2) + y(-4 + 24z - 75z^2 + 52z^3))H(3, 2, y) \Big\} / \Big(576(-1+y)^4y(-1 \\
& + z)^4z(-1+y+z)(y+z)^6 \Big);
\end{aligned}$$

$$\begin{aligned}
A_{6;C_F^2}^{(2)} = & \left\{ 4(-1+y)(-1+z)(y+z)(288y^{13}z - 3(-1+z)^5z^5(90 - 90z + 43z^2) + y^{12}(-129 - 1327z + 1720z^2 + 488z^3 \right. \\
& - 176z^4) + y^{11}(915 + 342z - 6679z^2 + 3734z^3 + 1168z^4 - 56z^5) + y(-1+z)^4z^4(1350 - 4968z + 5525z^2 - 2086z^3 \\
& - 175z^4 + 288z^5) + y^2(-1+z)^3z^3(-2700 + 15672z - 38367z^2 + 41471z^3 - 16563z^4 - 1519z^5 + 1720z^6) + y^{10}(-2910 \\
& + 11667z - 6846z^2 - 9291z^3 + 9388z^4 - 7000z^5 + 3264z^6) + y^9(5340 - 38596z + 84883z^2 - 66628z^3 + 1089z^4 + 39320z^5 \\
& - 36152z^6 + 10744z^7) + y^3(-1+z)^2z^2(2700 - 29448z + 105101z^2 - 188876z^3 + 176750z^4 - 72056z^5 - 359z^6 + 4710z^7 \\
& + 488z^8) + y^8(-6045 + 62541z - 210950z^2 + 320503z^3 - 225267z^4 + 21438z^5 + 93980z^6 - 69672z^7 + 15200z^8) + y^7(4179 \\
& - 59394z + 271749z^2 - 614432z^3 + 753510z^4 - 469026z^5 + 49426z^6 + 123492z^7 - 69672z^8 + 10744z^9) + y^6(-1620 + 33497z \\
& - 206288z^2 + 659603z^3 - 1187244z^4 + 1201898z^5 - 610940z^6 + 49426z^7 + 93980z^8 - 36152z^9 + 3264z^{10}) + y^4z(1350 \\
& - 23772z + 166697z^2 - 565574z^3 + 1068831z^4 - 1187244z^5 + 753510z^6 - 225267z^7 + 1089z^8 + 9388z^9 + 1168z^{10} \\
& - 176z^{11}) + y^5(270 - 10368z + 93483z^2 - 428526z^3 + 1068831z^4 - 1510552z^5 + 1201898z^6 - 469026z^7 + 21438z^8 \\
& + 39320z^9 - 7000z^{10} - 56z^{11})) - 3(-1+y)^4(-1+z)^4(-1+y+z)^2(y+z)^6(46 + 704y^3 - 112z + 254z^2 - 192z^3 \\
& + y^2(-717 + 404z) - 2y(-21 + 11z + 88z^2))H(0, y)^2 + 3(-1+y)^4(-1+z)^4(-1+y+z)^2(y+z)^6(-46 + 192y^3 - 42z \\
& + 717z^2 - 704z^3 + 2y^2(-127 + 88z) + y(112 + 22z - 404z^2))H(0, z)^2 + 9(-1+y)^4(-1+z)^4(-1+y+z)^2(y+z)^6(4 \\
& + 56z^3 + 34z - 101z^2 + 56z^3 + y^2(-101 + 84z) + y(34 - 76z + 84z^2))H(1, z)^2 + H(1, y)(-8(-1+y)^2(-1+z)^4(-1+y \\
& + z)(y+z)^6(150 + 136y^6 - 406z + 411z^2 - 155z^3 + y^5(-761 + 460z) + y^4(1819 - 2033z + 456z^2) + y^2(1859 - 3607z \\
& + 2367z^2 - 465z^3) + y^3(-2401 + 3730z - 1665z^2 + 164z^3) + y(-802 + 1856z - 1569z^2 + 474z^3)) - 96(-1+y)^4y(-1 \\
& + z)^4(-1+y+z)^2(y+z)^6(3 + 14y^2 - 3z + 3y(-5 + 2z))H(1, z)) + H(0, y)(8(-1+y)^2y(-1+y+z)^2(y
\end{aligned}$$

$$\begin{aligned}
& + z)^6(144y^5z + 12(-1+z)^3z(7 - 6z + z^2) + 4y^4z(-153 + 111z - 40z^2 + 10z^3) - 3y(-1+z)^2(-4 - 162z + 220z^2 \\
& - 108z^3 + 11z^4) + y^3(12 + 1112z - 1955z^2 + 1610z^3 - 799z^4 + 164z^5) + 2y^2(-12 - 511z + 1395z^2 - 1516z^3 + 831z^4 \\
& - 189z^5 + 2z^6)) + 144(-1+y)^4y(-1+z)^4(-1+y+z)^2(y+z)^6(4+12y^2-4z+y(-15+8z))H(1,z)) + 8(-1+y \\
& + z)(144y^{15}z + (-1+z)^5z^6(-132 + 340z - 341z^2 + 136z^3) + 4y^{14}(34 - 397z + 567z^2 - 176z^3 + 44z^4) + y^{13}(-1021 \\
& + 8884z - 22137z^2 + 20586z^3 - 8560z^4 + 1816z^5) + y(-1+z)^4z^5(468 - 3576z + 7726z^2 - 7779z^3 + 3972z^4 - 1012z^5 \\
& + 144z^6) + y^{12}(3405 - 30315z + 100809z^2 - 152893z^3 + 116054z^4 - 46660z^5 + 8448z^6) + 3y^2(-1+z)^3z^4(-748 + 5012z \\
& - 15992z^2 + 27958z^3 - 27830z^4 + 16002z^5 - 5111z^6 + 756z^7) + y^{11}(-6602 + 66866z - 275775z^2 + 575010z^3 - 652809z^4 \\
& + 420138z^5 - 149708z^6 + 23168z^7) + y^{10}(8150 - 98054z + 493695z^2 - 1321709z^3 + 2031803z^4 - 1859997z^5 + 1019924z^6 \\
& - 313380z^7 + 41296z^8) - y^3(-1+z)^2z^3(-1416 + 28792z - 145538z^2 + 374050z^3 - 574998z^4 + 551544z^5 - 328166z^6 \\
& + 113833z^7 - 19178z^8 + 704z^9) + y^9(-6561 + 96216z - 598074z^2 + 2006252z^3 - 3969623z^4 + 4828260z^5 - 3670950z^6 \\
& + 1713820z^7 - 448924z^8 + 49872z^9) + y^8(3361 - 62011z + 494076z^2 - 2075590z^3 + 5157019z^4 - 8018097z^5 + 8000348z^6 \\
& - 5125514z^7 + 2032884z^8 - 448924z^9 + 41296z^{10}) + 2y^7(-500 + 12419z - 137577z^2 + 734318z^3 - 2271456z^4 + 4429489z^5 \\
& - 5635698z^6 + 471974z^7 - 2562757z^8 + 856910z^9 - 156690z^{10} + 11584z^{11}) + y^4z^2(2244 - 31624z + 242798z^2 \\
& - 1036852z^3 + 2692286z^4 - 4542912z^5 + 5157019z^6 - 3969623z^7 + 2031803z^8 - 652809z^9 + 116054z^{10} - 8560z^{11} + 176z^{12}) \\
& + y^5z(468 - 21768z + 204538z^2 - 1036852z^3 + 3244920z^4 - 6575600z^5 + 8858978z^6 - 8018097z^7 + 4828260z^8 - 1859997z^9 \\
& + 420138z^{10} - 46660z^{11} + 1816z^{12}) + 2y^6(66 - 2724z + 49908z^2 - 346959z^3 + 1346143z^4 - 3287800z^5 + 5273177z^6 \\
& - 5635698z^7 + 4000174z^8 - 1835475z^9 + 509962z^{10} - 74854z^{11} + 4224z^{12}))H(2,y) + 9(-1+y)^4(-1+z)^4(-1+y+z)^2 \\
& + z)^6(4 + 56y^3 + 34z - 101z^2 + 56z^3 + y^2(-101 + 84z) + y(34 - 76z + 84z^2))H(2,y)^2 + H(0,z)(8(-1+z)^2z(-1+y \\
& + z)^2(y+z)^6(12(-1+z)^2z + y^6(12 - 33z + 4z^2) + 2y^5(-54 + 195z - 189z^2 + 82z^3) + y^4(336 - 1341z + 1662z^2 \\
& - 799z^3 + 40z^4) - 2y^3(240 - 1065z + 1516z^2 - 805z^3 + 80z^4) + y^2(324 - 1620z + 2790z^2 - 1955z^3 + 444z^4) \\
& + 2y(-42 + 231z - 511z^2 + 556z^3 - 306z^4 + 72z^5)) + 48(-1+y)^4y(-1+z)^4(-1+y+z)^2(y+z)^6(6 + 8y^2 - 6z \\
& + 3y(-5 + 4z))H(1,y) - 48(-1+y)^4(-1+z)^4(-1+y+z)^2(y+z)^6(8y^3 + 3y^2(-5 + 4z) + 6y(1+z - 4z^2) - 3z(4 \\
& - 15z + 12z^2))H(2,y)) + H(1,z)(8(-1+y+z)(144y^{15}z + 6(-1+z)^5z^6(3 - 2z + 2z^2) + 4y^{14}(34 - 397z + 567z^2 \\
& - 176z^3 + 44z^4) + y^{13}(-866 + 8100z - 20569z^2 + 19018z^3 - 7767z^4 + 1652z^5) + 2y(-1+z)^4z^5(-216 + 221z + 222z^2 \\
& - 456z^3 + 370z^4 - 234z^5 + 72z^6) + y^{12}(2374 - 23858z + 83917z^2 - 129245z^3 + 97321z^4 - 38669z^5 + 7008z^6) + y^2(-1 \\
& + z)^3z^4(6 - 780z - 2588z^2 + 13184z^3 - 18942z^4 + 14294z^5 - 6479z^6 + 1452z^7) + y^{11}(-3622 + 43744z - 199491z^2 \\
& + 436042z^3 - 501379z^4 + 321120z^5 - 113638z^6 + 17512z^7) + y^{10}(3290 - 50918z + 300333z^2 - 878721z^3 + 1407853z^4 \\
& - 1304275z^5 + 713376z^6 - 217490z^7 + 28280z^8) - y^3(-1+z)^2z^3(1584 - 2338z - 14788z^2 + 72720z^3 - 149820z^4 \\
& + 171732z^5 - 117066z^6 + 45939z^7 - 8478z^8 + 160z^9) + 2y^9(-863 + 18146z - 145902z^2 + 567991z^3 - 1216836z^4 \\
& + 1534256z^5 - 1178239z^6 + 547769z^7 - 141466z^8 + 15288z^9) + 2y^8(213 - 6663z + 89049z^2 - 480126z^3 + 1360821z^4 \\
& - 2265678z^5 + 2330148z^6 - 1502619z^7 + 590049z^8 - 126886z^9 + 11116z^{10}) + 2y^7(3 + 76z - 31201z^2 + 259264z^3 \\
& - 985699z^4 + 2156109z^5 - 2918981z^6 + 2511740z^7 - 1366047z^8 + 447153z^9 - 77957z^{10} + 5324z^{11}) + y^4z^2(-6 + 5026z \\
& + 3058z^2 - 165362z^3 + 688552z^4 - 1444642z^5 + 1850424z^6 - 1531142z^7 + 816755z^8 - 264717z^9 + 44437z^{10} - 2423z^{11} \\
& + 40z^{12}) + y^5z(-432 - 66z + 18020z^2 - 196646z^3 + 926280z^4 - 2346594z^5 + 3574134z^6 - 3448086z^7 + 2127944z^8 \\
& - 811205z^9 + 172740z^{10} - 16485z^{11} + 540z^{12}) + 2y^6(-9 + 845z + 4861z^2 - 81055z^3 + 437656z^4 - 1299435z^5 \\
& + 2341652z^6 - 2665679z^7 + 1940166z^8 - 884963z^9 + 236428z^{10} - 31919z^{11} + 1596z^{12})) + 48(-1+y)^4(-1+z)^4(-1+y \\
& + z)^2(y+z)^6(-4 + 28y^3 + 18z - 21z^2 + 8z^3 + 4y^2(-8 + 5z) + 2y(5 - 10z + 2z^2))H(2,y) - 144(-1+y)^4(-1 \\
& + z)^4(-1+y+z)^2(y+z)^6(12y^3 + y^2(-15 + 8z) + y(4 - 8z + 8z^2) + z(4 - 15z + 12z^2))H(3,y)) + 6(-1+y)^4(-1 \\
& + z)^4(-1+y+z)^2(y+z)^6(46 + 704y^3 - 112z + 254z^2 - 192z^3 + y^2(-717 + 404z) - 2y(-21 + 11z + 88z^2))H(0,0,y) \\
& - 6(-1+y)^4(-1+z)^4(-1+y+z)^2(y+z)^6(-46 + 192y^3 - 42z + 717z^2 - 704z^3 + 2y^2(-127 + 88z) + y(112 + 22z \\
& - 404z^2))H(0,0,z) - 96(-1+y)^4(-1+4y)(-1+z)^4(-1+y+z)^2(y+z)^6(2 + 2y^2 + 2y(-2+z) - 2z \\
& + z^2)H(0,1,y) - 144(-1+y)^4y(-1+z)^4(-1+y+z)^2(y+z)^6(4 + 12y^2 - 4z + y(-15 + 8z))H(0,1,z) + 48(-1 \\
& + y)^4(-1+z)^4(-1+y+z)^2(y+z)^6(52y^3 + y^2(-81 + 40z) - 2(2 - 2z + z^2) + 4y(9 - 8z + 2z^2))H(0,2,y) \\
& - 144(-1+y)^4y(-1+z)^4(-1+y+z)^2(y+z)^6(4 + 12y^2 - 4z + y(-15 + 8z))H(1,0,y) - 48(-1+y)^4y(-1+z)^4(-1 \\
& + y+z)^2(y+z)^6(6 + 8y^2 - 6z + 3y(-5 + 4z))H(1,0,z) + 48(-1+y)^4(-1+z)^4(-1+y+z)^2(y+z)^6(20y^3 \\
& + y^2(-9 + 8z) + 2(2 - 2z + z^2) - 4y(3 - 2z + 2z^2))H(1,1,y) + 6(-1+y)^4(-1+z)^4(-1+y+z)^2(y+z)^6(56y^3 \\
& + y^2(63 - 156z) - 18y(3 - 10z + 14z^2) - 3(4 + 34z - 101z^2 + 56z^3))H(1,1,z) - 96(-1+y)^4y(-1+z)^4(-1+y \\
& + z)^2(y+z)^6(3 + 14y^2 - 3z + 3y(-5 + 2z))H(1,2,y) + 48(-1+y)^4(-1+z)^4(-1+y+z)^2(y+z)^6(36y^3 \\
& + 3y^2(-15 + 8z) + z(-6 + 15z - 8z^2) - 6y(-2 + z + 2z^2))H(2,0,y) - 48(-1+y)^4(-1+z)^4(-1+y+z)^2(y \\
& + z)^6(36y^3 + 16y(-1+z)^2 + 4(-1+z)^2(-1+4z) + y^2(-47 + 32z))H(2,1,y) + 6(-1+y)^4(-1+z)^4(-1+y+z)^2(y
\end{aligned}$$

$$\begin{aligned}
& + z)^6(-76 + 184y^3 + 170z - 241z^2 + 184z^3 + y^2(-241 + 36z) + 2y(85 - 94z + 18z^2))H(2, 2, y) - 144(-1 + y)^4(-1 \\
& + z)^4(-1 + y + z)^2(y + z)^6(12y^3 + y^2(-15 + 8z) + y(4 - 8z + 8z^2) + z(4 - 15z + 12z^2))H(3, 2, y) \Big\} / (48(-1 \\
& + y)^4y(-1 + z)^4z(-1 + y + z)^2(y + z)^6); \\
\mathcal{A}_{6;n_f^2}^{(2)} & = \frac{1}{18} \mathcal{A}_0; \\
\mathcal{A}_{6;CAF}^{(2)} & = \left\{ -2(-1 + y)(-1 + z)(y + z)(1152y^{13}z - 9(-1 + z)^5z^5(90 - 94z + 41z^2) + 3y^{12}(-123 - 2483z + 4229z^2 \right. \\
& - 1283z^3 + 428z^4) + 3y(-1 + z)^4z^4(1350 - 5784z + 5943z^2 - 1088z^3 - 947z^4 + 384z^5) + 3y^{11}(897 + 5004z \\
& - 25436z^2 + 30556z^3 - 16597z^4 + 4808z^5) + 3y^2(-1 + z)^3z^3(-2700 + 13740z - 36361z^2 + 35633z^3 - 2149z^4 \\
& - 12749z^5 + 4229z^6) + y^{10}(-8730 + 9231z + 146355z^2 - 412685z^3 + 451131z^4 - 253782z^5 + 61568z^6) + 2y^9(8100 \\
& - 47868z - 594z^2 + 355100z^3 - 742645z^4 + 700596z^5 - 341189z^6 + 68500z^7) - y^3(-1 + z)^2z^2(-8100 + 99768z \\
& - 310125z^2 + 455122z^3 - 249510z^4 - 144438z^5 + 240896z^6 - 83970z^7 + 3849z^8) + y^8(-18405 + 190647z - 410874z^2 \\
& - 280262z^3 + 2163621z^4 - 3406317z^5 + 2683478z^6 - 1092120z^7 + 177144z^8) + y^7(12699 - 194892z + 695613z^2 \\
& - 809704z^3 - 883105z^4 + 3818004z^5 - 4987759z^6 + 3306568z^7 - 1092120z^8 + 137000z^9) + y^6(-4896 + 111537z \\
& - 565908z^2 + 1469879z^3 - 1595836z^4 - 916967z^5 + 4424978z^6 - 4987759z^7 + 2683478z^8 - 682378z^9 + 61568z^{10}) \\
& + y^4z(4050 - 65520z + 517761z^2 - 1698158z^3 + 2639853z^4 - 1595836z^5 - 883105z^6 + 2163621z^7 - 1485290z^8 \\
& + 451131z^9 - 49791z^{10} + 1284z^{11}) + y^5(810 - 33552z + 257043z^2 - 1175140z^3 + 2639853z^4 - 2346720z^5 - 916967z^6 \\
& + 3818004z^7 - 3406317z^8 + 1401192z^9 - 253782z^{10} + 14424z^{11})) + 9(-1 + y)^4(-1 + z)^4(-1 + y + z)(y + z)^6(-27 \\
& + 612y^4 + 7z - 18z^2 + 130z^3 - 92z^4 + 6y^3(-219 + 206z) + 6y^2(127 - 251z + 78z^2) - 3y(11 - 102z + 26z^2 \\
& + 52z^3))H(0, y)^2 - 9(-1 + y)^4(-1 + z)^4(-1 + y + z)(y + z)^6(27 + 92y^4 + 33z - 762z^2 + 1314z^3 - 612z^4 \\
& + 26y^3(-5 + 6z) + y^2(18 + 78z - 468z^2) - y(7 + 306z - 1506z^2 + 1236z^3))H(0, z)^2 - 9(-1 + y)^4(-1 + z)^4(-1 \\
& + y + z)(y + z)^6(-58 + 80y^4 + 136z + 27z^2 - 185z^3 + 80z^4 + 5y^3(-37 + 68z) + 3y^2(9 - 139z + 112z^2) + y(136 \\
& - 12z - 417z^2 + 340z^3))H(1, z)^2 + H(0, y)(-12(-1 + y)^2y(-1 + y + z)(y + z)^6(192y^6z + 4y^5z(-255 + 207z \\
& - 64z^2 + 16z^3) - 6(-1 + z)^4(1 + 18z - 47z^2 + 32z^3) + 3y(-1 + z)^3(3 + 6z + 242z^2 - 344z^3 + 134z^4) \\
& - y^2(-1 + z)^2(-63 - 1120z + 692z^2 + 644z^3 - 824z^4 + 208z^5) + y^4(27 + 2224z - 3883z^2 + 2826z^3 - 1250z^4 \\
& + 248z^5) - y^3(75 + 2315z - 5945z^2 + 5649z^3 - 2530z^4 + 376z^5 + 60z^6)) - 72(-1 + y)^4(-1 + z)^4(-1 + y + z)(y \\
& + z)^6(56y^4 - 3y^2(-7 + 9z) + y^3(-91 + 60z) + y(20 - 36z + 27z^2 - 12z^3) + 3(-2 + 4z - 3z^2 + z^3))H(1, z)) \\
& + H(1, y)(12(-1 + y)^3(-1 + z)^4(-1 + y + z)(y + z)^6(-406 + 388y^5 + 1020z - 1029z^2 + 383z^3 + y^4(-1877 + 1092z) \\
& + y^3(3592 - 3873z + 1116z^2) + y(1814 - 3714z + 3018z^2 - 859z^3) + y^2(-3511 + 5475z - 3111z^2 + 476z^3)) + 72(-1 \\
& + y)^4(-1 + z)^4(-1 + y + z)(y + z)^6(2 + 24y^4 - 4z + 3z^2 - z^3 + 4y^3(-7 + 10z) - 6y^2(2 + 3z + 2z^2) + y(14 \\
& - 3z^2 + 4z^3))H(1, z)) - 6(-1 + y + z)(384y^{15}z + (-1 + z)^5z^6(-726 + 1882z - 2105z^2 + 776z^3) + 8y^{14}(97 \\
& - 739z + 1077z^2 - 452z^3 + 113z^4) + y^{13}(-5985 + 40168z - 92560z^2 + 89128z^3 - 40267z^4 + 8364z^5) + y(-1 \\
& + z)^4z^5(2964 - 19836z + 41602z^2 - 41559z^3 + 20360z^4 - 4376z^5 + 384z^6) + y^{12}(20167 - 150791z + 451180z^2 \\
& - 659196z^3 + 502581z^4 - 202437z^5 + 35424z^6) + 2y^2(-1 + z)^3z^4(-6765 + 42879z - 127932z^2 + 212727z^3 \\
& - 204354z^4 + 112598z^5 - 33356z^6 + 4308z^7) + 2y^{11}(-19473 + 173943z - 646524z^2 + 1262820z^3 - 1387944z^4 \\
& + 876471z^5 - 304141z^6 + 45232z^7) + 2y^{10}(23690 - 260707z + 1196939z^2 - 2976262z^3 + 4350991z^4 - 3849912z^5 \\
& + 2048644z^6 - 608211z^7 + 77132z^8) - 2y^3(-1 + z)^2z^3(-4252 + 81656z - 390703z^2 + 946461z^3 - 1380495z^4 \\
& + 1270200z^5 - 730084z^6 + 245894z^7 - 40948z^8 + 1808z^9) + y^9(-37381 + 518516z - 2983546z^2 + 9301958z^3 \\
& - 17356961z^4 + 20206452z^5 - 14838192z^6 + 6708682z^7 - 1702288z^8 + 183528z^9) + y^8(18775 - 338839z + 2538420z^2 \\
& - 9955302z^3 + 23235465z^4 - 34337223z^5 + 32931038z^6 - 20432684z^7 + 7885302z^8 - 1702288z^9 + 154264z^{10}) \\
& + 2y^7(-2756 + 69365z - 731925z^2 + 3664120z^3 - 10625532z^4 + 19591238z^5 - 23845782z^6 + 19305676z^7 - 10216342z^8 \\
& + 3354341z^9 - 608211z^{10} + 45232z^{11}) + y^4z^2(13530 - 180320z + 1309202z^2 - 5314260z^3 + 13155096z^4 - 21251064z^5 \\
& + 23235465z^6 - 17356961z^7 + 8701982z^8 - 2775888z^9 + 502581z^{10} - 40267z^{11} + 904z^{12}) + y^5z(2964 - 126348z \\
& + 1116534z^2 - 5314260z^3 + 15703800z^4 - 30293056z^5 + 39182476z^6 - 34337223z^7 + 20206452z^8 - 7699824z^9 \\
& + 1752942z^{10} - 202437z^{11} + 8364z^{12}) + 2y^6(363 - 15846z + 276864z^2 - 1809523z^3 + 6577548z^4 - 15146528z^5 \\
& + 23154650z^6 - 23845782z^7 + 16465519z^8 - 7419096z^9 + 2048644z^{10} - 304141z^{11} + 17712z^{12}))H(2, y) - 9(-1 + y)^4(-1 \\
& + z)^4(-1 + y + z)(y + z)^6(-58 + 80y^4 + 136z + 27z^2 - 185z^3 + 80z^4 + 5y^3(-37 + 68z) + 3y^2(9 - 139z \\
& + 112z^2) + y(136 - 12z - 417z^2 + 340z^3))H(2, y)^2 + H(0, z)(12(-1 + z)^2z(-1 + y + z)(y + z)^6(-3(-1 + z)^3(2 \\
& + 9z) + 2y^7(96 - 201z + 104z^2) + 2y^6(-525 + 1119z - 620z^2 + 30z^3) - 4y^5(-597 + 1257z - 625z^2 - 94z^3
\end{aligned}$$

$$\begin{aligned}
& + 62z^4) - y(-1+z)^2(-84 - 159z + 760z^2 - 636z^3 + 192z^4) + y^2(-678 + 699z + 2869z^2 - 5945z^3 + 3883z^4 \\
& - 828z^5) - 2y^4(1443 - 2829z + 710z^2 + 1265z^3 - 625z^4 + 32z^5) + y^3(1944 - 3165z - 1860z^2 + 5649z^3 - 2826z^4 \\
& + 256z^5)) - 72(-1+y)^4(-1+z)^4(-1+y+z)(y+z)^6(-2+32y^4+4z-3z^2+z^3+y^3(-93+68z)+3y^2(29 \\
& - 39z+16z^2)-y(24-36z+15z^2+4z^3))H(1,y) + 288(-1+y)^4(-1+z)^4(-1+y+z)(y+z)^6(1+8y^4-4z \\
& - 6z^2+23z^3-14z^4+4y^3(-6+5z)+12y^2(2-3z+z^2)+y(-9+18z+3z^2-16z^3))H(2,y)) \\
& + H(1,z)(-6(-1+y+z)(384y^{15}z+(-1+z)^5z^6(86-122z+97z^2)+8y^{14}(97-739z+1077z^2-452z^3 \\
& + 113z^4)+y^{13}(-5219+36152z-84156z^2+80352z^3-35693z^4+7412z^5))+y(-1+z)^4z^5(-1908+2348z-286z^2 \\
& - 1305z^3+1608z^4-1272z^5+384z^6)+y^{12}(15045-117921z+362964z^2-532604z^3+400231z^4-158267z^5 \\
& + 27480z^6)+2y^2(-1+z)^3z^4(-675-195z-1902z^2+12975z^3-20676z^4+17018z^5-8414z^6+1980z^7) \\
& + 2y^{11}(-12039+115335z-450060z^2+899424z^3-987042z^4+612507z^5-208045z^6+30304z^7)+2y^{10}(11498 \\
& - 141313z+701873z^2-1830608z^3+2724693z^4-2395960z^5+1248128z^6-359939z^7+43932z^8)-2y^3(-1 \\
& + z)^2z^3(3868-2404z-34723z^2+117005z^3-200991z^4+214578z^5-145420z^6+58736z^7-11368z^8+256z^9) \\
& + y^9(-12895+213812z-1415134z^2+4813534z^3-9392031z^4+11059916z^5-8020592z^6+3525722z^7-858756z^8 \\
& + 87192z^9)+y^8(3685-89137z+912288z^2-4186350z^3+10584771z^4-16190181z^5+15575102z^6-9479600z^7 \\
& + 3525138z^8-718540z^9+59752z^{10})+2y^7(-112+5193z-179561z^2+1190012z^3-3904772z^4+7681554z^5 \\
& - 9620890z^6+7790928z^7-4023410z^8+1256653z^9-210091z^{10}+13920z^{11})+y^4z^2(1350+16400z+21642z^2 \\
& - 611924z^3+2286652z^4-4384532z^5+5218711z^6-4097291z^7+2122526z^8-683628z^9+116791z^{10}-6825z^{11} \\
& + 128z^{12})+y^5z(-1908-10644z+125622z^2-840744z^3+3311496z^4-7624456z^5+10838140z^6-9884853z^7 \\
& + 5831340z^8-2153460z^9+452070z^{10}-43743z^{11}+1524z^{12})+2y^6(-43+3050z+40106z^2-411629z^3+1786766z^4 \\
& - 4630398z^5+7634856z^6-8152400z^7+5636279z^8-2461502z^9+635000z^{10}-83925z^{11}+4224z^{12})) - 288(-1 \\
& + y)^4(-1+z)^4(-1+y+z)(y+z)^6(4y^3+4y^4+3(-1+z)z^2-3y^2(6-7z+6z^2)-2y(-5+9z-12z^2) \\
& + 6z^3))H(2,y) + 432(-1+y)^4(-1+z)^4(-1+y+z)^2(y+z)^6(12y^3+y^2(-15+8z)+y(4-8z+8z^2)+z(4 \\
& - 15z+12z^2))H(3,y)) - 18(-1+y)^4(-1+z)^4(-1+y+z)(y+z)^6(-27+612y^4+7z-18z^2+130z^3-92z^4 \\
& + 6y^3(-219+206z)+6y^2(127-251z+78z^2)-3y(11-102z+26z^2+52z^3))H(0,0,y) + 18(-1+y)^4(-1 \\
& + z)^4(-1+y+z)(y+z)^6(27+92y^4+33z-762z^2+1314z^3-612z^4+26y^3(-5+6z)+y^2(18+78z-468z^2) \\
& - y(7+306z-1506z^2+1236z^3))H(0,0,z) + 144(-1+y)^4y(-1+z)^4(-1+y+z)(y+z)^6(16y^3+y^2(-41+12z) \\
& - 2(7-6z+3z^2)+3y(13-9z+4z^2))H(0,1,y) + 72(-1+y)^4(-1+z)^4(-1+y+z)^2(y+z)^6(2+64y^3-2z \\
& + z^2+8y^2(-9+5z)-2y(-6+7z+2z^2))H(0,1,z) - 72(-1+y)^4(-1+z)^4(-1+y+z)(y+z)^6(104y^4+2(-1 \\
& + z)^3(-1+4z)+y^3(-245+148z)+3y^2(65-77z+28z^2)+8y(-7+12z-9z^2+2z^3))H(0,2,y) + 72(-1 \\
& + y)^4(-1+z)^4(-1+y+z)(y+z)^6(56y^4-3y^2(-7+9z)+y^3(-91+60z)+y(20-36z+27z^2-12z^3)+3(-2 \\
& + 4z-3z^2+z^3))H(1,0,y) + 72(-1+y)^4(-1+z)^4(-1+y+z)(y+z)^6(-2+32y^4+4z-3z^2+z^3+y^3(-93 \\
& + 68z)+3y^2(29-39z+16z^2)-y(24-36z+15z^2+4z^3))H(1,0,z) - 216(-1+y)^4y(-1+z)^4(-1+y+z)(y \\
& + z)^6(6+8y^3+4z-2z^2+y^2(-13+28z)+y(-1-27z+4z^2))H(1,1,y) + 18(-1+y)^4(-1+z)^4(-1+y+z)(y \\
& + z)^6(-50+16y^4+120z+39z^2-189z^3+80z^4+y^3(-253+356z)+y^2(327-741z+528z^2)+y(-40+228z \\
& - 549z^2+356z^3))H(1,1,z) + 72(-1+y)^4(-1+z)^4(-1+y+z)(y+z)^6(2+24y^4-4z+3z^2-z^3+4y^3(-7 \\
& + 10z)-6y^2(2+3z+2z^2)+y(14-3z^2+4z^3))H(1,2,y) - 288(-1+y)^4(-1+z)^4(-1+y+z)(y+z)^6(-1 \\
& + 14y^4+9z-24z^2+24z^3-8z^4+y^3(-23+16z)-3y^2(-2+z+4z^2)+y(4-18z+36z^2-20z^3))H(2,0,y) \\
& + 144(-1+y)^4(-1+z)^4(-1+y+z)(y+z)^6(4+32y^4-38z+87z^2-77z^3+24z^4+y^3(-75+68z)+3y^2(19 \\
& - 39z+20z^2)+y(-18+84z-111z^2+44z^3))H(2,1,y) - 18(-1+y)^4(-1+z)^4(-1+y+z)(y+z)^6(90+176y^4 \\
& - 280z+381z^2-367z^3+176z^4+y^3(-367+12z)-3y^2(-127+45z+48z^2)+y(-280+396z-135z^2 \\
& + 12z^3))H(2,2,y) + 432(-1+y)^4(-1+z)^4(-1+y+z)^2(y+z)^6(12y^3+y^2(-15+8z)+y(4-8z+8z^2)+z(4 \\
& - 15z+12z^2))H(3,2,y) \Big\} / \Big(144(-1+y)^4y(-1+z)^4z(-1+y+z)^2(y+z)^6 \Big);
\end{aligned}$$

$$\begin{aligned}
\mathcal{A}_{6;C_A n_f}^{(2)} = & \Big\{ (-1+y)(-1+z)(y+z)(864y^{12}z+7(-1+z)^4z^5(2-2z+z^2)+y^{11}(7-3181z+2877z^2+3053z^3-1028z^4) \\
& + y(-1+z)^3z^4(-70+138z+447z^2-697z^3-589z^4+864z^5)-2y^{10}(21-1831z+3460z^2+8127z^3-12227z^4 \\
& + 3314z^5)+y^9(112-93z-3293z^2+54841z^3-123339z^4+85304z^5-18716z^6)+y^2(-1+z)^2z^3(140-770z \\
& - 1605z^2+8180z^3-8502z^4-1166z^5+2877z^6)-y^8(168+2705z-24018z^2+117638z^3-307100z^4+350637z^5 \\
& - 170234z^6+30204z^7)+y^7(147+1554z-26467z^2+142908z^3-438373z^4+710452z^5-567495z^6+212662z^7 \\
& - 30204z^8)+y^6(-70+177z+10620z^2-97217z^3+373368z^4-794957z^5+925784z^6-567495z^7+170234z^8-18716z^9)
\end{aligned}$$

$$\begin{aligned}
& + y^3 z^2 (140 + 376z - 7503z^2 + 37294z^3 - 97217z^4 + 142908z^5 - 117638z^6 + 54841z^7 - 16254z^8 + 3053z^9) + y^5 (14 \\
& - 348z + 75z^2 + 37294z^3 - 197115z^4 + 514818z^5 - 794957z^6 + 710452z^7 - 350637z^8 + 85304z^9 - 6628z^{10}) + y^4 z (70 \\
& - 1050z - 7503z^2 + 62552z^3 - 197115z^4 + 373368z^5 - 438373z^6 + 307100z^7 - 123339z^8 + 24454z^9 - 1028z^{10})) + 12(-1 \\
& + y)^4 (y+z)^6 (72y^5 z - (-1+z)^5 (2-2z+z^2) + y^4 z (-171+177z-8z^2+2z^3) + y^3 (-1+z)^2 (-1+150z-33z^2 \\
& + 12z^3) + 3y^2 (-1+z)^3 (-1+25z-33z^2+22z^3) + y (-1+z)^4 (-4+30z-81z^2+64z^3)) H(0,y) + 27(-1+y)^4 (-1 \\
& + z)^4 z (-1+y+z)(y+z)^6 (3-12z+10z^2+y(-3+6z)) H(0,z) + 27(-1+y)^4 (-1+y+z)(y+z)^6 (10y^3+6y^2(-2+z)+y(3-6z \\
& + 6z^2) + z(3-12z+10z^2)) H(1,z)^2 + H(1,y) (12(-1+y)^4 (-1+z)^4 (y+z)^6 (22y^4+z(-1+3z)+2y^3(-29+8z) \\
& - 3y(7-6z+3z^2) + 3y^2(19-13z+6z^2)) - 72(-1+y)^4 y(3+10y^2+6y(-2+z)-3z) (-1+z)^4 (-1+y+z)(y+z)^6 H(1,z)) + 6(144y^{15}z - (-1+z)^5 z^6 (-2+44z-73z^2+44z^3) - 2y^{14}(22+371z-477z^2-80z^3+20z^4) \\
& + y^{13}(293+1168z-5070z^2+2496z^3+821z^4-140z^5) + y(-1+z)^4 z^5 (-24+332z-904z^2+1005z^3-360z^4 \\
& - 166z^5+144z^6) + y^{12}(-849+873z+9576z^2-16678z^3+5423z^4+311z^5+192z^6) + 6y^2(-1+z)^3 z^4 (5-169z \\
& + 700z^2-1162z^3+833z^4+15z^5-368z^6+159z^7) + 2y^{11}(696-3138z-1425z^2+18410z^3-21716z^4+10176z^5 \\
& - 3835z^6+976z^7) + 2y^{10}(-700+5626z-9744z^2-13652z^3+51737z^4-54675z^5+33289z^6-13437z^7+2420z^8) \\
& + 2y^3(-1+z)^2 z^3 (-168+1335z-5622z^2+12199z^3-12840z^4+3543z^5+5796z^6-5603z^7+1408z^8+80z^9) \\
& + y^9(869-11156z+40020z^2-28260z^3-100851z^4+231456z^5-227034z^6+134608z^7-45724z^8+6360z^9) + y^8(-313 \\
& + 6709z-39528z^2+82844z^3-7079z^4-224019z^5+385714z^6-333886z^7+169290z^8-45724z^9+4840z^{10}) + 2y^7(27 \\
& - 1188z+11322z^2-42860z^3+61782z^4+15764z^5-162079z^6+229116z^7-166943z^8+67304z^9-13437z^{10}+976z^{11}) \\
& + y^5 z (-24+1104z-16920z^2+80478z^3-172200z^4+157568z^5+31528z^6-224019z^7+231456z^8-109350z^9 \\
& + 20352z^{10}+311z^{11}-140z^{12}) + y^4 z^2 (-30+3342z-24582z^2+80478z^3-141088z^4+123564z^5-7079z^6-100851z^7 \\
& + 103474z^8-43432z^9+5423z^{10}+821z^{11}-40z^{12}) + 2y^6 (-1+214z-3666z^2+24778z^3-70544z^4+78784z^5 \\
& + 23768z^6-162079z^7+192857z^8-113517z^9+33289z^{10}-3835z^{11}+96z^{12}) H(2,y) - 108(-1+y)^4 (-1+z)^4 (-1+y \\
& + z)(y+z)^6 (10y^3+6y^2(-2+z)+y(3-6z+6z^2)+z(3-12z+10z^2)) H(2,y)^2 + H(0,z) (12(-1+z)^4 (y+z)^6 (2 \\
& - 4z+3z^2-z^3+y^7(-1+64z)+y^6(7-337z+66z^2)+y^5(-22+738z-297z^2+12z^3)+y^3(-45+584z-591z^2 \\
& + 228z^3-8z^4)+y^4(40-866z+570z^2-57z^3+2z^4)+y^2(31-225z+333z^2-334z^3+177z^4)+y(-12+46z \\
& - 84z^2+152z^3-171z^4+72z^5)) - 72(-1+y)^4 y(3+10y^2+6y(-2+z)-3z) (-1+z)^4 (-1+y+z)(y+z)^6 H(1,y) \\
& + 72(-1+y)^4 y(3+10y^2+6y(-2+z)-3z) (-1+z)^4 (-1+y+z)(y+z)^6 H(2,y) + H(1,z) (6(144y^{15}z + (-1 \\
& + z)^5 z^6 (2-2z+z^2) - 2y^{14}(22+371z-477z^2-80z^3+20z^4) + y^{13}(293+1168z-5070z^2+2496z^3+821z^4 \\
& - 140z^5) + y(-1+z)^4 z^5 (-24+78z-16z^2-225z^3+400z^4-342z^5+144z^6) + y^{12}(-843+831z+9720z^2 \\
& - 16954z^3+5717z^4+149z^5+228z^6) + 2y^2(-1+z)^3 z^4 (15-186z+305z^2+667z^3-2514z^4+3319z^5-2176z^6 \\
& + 609z^7) + 2y^{11}(683-3014z-1956z^2+19678z^3-23503z^4+11652z^5-4496z^6+1100z^7) + 2y^{10}(-678+5313z \\
& - 8022z^2-18773z^3+60879z^4-64750z^5+39999z^6-15912z^7+2808z^8) - 2y^3(-1+z)^2 z^3 (168-900z+2040z^2 \\
& + 85z^3-10206z^4+22176z^5-23052z^6+12257z^7-2704z^8+8z^9) + y^9(833-10292z+33702z^2-4660z^3-153421z^4 \\
& + 305336z^5-293084z^6+170960z^7-56910z^8+7824z^9) + y^8(-299+6023z-32496z^2+49134z^3+86751z^4-389079z^5 \\
& + 574814z^6-474284z^7+234114z^8-62510z^9+6680z^{10}) + 2y^7(26-1040z+8961z^2-27672z^3+8010z^4+134028z^5 \\
& - 332223z^6+391604z^7-268514z^8+106908z^9-22068z^{10}+1764z^{11}) + y^4 z^2 (-30+2672z-15902z^2+33612z^3 \\
& + 1816z^4-152124z^5+346211z^6-406001z^7+279114z^8-108142z^9+19425z^{10}-655z^{11}+4z^{12}) + y^5 z (-24+822z \\
& - 11768z^2+45164z^3-41376z^4-142688z^5+485144z^6-685563z^7+546704z^8-249740z^9+58512z^{10}-5199z^{11} \\
& + 156z^{12}) + 2y^6 (-1+187z-2784z^2+16395z^3-31152z^4-31320z^5+222248z^6-400783z^7+385277z^8-215282z^9 \\
& + 66695z^{10}-9876z^{11}+540z^{12})) + 72(-1+y)^4 (-1+z)^4 (-1+y+z)(y+z)^6 (10y^3+6y^2(-2+z)+y(3-6z+6z^2) \\
& + z(3-12z+10z^2)) H(2,y) - 54(-1+y)^4 (-1+z)^4 z (-1+y+z)(y+z)^6 (3-12z+10z^2+y(-3+6z)) H(0,0,y) \\
& - 54(-1+y)^4 y(3+10y^2+6y(-2+z)-3z) (-1+z)^4 (-1+y+z)(y+z)^6 H(0,0,z) + 72(-1+y)^4 y(3+10y^2 \\
& + 6y(-2+z)-3z) (-1+z)^4 (-1+y+z)(y+z)^6 H(1,0,z) + 72(-1+y)^4 (-1+z)^4 (-1+y+z)(y+z)^6 (40y^3 \\
& + 24y^2(-2+z)+3y(4-7z+6z^2)+3z(3-12z+10z^2)) H(1,1,z) - 72(-1+y)^4 y(3+10y^2+6y(-2+z) \\
& - 3z) (-1+z)^4 (-1+y+z)(y+z)^6 H(1,2,y) + 72(-1+y)^4 (-1+z)^4 z (-1+y+z)(y+z)^6 (3-12z+10z^2+y(-3 \\
& + 6z)) H(2,0,y) + 288(-1+y)^4 (-1+z)^4 (-1+y+z)(y+z)^6 (10y^3+6y^2(-2+z)+y(3-6z+6z^2)+z(3-12z \\
& + 10z^2)) H(2,2,y) \Big\} / \Big(144(-1+y)^4 y(-1+z)^4 z (-1+y+z)(y+z)^6 \Big);
\end{aligned}$$

$$\mathcal{A}_{6;C_F n_f}^{(2)} = \left\{ 45(-1+z)^3 z^6 (2-2z+z^2) + 3y^{11} (15-6z-39z^2+28z^3) - 3y(-1+z)^2 z^5 (180-528z+506z^2-167z^3 \right. \\
\left. + 6z^4) + 3y^{10} (-75+179z+81z^2-417z^3+224z^4) + y^9 (495-2538z+2541z^2+3020z^3-5974z^4+2432z^5) \right\}$$

$$\begin{aligned}
& + y^8(-585 + 5121z - 10623z^2 + 3201z^3 + 13112z^4 - 15226z^5 + 5024z^6) - 3y^2z^4(450 - 2184z + 4776z^2 - 5694z^3 \\
& + 3541z^4 - 847z^5 - 81z^6 + 39z^7) + 2y^7(180 - 2613z + 8541z^2 - 11754z^3 + 2089z^4 + 12163z^5 - 11756z^6 + 3180z^7) \\
& + y^3z^3(-1800 + 13656z - 34518z^2 + 41110z^3 - 23508z^4 + 3201z^5 + 3020z^6 - 1251z^7 + 84z^8) + 2y^4z^2(-675 + 6828z \\
& - 24831z^2 + 39456z^3 - 26784z^4 + 2089z^5 + 6556z^6 - 2987z^7 + 336z^8) + 2y^5z(-270 + 3276z - 17259z^2 + 39456z^3 \\
& - 38370z^4 + 7389z^5 + 12163z^6 - 7613z^7 + 1216z^8) + 2y^6(-45 + 1332z - 7164z^2 + 20555z^3 - 26784z^4 + 7389z^5 \\
& + 13973z^6 - 11756z^7 + 2512z^8) - 12(-1 + y)^2(-1 + 4y)(-1 + z)^2(y + z)^6(-2 + 2y^3 + 4z - 3z^2 + z^3 + y^2(-6 + 4z) \\
& + y(6 - 8z + 3z^2))H(1, y) + 3(-1 + y)^2(-1 + z)^2(32y^{10} + y^9(-101 + 244z) + 3y^8(37 - 241z + 280z^2) - z^6(-2 + 4z \\
& - 3z^2 + z^3) + 2y^7(-22 + 351z - 1125z^2 + 856z^3) + yz^5(-36 + 4z + 54z^2 - 39z^3 + 4z^4) + 6y^2z^4(69 - 146z \\
& + 118z^2 - 55z^3 + 12z^4) + 2y^3z^3(-348 - 98z + 825z^2 - 659z^3 + 200z^4) + 6y^5z(-6 - 206z + 527z^2 - 726z^3 \\
& + 332z^4) + 2y^4z^2(207 - 198z + 1263z^2 - 1518z^3 + 572z^4) + 2y^6(1 - 98z + 1110z^2 - 1987z^3 + 1132z^4))H(1, z) \\
& + 3(-1 + y)^2(-1 + z)^2(32y^{10} + 5y^9(-21 + 52z) + 3y^8(41 - 269z + 328z^2) + 6y^7(-10 + 145z - 469z^2 + 384z^3) \\
& + z^6(10 - 60z + 123z^2 - 105z^3 + 32z^4) + 6y^2z^4(89 - 302z + 516z^2 - 469z^3 + 164z^4) + yz^5(12 - 348z + 870z^2 \\
& - 807z^3 + 260z^4) + 6y^5z(2 - 302z + 927z^2 - 1400z^3 + 724z^4) + 2y^3z^3(-268 - 778z + 2781z^2 - 2961z^3 + 1152z^4) \\
& + 2y^4z^2(267 - 778z + 3213z^2 - 4200z^3 + 1860z^4) + 2y^6(5 - 174z + 1548z^2 - 2961z^3 + 1860z^4))H(2, y) \Big\} / \Big(36(-1 \\
& + y)^2y(-1 + z)^2z(-1 + y + z)(y + z)^6 \Big).
\end{aligned}$$

BIBLIOGRAPHY

- [1] “Figure credit: Wikipedia.” https://en.wikipedia.org/wiki/Standard_Model.
- [2] PARTICLE DATA GROUP collaboration, C. Patrignani et al., *Review of Particle Physics*, [Chin. Phys. C40](https://doi.org/10.1088/1674-113X/40/10/100001) (2016) 100001.
- [3] R. P. Feynman, *Relativistic cutoff for quantum electrodynamics*, [Phys. Rev. 74](https://doi.org/10.1103/PhysRev.74.1430) (1948) 1430–1438.
- [4] R. P. Feynman, *The Theory of positrons*, [Phys. Rev. 76](https://doi.org/10.1103/PhysRev.76.749) (1949) 749–759.
- [5] J. S. Schwinger, *Quantum electrodynamics. I A covariant formulation*, [Phys. Rev. 74](https://doi.org/10.1103/PhysRev.74.1439) (1948) 1439.
- [6] J. S. Schwinger, *Quantum electrodynamics. 2. Vacuum polarization and selfenergy*, [Phys. Rev. 75](https://doi.org/10.1103/PhysRev.75.651) (1948) 651.
- [7] T. Tati and S. Tomonaga, *Prog. Theor. Phys. 3*, 391 , (1948).
- [8] Z. Koba, T. Tati and S. Tomonaga, *Prog. theor. phys. 2*, 101 and 198, (1947).
- [9] J. C. Ward, *An Identity in Quantum Electrodynamics*, [Phys. Rev. 78](https://doi.org/10.1103/PhysRev.78.182) (1950) 182.

- [10] A. Petermann, *La normalisation des constantes dans la théorie des quanta* *Normalization of constants in the quanta theory*, *Helv. Phys. Acta* **26** (1953) 499–520.
- [11] M. Gell-Mann and F. E. Low, *Quantum electrodynamics at small distances*, *Phys. Rev.* **95** (1954) 1300–1312.
- [12] C.-N. Yang and R. L. Mills, *Conservation of Isotopic Spin and Isotopic Gauge Invariance*, *Phys. Rev.* **96** (1954) 191–195.
- [13] A. Salam, *On parity conservation and neutrino mass*, *Nuovo Cim.* **5** (1957) 299–301.
- [14] T. D. Lee and C.-N. Yang, *Parity Nonconservation and a Two Component Theory of the Neutrino*, *Phys. Rev.* **105** (1957) 1671–1675.
- [15] L. D. Landau, *On the conservation laws for weak interactions*, *Nucl. Phys.* **3** (1957) 127–131.
- [16] C. S. Wu, E. Ambler, R. W. Hayward, D. D. Hoppes and R. P. Hudson, *Experimental Test of Parity Conservation in Beta Decay*, *Phys. Rev.* **105** (1957) 1413–1414.
- [17] T. D. Lee and C.-N. Yang, *Question of Parity Conservation in Weak Interactions*, *Phys. Rev.* **104** (1956) 254–258.
- [18] F. Reines, C. L. Cowan, F. B. Harrison, A. D. McGuire and H. W. Kruse, *Detection of the free anti-neutrino*, *Phys. Rev.* **117** (1960) 159–173.
- [19] R. P. Feynman and M. Gell-Mann, *Theory of Fermi interaction*, *Phys. Rev.* **109** (1958) 193–198.

- [20] E. C. G. Sudarshan and R. e. Marshak, *Chirality invariance and the universal Fermi interaction*, *Phys. Rev.* **109** (1958) 1860–1860.
- [21] J. J. Sakurai, *MASS REVERSAL AND WEAK INTERACTIONS*, *Nuovo Cim.* **7** (1958) 649–660.
- [22] M. Gell-Mann, *A Schematic Model of Baryons and Mesons*, *Phys. Lett.* **8** (1964) 214–215.
- [23] G. Zweig, *An $SU(3)$ model for strong interaction symmetry and its breaking. Version 1*, .
- [24] G. Zweig, *An $SU(3)$ model for strong interaction symmetry and its breaking. Version 2*, in *DEVELOPMENTS IN THE QUARK THEORY OF HADRONS. VOL. 1. 1964 - 1978* (D. Lichtenberg and S. P. Rosen, eds.), pp. 22–101. 1964.
- [25] J. D. Bjorken and S. L. Glashow, *Elementary Particles and $SU(4)$* , *Phys. Lett.* **11** (1964) 255–257.
- [26] J. Goldstone, *Field Theories with Superconductor Solutions*, *Nuovo Cim.* **19** (1961) 154–164.
- [27] P. W. Higgs, *Broken symmetries, massless particles and gauge fields*, *Phys. Lett.* **12** (1964) 132–133.
- [28] F. Englert and R. Brout, *Broken Symmetry and the Mass of Gauge Vector Mesons*, *Phys. Rev. Lett.* **13** (1964) 321–323.
- [29] G. S. Guralnik, C. R. Hagen and T. W. B. Kibble, *Global Conservation Laws and Massless Particles*, *Phys. Rev. Lett.* **13** (1964) 585–587.
- [30] O. W. Greenberg, *Spin and Unitary Spin Independence in a Paraquark Model of Baryons and Mesons*, *Phys. Rev. Lett.* **13** (1964) 598–602.

- [31] M. Y. Han and Y. Nambu, *Three Triplet Model with Double SU(3) Symmetry*, *Phys. Rev.* **139** (1965) B1006–B1010.
- [32] S. Weinberg, *A Model of Leptons*, *Phys. Rev. Lett.* **19** (1967) 1264–1266.
- [33] A. Salam, *Weak and Electromagnetic Interactions*, *Conf. Proc. C680519* (1968) 367–377.
- [34] R. P. Feynman, *Photon hadron interactions - w.a. benjamin new york*, (1972).
- [35] R. P. Feynman, *Very high-energy collisions of hadrons*, *Phys. Rev. Lett.* **23** (1969) 1415–1417.
- [36] J. D. Bjorken and E. A. Paschos, *Inelastic Electron Proton and gamma Proton Scattering, and the Structure of the Nucleon*, *Phys. Rev.* **185** (1969) 1975–1982.
- [37] H. D. Politzer, *Reliable Perturbative Results for Strong Interactions?*, *Phys. Rev. Lett.* **30** (1973) 1346–1349.
- [38] D. J. Gross and F. Wilczek, *Ultraviolet Behavior of Nonabelian Gauge Theories*, *Phys. Rev. Lett.* **30** (1973) 1343–1346.
- [39] E598 collaboration, J. J. Aubert et al., *Experimental Observation of a Heavy Particle J*, *Phys. Rev. Lett.* **33** (1974) 1404–1406.
- [40] SLAC-SP-017 collaboration, J. E. Augustin et al., *Discovery of a Narrow Resonance in e+ e- Annihilation*, *Phys. Rev. Lett.* **33** (1974) 1406–1408.
- [41] UA1 collaboration, G. Arnison et al., *Experimental Observation of Isolated Large Transverse Energy Electrons with Associated Missing Energy at $s^{**}(1/2) = 540\text{-GeV}$* , *Phys. Lett.* **122B** (1983) 103–116.

- [42] UA1 collaboration, G. Arnison et al., *Experimental Observation of Lepton Pairs of Invariant Mass Around 95-GeV/c**2 at the CERN SPS Collider*, *Phys. Lett.* **126B** (1983) 398–410.
- [43] UA2 collaboration, M. Banner et al., *Observation of Single Isolated Electrons of High Transverse Momentum in Events with Missing Transverse Energy at the CERN anti-p p Collider*, *Phys. Lett.* **122B** (1983) 476–485.
- [44] UA2 collaboration, P. Bagnaia et al., *Evidence for Z0 —> e+ e- at the CERN anti-p p Collider*, *Phys. Lett.* **B129** (1983) 130–140.
- [45] CDF collaboration, F. Abe et al., *Observation of top quark production in pbar p collisions*, *Phys. Rev. Lett.* **74** (1995) 2626–2631, [[hep-ex/9503002](#)].
- [46] D0 collaboration, S. Abachi et al., *Observation of the top quark*, *Phys. Rev. Lett.* **74** (1995) 2632–2637, [[hep-ex/9503003](#)].
- [47] ATLAS collaboration, G. Aad et al., *Observation of a new particle in the search for the Standard Model Higgs boson with the ATLAS detector at the LHC*, *Phys. Lett.* **B716** (2012) 1–29, [[1207.7214](#)].
- [48] CMS collaboration, S. Chatrchyan et al., *Observation of a new boson at a mass of 125 GeV with the CMS experiment at the LHC*, *Phys. Lett.* **B716** (2012) 30–61, [[1207.7235](#)].
- [49] E. Noether, *Invariant Variation Problems*, *Gott. Nachr.* **1918** (1918) 235–257, [[physics/0503066](#)].
- [50] TASSO collaboration, R. Brandelik et al., *Evidence for Planar Events in e+ e- Annihilation at High-Energies*, *Phys. Lett.* **B86** (1979) 243–249.
- [51] D. P. Barber et al., *Discovery of Three Jet Events and a Test of Quantum Chromodynamics at PETRA Energies*, *Phys. Rev. Lett.* **43** (1979) 830.

- [52] PLUTO collaboration, C. Berger et al., *Evidence for Gluon Bremsstrahlung in $e+e-$ Annihilations at High-Energies*, *Phys. Lett.* **B86** (1979) 418–425.
- [53] JADE collaboration, W. Bartel et al., *Observation of Planar Three Jet Events in $e+e-$ Annihilation and Evidence for Gluon Bremsstrahlung*, *Phys. Lett.* **B91** (1980) 142–147.
- [54] H. Fritzsch, M. Gell-Mann and H. Leutwyler, *Advantages of the Color Octet Gluon Picture*, *Phys. Lett.* **B47** (1973) 365–368.
- [55] M. Breidenbach, J. I. Friedman, H. W. Kendall, E. D. Bloom, D. H. Coward, H. C. DeStaebler et al., *Observed Behavior of Highly Inelastic electron-Proton Scattering*, *Phys. Rev. Lett.* **23** (1969) 935–939.
- [56] E. D. Bloom et al., *High-Energy Inelastic $e p$ Scattering at 6-Degrees and 10-Degrees*, *Phys. Rev. Lett.* **23** (1969) 930–934.
- [57] S. L. Adler and W.-K. Tung, *Breakdown of asymptotic sum rules in perturbation theory*, *Phys. Rev. Lett.* **22** (1969) 978–981.
- [58] S. L. Adler and W.-K. Tung, *Bjorken limit in perturbation theory*, *Phys. Rev.* **D1** (1970) 2846–2859.
- [59] R. Jackiw and G. Preparata, *Probes for the constituents of the electromagnetic current and anomalous commutators*, *Phys. Rev. Lett.* **22** (1969) 975–977.
- [60] LHCb collaboration, R. Aaij et al., *Observation of $J/\psi\phi$ structures consistent with exotic states from amplitude analysis of $B^+ \rightarrow J/\psi\phi K^+$ decays*, *Phys. Rev. Lett.* **118** (2017) 022003, [[1606.07895](#)].
- [61] LHCb collaboration, R. Aaij et al., *Amplitude analysis of $B^+ \rightarrow J/\psi\phi K^+$ decays*, *Phys. Rev.* **D95** (2017) 012002, [[1606.07898](#)].

- [62] LHCb collaboration, R. Aaij et al., *Observation of $J/\psi p$ Resonances Consistent with Pentaquark States in $\Lambda_b^0 \rightarrow J/\psi K^- p$ Decays*, *Phys. Rev. Lett.* **115** (2015) 072001, [[1507.03414](#)].
- [63] P. A. Baikov, K. G. Chetyrkin and J. H. Khn, *Five-Loop Running of the QCD coupling constant*, [1606.08659](#).
- [64] T. Kinoshita, *Mass singularities of Feynman amplitudes*, *J. Math. Phys.* **3** (1962) 650–677.
- [65] T. D. Lee and M. Nauenberg, *Degenerate Systems and Mass Singularities*, *Phys. Rev.* **133** (1964) B1549–B1562.
- [66] G. Passarino and M. J. G. Veltman, *One Loop Corrections for $e+ e-$ Annihilation Into $\mu\mu+$ $\mu\mu-$ in the Weinberg Model*, *Nucl. Phys.* **B160** (1979) 151–207.
- [67] G. Ossola, C. G. Papadopoulos and R. Pittau, *Reducing full one-loop amplitudes to scalar integrals at the integrand level*, *Nucl. Phys.* **B763** (2007) 147–169, [[hep-ph/0609007](#)].
- [68] G. Ossola, C. G. Papadopoulos and R. Pittau, *Numerical evaluation of six-photon amplitudes*, *JHEP* **07** (2007) 085, [[0704.1271](#)].
- [69] S. Frixione, Z. Kunszt and A. Signer, *Three jet cross-sections to next-to-leading order*, *Nucl. Phys.* **B467** (1996) 399–442, [[hep-ph/9512328](#)].
- [70] S. Frixione, *A General approach to jet cross-sections in QCD*, *Nucl. Phys.* **B507** (1997) 295–314, [[hep-ph/9706545](#)].
- [71] S. Moch, J. A. M. Vermaseren and A. Vogt, *Next-to-next-to leading order QCD corrections to the photon's parton structure*, *Nucl. Phys.* **B621** (2002) 413–458, [[hep-ph/0110331](#)].

- [72] S. Moch, J. A. M. Vermaseren and A. Vogt, *The Three loop splitting functions in QCD: The Nonsinglet case*, *Nucl. Phys.* **B688** (2004) 101–134, [[hep-ph/0403192](#)].
- [73] A. Vogt, S. Moch and J. A. M. Vermaseren, *The Three-loop splitting functions in QCD: The Singlet case*, *Nucl. Phys.* **B691** (2004) 129–181, [[hep-ph/0404111](#)].
- [74] A. Vogt, S. Moch and J. Vermaseren, *Photon-parton splitting functions at the next-to-next-to-leading order of QCD*, *Acta Phys. Polon.* **B37** (2006) 683–688, [[hep-ph/0511112](#)].
- [75] K. Ellis, *Introduction to QCD at Colliders - lecture given at Fermilab*, 2006.
- [76] J. F. Donoghue, *General relativity as an effective field theory: The leading quantum corrections*, *Phys. Rev.* **D50** (1994) 3874–3888, [[gr-qc/9405057](#)].
- [77] A. Zee, *Quantum Field Theory in a Nutshell: (Second Edition)*. In a Nutshell. Princeton University Press, 2010.
- [78] S. Weinberg, *Gravitation and cosmology: principles and applications of the general theory of relativity*. Wiley, 1972.
- [79] T. Kaluza, *On the Problem of Unity in Physics*, *Sitzungsber. Preuss. Akad. Wiss. Berlin (Math. Phys.)* **1921** (1921) 966–972.
- [80] O. Klein, *The Atomicity of Electricity as a Quantum Theory Law*, *Nature* **118** (1926) 516.
- [81] N. Arkani-Hamed, S. Dimopoulos and G. Dvali, *The Hierarchy problem and new dimensions at a millimeter*, *Phys.Lett.* **B429** (1998) 263–272, [[hep-ph/9803315](#)].
- [82] I. Antoniadis, N. Arkani-Hamed, S. Dimopoulos and G. Dvali, *New dimensions at a millimeter to a Fermi and superstrings at a TeV*, *Phys.Lett.* **B436** (1998) 257–263, [[hep-ph/9804398](#)].

- [83] N. Arkani-Hamed, S. Dimopoulos and G. R. Dvali, *Phenomenology, astrophysics and cosmology of theories with submillimeter dimensions and TeV scale quantum gravity*, *Phys. Rev.* **D59** (1999) 086004, [[hep-ph/9807344](#)].
- [84] ATLAS COLLABORATION collaboration, G. Aad et al., *Search for Extra Dimensions in diphoton events using proton-proton collisions recorded at $\sqrt{s} = 7$ TeV with the ATLAS detector at the LHC*, *New J.Phys.* **15** (2013) 043007, [[1210.8389](#)].
- [85] CMS COLLABORATION collaboration, S. Chatrchyan et al., *Search for signatures of extra dimensions in the diphoton mass spectrum at the Large Hadron Collider*, *Phys.Rev.Lett.* **108** (2012) 111801, [[1112.0688](#)].
- [86] G. L. Landsberg, *Extra dimensions and more...*, in *Proceedings, 36th Rencontres de Moriond on QCD and High Energy Hadronic Interactions: Les Arcs, France, Mar 17-24, 2001*, pp. 349–352, 2002. [hep-ex/0105039](#).
- [87] DELPHI collaboration, P. Abreu et al., *Photon events with missing energy at $s^{**}(1/2) = 183\text{-GeV to } 189\text{-GeV}$* , *Eur. Phys. J.* **C17** (2000) 53–65, [[hep-ex/0103044](#)].
- [88] T. Han, J. D. Lykken and R.-J. Zhang, *On Kaluza-Klein states from large extra dimensions*, *Phys.Rev.* **D59** (1999) 105006, [[hep-ph/9811350](#)].
- [89] H. Davoudiasl, J. Hewett and T. Rizzo, *Phenomenology of the Randall-Sundrum Gauge Hierarchy Model*, *Phys.Rev.Lett.* **84** (2000) 2080, [[hep-ph/9909255](#)].
- [90] G. F. Giudice, R. Rattazzi and J. D. Wells, *Quantum gravity and extra dimensions at high-energy colliders*, *Nucl.Phys.* **B544** (1999) 3–38, [[hep-ph/9811291](#)].
- [91] W. D. Goldberger and M. B. Wise, *Modulus stabilization with bulk fields*, *Phys.Rev.Lett.* **83** (1999) 4922–4925, [[hep-ph/9907447](#)].

- [92] W. D. Goldberger and M. B. Wise, *Phenomenology of a stabilized modulus*, *Phys.Lett.* **B475** (2000) 275–279, [[hep-ph/9911457](#)].
- [93] H. Davoudiasl, J. Hewett and T. Rizzo, *Experimental probes of localized gravity: On and off the wall*, *Phys.Rev.* **D63** (2001) 075004, [[hep-ph/0006041](#)].
- [94] M. Kumar, P. Mathews, V. Ravindran and A. Tripathi, *Direct photon pair production at the LHC to order α_s in TeV scale gravity models*, *Nucl.Phys.* **B818** (2009) 28–51, [[0902.4894](#)].
- [95] S. Kumar Rai and S. Raychaudhuri, *Single photon signals for warped quantum gravity at a linear e+ e- collider*, *JHEP* **0310** (2003) 020, [[hep-ph/0307096](#)].
- [96] ATLAS collaboration, G. Aad et al., *Evidence for Electroweak Production of $W^\pm W^\pm jj$ in pp Collisions at $\sqrt{s} = 8$ TeV with the ATLAS Detector*, *Phys. Rev. Lett.* **113** (2014) 141803, [[1405.6241](#)].
- [97] ATLAS collaboration, G. Aad et al., *Evidence of W Production in pp Collisions at $s=8$ TeV and Limits on Anomalous Quartic Gauge Couplings with the ATLAS Detector*, *Phys. Rev. Lett.* **115** (2015) 031802, [[1503.03243](#)].
- [98] CMS collaboration, S. Chatrchyan et al., *Search for $WW\gamma$ and $WZ\gamma$ production and constraints on anomalous quartic gauge couplings in pp collisions at $\sqrt{s} = 8$ TeV*, *Phys. Rev. D90* (2014) 032008, [[1404.4619](#)].
- [99] L. Randall and R. Sundrum, *A Large mass hierarchy from a small extra dimension*, *Phys.Rev.Lett.* **83** (1999) 3370–3373, [[hep-ph/9905221](#)].
- [100] N. Agarwal, V. Ravindran, V. K. Tiwari and A. Tripathi, *Next-to-leading order QCD corrections to the Z boson pair production at the LHC in Randall Sundrum model*, *Phys.Lett.* **B686** (2010) 244–248, [[0910.1551](#)].

- [101] N. Agarwal, V. Ravindran, V. K. Tiwari and A. Tripathi, *Next-to-leading order QCD corrections to W^+W^- production at the LHC in Randall Sundrum model*, *Phys.Lett.* **B690** (2010) 390–395, [[1003.5445](#)].
- [102] P. Mathews, V. Ravindran and K. Sridhar, *NLO-QCD corrections to dilepton production in the Randall-Sundrum model*, *JHEP* **0510** (2005) 031, [[hep-ph/0506158](#)].
- [103] G. Das, P. Mathews, V. Ravindran and S. Seth, *RS resonance in di-final state production at the LHC to NLO+PS accuracy*, *JHEP* **10** (2014) 188, [[1408.3970](#)].
- [104] G. Bozzi, F. Campanario, M. Rauch and D. Zeppenfeld, *$Z\gamma\gamma$ production with leptonic decays and triple photon production at next-to-leading order QCD*, *Phys.Rev.* **D84** (2011) 074028, [[1107.3149](#)].
- [105] T. Binoth, G. Ossola, C. Papadopoulos and R. Pittau, *NLO QCD corrections to tri-boson production*, *JHEP* **0806** (2008) 082, [[0804.0350](#)].
- [106] G. Bozzi, F. Campanario, V. Hankele and D. Zeppenfeld, *NLO QCD corrections to $W+W-$ gamma and $Z Z$ gamma production with leptonic decays*, *Phys.Rev.* **D81** (2010) 094030, [[0911.0438](#)].
- [107] A. Lazopoulos, K. Melnikov and F. Petriello, *QCD corrections to tri-boson production*, *Phys.Rev.* **D76** (2007) 014001, [[hep-ph/0703273](#)].
- [108] J. M. Campbell and C. Williams, *Triphoton production at hadron colliders*, [**1403.2641**](#).
- [109] M. Mandal, P. Mathews, V. Ravindran and S. Seth, *Three photon production to NLO+PS accuracy at the LHC*, [**1403.2917**](#).

- [110] M. Kumar, P. Mathews, V. Ravindran and S. Seth, *Neutral triple electroweak gauge boson production in the large extra-dimension model at the LHC*, *Phys.Rev.* **D85** (2012) 094507, [[1111.7063](#)].
- [111] R.-C. Jiang, X.-Z. Li, W.-G. Ma, L. Guo and R.-Y. Zhang, *Triple Z^0 -boson production in large extra dimensions model at ILC*, *Chin.Phys.Lett.* **29** (2012) 111101, [[1211.6800](#)].
- [112] H. Sun and Y.-J. Zhou, *Neutral Triple Gauge Boson production in the large extra dimensions model at linear colliders*, *Phys.Rev.* **D86** (2012) 075003, [[1209.2214](#)].
- [113] S. Catani, F. Krauss, R. Kuhn and B. Webber, *QCD matrix elements + parton showers*, *JHEP* **0111** (2001) 063, [[hep-ph/0109231](#)].
- [114] F. Krauss, *Matrix elements and parton showers in hadronic interactions*, *JHEP* **0208** (2002) 015, [[hep-ph/0205283](#)].
- [115] J. Alwall, S. Hoche, F. Krauss, N. Lavesson, L. Lonnblad et al., *Comparative study of various algorithms for the merging of parton showers and matrix elements in hadronic collisions*, *Eur.Phys.J.* **C53** (2008) 473–500, [[0706.2569](#)].
- [116] J. Alwall, S. de Visscher and F. Maltoni, *QCD radiation in the production of heavy colored particles at the LHC*, *JHEP* **0902** (2009) 017, [[0810.5350](#)].
- [117] T. Sjostrand, S. Mrenna and P. Z. Skands, *PYTHIA 6.4 Physics and Manual*, *JHEP* **05** (2006) 026, [[hep-ph/0603175](#)].
- [118] J. Alwall, R. Frederix, S. Frixione, V. Hirschi, F. Maltoni, O. Mattelaer et al., *The automated computation of tree-level and next-to-leading order differential cross sections, and their matching to parton shower simulations*, *JHEP* **07** (2014) 079, [[1405.0301](#)].

- [119] A. Alloul, N. D. Christensen, C. Degrande, C. Duhr and B. Fuks, *FeynRules 2.0 - A complete toolbox for tree-level phenomenology*, *Comput.Phys.Commun.* **185** (2014) 2250–2300, [[1310.1921](#)].
- [120] ATLAS COLLABORATION collaboration, G. Aad et al., *Search for Extra Dimensions using diphoton events in 7 TeV proton-proton collisions with the ATLAS detector*, *Phys.Lett.* **B710** (2012) 538–556, [[1112.2194](#)].
- [121] CMS collaboration, V. Khachatryan et al., *Search for resonances and quantum black holes using dijet mass spectra in proton-proton collisions at $\sqrt{s}=8$ TeV*, *Phys.Rev.* **D91** (2015) 052009, [[1501.04198](#)].
- [122] K. Hagiwara, J. Kanzaki, Q. Li and K. Mawatari, *HELAS and MadGraph/MadEvent with spin-2 particles*, *Eur.Phys.J.* **C56** (2008) 435–447, [[0805.2554](#)].
- [123] S. Frixione, *Isolated photons in perturbative QCD*, *Phys.Lett.* **B429** (1998) 369–374, [[hep-ph/9801442](#)].
- [124] R. Frederix, S. Frixione, V. Hirschi, F. Maltoni, R. Pittau and P. Torrielli, *Four-lepton production at hadron colliders: aMC@NLO predictions with theoretical uncertainties*, *JHEP* **02** (2012) 099, [[1110.4738](#)].
- [125] D. Atwood and S. K. Gupta, *Probing Randall-Sundram Model using triphotons at the LHC*, [\[1006.4370\]\(#\)](#).
- [126] CMS COLLABORATION collaboration, S. Chatrchyan et al., *Search for Resonances in the Dilepton Mass Distribution in pp Collisions at $\sqrt(s)=7$ TeV*, *JHEP* **1105** (2011) 093, [[1103.0981](#)].

- [127] P. Mathews, V. Ravindran, K. Sridhar and W. van Neerven, *Next-to-leading order QCD corrections to the Drell-Yan cross section in models of TeV-scale gravity*, *Nucl.Phys.* **B713** (2005) 333–377, [[hep-ph/0411018](#)].
- [128] M. Kumar, P. Mathews and V. Ravindran, *PDF and scale uncertainties of various DY distributions in ADD and RS models at hadron colliders*, *Eur.Phys.J.* **C49** (2007) 599–611, [[hep-ph/0604135](#)].
- [129] M. Kumar, P. Mathews, V. Ravindran and A. Tripathi, *Diphoton signals in theories with large extra dimensions to NLO QCD at hadron colliders*, *Phys.Lett.* **B672** (2009) 45–50, [[0811.1670](#)].
- [130] N. Agarwal, V. Ravindran, V. Tiwari and A. Tripathi, *Z boson pair production at the LHC to $O(\alpha(s))$ in TeV scale gravity models*, *Nucl.Phys.* **B830** (2010) 248–270, [[0909.2651](#)].
- [131] N. Agarwal, V. Ravindran, V. K. Tiwari and A. Tripathi, *W^+W^- production in Large extra dimension model at next-to-leading order in QCD at the LHC*, *Phys.Rev.* **D82** (2010) 036001, [[1003.5450](#)].
- [132] S. A. Li, C. S. Li, H. T. Li and J. Gao, *Constraints on Randall-Sundrum model from the events of dijet production with QCD next-to-leading order accuracy at the LHC*, [1408.2762](#).
- [133] R. Frederix, M. K. Mandal, P. Mathews, V. Ravindran, S. Seth et al., *Diphoton production in the ADD model to NLO+parton shower accuracy at the LHC*, *JHEP* **1212** (2012) 102, [[1209.6527](#)].
- [134] R. Frederix, M. Mandal, P. Mathews, V. Ravindran and S. Seth, *Drell-Yan, ZZ, W^+W^- production in SM & ADD model to NLO+PS accuracy at the LHC*, *Eur.Phys.J.* **C74** (2014) 2745, [[1307.7013](#)].

- [135] S. Frixione and B. R. Webber, *Matching NLO QCD computations and parton shower simulations*, *JHEP* **0206** (2002) 029, [[hep-ph/0204244](#)].
- [136] J. Alwall, M. Herquet, F. Maltoni, O. Mattelaer and T. Stelzer, *MadGraph 5 : Going Beyond*, *JHEP* **1106** (2011) 128, [[1106.0522](#)].
- [137] R. Frederix, S. Frixione, F. Maltoni and T. Stelzer, *Automation of next-to-leading order computations in QCD: The FKS subtraction*, *JHEP* **0910** (2009) 003, [[0908.4272](#)].
- [138] G. Corcella, I. Knowles, G. Marchesini, S. Moretti, K. Odagiri et al., *HERWIG 6: An Event generator for hadron emission reactions with interfering gluons (including supersymmetric processes)*, *JHEP* **0101** (2001) 010, [[hep-ph/0011363](#)].
- [139] P. Artoisenet, R. Frederix, O. Mattelaer and R. Rietkerk, *Automatic spin-entangled decays of heavy resonances in Monte Carlo simulations*, *JHEP* **1303** (2013) 015, [[1212.3460](#)].
- [140] H. Murayama, I. Watanabe and K. Hagiwara, *HELAS: HELicity amplitude subroutines for Feynman diagram evaluations*, *KEK-91-11* (1992) .
- [141] P. de Aquino, K. Hagiwara, Q. Li and F. Maltoni, *Simulating graviton production at hadron colliders*, *JHEP* **1106** (2011) 132, [[1101.5499](#)].
- [142] A. Martin, W. Stirling, R. Thorne and G. Watt, *Parton distributions for the LHC*, *Eur.Phys.J.* **C63** (2009) 189–285, [[0901.0002](#)].
- [143] ATLAS, CDF, CMS, D0 collaboration, Y. R. Peters, *Top anti-top Asymmetries at the Tevatron and the LHC*, in *Proceedings, 32nd International Symposium on Physics in Collision (PIC 2012): Strbske Pleso, Slovakia, September 12-15, 2012*, pp. 27–37, 2012. [1211.6028](#).

- [144] M. Czakon, P. Fiedler and A. Mitov, *Resolving the Tevatron Top Quark Forward-Backward Asymmetry Puzzle: Fully Differential Next-to-Next-to-Leading-Order Calculation*, *Phys. Rev. Lett.* **115** (2015) 052001, [[1411.3007](#)].
- [145] C. Anastasiou, C. Duhr, F. Dulat, F. Herzog and B. Mistlberger, *Higgs Boson Gluon-Fusion Production in QCD at Three Loops*, *Phys. Rev. Lett.* **114** (2015) 212001, [[1503.06056](#)].
- [146] S. Catani and M. Grazzini, *An NNLO subtraction formalism in hadron collisions and its application to Higgs boson production at the LHC*, *Phys. Rev. Lett.* **98** (2007) 222002, [[hep-ph/0703012](#)].
- [147] J. Gaunt, M. Stahlhofen, F. J. Tackmann and J. R. Walsh, *N-jettiness Subtractions for NNLO QCD Calculations*, *JHEP* **09** (2015) 058, [[1505.04794](#)].
- [148] A. Gehrmann-De Ridder, T. Gehrmann and E. W. N. Glover, *Antenna subtraction at NNLO*, *JHEP* **09** (2005) 056, [[hep-ph/0505111](#)].
- [149] N. N. Bogoliubov and O. S. Parasiuk, *On the Multiplication of the causal function in the quantum theory of fields*, *Acta Math.* **97** (1957) 227–266.
- [150] K. Hepp, *Proof of the Bogolyubov-Parasiuk theorem on renormalization*, *Commun. Math. Phys.* **2** (1966) 301–326.
- [151] W. Zimmermann, *Convergence of Bogolyubov’s method of renormalization in momentum space*, *Commun. Math. Phys.* **15** (1969) 208–234.
- [152] G. Heinrich, *Sector Decomposition*, *Int. J. Mod. Phys.* **A23** (2008) 1457–1486, [[0803.4177](#)].
- [153] L. Randall and R. Sundrum, *An Alternative to compactification*, *Phys. Rev. Lett.* **83** (1999) 4690–4693, [[hep-th/9906064](#)].

- [154] D. de Florian, M. Mahakhud, P. Mathews, J. Mazzitelli and V. Ravindran, *Quark and gluon spin-2 form factors to two-loops in QCD*, *JHEP* **02** (2014) 035, [[1312.6528](#)].
- [155] T. Ahmed, G. Das, P. Mathews, N. Rana and V. Ravindran, *Spin-2 Form Factors at Three Loop in QCD*, *JHEP* **12** (2015) 084, [[1508.05043](#)].
- [156] D. de Florian, M. Mahakhud, P. Mathews, J. Mazzitelli and V. Ravindran, *Next-to-Next-to-Leading Order QCD Corrections in Models of TeV-Scale Gravity*, *JHEP* **1404** (2014) 028, [[1312.7173](#)].
- [157] T. Ahmed, P. Banerjee, P. K. Dhani, M. C. Kumar, P. Mathews, N. Rana et al., *NNLO QCD Corrections to the Drell-Yan Cross Section in Models of TeV-Scale Gravity*, [1606.08454](#).
- [158] R. N. Lee, *Group structure of the integration-by-part identities and its application to the reduction of multiloop integrals*, *JHEP* **07** (2008) 031, [[0804.3008](#)].
- [159] E. Remiddi, *Dispersion Relations for Feynman Graphs*, *Helv. Phys. Acta* **54** (1982) 364.
- [160] S. Laporta and E. Remiddi, *Progress in the analytical evaluation of the electron ($g-2$) in QED: The Scalar part of the triple cross graphs*, *Phys. Lett.* **B356** (1995) 390–397.
- [161] S. Laporta and E. Remiddi, *The Analytical value of the electron ($g-2$) at order alpha**3 in QED*, *Phys. Lett.* **B379** (1996) 283–291, [[hep-ph/9602417](#)].
- [162] A. V. Kotikov, *Differential equations method: New technique for massive Feynman diagrams calculation*, *Phys. Lett.* **B254** (1991) 158–164.
- [163] T. Gehrmann and E. Remiddi, *Differential equations for two loop four point functions*, *Nucl. Phys.* **B580** (2000) 485–518, [[hep-ph/9912329](#)].

- [164] M. Beneke and V. A. Smirnov, *Asymptotic expansion of Feynman integrals near threshold*, *Nucl. Phys.* **B522** (1998) 321–344, [[hep-ph/9711391](#)].
- [165] V. A. Smirnov, *Applied asymptotic expansions in momenta and masses*, *Springer Tracts Mod. Phys.* **177** (2002) 1–262.
- [166] V. A. Smirnov, *Analytic tools for Feynman integrals*, *Springer Tracts Mod. Phys.* **250** (2012) 1–296.
- [167] S. Karg, M. Kramer, Q. Li and D. Zeppenfeld, *NLO QCD corrections to graviton production at hadron colliders*, *Phys. Rev.* **D81** (2010) 094036, [[0911.5095](#)].
- [168] T. Ahmed, M. Mahakhud, P. Mathews, N. Rana and V. Ravindran, *Two-Loop QCD Correction to massive spin-2 resonance → 3 gluons*, *JHEP* **1405** (2014) 107, [[1404.0028](#)].
- [169] T. Gehrmann and E. Remiddi, *Analytic continuation of massless two loop four point functions*, *Nucl. Phys.* **B640** (2002) 379–411, [[hep-ph/0207020](#)].
- [170] S. Catani, *The Singular behavior of QCD amplitudes at two loop order*, *Phys. Lett.* **B427** (1998) 161–171, [[hep-ph/9802439](#)].
- [171] F. V. Tkachov, *A Theorem on Analytical Calculability of Four Loop Renormalization Group Functions*, *Phys. Lett.* **B100** (1981) 65–68.
- [172] K. G. Chetyrkin and F. V. Tkachov, *Integration by Parts: The Algorithm to Calculate beta Functions in 4 Loops*, *Nucl. Phys.* **B192** (1981) 159–204.
- [173] T. Binoth and G. Heinrich, *An automatized algorithm to compute infrared divergent multiloop integrals*, *Nucl. Phys.* **B585** (2000) 741–759, [[hep-ph/0004013](#)].

- [174] V. A. Smirnov, *Analytical result for dimensionally regularized massless master double box with one leg off-shell*, *Phys. Lett.* **B491** (2000) 130–136, [[hep-ph/0007032](#)].
- [175] V. A. Smirnov, *Analytical result for dimensionally regularized massless master nonplanar double box with one leg off-shell*, *Phys. Lett.* **B500** (2001) 330–337, [[hep-ph/0011056](#)].
- [176] T. Gehrmann and E. Remiddi, *Two loop master integrals for gamma* → 3 jets: The Planar topologies*, *Nucl. Phys.* **B601** (2001) 248–286, [[hep-ph/0008287](#)].
- [177] T. Gehrmann and E. Remiddi, *Two loop master integrals for gamma* → 3 jets: The Nonplanar topologies*, *Nucl. Phys.* **B601** (2001) 287–317, [[hep-ph/0101124](#)].
- [178] G. F. Sterman and M. E. Tejeda-Yeomans, *Multiloop amplitudes and resummation*, *Phys. Lett.* **B552** (2003) 48–56, [[hep-ph/0210130](#)].
- [179] E. Remiddi and J. A. M. Vermaseren, *Harmonic polylogarithms*, *Int. J. Mod. Phys.* **A15** (2000) 725–754, [[hep-ph/9905237](#)].
- [180] S. M. Aybat, L. J. Dixon and G. F. Sterman, *The Two-loop anomalous dimension matrix for soft gluon exchange*, *Phys. Rev. Lett.* **97** (2006) 072001, [[hep-ph/0606254](#)].
- [181] S. M. Aybat, L. J. Dixon and G. F. Sterman, *The Two-loop soft anomalous dimension matrix and resummation at next-to-next-to leading pole*, *Phys. Rev.* **D74** (2006) 074004, [[hep-ph/0607309](#)].
- [182] V. Ravindran, J. Smith and W. L. van Neerven, *Two-loop corrections to Higgs boson production*, *Nucl. Phys.* **B704** (2005) 332–348, [[hep-ph/0408315](#)].
- [183] S. Moch, J. A. M. Vermaseren and A. Vogt, *Three-loop results for quark and gluon form-factors*, *Phys. Lett.* **B625** (2005) 245–252, [[hep-ph/0508055](#)].

- [184] T. Becher and M. Neubert, *Infrared singularities of scattering amplitudes in perturbative QCD*, *Phys. Rev. Lett.* **102** (2009) 162001, [[0901.0722](#)].
- [185] E. Gardi and L. Magnea, *Factorization constraints for soft anomalous dimensions in QCD scattering amplitudes*, *JHEP* **03** (2009) 079, [[0901.1091](#)].
- [186] J. A. M. Vermaseren, *New features of FORM*, [math-ph/0010025](#).
- [187] A. von Manteuffel and C. Studerus, *Reduze 2 - Distributed Feynman Integral Reduction*, [1201.4330](#).
- [188] R. N. Lee, *Presenting LiteRed: a tool for the Loop InTEgrals REDuction*, [1212.2685](#).
- [189] R. N. Lee, *LiteRed 1.4: a powerful tool for reduction of multiloop integrals*, *J. Phys. Conf. Ser.* **523** (2014) 012059, [[1310.1145](#)].
- [190] P. Nogueira, *Automatic Feynman graph generation*, *J. Comput. Phys.* **105** (1993) 279–289.
- [191] P. Mathews, V. Ravindran and K. Sridhar, *NLO - QCD corrections to e+ e- → $\gamma\gamma$ hadrons in models of TeV-scale gravity*, *JHEP* **08** (2004) 048, [[hep-ph/0405292](#)].
- [192] S. Laporta, *High precision calculation of multiloop Feynman integrals by difference equations*, *Int. J. Mod. Phys. A* **15** (2000) 5087–5159, [[hep-ph/0102033](#)].
- [193] P. Nason, *MINT: A Computer program for adaptive Monte Carlo integration and generation of unweighted distributions*, [0709.2085](#).
- [194] R. N. Lee and A. A. Pomeransky, *Critical points and number of master integrals*, *JHEP* **11** (2013) 165, [[1308.6676](#)].
- [195] A. V. Kotikov, *Differential equations method: The Calculation of vertex type Feynman diagrams*, *Phys. Lett. B* **259** (1991) 314–322.

- [196] V. A. Smirnov, *Analytical result for dimensionally regularized massless on shell double box*, *Phys. Lett.* **B460** (1999) 397–404, [[hep-ph/9905323](#)].
- [197] J. B. Tausk, *Nonplanar massless two loop Feynman diagrams with four on-shell legs*, *Phys. Lett.* **B469** (1999) 225–234, [[hep-ph/9909506](#)].
- [198] T. Ahmed, M. Mahakhud, P. Mathews, N. Rana and V. Ravindran, *Two-loop QCD corrections to Higgs $\rightarrow b + \bar{b} + g$ amplitude*, *JHEP* **08** (2014) 075, [[1405.2324](#)].
- [199] T. Ahmed, G. Das, P. Mathews, N. Rana and V. Ravindran, *The two-loop QCD correction to massive spin-2 resonance $\rightarrow q\bar{q}g$* , *Eur. Phys. J.* **C76** (2016) 667, [[1608.05906](#)].
- [200] F. Jegerlehner, *Facts of life with gamma(5)*, *Eur. Phys. J.* **C18** (2001) 673–679, [[hep-th/0005255](#)].